Technology for Electric and Hybrid Vehicles

Engine

Turbine Generator

Inter Cooler

Injection pump

Dynamometer Controller

Intake Manifold

DC Dynamometer

Wastegate Control

Intake Air

Compressor

Power Turbine

Turbine

Generator

Register for Emergency Stop

Voltage

Controller

Current

Resistance Load

Exhaust

Second Prototype   Turbine

Generator

First Prototype

Turbine   Generator

SAE INTERNATIONAL® ···· SP-1331 ····

Technology for Electric and Hybrid Vehicles

SP-1331

GLOBAL MOBILITY *DATABASE*

All SAE papers, standards, and selected books are abstracted and indexed in the Global Mobility Database

PREFACE

This Special Publication, <u>Technology for Electric and Hybrid Vehicles</u> (SP-1331), is a collection of papers from the "Electric Vehicle Technology" and "Engines and Fuel Technology for Hybrid Vehicles" sessions of the 1998 SAE International Congress and Exposition.

Hybrid vehicles are now a reality in Japan, and they could soon be coming to the United States. The heart of the Toyota Prius hybrid vehicle is its fuel-efficient engine and unique transmission, coupled with a limited-range battery. The hybrid vehicle's advantage is its ability to run the engine at its "sweet spot" to minimize emissions of criteria pollutants or minimize energy consumption and CO_2 production, depending on the control strategy. The key technical measure of success for a hybrid vehicle is a well designed engine--electrical-battery system that is matched to the load demand.

The papers from the "Engines and Fuel Technology for Hybrid Vehicles" session focus on leading-edge engine design, engine management, and fuel strategies for low emission, high mileage hybrid cars and commercial vehicles.

The papers from the "Electric Vehicle Technology" session focus on hybrid vehicle control technology, energy storage, and management for hybrid vehicles and simulation development.

<div align="right">

Bradford Bates
Ford Research Laboratory

Frank Stodolsksy
Argonne National Laboratory

Session Organizers

</div>

TABLE OF CONTENTS

An Algorithm of Optimum Torque Control for Hybrid Vehicle

Yoshishige Ohyama
Hitachi Car Engineering Co., Ltd.

Abstract

An algorithm for a fuel efficient hybrid drivetrain control system that can attain fewer exhaust emissions and higher fuel economy was investigated. The system integrates a lean burn engine with high supercharging, an exhaust gas recycle system, an electric machine for power assist, and an electronically controlled gear transmission. Smooth switching of the power source, the air-fuel ratio, pressure ratio, exhaust gas ratio as a function of the target torque were analyzed. The estimation of air mass in cylinder by using an air flow meter was investegated to control the air-fuel ratio precisely during transients.

1.INTRODUCTION

Consumers are inceasing their demands for vehicles that are more fuel efficient, environmentally friendly, and affordable. Some form of electric and hybrid vehicle is increasingly being viewed as one answer to user demands. Thus, introduction of a future car system integrating an internal combustion engine and an electric machine seems inevitable [1]. While electric vehicles and hybrid-electric vehicles are still dominant [2-4], conventional hybrid systems, with their complicated energy management and storage systems, may not be the final answer to the ultimate high-mileage, low-emissions passenger vehicle. Many of today's hybrid and electric designs are simply too complex, heavy and costly to be considered a viable supercar-type vehicle.

Minimal hybridization will present the best solution to the low-emitting, high-economy passenger vehicle of the future [1]. The internal combustion engine will continue to dominate the world passenger-vehicle market for at least the next 25 years [5]. The engine will require better efficiency and lowered emissions output which means that fuels will similarly require refinement, so that the engines can eventually be refined to the point that they produce almost no harmful emissions. Internal combustion engines using synthetic fuel made of natural gas, similar to light quality gasoline, seem to be the most promising advancement in the near future [5].

To reduce the system's cost and increase its efficiency, the engine is driven at the lowest possible speed at the maximum gear ratio of the transmission at low vehicle speed. Thus, the capacity of the electric machine and battery can be kept small. Systems that combine an integrated interactive hybrid drivetrain control system, such as to give lean burn, with an electronically controlled transmission, and electric machine control systems mentioned above, have been partially examined [1]. The optimum combination of two power sources-a hybrid drivetrain with an internal combustion engine and a small electric machine-would make it possible to get significant reductions in fuel consumption and exhaust emissions. The control system without the electric machine has been already investigated [6], as well as the control system with the electric machine and a continuously variable transmission [7]. A control system with the electric machine and simple gear transmission was presented [8]. A concept for an advanced hybrid control system was investegated that combined a high supercharging engine and a small electric machine [9]. In this paper, an algorithm for an advanced hybrid drivetrain control system

that combines the engine drivetrain control system and electric machine systems is investegated.

2. SYSTEM CONCEPT

2.1 Outline

Idealized, the concept would include an engine and electric machine drivetrain, such as in Figure 1 and Table 1. The electric machine is usually functioned as an electric motor. On one hand this provides fuel saving and lower exhaust emissions while using the engine system such as direct injection stratified charge sytem [10], or rapid combustion system with high dispersed fuel-air mixture [11] and high supercharging, on the other hand, it allows for short-distance driving and low load driving with the electric machine such as electrically exited synchronous drive with power inverter. The engine brake, wheel brake, and regeneration by the electric machine are controlled optimally during deceleration and downhill travel. A transmission with electronically controlled synchromesh gear sets is used for this purpose.
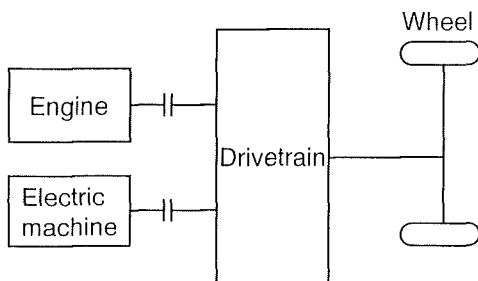
Fig. 1 Hybrid drivetrain

Table 1   Hybrid   drivetrain

(1) Engine
    (a) Rapid combustion with high dispersed mixture
    (b) High supercharging
        → lower nitrogen oxides emissions

(2) Electric machine
    Electrically exited synchronous drive
    with power inverter
        → short distance and low load driving

(3) Transmission
    Electronically controlled synchromesh gear set
        → lower power loss

2.2 Basic control technique

The aim of the control system is to obtain a smooth drivetrain force change relative to the torque set point, which is given by the accelerator position, over a wide range of vehicle speeds and loads. The system should be able to cope with large changes in engine load and drivetrain switches from the electric machine to the engine and from the engine to the electric machine without increasing nitrogen oxides emissions, and without degrading driveability.
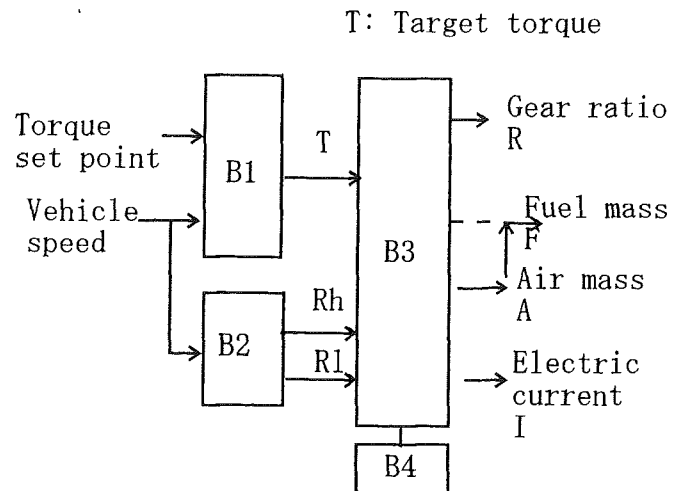
Fig. 2   Control system

As shown in Figure 2, the target drivetrain torque T is calculated as a function of the torque set point and the vehicle speed in block1 (B1). The upper and lower limits of the equivalent gear ratio Rh and Rl are calculated as a function of the vehicle speed in B2. The equivalent gear ratio R, fuel mass F, and air mass A are simultaneously calculated as a function of the target torque T, taking the limit Rh and Rl in consideration in B3. Some control strategies such as the dynamic compensation described in section 3.7 are executed in B4. Fuel mass F is delivered with an electronically controlled fuel injector as shown elsewhere [10]. Fuel is injected directly into the cylinders. Therefore, the system is free from transient fuel compensation which is commonly in port injection systems [8]. The air mass A is controlled with an electronically controlled throttle valve and air bypass valve as described later. The fuel mass may be set by the target torque directly, as in diesel engines. But the estimation of the air mass by the accelerator position is not accurate. Therefore,the fuel mass is controlled

2

by the air mass which is generally measured by the air flow meter, to control the air-fuel ratio precisely [12].

Under stratified charge conditions, the accelerator pedal opening angle, rather than the intake manifold pressure, is the most important information for determining the quantity of injected fuel. But, information about the amount of intake air has also importance in actual engine operation to control the air-fuel ratio A/F precisely.

The gear ratio R is controlled with an electronically controlled transmission [13-16]. The command electronics for an electrically excited synchronous drive can be easily accomplished. In the case of a synchronous drive, an inverter provides optimal control of rotor excitation, stator current amplitude I, and stator current phase. A power inverter with insulated gate bipolar transistors transforms the battery voltage into the rotating voltage system for the motor driving of the electric machine. An additional chopper controls the DC current for the rotor. Then, the drivetrain output torque is obtained, which is equal to the target torque T if there are neither calculation nor control errors.

2.3 Air-fuel ratio control

As the target torque T increases, the drivetrain switched from the electric machine to the engine. The fuel mass F, air mass A of the engine and the electric current I are changed stepwise.

The air mass and fuel mass of the engine are changed frequently as the target torque changes. The air-fuel ratio must be controlled during the transient conditions precisely to reduce exhaust emissions and improve driveability. It was determined that the volumetric efficiency during and immediately following a transient, at any engine temperature, was not equal to the staedy-state value. The transient volumetric efficiency was found to be as large as 10% different from the steady-state value. The volumetric efficiency is dependent upon instantaneous cylinder wall and valve temperature. To control the the air-fuel ratio A/F during transients accurately, the engine controller needs precise predictions or measurements of the amount of intake air, and the amount of fuel injected that will go directly in-cylinder [12].

The intake system of the engine is equipped with a compressor for supercharging and an exhaust gas recycle system, as shown in Figure 3. Wt, Wc, Wb, Wh, Wr, and We are the air or gas mass flow rate at the upstream throttle valve, at the outlet of the compressor, at the bypass valve, at the downstream throttle valve, at the exhaust gas recycle valve, and at the intake port of the engine, respectively. In conventional engine control systems, the air flow into the cylinders should be predicted based on the movement of the throttle plate [12]. The air intake process is modeled through the manifold abusolute pressure observer model. The observer is based on the estimated throttle opening [12]. With stratified
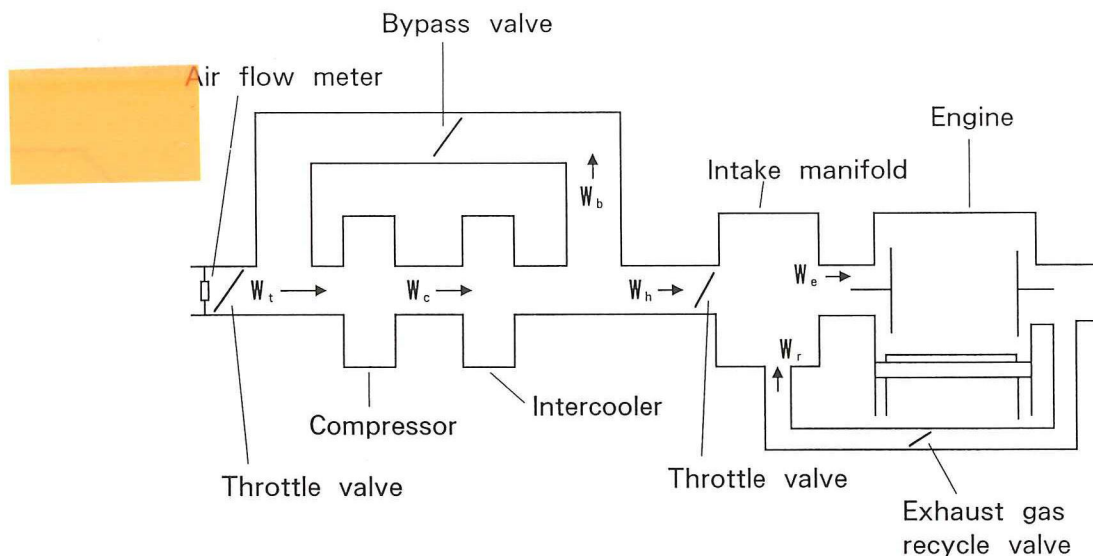
Fig. 3 Intake system

Table 2　　　　　Calculation conditions

Type	4-stroke 4 cylinder	
Cylinder volume per cylinder	4×10^{-4}	m³
Maximum air mass per cylinder at atmospheric pressure A0	4.8×10^{-4}	kg
Maximum exhaust gas recycle ratio	40	%
Maximum exhaust recycle mass per cylinder G0	1.9×10^{-4}	kg
Sum of A0 and G0　　GvO	6.7×10^{-4}	kg
Maximum fuel mass per cylinder at atmospheric pressure F0	4.8×10^{-5}	kg
Maximum air-fuel ratio	40	
Atmospheric pressure	9.8×10^{4}	Pa
Maximum pressure ratio of compressor	2	
Torque T	$1.92 \times 10^{6} \times F{-}19.2$	Nm
Cylinder volume per cylinder	4×10^{-4}	m³
Thermal efficiency of engine	30	%
Maximum output power of electric machine	10.5	kW

charge engines, nearly unthrottled operation is realized. Under these conditions, the estimation of the air flow based on movement of the throttle plate is not accurate due to the small pressure differential accross the throttle plate. Therefore, the model based on the air flow meter was investigated in this paper.

3. ANALYSIS

3.1 Simulation conditions

A 4 cylinder, 4-stroke engine with a cylinder volume of 4 $\times 10^{-4}$ m³ was used for testing. The engine was equipped with a direct injection stratified charge system [10], a supercharger and an exhaust gas recycle (EGR) system. The air-fuel ratio A/F was set between 11 and 40. The maximum ratio of the EGR was 40 %. The maximum pressure ratio of the superchager was 2. The air mass A was controlled by opening and closing of the throttle valve or the bypass valve in Figure 3. The relevant gear ratios from 1st-5th for a stepped transmission were 3.5, 2.0, 1.3, 1.0 and 0.73, respectively. Fuel mass F was controlled with electronically controlled fuel injectors. Table 2 shows the calculation conditions. The output power of the electric machine was 10.5 kW, and the torque was 50 Nm at the speed of 2000 rpm.

3.2 Smooth switching of power source

As the target torque T increases in Figure 4, the

drivetrain switches from the electric machine to the engine. The switching is carried out by simultaneously decreasing the power of the electric machine and increasing the engine power. At T=50 Nm in Figure 4, the power source is switched from the electric machine to the engine. The fuel mass F, air mass A and the exhaust recylce mass G are increased stepwise simultaneously to keep the air-fuel ratio 15 and the EGR ratio 40 %. As the target torque T increases further, the supercharger starts, the air mass A is increased more than A0, and the EGR mass is also increased. At T=162 Nm, the air mass A and the EGR mass G becomes doubled,
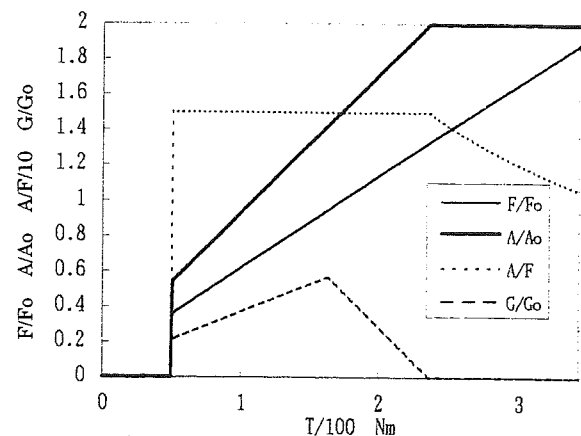
Fig. 4 Fuel mass F, air mass A and EGR mass G versus target torque

which is limited by the pressure ratio of the supercharger. At T=243 Nm, the EGR mass G is decreased and the air mass A is doubled. When the target torque increases further, A/F becomes lower than 15, and the air mass must be controlled by using the throttle valve and the bypass valve.

3.3 Lean burn control by supercharging

Figures 5 (a), (b) and (c) show the simulation results with high supercharging and lean burn. When the target torque is more than T1= 50 Nm, the power source switched from the electric machine to the engine. When the air mass ratio A/A0 becomes more than 1 , the supercharge starts, the air mass ratio A/A0 is finally doubled. In Figure 5(a), at T=50 Nm, the supercharger starts simultaneously with the switching to the engine. When the target torque becomes higher than T2, The air-fuel ratio A/F becomes lower than 40. In Figure 5(b), the supercharger starts at T= 78 Nm. The air-fuel ratio A/F is increased temporally from 20 to 40. When the target torque becomes T3, the air mass A is decreased by decreasing the air-fuel ratio from 20 to 15 stepwise ,without passing into the high nitorogen oxide emission region.

Figure 5 (c) shows the result with high supercharging when pressure is controlled by the bypass valve proportionally to keep the air-fuel ratio at 15. When the target torque becomes T2, the air mass is decreased slightly to decrease the air-fuel ratio from 20 to 15 by controlling the throttle valve. When the target torque increases further, the supercharger starts again and the pressure is controlled by the bypass valve.

3.4 Smooth gear shift with exhaust gas recycle control

Figures 6 (a)-(d) show the results when the gear is shifted from 4th to 2nd at the target torques are Tg=100 Nm, 170 Nm, 238 Nm, and 300 Nm, respectively. The engine torque must be changed simultaneously, so that the output torque remains the same during the shift operation. The engine torque is controlled by decreasing the mass of fuel. The air mass and EGR mass are decreased simultaneously to keep the air-fuel ratio at 15 and EGR ratio at 40%. The air mass is controlled by opening and closing the
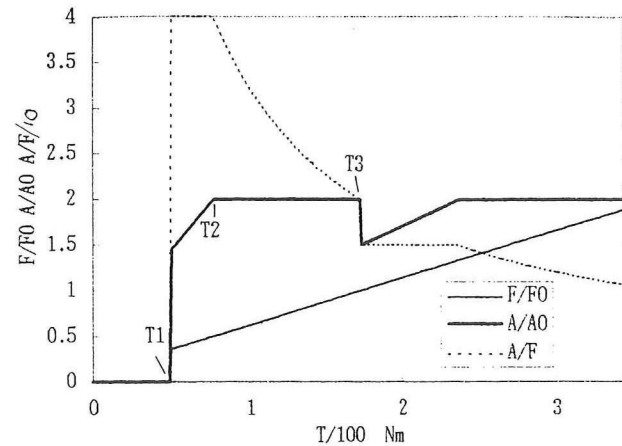
(a) Early supercharging
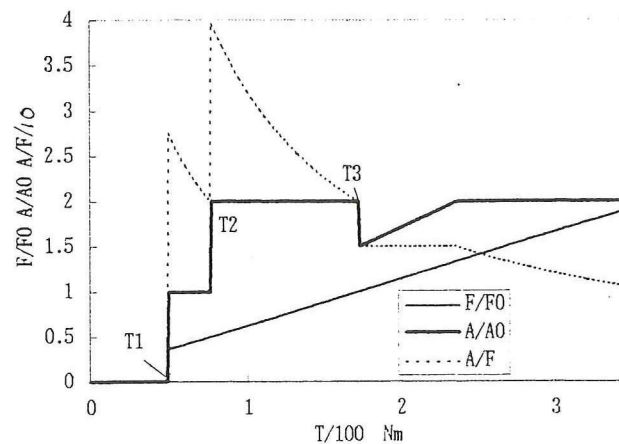
(b) Late supercharging
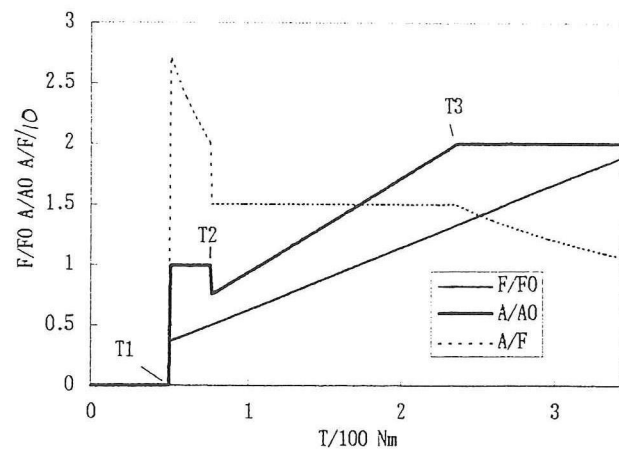
(c) Proportional supercharging

Fig. 5   Fuel mass F, air mass A and EGR mass G versus target torque T

throttle valve and the bypass valve. When the target torque becomes higer than T3 (Figures 6 (a)-(c)), the EGR mass G decreases. When the target torque T
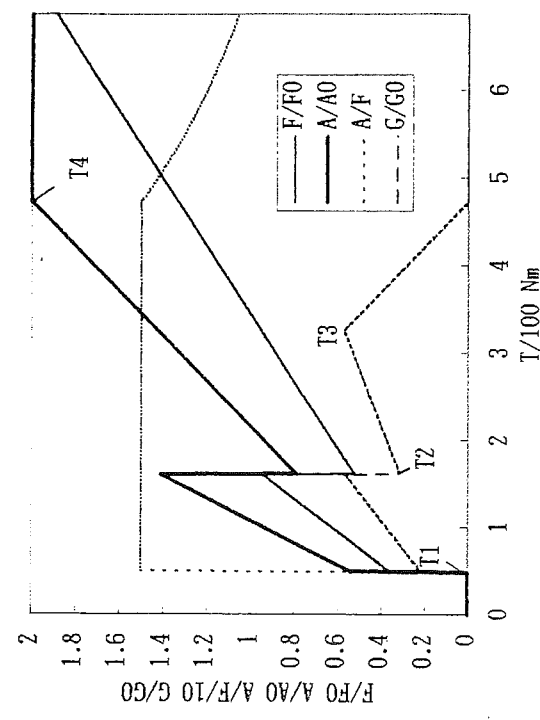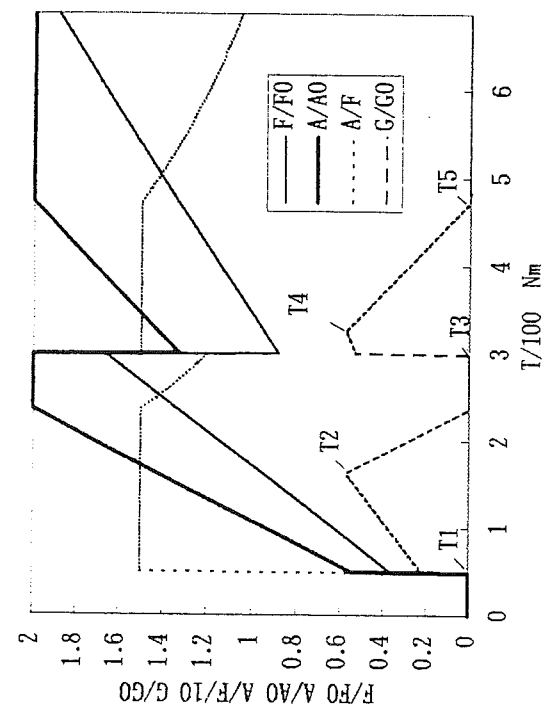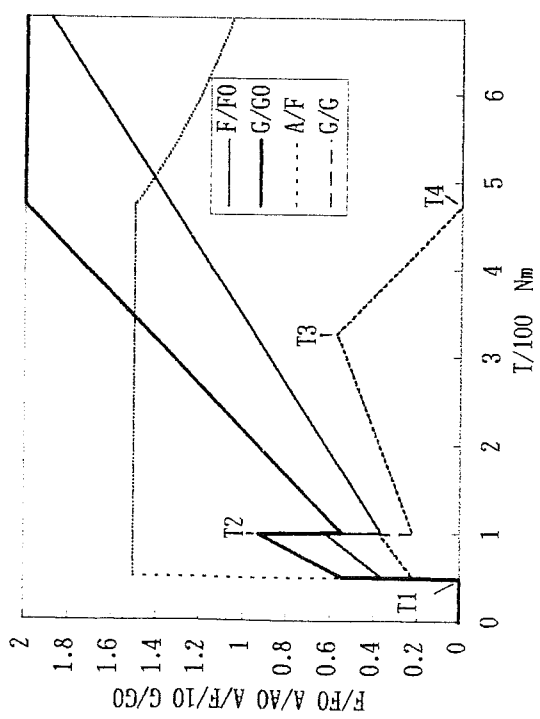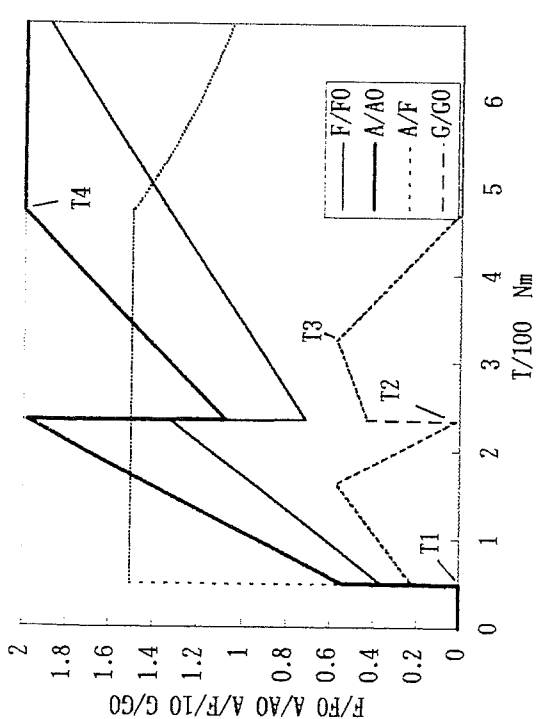
Fig. 6 Fuel mass F, air mass A, EGR mass
and air-fuel ratio A/F versus traget torque T

becomes higher than T4 (Figures 6 (a)-(c)), the air-fuel ratio becomes lower than 15. As the target torque at the gear shift Tg becomes higher, the region of supercharging increases. In Figure 6 (d),the air-fuel ratio becomes less than 15 at T=230-300 Nm, resulting in the increase of carbon monoxide emission.

Figures 7 (a) and (b) show the total mass Gv (the sum of air mass and EGR mass) as a function of the target torque T. Tg is the target torque at gear shift .The gear is shifted from 4th to 2nd. The total mass ratio Gv/Gv0 is lowered when the Tg becomes lower. Thus, the target torque T when the supercharger starts , becomes higher. When Tg is 100 Nm, the supercharger starts at the target torque T of less than 100 Nm.

3.5 Smooth gear shift with lean burn control

Figures 8 (a)-(c) show the results when the gear is shifted from 4th to 2nd at the target torque Tg=70 Nm, 170 Nm and 238 Nm, respectively. As Tg becomes higher, the target torque when the superchager starts becomes lower. The engine torque must be changed so that the output torque remains the same during the shift operation. The engine torque can be controlled by controlling the fuel mass only. The air mass remains the same during the shift operation.

(a) Tg= 70 Nm

(b) Tg= 170 Nm

(a) Tg= 70 Nm

(c) Tg= 238 Nm

Fig. 7   Total mass Gv as a function of
the target torque T
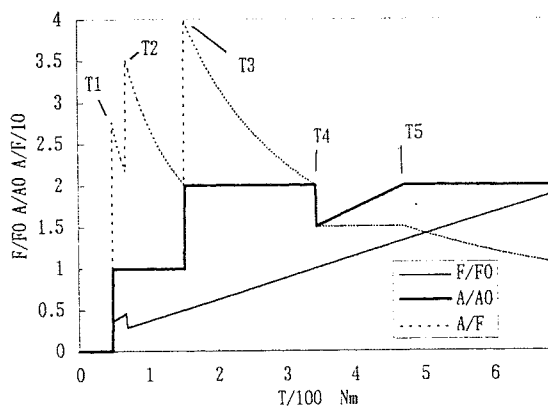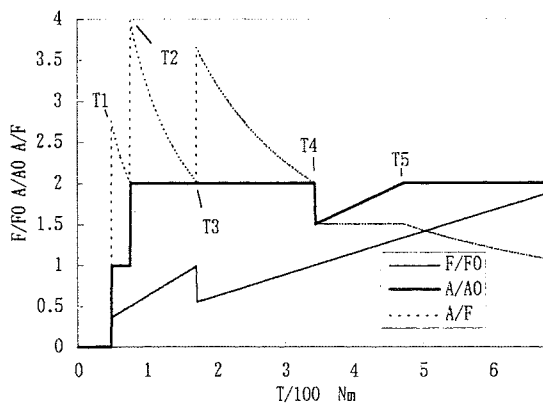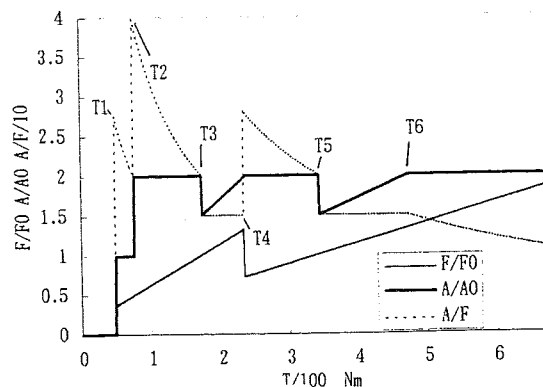
Fig. 8   Fuel mass F, air mass A, EGR mass
as a function of the target torque T

Figures 9 (a) and (b) show the results when gear is shifted from 4th to 2nd at the target torque Tg=70 Nm, 171 Nm, respectively. As the target torque at gear shift Tg becomes higher, the region of supercharging becomes wider, the region of the air-fuel ratio A/F of more than 20 becomes narrower.
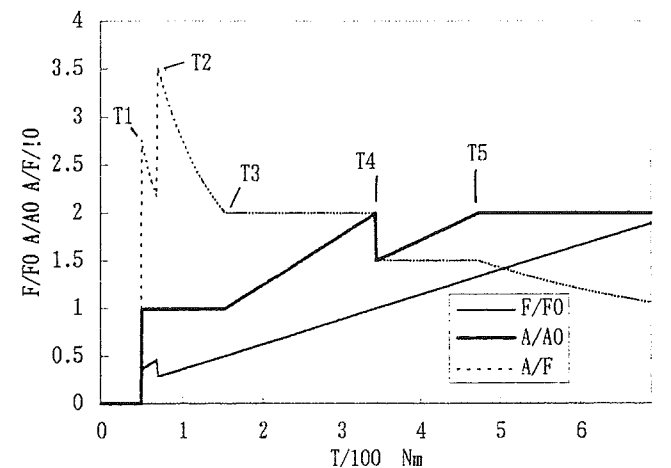
(a) Tg= 70 Nm
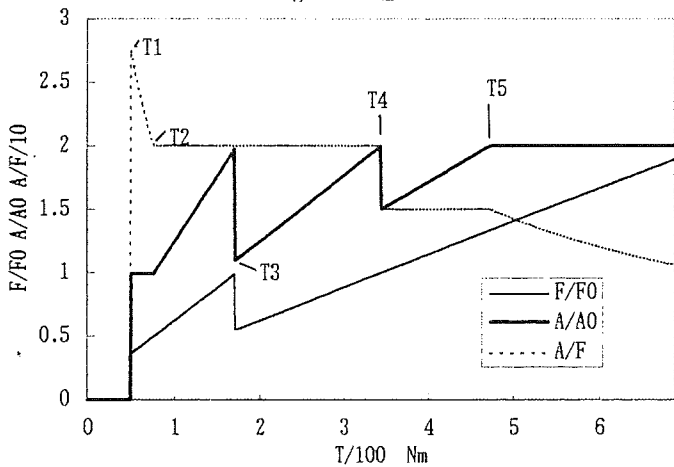
(b) Tg= 170 Nm

Fig. 9   Fuel mass F, air mass A, EGR mass
as a function of the target torque T

3.6 Air-fuel ratio control

As mentioned before, the fuel mass is controlled by the air mass which is generally measured by the air flow meter. During switching from the electric machine to the engine, the air mass increases stepwise against the target torque T to maintain the air-fuel ratio adequately. The accuracy of maintaining the air-fuel ratio for operation during transient conditions depends on the accuracy of the estimated air mass entering the engine cylinders. It is necessary

to estimate this air mass in advance of fuel injection timing and before placing the fuel in the cylinders. In case of gasoline direct injection the fuel injection is free from compensation for the fueling dynamics. When the capacity of the compressor, the surge tank and the intercooler in the intake system [17] is larger in Figure 3, the air mass going through the air flow meter increases temporarily to fill the surge tank and intercooler during throttle opening and the compressor starting. The air mass must be compensated also according to the response lag of the air flow meter and the filling lag of the EGR.

The filling spike must be compensated to reduce fluctuation of the air-fuel ratio which is apt to increase exhaust emissions. This compensation is attained by using the aerodynamic model of the intake system [13]. The air mass into the cylinder is calculated by using the intake manifold filling dynamics and the compressor dynamics. Then, the model of the intake system to predict future air mass is applied. Some simulation results, obtained by the method mentioned above, are shown in Figure 10 which has samples of the traces for air mass flow rate Wa, Wc, Wb, Wh, and We and the pressure pi (10^5 Pa) at the intercooler when the compressor is started during 0-0.2 s and the bypass valve is closed during 0.3-0.4 s. Wa is the measuring value by the air flow meter. The estimated air mass, We, is close to the air mass

Time s
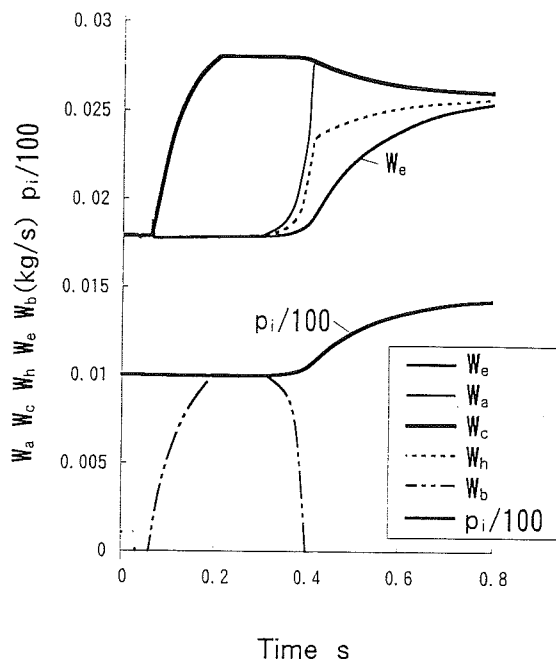
Fig. 10   Air flow during bypass valve control

entering the cylinder. It is seen that the air mass can be estimated at the beginning of the intake stroke, resulting in the fuel supply without any delay, thus a precise air-fuel ratio control.

3.7 Control strategies

(1) Dymamic compensation

Good acceleration performance will require some modification for the strategy mentioned in section 3.6. The output torque is reduced during the change in gear ratio and the power source (engine, electric machine) because part of the engine torque is used to accelerate the engine itself. The power is controlled by compensating the fuel mass and air mass through dynamic models, resulting in smooth switching and reduced drivetrain vibration.

(2) Damping of the torque oscillation

The torque of the engine is controlled during acceleration by monitoring differences between engine and wheel speeds in order to provide a measure of phase differences in the event of engine torque oscillating. The difference between the engine and wheel signals is integrated and fed to an ignition angle correction circuit in order to damp out the torque oscillations [18]. Or, the fuel mass is compensated in place of the ignition angle. In the case of the transmission without power shift, the oscillation will increase when the fuel mass is increased stepwise after the gear engagement. The fuel mass is controlled, taking the oscillation into consideration or, the control is executed by estimating the torque by engine speed signal [19].

(3)Block of the shift

The control system compares and calculates the difference between two stationary torques calculated at different times. Then it recognizes whether the vehicle is on the crest of a hill or in a valley, and whether the vehicle is traveling uphill or downhill over the crest of the hill or through a valley. The gear shift is blocked according to this information to avoid frequent gear shifts.

(4) Integration of brake control

Full utilization of regenerative braking increases electric machine operating range by 25% [20]. The engine brake, wheel brake, and regeneration by the electric machine are controlled optimally during downhill travel. However, available regenerative braking methods vary for several operating conditions such as state of battery charge and vehicle speed.

Regeneration cannot be executed when the battery charge is full. Integration of brake and drivetrain controls allows maximum energy recovery with minimal friction braking. This dynamic interaction between the vehicle's brake and drivetrain systems also improves driveability.

(5) Power assist with electric machine

The electric machine is connected between the engine and transmission or between the transmission and the wheel. In the former, the electric machine can assist synchronization of the gear sets during the shift operation in the synchromesh transmission. The operating force becomes unnecessary, and the friction cones for synchronism are eliminated. Therefore, the gear shift mechanism in the synchromesh transmission becomes very simple. In the latter, the electric machine can assist power supply to the wheel during the shift operation in the synchromesh transmission, resulting in better driveability.

3.8 Future outlook

The system mentioned above is a concept, although some components and subsystems have been tested already. More detailed analysis would be conducted to demonstrate the magnitude of the efficiency gains by introducing all components and subsystems in a testing vehicle.

4. SUMMARY

A fuel efficient engine drivetrain control system was proposed which combines a lean burn engine with a supercharging, an exhaust gas recycle, an electric machine for power assist, and an electronically controlled trasmission. The smooth switching of power source, the lean burn control with supercharging, the smooth gear shift with exhaust gas recycle control and lean burn control, and the air-fuel ratio control by using an air flow meter were analyzed to attain better fuel economy and better driveability.

References

[1] Y. Ohyama, An Advanced Engine Drivetrain Control System, SAE Technical Paper Series No.970291, International Congress & Exposition,

Detroit, Michigan, February 24-27, 1997

[2] Hybrid Honda adds smooth power boost, WARD'S Engine and Vehicle Technology Update, p.2, November 1,1996

[3] Carb to test Mitubishi hybrid-electric vehicle, WARD'S Engine and Vehicle Technology Update, p.7, June 1, 1995

[4] Toyota explains its 70-mpg semi-hybrid, WARD'S Engine and Vehicle Technology Update, p.5, November 15,1995

[5] W. Kalkert, W.Adams, Future Powertrain Systems, AVL Conference "Engine and Environment" '94,Graz, Austria, June 16, 1994

[6] Y. Ohyama, An advanced engine drivetrain control system that improves fuel economy and lowers exhaust emissions, 5th International Congress, European Automobile Engineers Cooperation, Strasburg, 21-23 June 1995.

[7] Y. Ohyama, A new engine drivetrain control system, 29th International Symposium on Automotive Technology & Automation, Florence, Italy, 3-6 June 1996

[8] Y. Ohyama, A Fuel Efficient Engine Drivetrain Control System, 9th International Pacific Conference on Automotive Engineering, Bali, Indonesia, November 16-21,1997

[9] Y.Ohyama, A Fuel Efficient Hybrid Drivetrain Control System, Autotech '97, 4-6 November, 1997, Birmingham, U.K.

[10] Y. Ohyama, M. Fujieda, A new engine control system using direct fuel injection and variable valve timing, SAE Paper No.950973, 1995 SAE International Congress and Exposition, Detroit, Feburuary 27-March 2, 1995

[11] S. Nakahara, J. Mitzuda, Y. Sato, H. Yamnagihara, A study of Rapid Combustion with High Dispersed Fuel-Air Mixure under High Load Operation, 1997 JSAE Spring Convention, Paper No. 972496, Yokohama, Japan, May 1997

[12] N. P. Fekete, U. Nester, I. Gruden, J. D. Powell, Model-Based Air-Fuel Ratio Control of a Lean Multi-Cylinder Engine, SAE Paper 950846, International Congress and Exposition, Detroit, Michigan, February 27-March 2, 1995

[13] H. Machida, H. Itoh, T. Imanishi, H. Tanaka, Design Principle of High Power Traction Drive CVT, SAE Paper 950675, International Congress and Exposition, Detroit, February 27-March 2, 1995

[14] A. Norzi, G. Cuzzucoli, How Electronic Controls Make It Possible to Automate Conventional Transmission for Commercial Vehicles, FISITA'94 Technical Paper 945233 ,17-21 October 1994, Beijing

[15] A. Hedman, Synchromesh Transmissions with Power-Shifting Ability-Improved Truck Performance, SIA 9506A18, 5th International Congress, European Automobile Engineers Cooperation, Strasbourg, 21-23 June 1995

[16] Transmission Antonov: la serie en 1998, Ingenieurs de L'Automobile,novembre-decembre 1996, p.34-35

[17] Yoshishige Ohyama, Yutaka Nishimura, Minoru Ohsuga, Teruo Yamauchi, Hot-Wire Air Flow Meter for Gasoline Fuel-Injection System, 1996 JSAE Autumn Convention Proceedings No 965, October 4-6, Sapporo, Japan

[18] PCT Patent No. WO 90/06441, 14 June 1990

[19] S. Drakunov, G.Rizzoni, Y. Y. Wang, On-Line Estimation of Indicated Torque in IC Engines Using Nonlinear Observers, SAE Paper 950840, International Congress and Exposition, Detroit, Michigan, February 27-March 2, 1995

[20] D. E. Schenk, R. L. Wells, J. E. Miller, Intelligent Braking for Current and Future Vehicles, SAE Paper 950762, Interntional Congress and Exposition, Detroit, Michigan, February 27-March 2, 1995

Energy Regeneration of Heavy Duty Diesel Powered Vehicles

Matsuo Odaka, Noriyuki Koike
Traffic Safety and Nuisance Research Institute
Ministry of Transport, Japan

Yoshito Hijikata, Toshihide Miyajima
Hino Motors, Ltd.

ABSTRACT

The objective of this study is to improve fuel economy and reduce carbon dioxide emissions in diesel-electric hybrid automotive powertrains by developing an exhaust gas turbine generator system which utilizes exhaust gas energy from the turbocharger waste gate.

The design of the exhaust gas turbine generator was based on a conventional turbocharger for a direct-injection diesel engine.

Data from steady-state bench tests using air indicates about 50% of the turbine input energy can be converted to electric energy. Turbine generator output averaged 3 kW, while a maximum of about 6 kW was observed. Based on this data, we estimate that energy consumption in a vehicle could be reduced between 5% and 10%.

Engine tests were conducted under both steady-state and transient conditions. These tests revealed that optimal performance occurred under high-speed, high-load conditions, typical of highway or uphill driving, and that performance at iow-speed, low-loads was relatively poor.

The efficiency at low engine speeds could be improved by controlling the inlet flow to the turbine generator.

INTRODUCTION

In the automotive field, many effort has been made to reduce carbon dioxide (CO_2) emission by reducing fuel consumption with combustion improvement of the engine or reducing power train and driving resistance.

Thermal efficiency has been pursued to almost its maximum in the case of automotive diesel engines and further improvement of fuel consumption by means of engine modification seems to be very difficult.

However, only 20 to 30% of total fuel energy consumed is used for net engine power output and the remainder was wasted. To achieve the notable fuel consumption improvement and consequent CO_2 reduction, recovering these wasted energies, such as kinetic energy at deceleration and exhaust gas heat energy etc., and converting (regenerating) them to the energy useful for vehicle driving source is required.

In this effort, an exhaust heat energy regeneration technique has been experimentally studied with an exhaust turbine generator system.

APPROACH

Today, energy regeneration systems of diesel powered vehicles where a part of the wasted energy is regenerated and used as auxiliary power source are made practicable in Japan as pressure storage type hybrid systems and a diesel-electric hybrid system (**HIMR**: Hybrid Inverter controlled Motor & Retarder System)[1].

However, these systems regenerate only decelerating energy mechanically or electrically and uses it as auxiliary power source. Therefore, these system can fulfill its function only under driving conditions with high in frequency of acceleration and deceleration and may suitable under urban driving conditions which has relatively low average speed.

This study aims at the improvement of the total energy consumption efficiency by regenerating wasted energies mainly at high speed and heavy load engine operating regions such as highway or long uphill driving and adding them to the existing hybrid system.

In this study, we consider regenerating exhaust heat energy to electric energy, which is the most convenient energy to use, and then applying them to HIMR system.

A turbine generator system, in which a generator is driven by a exhaust power turbine, was developed for exhaust energy regeneration and conversion to electric energy. At first, amount of the energy which can be
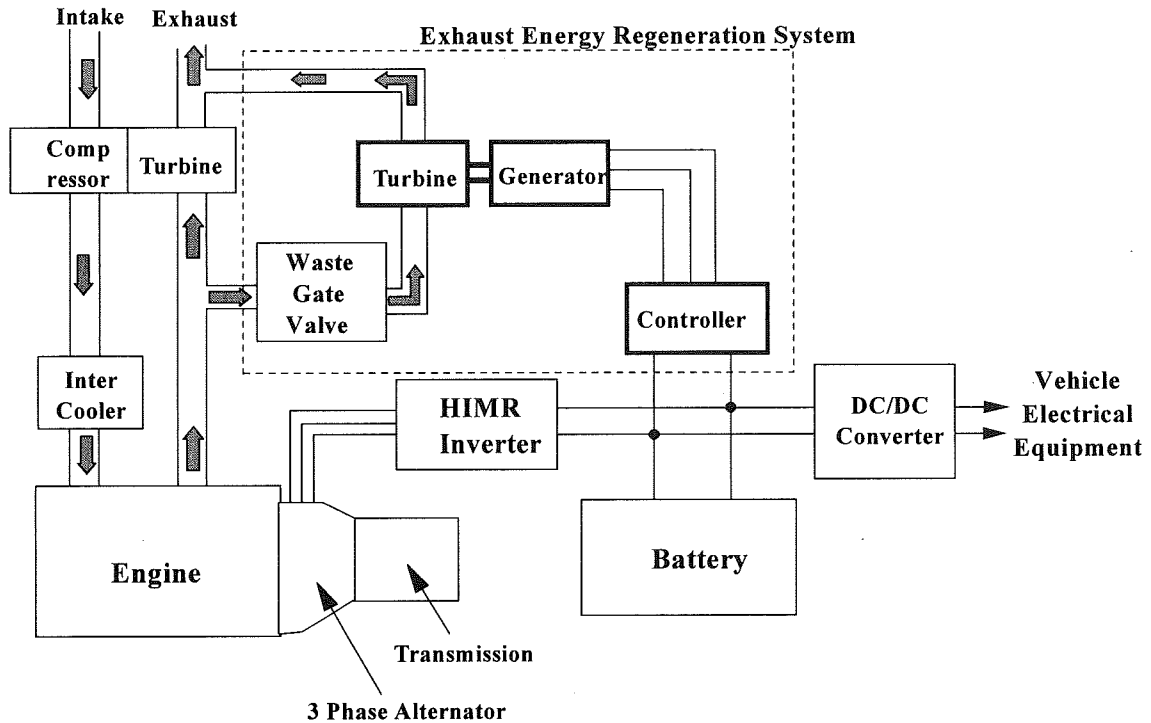
Fig.1 Exhaust Energy Regeneration System

regenerated was theoretically studied for a typical diesel engine and the basic estimation of possible regenerated power has been done. Then the performance target of a turbine generator system was settled based on the estimation and the system has been designed and made for trial followed by the component test for performance evaluation.

Finally, the system was connected to a complete engine system for evaluating the energy regeneration effect under actual driving conditions.

DESIGN AND DEVELOPMENT OF THE EXHAUST ENERGY REGENERATION SYSTEM

OUTLINE OF THE EXHAUST ENERGY REGENERATION SYSTEM

Since this system should not affect the engine basic performance, regeneration of exhaust gas heat energy from a waste-gate valve of a turbo charged diesel engine was considered.

Fig.1 shows the schematic of the energy regeneration system. An exhaust gas bypass valve (waste gate valve) is located between the engine and the turbo charger turbine and the bypassed exhaust gas is introduced to a power turbine which is directly connected with an alternative current generator. The bypassed exhaust gas drives the power turbine which drives the generator. Then, the exhaust heat energy is converted to electric energy. The system controller governs the control of the generated power and the conversion of AC to DC for charging batteries.

ESTIMATION OF ENERGY REGENERATION PERFORMANCE

Amount of a turbine power generated by combustion gas was estimated as following.
The turbine work L is generally indicated as the following equation.

$$L = Gg \cdot Cp \cdot T_{vt} \cdot (1 - \frac{1}{\pi_t^{(\kappa-1)/\kappa}}) \cdot \eta$$

Where

Cp : specific heat at constant pressure = 0.28

κ : ratio of specific heat = 1.36

T_{vt} : turbine inlet gas temperature

π_t : expansion ratio

Gg : turbine gas flow rate

η : turbine efficiency

Fig.2 shows the estimation results of turbine power outputs with assumptions of turbine efficiency η =65% , and expansion ratio π_t =2.0. The figure indicates that about 7 kW could be obtained as maximum turbine output under the turbine inlet gas temperature of 600

FMC 1016

deg.C and the gas flow rate of 4 kg/min.

Fig.3 shows the estimated turbine power at different engine operating points of a direct injection diesel engine with 8000 cm³ swept volume based on measured exhaust temperatures, expansion ratios and gas flow rates from the waste gate. As shown in the figure, regained turbine power is very little at low engine speed regions because of lower gas flow rates and temperature. On the contrary, it goes up rapidly at high speed and heavy load regions. Thereby this energy regeneration system may work effectively at high speed and heavy load regions.

DESIGN OF TURBINE GENERATOR SYSTEM

To evaluate this concept experimentally, a turbine generator system was developed based on the above estimates.

Generator type

Generally speaking, a permanent magnet type or a crow pole type is used as an high speed generator. Although a crow pole generator is more suitable for very high speed operations, the size and weight may become large due to its complicated mechanism. Thereby, permanent magnet type was selected for this system due to its high generating efficiency and potential for smaller size and lower weight.

Table 1 shows the projected specification of the generator. The normal operating speed range is 50,000 to 80,000 rpm and the continuous maximum output is aimed at 6 kW with the estimation of 90% in energy conversion efficiency .

Power turbine

A turbo charger turbine for a diesel engine was applied as the power turbine and a variable nozzle was added for optimization of the system efficiency. At first

Fig.2 Estimation of Turbine Output Power
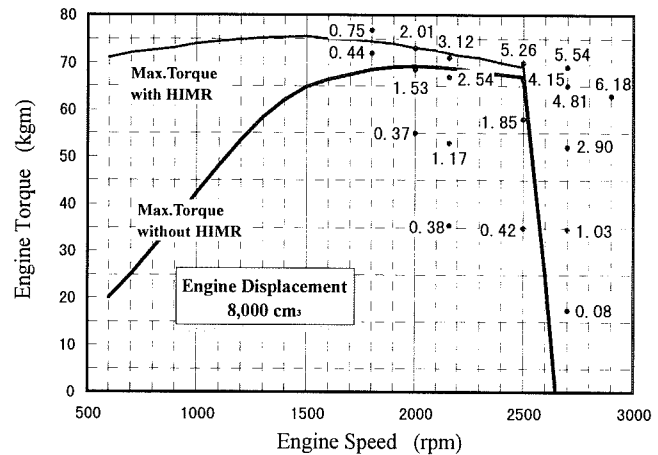
Fig.3 Estimated Turbine Power
at Different Engine Operating Points

Table 1 Generator Specification

Generator Type	Three Phase Permanent Magnet Type Synchronous Generator
Rating Power Output Voltage Number of Poles Speed Rated Time	6kw (80,000rpm) AC200V 2 80,000rpm (1333Hz) Continuous
Operating Speed Range	50,000 to 80,000rpm
Over Speed Max.	84,000rpm (105%)
Bearing	Ball Bearing
Weight	Approximately 10kg
Size	115mm φ × 170mmL

Fig.4 Prototype Turbine Generators

Altanator Output I × V [kW]
Controller Output $I_0 × V_0$ [kW]
System Efficiency $I_0 × V_0/Wa × 100$ [%]
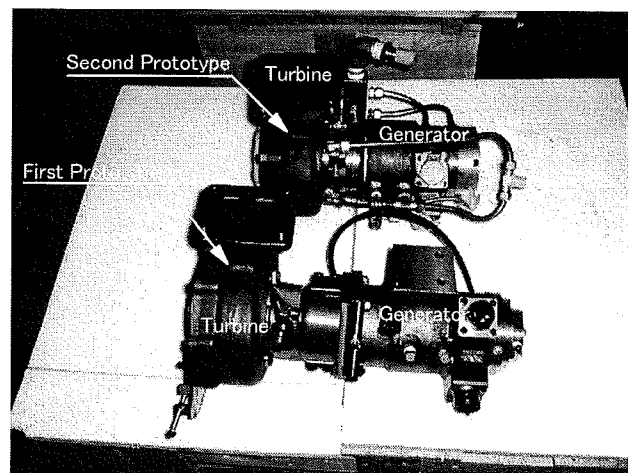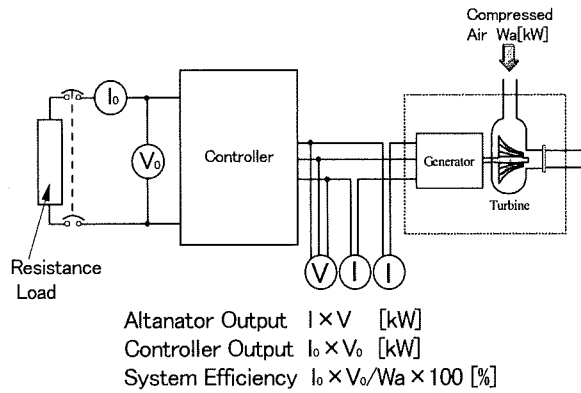
Fig.5 Schematic of Component Test

prototype, a coupling was used to connect the generator and the turbine shaft. However, increase in vibration due to eccentricity between both shafts was observed at a spinning test and the second prototype in which the turbine shaft was integrated with the generator shaft was made. Fig.4 shows both prototypes. The generator part is smaller at the second prototype. A water cooling system is used for cooling of the field coil in the generator.

EXPERIMENTAL RESULTS AND DISCUSSION

COMPONENT PERFORMANCE TEST

Component performance tests have been conducted to evaluate the steady state performance of the prototype turbine generator system. Fig.5 shows the test system. At the test, compressed air from an high pressure air source was used instead of real automotive exhaust gas for driving the power turbine.

The generator current was adjusted with a controller and a resistance load was used for absorption of generated electric power.

The generator output power was observed according to the turbine speed and the generator load current. The voltage and the current was measured between the generator and the controller and between the controller and the resistor to calculate output power and efficiency as indicated in the figure.

Fig.6 shows measured results of the controller output power versus turbine speeds. The maximum output was about 6 kW at 80,000 rpm and this is close to the estimated value. The efficiency of the generator itself varied with load currents and turbine speeds though, it was 70% or higher at lowest as shown in Fig.7.

The measured over all system efficiency was shown in Fig.8. As shown in the figure, about 50% of the turbine input energy can be converted to electric energy under wide operating ranges.

Based on these results, 5 to 10% of energy consumption improvement may be expected from the calculation of energy regeneration effects with an assumption that
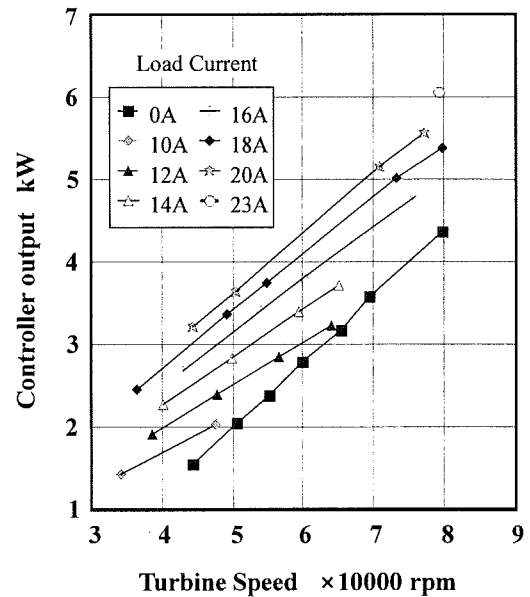
Fig.6 Controller Output Power versus Turbine Speeds
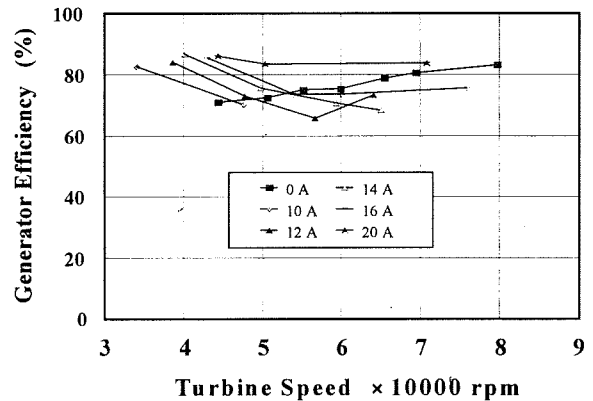
Fig.7 Generator Efficiency versus Turbine Speed
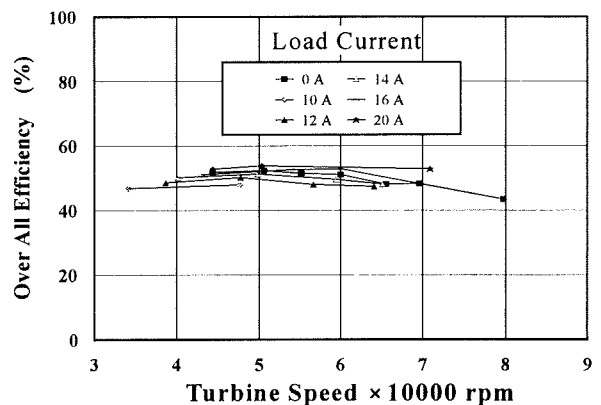
Fig.8 Overall System Efficiency
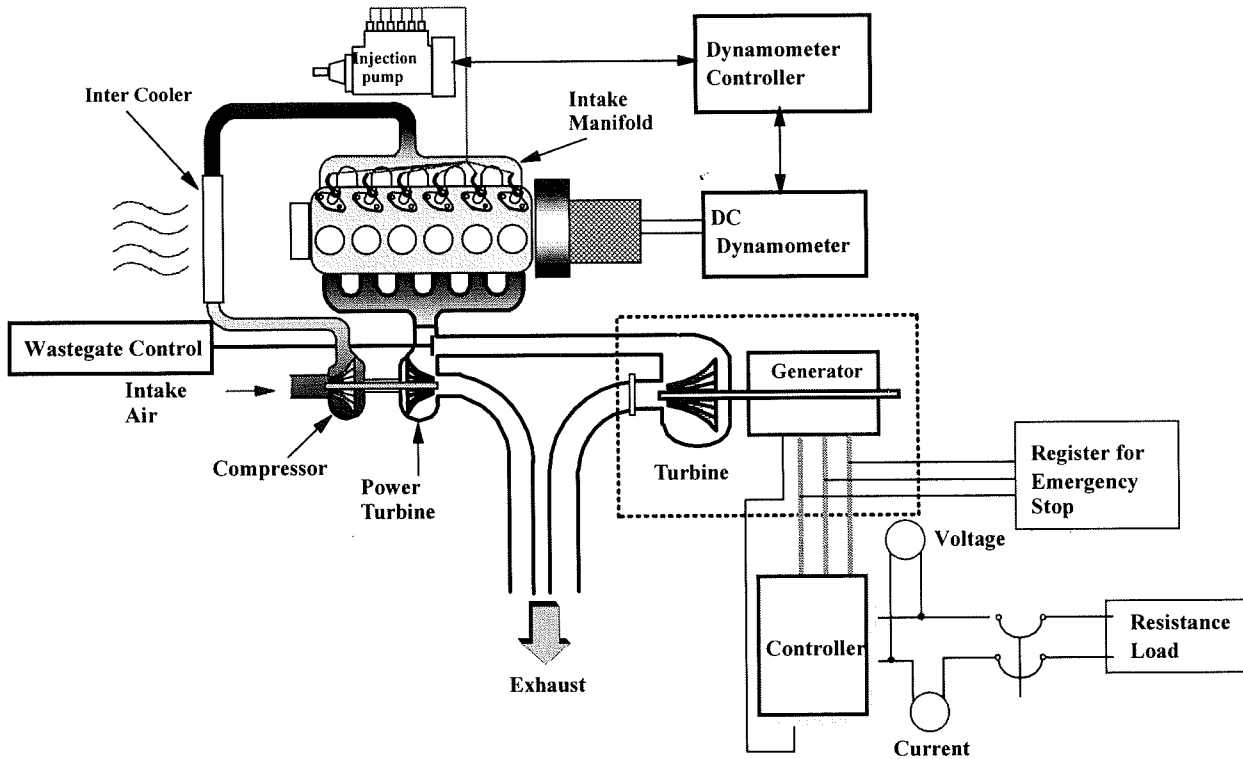
Fig.9 Schematic of Engine Dynamometer Test System
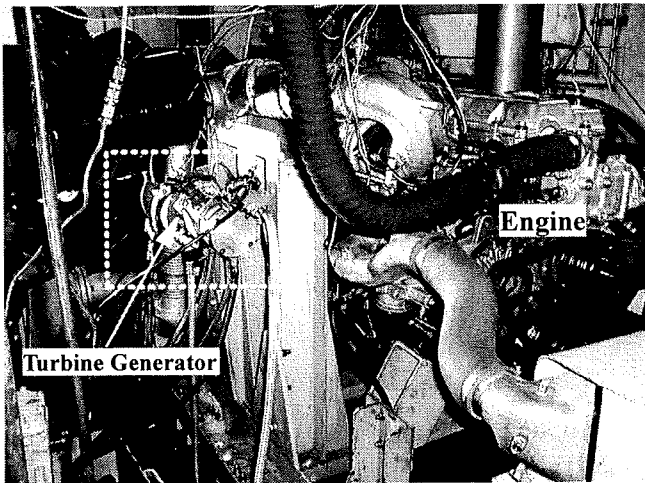
Fig.10 Turbine Generator and Test Engine
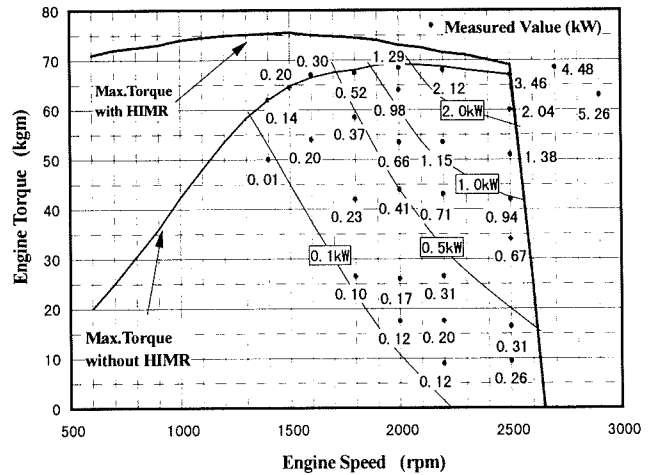
Fig.11 Steady-state Engine Test Result

average exhaust energy regeneration electric power is 3 kW under various driving conditions

ENERGY REGENERATION EFFECT AT THE ENGINE DYNAMOMETER TEST

The prototype turbine generator system was then connected to a turbo charged diesel engine on a dynamometer test bed to evaluate exhaust energy regeneration performances.
Fig.9 shows the schematic of the engine test system.

The test engine was a turbo charged direct injection diesel engine with 8,000 cm^3 in displacement.
As shown in Fig.10, the turbine generator was located separately from the engine and the engine exhaust gas was introduced to the power turbine from the waste gate of the turbo charger with a flexible pipe. The generated power was absorbed by resistance load.
The performance evaluation has been conducted not only under steady-state but also transient operations which represent the engine behavior under actual driving conditions.

Table 2 Characteristics of Engine Operating Pattern

Name of Pattern	Operating Time (sec)	Equivalent Driving Distance (km)	Average Speed (km/h)	Ratio of 4 mode (time %)				Total Work (kWh)
				Idling	Acceleration	Cruising	Deceleration	
F20	789	4.726	21.56	34.7	24.9	17.7	22.7	5.79
F40	806	8.870	39.32	13	25.6	38.4	23	8.68
HW1	766	15.290	71.86	2.7	7.8	82	7.5	14.93
High speed Mode	725	Max. Engine Speed 2500rpm	Max. Engine Torque 65kgm	0	0	100	0	19.92

Steady state test results

Fig.11 shows results of regenerated electric power measurements under various engine operating points. The maximum output was gained at a point of engine full load with 2900 rpm in engine speed and was about 5.3 kW. This value was about 85% of the estimated value as shown in Fig.3 and other measured values were also lower than the estimates in most operating points. This may be caused by lowered exhaust temperature due to the distance between the waste gate and the turbine inlet. As shown in Fig.10,

1 kW or higher output was regenerated at the regions of over 2000 rpm in engine speed and 1/2 or higher in engine load. The experiments suggest that this system may be effective under driving conditions where relatively heavy load engine operating regions are mainly used.

On the contrary, energy regeneration effects at low-speed, low-loads were little because the exhaust energy is not so large at these operating regions and most of the exhaust energy is consumed by the turbo charger.

Transient engine test results

To evaluate exhaust energy regeneration effects under actual driving conditions, transient engine tests were conducted under 4 different engine transient modes based on vehicle driving patterns with different average vehicle speeds.

Table 2 shows the characteristics of each engine operating pattern. Among these patterns, F20 and F40 are constructed from actual vehicle driving patterns with average speed of 20 and 40 km/h respectively and represents urban driving conditions. HW1 represents the engine conditions under highway driving conditions and High Speed Mode is a combined operating pattern with highway and long distance uphill driving and the
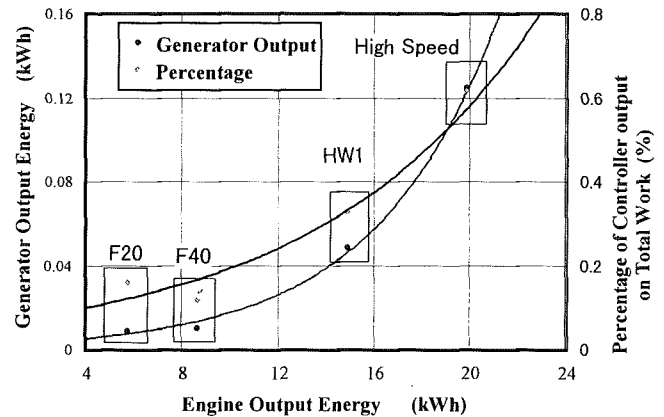
Fig.12 Regenerated Energy at Transient Test

total engine work is the highest among these four patterns. Relations between the total required engine work and total regenerated electric energy under the driving of each pattern are shown in Fig.12. Regenerated electric energy goes up almost exponentially according to the increase in required engine work.

The percentage for engine work shows the same tendency also. The highest regeneration energy was gained at High Speed Mode pattern and it was 0.125 kWh in total and 0.6% of required engine work.

Fig.13(a),(b),(c),(d) show frequency distribution of engine operating regions under the tested each engine operating patterns. At F20 and F40, the engine was operated at mostly low engine speed regions and the amount of the regeneration energy was very small because sufficient regeneration could not be expected at these regions as indicated by the steady state test.

In the case of HW1, the engine was mostly operated in

16
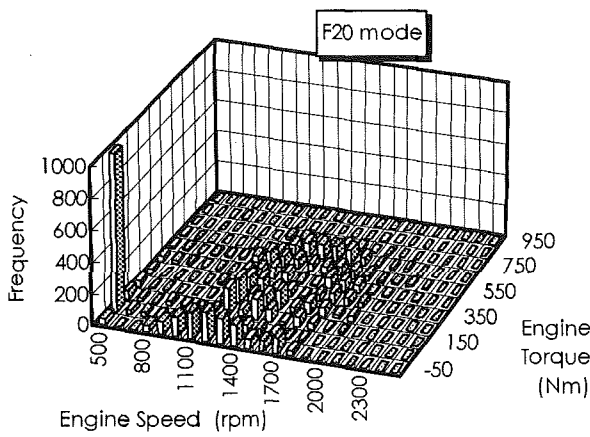
Fig.13(a) frequency distribution of engine operating regions under F20 Engine Operation Pattern
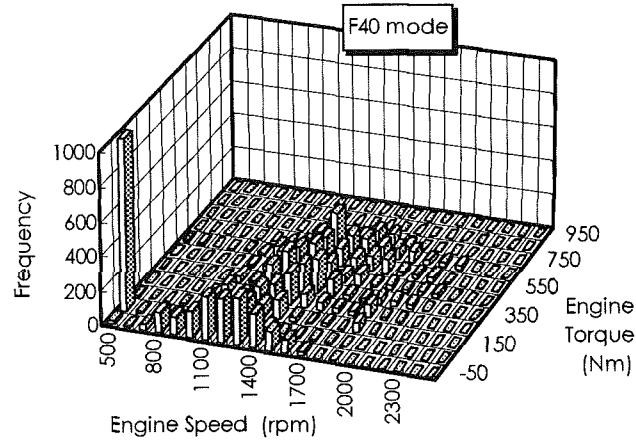
Fig.13(b) frequency distribution of engine operating regions under F40 Engine Operation Pattern
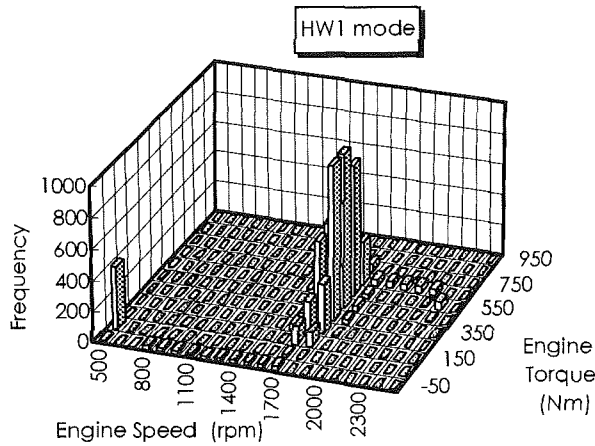
Fig.13(c) frequency distribution of engine operating regions under HW1 Engine Operation Pattern
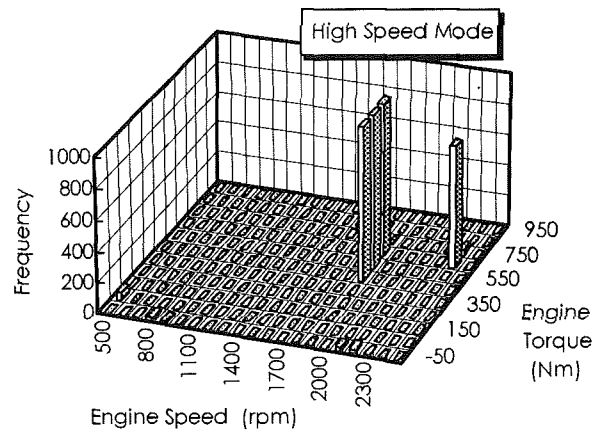
Fig.13(d) frequency distribution of engine operating regions under High Speed Mode Engine Operation Pattern

the vicinity of 1800 rpm where regenerating power starts to go up and thereby the energy regeneration effect went up from the case of F20 or F40.

At High Speed Mode, the engine operating regions were limited to heavy load regions of over 1900 rpm and then it is considered that this is the reason of increase in regenerated energy at this case.

Then, based on these results, as the higher the frequency of high speed and heavy load engine operations, the higher regenerating effect of the turbine generator system can be obtained and therefore it is also experimentally clarified that the exhaust heat energy regeneration will be suited for highway or long distance uphill driving.

EVALUATION OF THE EXHAUST HEAT ENERGY REGENERATION

A technical possibility for converting exhaust heat energy to electric energy was assured by this study. However, in spite of the 50% in overall efficiency was obtained by the component test, exhaust energy regeneration efficiency of the engine test under transient conditions was much lower than expected. For this reason, it can be pointed out that the matching with the engine was not good at low speed and light load regions. If the generating efficiency at lower engine speed regions were improved by controlling the exhaust gas flow to the turbine, the total regeneration efficiency could be increased.

The overall efficiency of the turbine generator itself is 50% or higher and then, by optimizing the system particularly at low engine speed regions, 5 to 10% reduction of energy consumption could be possible.

CONCLUSION

1. A vehicle energy regeneration system where exhaust energy was regenerated and converted to electric energy has been developed. The overall efficiency of the system was over 50% under wide range of the operating points in steady-state tests.

2. At the engine test combined with a heavy duty diesel engine, the energy regeneration efficiency under various transient driving conditions was much lower than the component test results. However, the improvement of the total system efficiency could be possible if the generating efficiency at lower engine speed regions were improved by controlling the exhaust gas flow introduced into the turbine.

3. Based on an optimized system, we think that energy consumption in a vehicle could be reduced between 5% and 10% and prospect is obtained for improving fuel consumption and consequent CO_2 reduction from diesel vehicles by adding the regenerated electric energy to the diesel - electric hybrid system for utilizing wasted energy.

REFERENCES

1) Yamamoto, Sekiya, Suzuki: Application of hybrid inverter controlled motor & retarder system to dust gathering vehicles EVS-11 Florence SYMPOSIUM PROCEEDINGS

Development of the Hybrid/Battery ECU for the Toyota Hybrid System

Akira Nagasaka, Mitsuhiro Nada, Hidetsugu Hamada, Shu Hiramatsu, Yoshiaki Kikuchi
Toyota Motor Corporation

Hidetoshi Kato
Denso Corporation

ABSTRACT

For energy saving and global warming prevention, Toyota has developed Toyota Hybrid System (THS) for mass-produced passenger cars, which achieves drastic improvement in fuel efficiency and reduction in exhaust emissions compared to conventional gasoline engine cars.

The THS has two motive power sources which engage depending on driving conditions. It's power is supplied either from an engine (controlled by the engine ECU) or an electric motor (controlled by the motor ECU) which is powered by a high-voltage battery (monitored by the battery ECU). These ECUs are controlled by a hybrid ECU. Each ECU has been developed with a fail-safe system in mind, to ensure driver safety in case of vehicle breakdowns.

Among these ECUs, this paper reports particularly on the newly introduced ECUs: hybrid ECU and battery ECU. In the development of these ECUs, special attention was focused on fail-safe performance.

INTRODUCTION

Reducing carbon dioxide (CO_2) emissions to alleviate global warming has become an international issue in recent years. From an automaker's point of view, the most important factors in reducing CO_2 emissions are improving fuel economy and achieving cleaner exhaust emissions.

Toyota has developed a highly advanced hybrid system for powering mass-produced passenger cars. The THS uses a gasoline engine, electric motor, and electric generator to achieve nearly twice the fuel efficiency of conventional gasoline engine cars and significantly reduce exhaust emissions. The THS has two motive power sources which engage depending on driving conditions. An improved efficiency gasoline engine provides the main power to drive the wheels, as in conventional automobiles. Drive power can also be supplied by an electric motor, which derives its electricity from the nickel-metal hydride battery and an electric generator.

This paper reports on the development of the hybrid electronic control unit (ECU) , which gives commands to the ECUs that directly govern the hybrid drive system, and of the battery ECU, which monitors the charging/discharging state of the battery, particularly the development processes that focus on the fail-safe mechanism.

SYSTEM OUTLINE

Before we introduce the development processes of the hybrid ECU and the battery ECU, we will explain the construction of this hybrid control system and summarize of its operation.

As shown in Fig.1, the THS is driven by both an engine and a motor, with the engine providing the primary power. The system divides the engine's power with a power split device that uses a planetary gear to send power to both the drive shaft and the generator. Some of the electricity from the generator drives the motor; the remainder, after being converted to DC by an inverter, is stored in the battery.
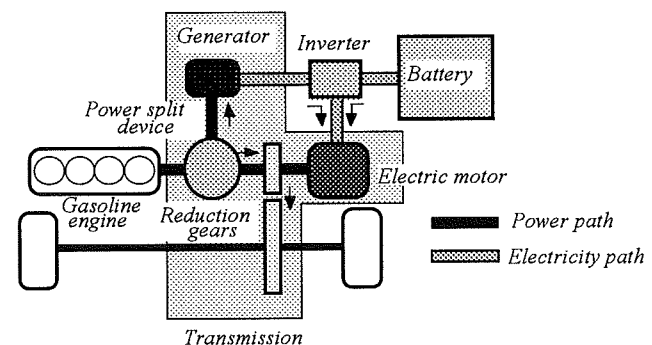
Fig.1 Toyota Hybrid System

With an electronically controlled continuously variable transmission and an electric motor that assists the engine, the THS vehicle achieves smooth acceleration and deceleration, as well as excellent response. In particular, initial acceleration takes advantage of the motor's characteristics —high torque at low speeds. For maximum acceleration when the throttle is fully opened,

19

power from both engine and motor drives the vehicle, with energy from the battery boosting the motor's output. (Fig.2)
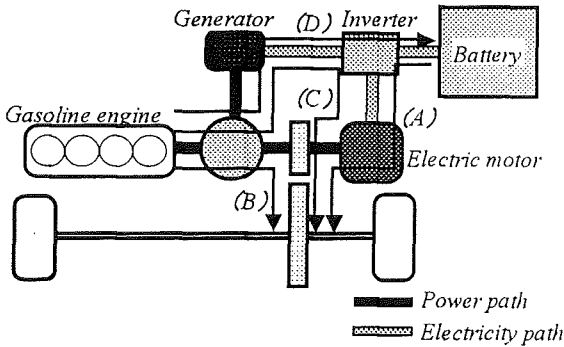
Fig.2 Operating Conditions
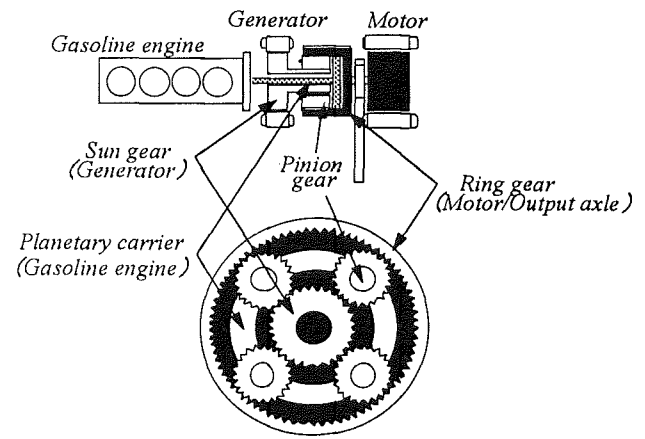
Fig.3 Power Split Device

When starting out, driving at extremely low speeds, going down a moderate slope, or operating in other conditions in which the engine is not at peak efficiency, the engine shuts down and the motor drives the vehicle.(A)

For normal driving conditions, the power split device separates the engine power into two paths. One path drives the wheels.(B) The other drives the generator to produce electricity for the motor, which provides additional driving force to the wheels.(C) The system controls the ratio of power to each path for maximum efficiency.

During full throttle acceleration, the battery also supplies power, boosting the motor's output.(A)

During deceleration and braking, the inertia of the wheels turns the motor, which then acts as a generator. The recovered electricity is stored in the battery.(A) The battery is regulated to maintain a constant charge. When the battery gets low, the generator routes power to recharge it.(D)

And the engine automatically shuts off when the vehicle is stopped.

THS TRANSMISSION (FIG.1)

The THS transmission consists of the power split device, the generator, the motor, and reduction gears. The power split device divides the power from the engine, sending one portion to the drive shaft, and the other to the generator. In other words, engine power is transmitted to the drive shaft via a mechanical path and an electrical path. The THS transmission also functions as an electronically controlled continuously variable transmission by smoothly adjusting the speed of the engine, generator, and motor when accelerating or decelerating.

The power split device uses a planetary gear.(Fig.3) The rotating shaft of the planetary carrier is connected to the engine, and uses a pinion gear to transmit power to the outer ring gear and the inner sun gear. The shaft of the ring gear connects directly to the motor and to the drive shaft through reduction gears, driving the wheels. The shaft of the sun gear connects to the generator.

The following graph (Fig.4) shows how the engine, generator, and motor operate under different condition.

The three vertical lines in the diagram show the shafts in the planetary
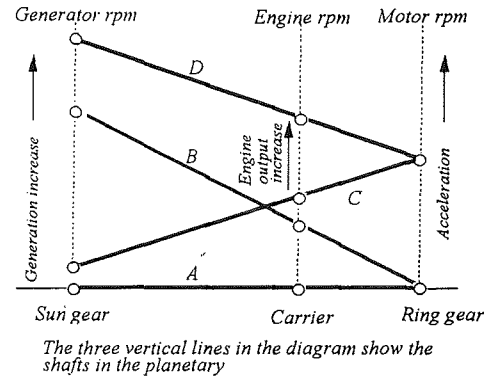
Fig.4 Power Interaction Diagram

When the vehicle is stopped, the engine, generator, and motor are stopped.(A) The generator acts as a starter to crank the engine. After the engine starts up, the generator begins to produce electricity, operating the motor, which supplies power for the vehicle to start out.(B)

For normal driving conditions, the engine supplies enough power, so there is virtually no need to generate electricity.(C)

As the vehicle accelerates from cruising speeds, engine speed increases, the generator produces electricity, and the motor sends additional power to the drive shaft to assist the acceleration.(D)

The system can change the engine speed by controlling the generator's revolutions. And some of the engine's output is transmitted to the motor via the generator as supplemental power for acceleration. This means that the system does not need a conventional transmission.

REGENERATIVE BRAKING SYSTEM (FIG.5)
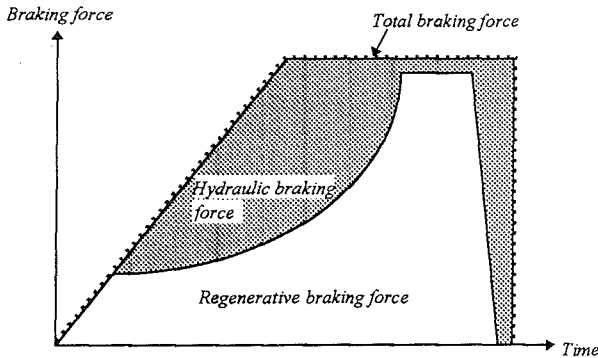
Fig.5 Regenerative Braking System

When the vehicle slows down, either by engine braking or by applying the brakes, the motor acts as a generator and converts kinetic energy into electricity, which is stored in the battery. This regenerative braking system is especially useful in the repetitive acceleration and deceleration of city driving, and is a very effective method of recovering energy. When the driver applies the brakes, the hydraulic and regenerative braking systems are controlled in a cooperative manner to maximize energy regeneration.

ADVANCED SYSTEM CONTROL AND ECU SCHEMATIC(FIG.6)
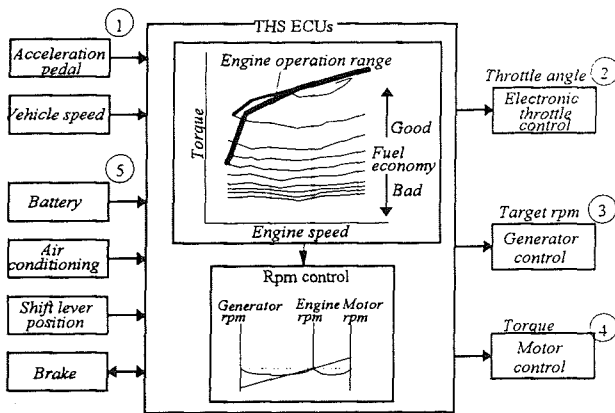
Fig.6 THS Control System

The THS calculates the desired operating condition and the existing operating condition, then the system accurately controls the engine, motor, generator, battery, and other components in real time.

By matching engine speed to operating conditions and the electronic throttle opening, the THS ECUs keep the engine operating in a predetermined high torque range, maximizing fuel economy.

When the driver presses the accelerator pedal ①, the electronic throttle opens in response to a signal from the ECU ②; engine speeds are also controlled ③. At the

same time, the ECU determines the allocation of engine power between the drive shaft and the generator ④. The carefully controlled combination of the engine's direct drive force and the motor's drive force propels the vehicle.

If the battery gets low, the ECU commands the engine to provide output to the generator to recharge it ⑤.

Performance of the THS vehicles is determined by the sum total of the engine's direct driving force, and the driving force of the motor, powered by the generator and battery.

At low vehicle speeds, this overall drive force comes mainly from the motor. With the power split device functioning like an electronic continuously variable transmission, the vehicle achieves much smoother acceleration and deceleration performance than vehicles with conventional engines.

ECU CONFIGURATION AND CONTROL.

In this section, we will describe the ECU configuration that can effect the control of this hybrid system. As shown in Fig.7, this system consists of the following five ECUs: the motor ECU and the engine ECU that control the motive force (electrical motor and engine), the brake ECU that controls the brakes, the battery ECU that monitors the battery, and the hybrid ECU that controls these ECUs. An outline of the control of the ECUs is given below.
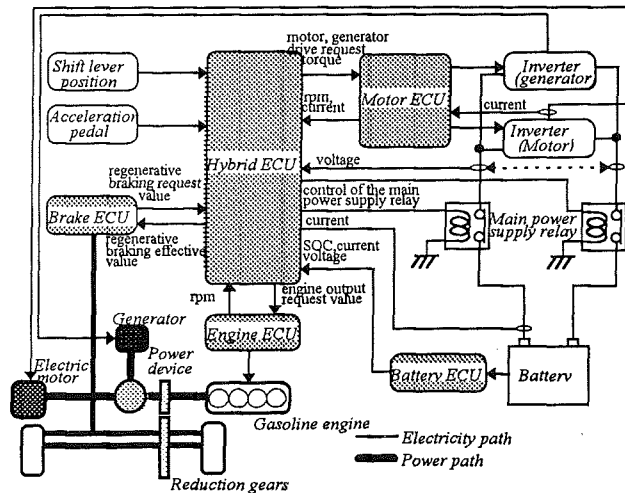
Fig.7 ECU Schematic

1.HYBRID ECU

This ECU controls the drive force of the hybrid vehicle by calculating the engine output, motor drive torque, and the generator drive torque based on information such as the accelerator opening and shift position. Request values are sent to the ECUs.

2.MOTOR ECU

In accordance with the drive output value requested by

the hybrid ECU, the motor ECU controls the inverters of the generator to output a three-phase DC current in order to generate the desired torque. An electrical feedback control (causes the motor to generate torque by feeding back the current and by controlling the amount and the phase of the current).

3.ENGINE ECU

This ECU controls the electronic throttle in accordance with the engine output value requested from the hybrid ECU, as well as various conditions such as water temperature (similar to those of the conventional gasoline engine control).

4.BRAKE ECU

By coordinating the braking effort with the regenerative braking that is executed by the motor, this ECU controls in such a manner that the entire brake force becomes equal to that of a vehicle that is equipped with an ordinary hydraulic brake system. This brake system is one in which the regenerative brake system has been added to the conventional hydraulic brake system. (Fig. 7).

5.BATTERY ECU

This ECU monitors the charging state of the battery.

THS SAFETY FEATURES

The THS incorporates safety features to avoid situations like unintended acceleration and braking, or significant current leakage from the high voltage system. Four types of fail-safe functions are provided, and each of them are described below.

1.SHUTTING OFF THE HIGH-VOLTAGE POWER SUPPLY(FIG.8)
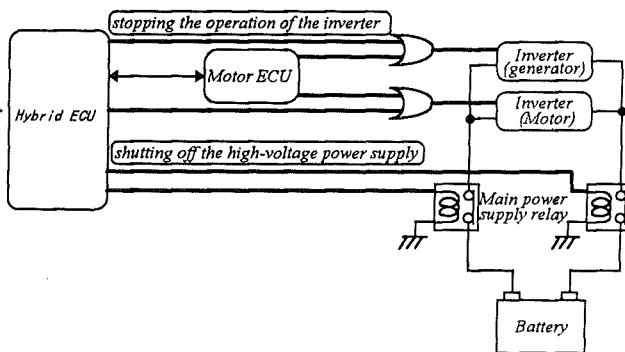
Fig.8 Fail-Safe

The hybrid ECU turns off the main power supply relay to cut off the energy supplied by the battery to the motor and by the generator to the battery, thus preventing the drive force from being generated by the battery and protecting the battery from abnormal conditions. This shut-off state is maintained until the ignition switch is turned OFF. In order for the power to be reinstated, the ignition key must be re-inserted and the area of the malfunction must revert to its normal state. This action is applicable to a malfunction that could cause danger if a return to normal vehicle operation is allowed.

Because the system cannot be stopped if the main power supply relays become fused, the following measures are taken to prevent the relays from becoming fused:
- Zero current is applied to the relays when activating (for connecting and disconnecting) the relays.
- A relay is provided for both the positive and negative sides of the battery, and they do not activate simultaneously.
- During their activation, the relays are checked for fusing, and if a malfunction is detected, the relays are prohibited from connecting.
- If a malfunction is detected in the relay drive circuit, the relays are prohibited from connecting.
- When the microprocessor is reset, a shut-off command is output to prevent the power supply from remaining in the connected state.
- By turning OFF the ignition key, the negative-side relay is shut off through a hardware electronic circuit.

2.STOPPING THE OPERATION OF THE INVERTER(FIG.8)

This action is applicable for malfunctions that are minor and the system can be permitted to revert to its normal operation. It is a method that shuts off the drive force that is provided by the inverter to the axle. The shut-off command is output by the hybrid ECU to the motor ECU. However, the inverter could shut off by itself as a means of self protection; even in such a case, a shutoff command is output by the ECU. If a shutoff command is output, the torque command that is output by the hybrid ECU to the motor ECU simultaneously becomes zero.

Two systems of microprocessors, the hybrid ECU and the motor ECU, command the stoppage.

3.STOPPING THE ENGINE

This action stops the engine in case of no electrical generation due to a malfunction in the engine system or in the generator system. This action is maintained until the ignition key is turned OFF.

4.STOPPING THE REGENERATION BRAKING

This action is executed in order to specify brake control only to the hydraulic brake system in case it is not possible to coordinate regenerative braking. This action is canceled after it has been verified that the system has returned to normal.

HYBRID ECU

Before designing our safety features, we performed an FTA (Fault Tree Analysis) on the entire system and the ECUs. Through the FTA, we identified the parts that could cause problems, to which we added a monitor or fail-safe mechanism. In this section, we will describe the hybrid ECU, which comprehensively controls the ECUs, particularly the development processes that focus on the

22

fail-safe mechanism.

1.CONDUCTING FTA ON ECU AND DETERMINING APPLICABLE PARTS

As mentioned earlier, in the hybrid system, the drive system is controlled directly by other ECUs. Therefore, as for the hybrid ECU, it is extremely important that the command (request) values to those ECUs are correctly calculated and transmitted to the ECUs. Therefore, we conducted an FTA on this aspect. As a result of this analysis, the items given below have been brought out as the most important particulars. Because the detection of leakage current from the high voltage system is delegated to the battery ECU, the description below describes the four particulars. (Fig.9)
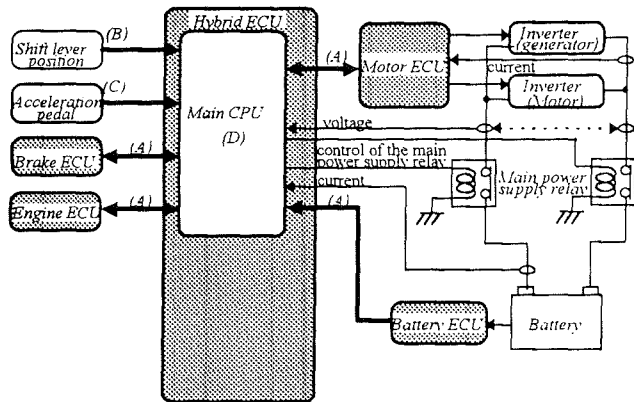
Fig.9 Hybrid ECU

(A)Malfunction in transmission between ECUs
(B)Malfunction in the shift sensor system
(C)Malfunction in the accelerator sensor system
(D)Malfunction in the CPU that governs control (hereafter called "main CPU")

2.MALFUNCTION DETECTION AND FAIL-SAFE FUNCTION FOR EACH ITEM.

In terms of the particulars listed in section 1, this section describes the methods for detecting malfunctions and the fail-safe actions to be taken.
(A)MALFUNCTION IN THE COMMUNICATION BETWEEN ECUS
The data communication between the ECUs is implemented through a handshake system that uses serial communication.

The communication cables adopt a differential method that increases the noise margin against electrical noise.

The methods (framing error, sum or mirror check error, periodic communication) are used to detect malfunctions, not only malfunctions of the communication cables, but also the corruption of communication data due to electrical noise and the like.

Fail-safe is given below:
①Malfunction in communication with the motor ECU
As mentioned earlier, the motor ECU controls the motor and the generator. As such, because the motor

ECU takes direct control of the driving of the vehicle, the vehicle cannot be driven if the communication with the ECU malfunctions. Therefore, this action stops the operation of the motor and the generator's inverter.
②Malfunction in communication with the engine ECU
Ordinarily, the hybrid ECU outputs a power request to the engine ECU, and in accordance with this request, the engine ECU controls the electronic throttle. At that time, the control of the engine rpm is carried out by the hybrid ECU, which controls the rpm of the generator.

In the case of a communication malfunction, the hybrid ECU would not be able to monitor the engine's drive force, and thus cannot distribute the drive force. For this reason, the engine's drive force is applied only to the generator, and the driving of the axle is delegated only to the motor. At this time, the engine rpm is controlled by the engine ECU to a level that is appropriate for the vehicle speed.
③Malfunction in communication with the brake ECU
In the case of a communication malfunction, the brake ECU will not be able to receive the regenerative braking execution value from the hybrid ECU, and thus will not be able to execute a command to the hydraulic brake system. For this reason, if a communication malfunction occurs, regenerative braking is prohibited and the brake ECU controls the brakes using only the hydraulic brake system.
④Malfunction in communication with the battery ECU
In the case of a communication malfunction, the ECU will not be able to receive the discharge request value, and if it continues to execute control, the possibility of overcharging or over discharging becomes great. For this reason, if a malfunction occurs, the vehicle is driven under a control strategy that does not involve the charging or discharging of the battery.
(B)MALFUNCTION OF THE SHIFT SENSOR
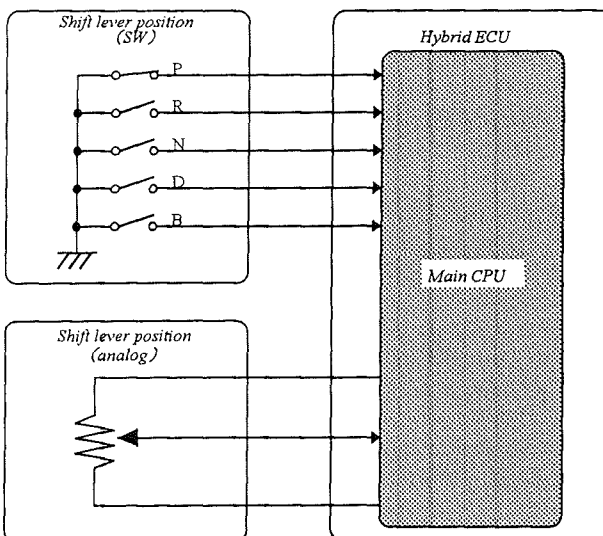
Fig.10 Shift Lever Position 1

In the THS, the step-less shifting and the vehicle's forward/reverse movement are controlled by planetary gears. For this reason, the shift position is not determined through the use of a conventional mechanical linkage,

but through the use of a shift-by-wire system. The shift sensor's electrical signal directly becomes the shift position that is used by the control. For this reason, we believed that the shift-by-wire system is particularly important for the hybrid system, and thus adopted a multiplex system (Fig.10).
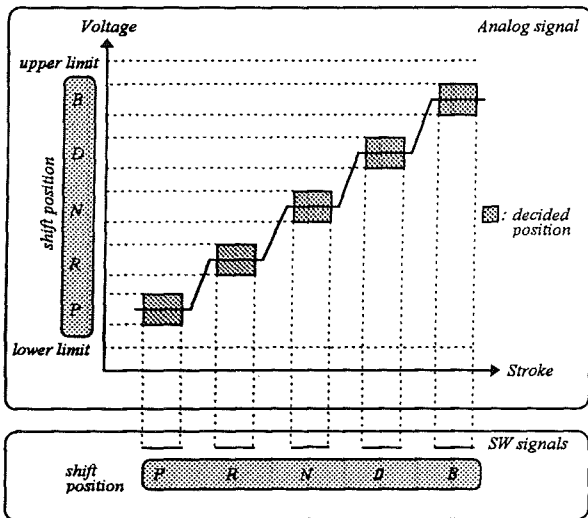
Fig.11 Shift Lever Position 2

Fig.12 Accelerator Sensor 1

Fig.13 Accelerator Sensor 2

As shown in Fig.10 and 11, the shift-by-wire system consists of 5 switch signals (P, R, N, D, B) and 1 analog signal. The shaded portion in Fig.11 shows a state in which the shift positions of the signals of the 2 systems match. Ordinarily, if the driver releases his/her hand away from the shifter, the shifter is mechanically fixed to be within the shaded portion. If the shifter remains in an area other than the shaded portion longer than a prescribed length of time, the control renders it as being in the N position, which does not produce a drive force.

Methods for detecting malfunctions are given below.
· If a multiple number of switch signals are input.
· If the analog voltage is above or below the upper and lower limits.
· If the analog voltage signal is not within a specified value when one of the switch signals is ON.
· If the switch does not turn ON in spite of having executed a certain shift operation for a prescribed number of times or more.

If the shift sensor malfunctions, the shifter position that is used by the control is the N position, which does not allow the drive force to be produced. At that time, the shift display remains blank. Even if the system reverts to normal in the interim, this action is maintained until the ignition key is turned OFF.

(C)MALFUNCTION OF THE ACCELERATOR SENSOR

Because the accelerator is also controlled electronically through the electronic throttle, an accelerator-by-wire system has been adopted, similar to that of the shift system. Thus, the electrical signal of the accelerator sensor directly becomes the amount of acceleration that is used by the control. For this reason, we believed that the accelerator-by-wire system is particularly important for the hybrid system, and thus adopted a multiplex system(Fig.12).
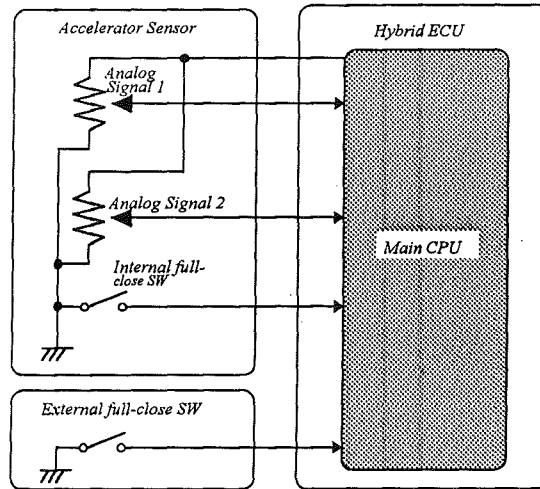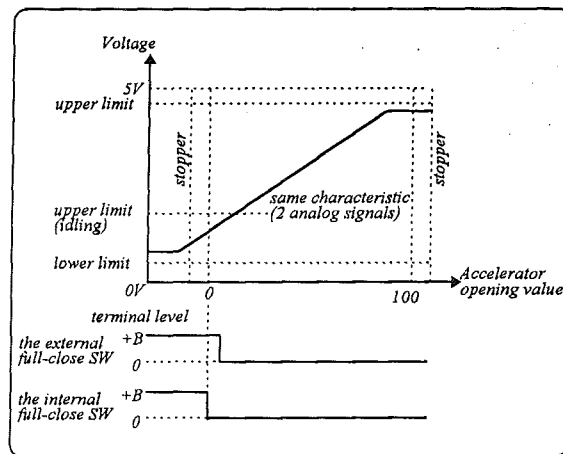
As shown in Fig.12 and 13, the accelerator-by-wire system consists of 2 analog signals and 2 full-close switches. Furthermore, an internal full-close switch is used to implement the full-close teaching for the analog signal's full-close position.

A malfunction is detected by mutually checking the 2 analog signals and the 2 full-close switches.

If the accelerator sensor malfunctions at a time when the brake pedal is not pressed, the accelerator opening is regulated in accordance with the vehicle speed to enable limp-mode driving. If the brake pedal is pressed, the accelerator opening is rendered to 0.

(D)MALFUNCTION IN THE MAIN CPU

Two types of malfunctions could occur in the CPU, as follows:
①the program in the CPU goes out of control
②the RAM in the CPU becomes damaged or the entered data becomes corrupted

The methods for addressing these two types of malfunctions are explained below:

24

①Program in the CPU goes out of control

A monitor CPU is provided to monitor whether the main CPU goes out of control. Furthermore, this CPU is monitored by a hardware-based electronic circuit (called a "monitor IC") (Fig.14).
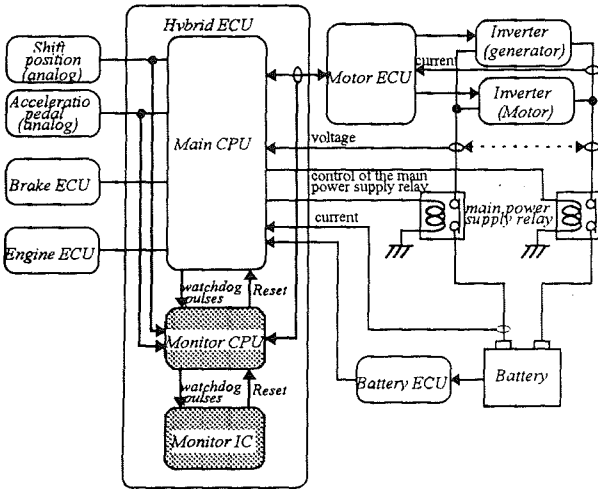
Fig.14 Monitor CPU, IC

The monitor CPU and the monitor IC will judge that a malfunction has occurred if a pulse from the main CPU (or the monitor CPU) is not received within a definite period, and resets (initializes) that CPU. Therefore, the main power supply relay, which is under the control of the main CPU, turns OFF.

When the monitor CPU is malfunction, the monitor IC resets the monitor CPU, and as a result, the monitor CPU resets the main CPU. Therefore, the main power supply relay, which is under the control of the main CPU, turns OFF.

②Damaging or corrupting the RAM in the CPU

The RAM values are not used directly for the important signals used for control. Instead, function call outs are used for checking the RAM for damage.

The fail-safe varies with the RAM that is used. For example, in the case of the RAM that is used for the shifter, the shift position used for control is N.

③ ①+②

The shift position sensor and the accelerator sensor (one of each system) are used as inputs. The request torque that is output by the main CPU and the torque that is obtained by the monitor CPU are compared. If the request torque is over or under the upper and lower limits of the torque calculated by the monitor CPU (these torque limits vary according to the accelerator opening and the shift position), the condition is judged to be abnormal.

When it is abnormal, the monitor CPU resets the main CPU.

3.SYSTEM MONITOR FUNCTION

Up until section 2, we described the monitoring of the hybrid ECU itself and its fail-safe functions. However, the hybrid ECU also monitors the hybrid system (the current to the motor, the energy) , a function that we will describe in this section.

The hybrid ECU calculates the current based on the torque command value that is output to the motor ECU. This value and the current that actually flows to the inverter are compared to detect any malfunction.

The following comparisons are made to detect a malfunction:
· the amperage that actually flows to the battery and the actual power value that is obtained from the voltage at that time.
· the torque values of the motor and the generator and the estimated power value based on the rpm from which the amount of loss has been deducted.

BATTERY ECU

This section describes the battery ECU provided in the THS. In the development of this ECU, special attention was focused on fail-safe performance.

First, we will describe battery control, which is carried out in cooperation with the hybrid ECU. Next, we will conduct an FTA for the entire system against abnormalities with the high-voltage section, one of the critical hazards for the vehicle, to identify those components causing the abnormalities. We will also describe the fail-safe mechanism which has been introduced in the system.

1. BATTERY CONTROL

Battery control has two main roles.

The first is to control the optimum charging state of the high-voltage battery. This is done by the battery ECU in cooperation with the hybrid ECU, by monitoring the charging state and outputting a charging/discharging request to the hybrid ECU. By constantly regulating the remaining capacity of the battery to the center value, it is possible to optimize battery performance over the whole driving range, that is the discharging performance required for helping the motor during acceleration and charging performance required for re-generation during deceleration, thereby improving driving performance.
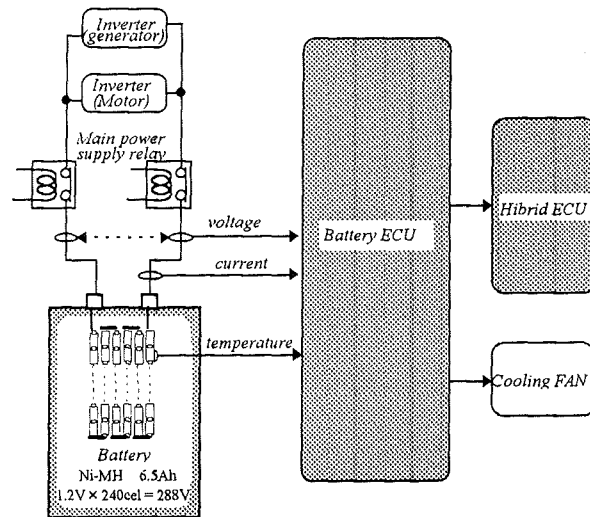
Fig.15 Battery ECU Schematic

The second is to optimize the performance of the battery. This is done by the battery ECU, by detecting the battery temperature and controlling the cooling fan to maintain the battery at the optimum temperature. As shown in Fig. 15, the voltage, temperature and current of the battery are input to the battery ECU, which then sends the control information to the hybrid ECU as well as controlling the cooling fan.

2. CONDUCTING AN FTA AGAINST ABNORMALITY WITH HIGH-VOLTAGE SECTION AND IDENTIFYING THE CAUSE (FIG. 16)
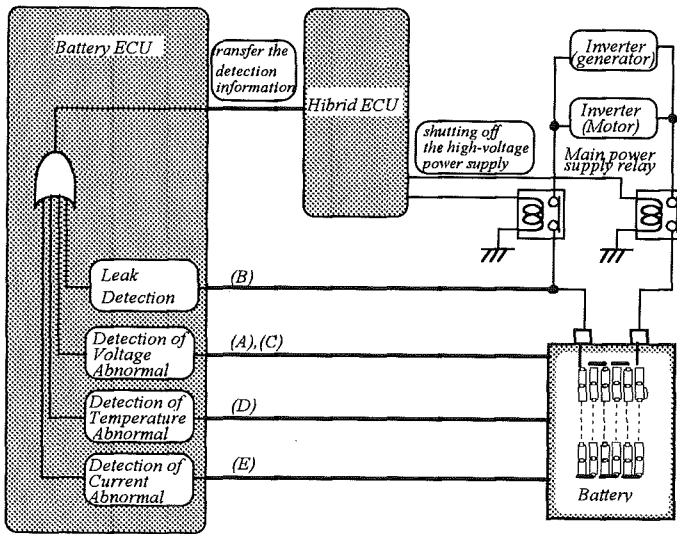
Fig.16 Fail-Safe

The system uses an Ni-MH type battery to reduce the weight of the power section. A total of 240 cells are connected in series to provide high voltage (rated voltage: 288V). We conducted an FTA for abnormalities with the high-voltage section, which is one of the critical hazards for the vehicle. From the results, the following abnormalities were considered to be critical hazards: (A) abnormality with the battery itself, (B) leakage from the high-voltage section, (C) abnormality with the battery voltage detection section, (D) abnormality with the battery temperature detection section, (E) abnormality with the battery current detection section and (F) communication error with hybrid ECU. No description for communication error with hybrid ECU is given here since it has already been given in this paper.

3. DETECTION OF EACH HAZARD AND FAIL-SAFE

A description of the detection method and fail-safe is given below for each hazard.

(A) ABNORMALITY WITH THE BATTERY ITSELF

The high-voltage battery may be over-charged or over-discharged due to faulty charge/discharge control, increase in capacity fluctuation between battery cells connected in series or leakage of electrolyte. If the battery is over-charged or over-discharged in such a situation, the battery will get extremely hot, resulting in leakage of electrolyte and other problems. To prevent such problems, the voltage, temperature and current of the battery are detected as shown in Fig. 16, to ensure

detection of battery abnormality.

Firstly, the high-voltage is divided into blocks, and the total voltage of the entire high-voltage battery and the voltage of each block are measured to detect a voltage abnormality in the battery.

Secondly, a multiple number of sensors are employed to detect the temperature of the high-voltage battery. This is necessary for safe and optimum control of the entire battery, since the battery consists of 240 cells as explained earlier. As shown in Fig. 17, the temperature sensor consists of thermisters installed on some battery cells to control cooling and detect abnormal heat generation on the cells.

Thirdly, the current of the high-voltage battery is detected by a current sensor, to constantly monitor abnormal current during normal charge/discharge control.
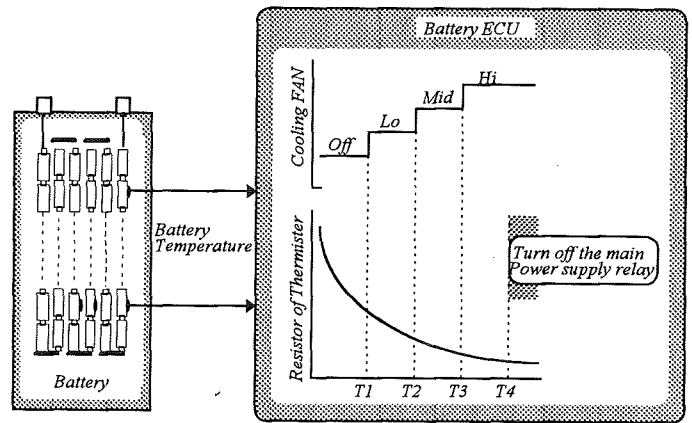
Fig.17 Battery Temperature Detection

By using the above battery voltage, temperature and current detection functions, the battery ECU ensures detection of any abnormality occurring with the battery. If a battery abnormality occurs, the battery ECU transfers the detection information to the hybrid ECU, which then issues an alarm, restricts the charge/discharge amount of the battery, and turns off the main power relay to isolate the battery from the system.

(B) LEAKAGE FROM THE HIGH-VOLTAGE SECTION

Leakage from the high-voltage section is acknowledged when a drop of the insulation resistance between the high-voltage power supply and vehicle body below the specified level is detected by the leakage sensor circuit. If leakage is detected, the battery ECU transfers the detection information to the hybrid ECU and requests it to issue an alarm. As shown in Fig. 18, the leakage sensor circuit applies a voltage periodically between the high-voltage power supply and vehicle body to measure the insulation resistance.

Furthermore, to ensure proper operation of the leakage sensor circuit, a semiconductor switch is used to connect a specified resistance between the high-voltage power supply and vehicle body for a certain duration when the ignition key is turned on. If an abnormality with the leakage sensor circuit is detected, the battery ECU transfers the detection information to the hybrid ECU and requests it to issue an alarm.

26
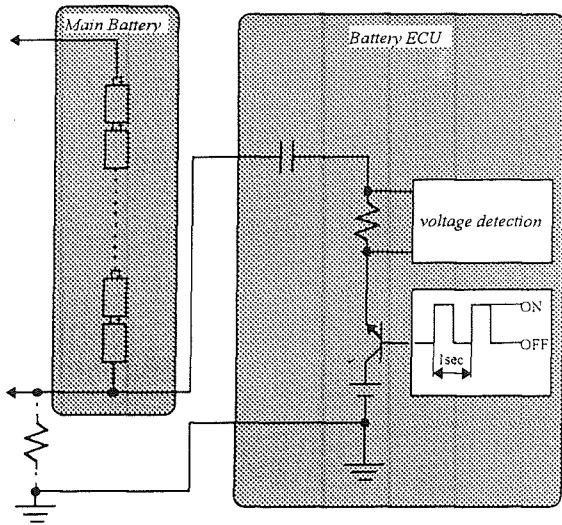
Fig.18 Leak Detection

(C) ABNORMALITY WITH THE BATTERY VOLTAGE DETECTION SECTION

Abnormalities with the battery voltage detection section include wire breakage and accuracy problems of the voltage detection section. For detection of accuracy abnormalities, the battery is divided into blocks as shown in Fig. 19 and the voltage of each block is detected. This enables judgment similar to that for fluctuation of the detected voltage of each block. If an abnormality with the battery voltage detection section is detected, the battery ECU transfers the detection information to the hybrid ECU and requests it to issue an alarm. In the worst case, the main power relay will be turned off to isolate the battery from the system.
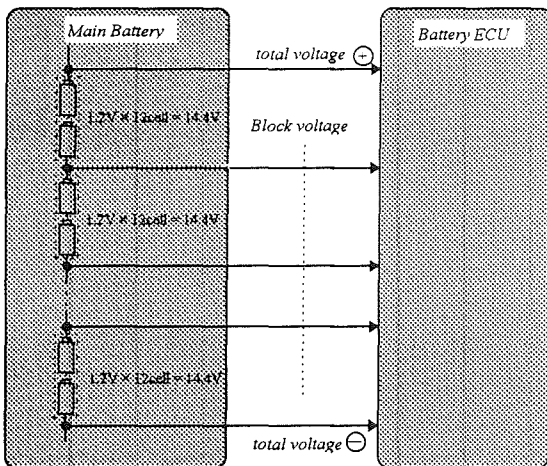
Fig.19 Battery voltage Detection

(D) ABNORMALITY WITH THE BATTERY TEMPERATURE DETECTION SECTION

Fig. 17 shows the battery temperature detection section. Wire breakage and short-circuit of each sensor are detected. If a battery temperature abnormality is detected, the battery ECU transfers the detection

information to the hybrid ECU and requests it to issue an alarm. In the worst case, the main power relay will be turned off to isolate the battery from the system.

(E) ABNORMALITY WITH THE BATTERY CURRENT DETECTION SECTION

Whether or not the battery current is abnormal is judged by checking fluctuation of the battery current and voltage values input to the battery ECU in relation to time. If an abnormality with the battery temperature detection section is detected, the battery ECU transfers the detection information to the hybrid ECU and requests it to issue an alarm. In the worst case, the main power relay will be turned off to isolate the battery from the system.

CONCLUSION

The THS incorporates the technologies of clean, high-efficiency gasoline engines, electric vehicle power systems based on nickel-metal hydride batteries, advanced automatic transmissions, and precision power control. The combination of these technologies into a single power train unit provides clean emissions and outstanding fuel consumption. And we believe that the THS contributes to reducing CO_2 emissions to alleviate global warming.

This hybrid control system provides fail-safe functions, as previously described, to ensure that the vehicle does not encounter danger in case of a system malfunction. Furthermore, in terms of the malfunction monitoring functions and protective functions, it is particularly important to adopt a multiplex system to ensure an even higher level of fail-safe performance. We believe that we have developed an extremely safe system for THS.

ACKNOWLEDGMENTS

REFERENCES

1. Shinichi Abe, Shoichi Sasaki, Hideaki Matsui, Kaoru Kubo, "Development of Hybrid System for Mass Productive Passenger Car" , JSAE 9739543, 1997
2. Katsuhiko Hirose, Toshifumi Takaoka, Tatehito Ueda, Yukio Kobayashi, "The New High Expansion Ratio Gasoline Engine for the TOYOTA Hybrid System" , JSAE 9739552, 1997

HYBRID POWER UNIT DEVELOPMENT FOR FIAT MULTIPLA VEHICLE

A. Caraceni, G. Cipolla
ELASIS ScPA - Motori

R. Barbiero
FIAT AUTO - VAMIA

ABSTRACT

In the "scenario" of increasing concerns for environmental pollution, hybrid vehicles will play a significant role in the near future. Compared to electric vehicles, the hybrid ones have an unrestricted driving range, higher performance and transport capability, still fulfilling ZEV emission regulation.

The hybrid vehicle features a power train that integrates a thermal engine with an electric motor. Among the several possible configurations for hybrid vehicle, the parallel hybrid one has been chosen for the FIAT MULTIPLA, for the following reasons:

- lower weight and volume of the electric unit to obtain the same driving mission;

- higher global efficiency of the system, due to direct thermal to mechanical energy conversion;

- a better vehicle performance (acceleration and max speed), thanks to the contribution of both motors to traction.

In the development of a hybrid parallel concept, the critical aspects to be overcome are related to the system mechanical complexity and the simultaneous control of the two motors.

In this paper the Fiat Auto and Elasis approach to the hybrid vehicle is presented with particular reference to the powertrain unit and its control strategies.

INTRODUCTION

In the last years the European legislation and environmental issues have focused the attention to the inconvenience produced by traffic density in our most congested European urban centers. Electric vehicles, as reported by several studies performed in different European cities, could substitute less than 10 % of the vehicles in circulation in the cities, provided that they can assure a real range of more than 80 km. On the contrary hybrid vehicle would allow a substitution of a bigger portion of the vehicle city park, thanks to their "range extension" and "peak performance" features.

The hybrid vehicle seems to be a very promising answer to today's different demands such as:

- free driving in emission protected zones

- ability to match different condition in urban or extra urban driving

- unrestricted range and transport capabilities like thermal vehicles

- same or similar driving characteristics as a conventional vehicle

- reduced dependency on batteries

- use of existing infrastructure

- commercially interesting image.

The mass production feasibility of the electric vehicle remains nowadays a big concern, primarily because of the battery problems. In case of the hybrid vehicle, battery dependency is reduced and so the hybrid vehicle is more acceptable to the public.

Conventional vehicles, especially those equipped with gasoline engines, have lower fuel economy and higher emissions especially in short range distance driving during warm-up phases, but offer high performance, long

distance and high transportation capability.

Although hybrid vehicles suffer from a higher weight if compared to conventional internal combustion driven and pure electric vehicles, they may offer a possibility of satisfying personal and commercial needs with lower emissions and higher global efficiency.

On the other hand hybrid vehicles have higher complexity than their counterparts. The main disadvantages can be summarized as:

- higher number of components

- higher weight

- more sophisticated vehicle electronic control strategies

- higher costs.

The hybrid powertrain structure and power size must be carefully selected to minimize the above mentioned disadvantages. Hybrid propulsion systems can be arranged, in a variety of configurations, in two basic categories: series and parallel (Fig 1).

SERIES

PARALLEL

——▷ Regenerative power ——▶ Engine power

Figure 1
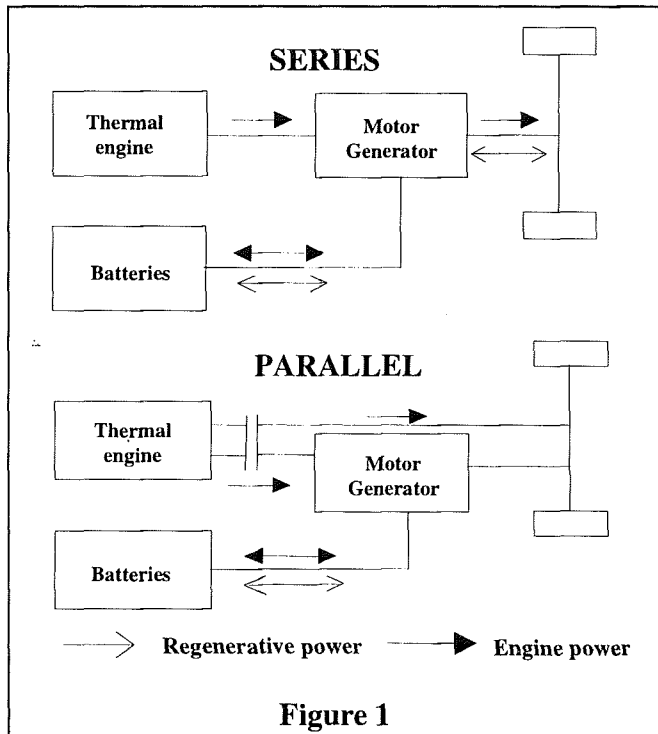
In the series arrangement, all energy from thermal engine is converted into electricity. The parallel arrangement has in addition a direct mechanical connection to the transmission driveline which could include a conventional gearbox. The topology and the details of a hybrid propulsion system will depend heavily on the mission that the vehicle is intended to fulfill and on the constrains of today's technology availability for mass production.

The global objectives of Fiat MULTIPLA hybrid vehicle and its powertrain subsystems characteristics are discussed in the following paragraphs.

MAIN VEHICLE OBJECTIVES

The goal of the present research activity is to design a hybrid vehicle, suitable for mass production, derived from the "MULTIPLA" equipped with a 1.6 litres gasoline engine, with similar characteristics as far as it concerns comfort, habitability and safety.

The daily vehicle mission could be summarized as 105 km per day with 1/3 on urban driving in hybrid mode, 1/3 in pure electric and 1/3 in hybrid mode on extraurban driving.

The emission levels must be equivalent to ZEV in pure electric and according to the European limits for year 2005 (EEC phase IV) in hybrid or thermal mode. Tab 1 shows the main vehicle performance requirements.

Performance requirements		Hybrid	Thermal	Electric
Top speed (km/h)		≥ 150		≥ 100
Continuous speed (km/h)		≥ 130	≥ 130	≥ 80
Acceleration (s)	0 – 100 km/h	<18	>30	-
	0 – 80 km/h	<12	<20	<40
	0 – 50 km/h	<6	<9	<13
Acceleration 3rd gear (s)	40 – 80 km/h	<10	-	-
Fuel consumption (ECE+EUDC) (l/100km)		-	<10	-
Emission		ECE IV	ECE III	ZEV

Table 1

In this paper the impact of these requirements on the powertrain will be examined.

POSSIBLE HYBRID CONFIGURATION

Throughout a preliminary investigation with mathematical simulation models, the deployment of overall objectives has been performed into subsystems specification as a function of possible powertrain configurations. For each of the possible solutions a weighted analysis of positive and negative aspects has been carried out.

The results of this analysis can be summarized as

30

follows:

Dual mode - The addition of an independent electric power train on the thermal vehicle leads to the simplest hybrid configuration. The two power trains operate in alternative, to meet the requirements of the circulation in typical urban areas (electric traction) or those of the extraurban missions (thermal engine).

Typical mission: extraurban driving, with limited operation in ZEV urban area.

Advantages:

• simplicity

• no integration of the two powertrain possibility to have a two axles drive system in case of critical mobility

Disadvantages:

• critical layout due to the two traction axles, with considerable modification on structure and mechanics;

• not optimized system in terms of energy consumption and emissions

Series Hybrid - The thermal engine coupled to an electric generator is used as a generating unit and motion is assured by an electric power train.

Typical mission: driving in large ZEV urban area

Advantages:

• small size thermal engine and its utilization within the most favorable working conditions in terms of efficiency and emissions;

• gearbox is not mandatory

• equal vehicle performance in electric and hybrid modes.

Disadvantages:

• number of installed components which have impact on the vehicle in terms of weight, volume and cost

• low efficiency over constant speed as a consequence of the energy conversions

• performance and operating range limited by battery

high installed electric power

Parallel Hybrid - Thermal engine and electric motor add

on the same shaft their respective torque to achieve the desired performance.

Typical mission: ZEV urban driving and full-performance extraurban driving

Advantages:

• low installed electric power, related to the urban mission

• thermal engine can be downsized without penalizing vehicle performance leading to a fuel economy benefit.

• operating range in hybrid mode depending on vehicle fuel tank only

• addition of electric power to the thermal for peak performance

• flexibility in changing the vehicle mission.

Disadvantages:

• mechanical complexity

• gearbox and specific coupling interface needed

• system control complexity due to the management necessity of the two propulsion systems.

The vehicle mission and performance, the uncertainties of the evolution of the market, and cost constrain, requiring a strong attention to the "carry over" opportunities among the various production vehicles, have led to the choice of the parallel configuration (fig.2).
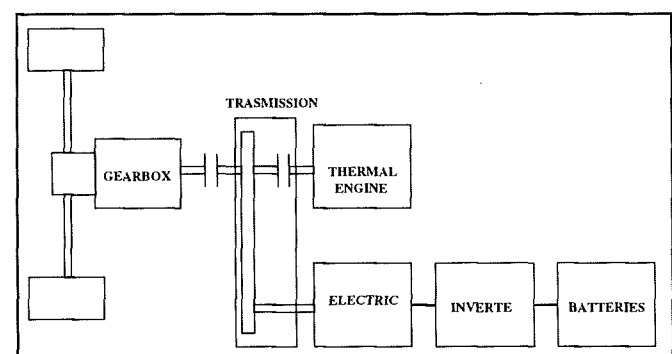
Figure 2

POWERTRAIN DESCRIPTION

Fig. 3 shows the powertrain where the thermal engine, the electric motor, the interface and gearbox are visible.
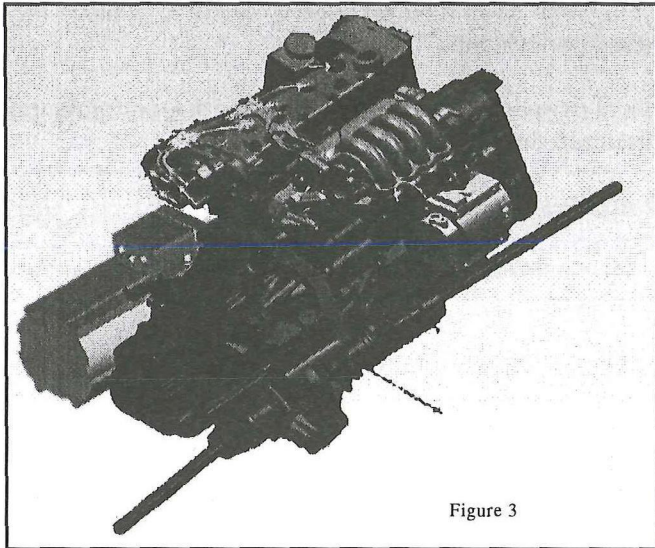
Figure 3

Thermal engine

The thermal engine chosen for this application is the new FIRE 1242 16 valves, just in production on the Lancia Y and on the Fiat PUNTO. An engine section is visible in fig. 4 and fig. 5 shows the engine torque and power characteristics.
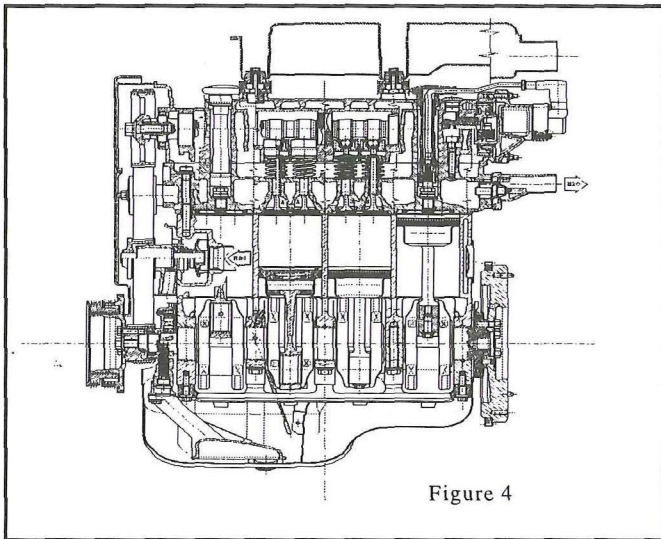
Figure 4
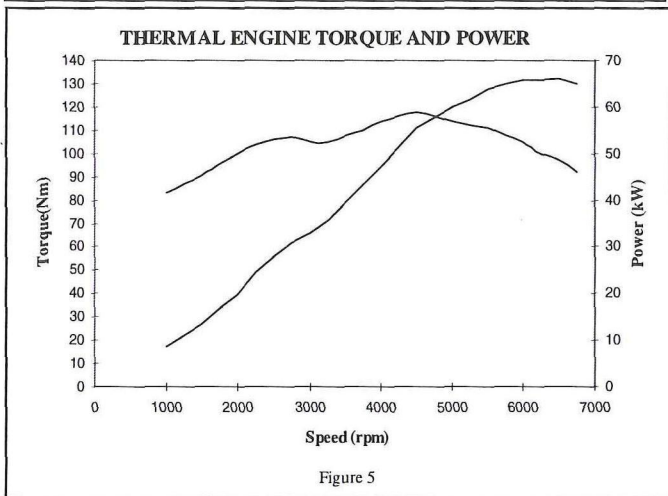
Figure 5

For the hybrid application some modifications of the series production thermal engine are required, mainly in the electronic control package which features a drive-by-wire system. Engine ECU re-calibration is of course necessary to optimize fuel economy, emission and driveability for the hybrid application. Table 2 reports the main engine characteristics.

ENGINE CHARACTERISTICS Table 2	
Weight	106 kg
Height	670 mm
Length	600 mm
Width	550mm
Displacement	1242cm^3
N. valve	16
Compression ratio	10.2
Injection system	MPI
Max torque	115Nm@4750rpm
Max power	65.5kW@6250rpm

The choice of a gasoline engine versus a diesel engine has been done mainly because the handicap of the diesel engine is the relatively high NOx emission, which with today's technology cannot be reduced to the same extent as a gasoline engine equipped with a three-way catalyst.

Electric motor and inverter

The electric drive system is based on an induction motor with vector control inverter.

Table 3 and table 4 reports the main motor and inverters characteristics.

ELECTRIC MOTOR CHARACTERISTICS Table 3	
Base speed	2500 rpm
Maximum speed at rated power	9000 rpm
Cut-off-speed (max. power peak)	6500 rpm
Over speed @ zero torque	10000 rpm
Rated torque	65 Nm
Max torque (5')	123 Nm
Rated power	15 kW
Max power (5')	30 kW
Peak power @ max peed	22 kW
Weight	41.5 kg
Diameter	200 mm
length	360 mm

32

INVERTER CHARACTERISTICS Table 4	
Control algorithm	Torque - vector
Power switches	IBGT
Switching frequency	6 kHz
Power section input voltage	
Rated	160 - 260 V
Allowed	140 - 280 V
Control section input voltage	6 – 16 V
Max input current	280 A
Weight	17 kg
L x W x H	440x204x176 mm

Fig 6 shows the motor torque and power characteristics.

ELECTRIC MOTOR TORQUE AND

Figure 6
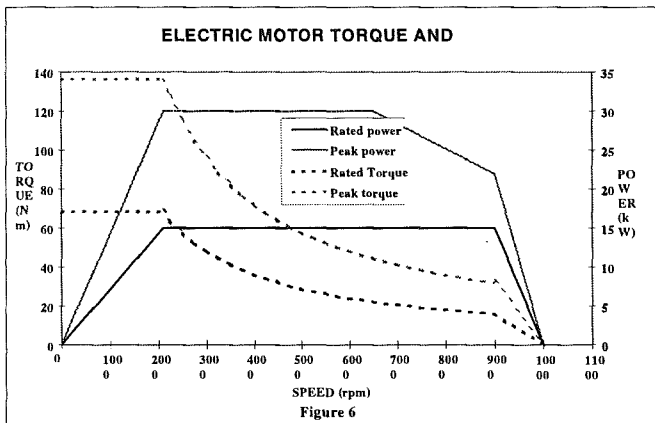
The motor features a low weight, reduced dimensions, and high utilization range with good efficiency (fig. 7).

Electric motor and inverter mesured efficiency
1st quadrant @ voltage 240 [V]

Figure 7
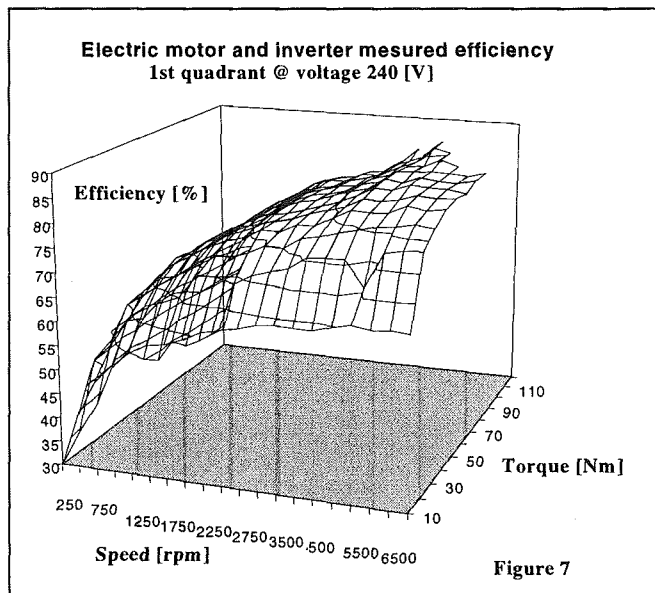
The motor, the inverter and the battery management have been designed for the application to the Fiat 600 electric vehicle, under development at Fiat Auto and Elasis.

Transmission

To minimize modifications and to make the solution compatible with the industrial needs, the integration of the two engines has been implemented through a parallel axle transmission (fig. 8).

Figure 8
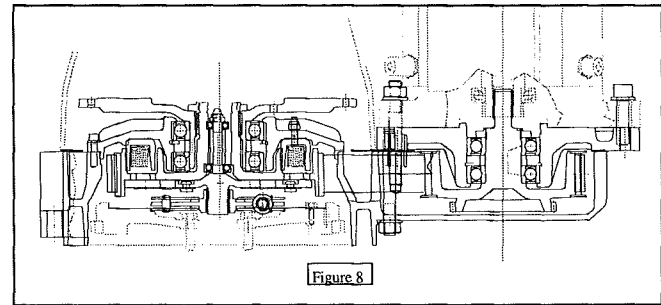
The mechanical coupling between the two axles is performed throughout a toothed belt. An electromagnetic clutch has been designed and manufactured to the connection and disconnection of the thermal engine. This allows for an automatic switching from electric to hybrid mode during vehicle operation, based on the drive train control strategies. The transmission to the vehicle wheels is performed by a normal production manually shifted 5 speed gearbox.

The main results of a simulation activity on vehicle performance with the above described powertrain components is shown in table 5.

PERFORMANCE		HYBRID	THERMAL	ELECTRIC	REFER. CONV. VEHICLE
Top speed (km/h)		176		116	173
Continuous speed (km/h)		166	148	86	
Acceleration (s)	0 – 100 km/h	15.5	26.8		12.4
	0 – 80 km/h	10.5	17.9	28.0	8.3
	0 – 50 km/h	4.9	8.7	10.3	4.1
Acceleration in 3rd (s)	40 – 80 km/h	8.3	17.6	21.0	7.5
Acceleration in 4th (s)	60 – 100 km/h	12.0	28.1		10.8
Acceleration in 5th (s)	80 – 120 km/h	18.3			15.9

Table 5

VEHICLE OPERATING MODES

The driver can select between the following four operating modes:

- hybrid mode

- electric mode

- economy mode

- recharge mode

In hybrid mode both the thermal engine and the electric motor are connected to the driveline to assure vehicle nominal performance and to minimize fuel consumption and emissions.

The vehicle operation can be divided into two basic modes: constant speed (cruising) and acceleration or deceleration.

In cruising mode, relatively low power is required from the drive train. However, a large amount of energy is consumed in a long trip. In acceleration mode, a high peak of power is required but not much energy is consumed due to its brief and transient occurrence. When maximum vehicle performance is not required, a proper combination of thermal engine operation for cruising, and electric motor for acceleration can be used to minimize fuel consumption and emissions. Furthermore when the vehicle operates with light loads it is convenient to use electric power instead of thermal one because of the high specific fuel consumption of the gasoline engine.

The electric motor acts as a generator to recover energy during deceleration and braking.

The driver operates the vehicle in conventional way, using accelerator, brake, clutch and gear shift.

The powertrain management controls takes care of not discharging the battery below a certain threshold; if the threshold is reached the system does not allow the use of electric motor automatically switching in economy mode.

In electric mode the thermal engine is shut down and mechanically disconnected through the electromagnetic clutch. In this mode, driving could be done without use of the manual gearbox, and the battery can be fully discharged.

Thermal engine starts only if cabin cooling or heating is required.

In economy mode all the torque necessary for vehicle operation is provided by the thermal engine. Braking energy is always recovered.

In recharge mode the thermal engine delivers power both for traction and for battery recharge. As a general consideration it is always convenient, from an economical point of view, to recharge battery from the electric distribution through the on-board electric battery charger. In this operation mode optimization of recharge strategies is necessary as a function of the battery state of charge and/or fuel economy and emissions. Fig 9 shows a typical torque management.

1. The electric motor provides all the required torque where engine has high specific fuel consumption
2. The engine delivers torque with limited torque gradient; the electric motor deliveres complementary torque
3. The engine delivers the total requested torque
4. Electric motor torque is added when the requested torque is higher than the maximum engine torque
5. Braking torque is provided by the electric motor to recharge the batteries
6. The electric motor recharges the batteries; the thermal engine delivers torque for both traction and recharge
7. The electric motor does not deliver any positive torque for traction (limited vehicle performance)

Figure 9

CONTROL SYSTEM AND MANAGEMENT STRATEGIES

The hybrid system is managed by a Vehicle Management Unit (VMU) which implements the working strategies of the vehicle and activates the two drive trains through the inverter for the electric motor and the engine electronic control unit respectively. System diagnosis, driver's controls, dashboard warning lights' management and battery state of charge are also accomplished by the VMU. Fig. 10 shows the control system scheme.

Figure 10
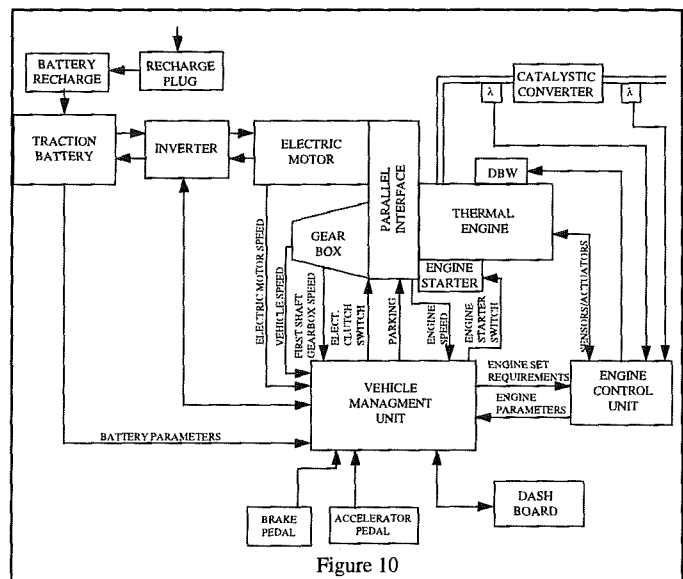
Parameters from engine and vehicle ECU, are exchanged through CAN protocol. The driver, through the accelerator pedal position, sets the required traction torque; this is then splitted (in hybrid mode) between the engine and the motor as a function of vehicle operating condition and battery state of charge to optimize fuel economy, emission and driveability. The electric torque request is then actuated through the inverter. The thermal engine torque request is supplied to the engine

34

control unit that set the throttle angle accordingly.

When the accelerator pedal is released, a regenerative braking occurs while the electromagnetic clutch is disengaged.

The braking effect, and the corresponding energy recovery is increased pushing the brake pedal.

SIMULATION STUDIES

A simulation package based on SIMULINK™ has been developed. SIMULINK™ is a program for simulating dynamic systems based on MATLAB™ which is a powerful numerical math program. Individual components of the drive train could be easily represented by simulation blocks. They can be connected to constitute a mathematical model of the entire power train. The model includes the possibility to implement different torque split strategies and to evaluate the effect on parameters such as fuel consumption, emission, battery state of charge etc.

Fig 11 shows the top level block diagram of the hybrid powertrain.

PARALLEL HYBRID PROPULSION SYSTEM
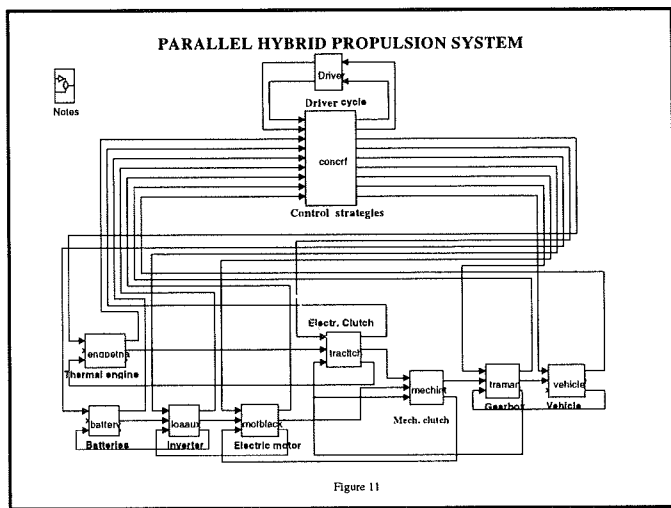
Figure 11

Figure 12 and 13 show a typical torque split on ECE and on EUDC which is obtained by limiting the thermal engine torque increase at 1 daNm/s.

Torque splitting on ECE
Thermal engine torque gradient limited @1daNm/s

Figure 12

Torque splitting on EUDC
Thermal engine torque gradient limited @1daNm/s
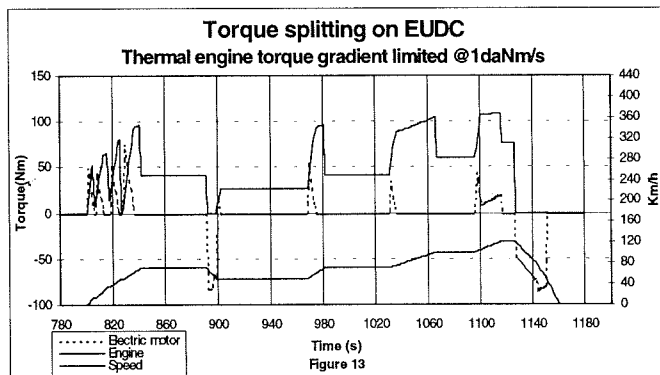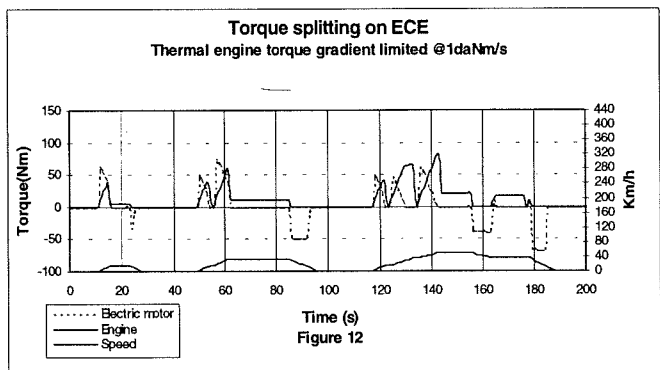
Figure 13

Fig 14 shows the effect of different thermal engine torque increase limitation on tailpipe emission, fuel consumption and electric energy consumption.

ENGINE TRANSIENT TORQUE LIMITATION EFFECT ON ECE+EUDC
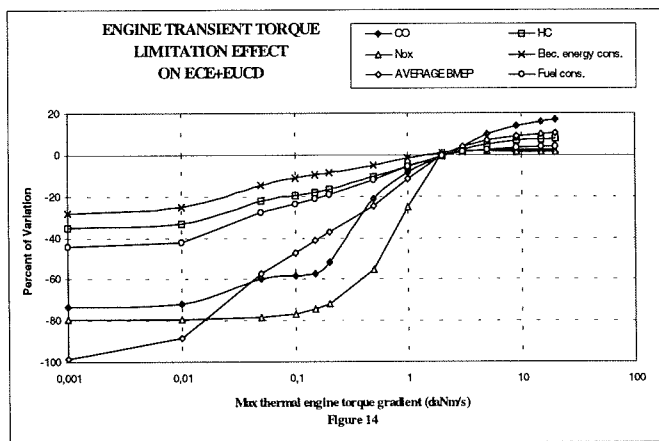
Figure 14

Figure 15 shows the effect of different constant recharging thermal engine torque on tailpipe emission, fuel consumption and electric energy consumption, when the thermal engine torque gradient is limited at 2 Nm/s.

USE OF CONSTANT RECHARGING TORQUE EFFECT ON ECE+EUDC
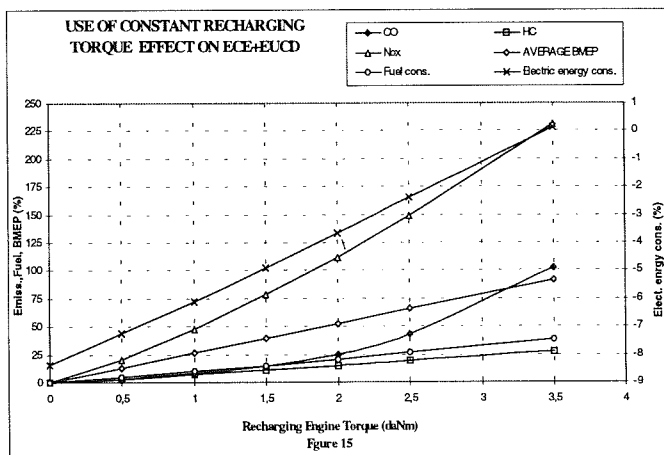
Figure 15

Fig 16 shows the effect of different constant electric motor equivalent torque on tailpipe emission, fuel consumption and electric energy consumption, when the thermal engine torque gradient is limited at 9 Nm/s.

CONSTANT ELECTRIC TORQUE EFFECT ON ECE+EUCD
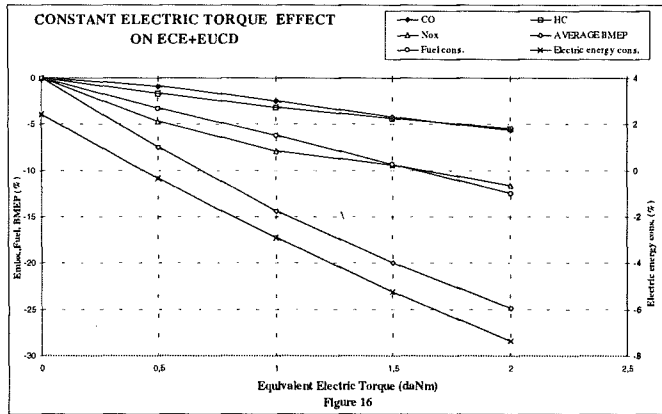
Figure 16

Figure 17 reports the kinetic energy breakdown during decelerations phases on ECE, EUDC, and at two deceleration rates.

CALCULATED ENERGY BREAKDOWN
Figure 17

- Energy saving
- Electric losses
- Aerodynamycs+rollyng+transmission losses
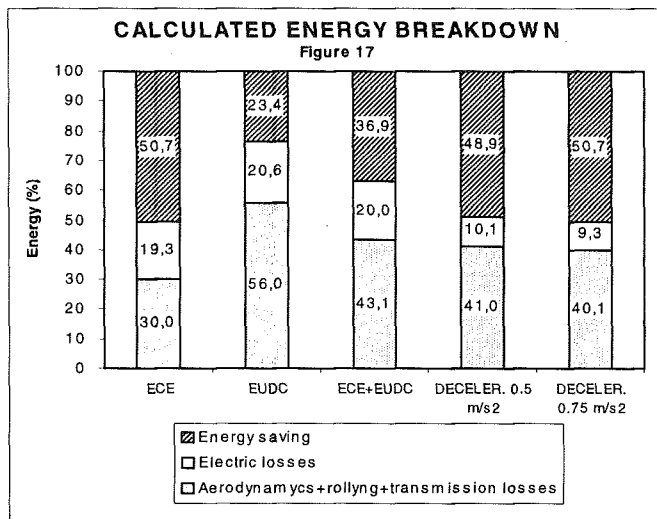
Figure 18 shows the electric range autonomy on ECE, and at two constat speed.

ELECTRIC RANGE

Figure 18
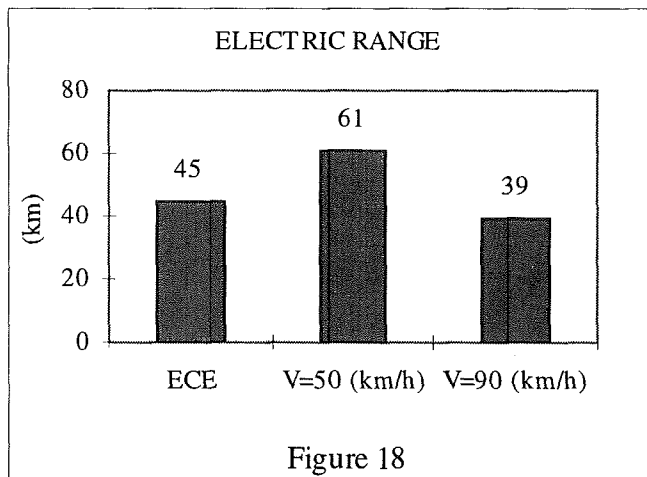
CONCLUSION

The hybrid drive system presented in this paper is envisaged to use as much as possible series components to minimize development time and costs. At present time it is hard to predict which type of hybrid vehicle will be the best choice for the future traffic and legislation scenario. Our studies showed that the parallel hybrid configuration could be the right choice.

It is important to remark that the objective of the present research work is of identifying and prototyping a powertrain for a hybrid vehicle suitable for mass production. As a consequence, the focus of the research project has been the "system optimization", i.e. identification of optimum configuration and control strategies using "conventional present technology".

At this stage the research and development activities of power train functions and control strategies, using current level of technology on batteries, electric motor and combustion engine, have shown good results in fuel economy, emissions and performance. Further improvements in this area are still possible and will be the main goals of the future activity.

ACKNOWLEDGMENTS

The Development of a Simulation Software Tool for Evaluating Advanced Powertrain Solutions and New Technology Vehicles

Jaimie Swann and Andy Green
Motor Industry Research Association (MIRA)

ABSTRACT

The drive for developing advanced powertrain solutions such as electric, hybrid and fuel cell vehicle traction systems is increasing, principally to meet increasingly stringent legislative demands and partly to satisfy intuitive customer requirements. However, to achieve the potential benefits such technologies offer, these complex systems must be optimized for the particular vehicle and its operating environment. There is therefore, an increasing demand from potential users of new vehicle technologies ranging from system designers to transport operators, for a rapid and cost effective evaluation tool capable of modelling advanced powertrain solutions and the potential effects on the environment.

INTRODUCTION

The *FLEETS* - ENERGY project started in April 1996 and is part funded by the JOULE-THERMIE programme. The objective is to develop a validated simulation tool for advancing and optimizing new technology vehicles (including electric and hybrid vehicles). The modelling capabilities of the Vehicle Mission Simulation program (VMS) will enable users to objectively evaluate conceptual designs of advanced powertrain vehicles operating over any given drive cycle or performance criteria.

This collaborative project consists of 21 different organizations from all over Europe including; research organizations, powertrain specialists, OEM's, transport operators, energy utilities and transport planners. All provide specific expertise in the areas of technical input, research collaboration and end user evaluation of the simulation tool.

The overall project is divided into eight main 'work packages' including Systems Identification, Systems Modelling, Data Acquisition, Software Implementation and Vehicle Simulation/Validation. This paper will describe the objectives and approach used to developing the simulation tool, the modelling techniques applied and what validation procedures will be used.

OBJECTIVES

The main objective of the project is to produce a simulation software tool that can assist in the development, assessment and implementation of advanced vehicle designs. To achieve this, the software must be capable of the following:

- Perform simulation of any Vehicle/Powertrain over given drive cycle.
- Model effect-cause and cause-effect drive cycle data.
- Perform multiple simulations.
- Allow users to design virtual vehicle layouts.
- Model all major subsystems affecting energy consumption and transmission.
- Predict operational costs and environmental effects.

These features will be made available to the user in an intuitive way and be flexible enough to be applied to a wide variety of applications ranging from vehicle/system design to route optimization. It is intended that this tool will promote the understanding of energy-environment-transport systems using new vehicle technologies and enhance the confidence in such systems.

A major aim of the project is to ensure that the simulation tool and in turn the individual component models are validated against 'real-life' data. This will be achieved by collecting on-vehicle data measurements and using the results to correlate simulation calculations and component models.

Programs of a similar type to VMS are available at vehicle OEM's, however the key difference with this project is that the software tool is intended for a much wider range of users, both technical and non technical. It will also be generic, modelling any manufacturer's vehicle, provided system data is available, and will run on standard PCs rather than specialist workstations.

USERS AND POTENTIAL APPLICATIONS

The simulation tool is targeted at three main groups of users; Engineers, Operators and Suppliers, Decision Makers. These three user groups have different requirements as detailed below. However, much of the

core functionality is common to all groups and is essential for a reasonable level of accuracy in predicting the characteristics of new technology vehicles. The main difference will be in the level of engineering detail each group is interested in, for example, systems engineers may need detailed second by second component data while at the policy support level only overall energy usage and generic vehicle types may be required. Three typical applications for these main user groups are described below.

System Designers and Engineers:

One of the primary aims of VMS is to provide engineers with a tool that will help reduce the time (and therefore the cost) of design and development of new technology vehicles. For example, the capability of VMS to perform multiple simulations on flexible powertrain configurations in both drive cycle and performance modes allows system designers to analyze system interactions at the parameter level and consequently perform powertrain matching and optimization. This effectively reduces the need for expensive prototype builds and vehicle testing. Likewise, component suppliers would be able to utilize the extensive component database to select components for different simulations, allowing them to optimize components for specific systems/vehicles.

Bus Operators and Local Authorities:

It is intended that transport operators using VMS will gain greater confidence in new technology vehicles meeting their requirements by assessing alternative fueled and hybrid buses over new or existing routes with respect to conventionally powered vehicles. Users would be able to evaluate the comparative running costs of the various vehicle types and optimize route parameters such as refueling locations and the number/location of passenger/cargo pick up points. As a result transport operators would be able to use the simulation tool to determine strategically what vehicle types would be best suited for specific routes and predict the comparative running costs.

Urban Planners and Policy Makers:

The implementation of efficient road based transport systems and the associated infrastructures based on new technology vehicles, requires major expenditure and potentially, changes to regulations. Urban Authorities and Planners could utilize both the database and simulation capabilities to assess the viability of such changes and increase confidence that they will have the desired effect.

SIMULATION TOOL SCOPE AND MAJOR FEATURES

The VMS simulation tool, by necessity, has a very broad scope, as described in Table 1, to allow it to meet the objectives described previously. To cope with this requirement, the software is based on a pragmatic mix of design parameters, experimentally derived data and calculations. This flexible approach allows a wide range of vehicles and systems to be included while keeping the simulation tool as easy to use and accurate as possible.

Table 1- VMS Scope

Category	Scope
Route and Infrastructure	Any Route Profile Fuel Delivery Infrastructure Vehicle 'Control' Telematics
Vehicle	Any powered, road based wheeled vehicle.
Powertrain	Internal Combustion Electric Series Hybrid Parallel Hybrid
Fuel	electric liquid hydrocarbons gaseous hydrocarbons
Primary Parameters Modeled	Efficiency Energy/Power Speed Fuel Usage Emissions Cost

Whilst the software is based on 'Windows' user interface standards it also has an underlying relational database, simulation 'objects' to represent real world systems and finally the ability to produce output on screen or as printed results graphs and reports. Results analysis and presentation is key to assisting the user in understanding what has happened during a simulation. Important features here, include the ability to compare the results from several simulations in a graphical form and to print out user defined reports.

TECHNICAL APPROACH

The project includes a number of key work packages as described below:

SYSTEM IDENTIFICATION

The objective was to identify system boundaries, parameters, interactions and data formats. This also included a literature search to review existing models and parameter data. Over 50 different vehicle systems have been examined in detail, this includes systems from conventional engines to electric traction motors and fuel cells. Refer to Appendix 1 for example of powertrain parameter interaction diagram.

DATA ACQUISITION

Accurate data is essential to the validation and operation of the simulation program. This work package includes the collection of data on routes, vehicles and systems. The information is obtained by both physical on-vehicle data measurements and from historical or paper based sources. A detailed specification for data measurement has been completed and 10 vehicles (listed in Table 2) out of a possible 23, have been identified for on-board data measurement. The selection was based upon a number of criteria including:

- vehicle type
- vehicle usage
- fuel type
- the amount of existing system/component information available.

Table 2 - Selected vehicles

Owner	Veh Type	P/T Type	Location
KVG	InterUrban Bus	Diesel	Salzgitter
KVG	Bus	Diesel	Salzgitter
KVG	Bus	Nat Gas	Salzgitter
CCT	MiniBus/Van	EV	London
CCT	MiniBus/Van	Nat Gas	London
CCT	MiniBus/Van	Diesel	London
STCR	Bus	Diesel	La Rochelle
EIGSI	Car	EV	La Rochelle
Trans de Barc	Bus	Diesel	Barcelona
Trans de Barc	Bus	Diesel	Barcelona

Detailed information to be collected on each vehicle includes:

- vehicle data including vehicle speed and payload
- route information such as road gradient, wind speed and ambient air temperature
- driver interactions such as brake/accelerator pedal movement
- component data including engine speed, battery current and operating temperatures

SYSTEM MODELLING

This work package concentrated on defining the simulation algorithms which are used to model the vehicles and powertrains, as well as the optimization procedures and control strategies (particularly for hybrid vehicles). Algorithm Identification sheets were formulated and circulated to the main partners of the project, they were designed to capture information on the following parameters for each system type;

- conceptual and detailed modelling procedures.
- component/system algorithms for both 'cause-effect' and 'effect-cause' calculations.
- optimization procedures
- data conversion routines
- block diagrams for components and interactions
- control strategy

Alternative models were considered to allow the VMS tool to work with different levels of data and to be used at both the 'concept' and 'detailed' ends of transport system development. The modelling algorithms for each system also had to conform to a standard format in terms of the inputs/outputs they would produce. This allowed the interactions between components to be modeled using standard connections (i.e. mechanical, electrical, thermal and chemical) and in turn allow standard link parameters (refer to figure 1) to be passed between different components in a consistent manner, independent of vehicle/powertrain layout or conformance to drive cycle.

Figure 1 - Standard component interaction (Engine)
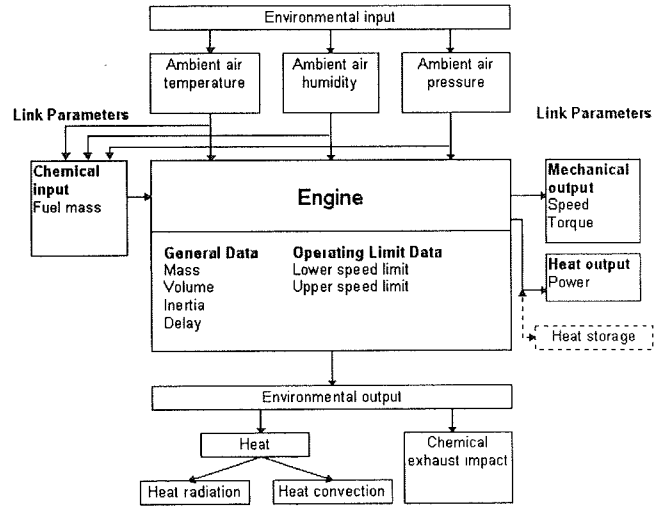
The modelling approach used for component interaction is based on the 'quasi static' method for solving a components state at a definitive time increment in the drive cycle. This method assumes a state of equilibrium exists for each component during the calculation procedure per time increment. The effects of transients (particularly for the major components) can be accommodated if the underlying component maps are made available.

This methodology also allows the flexibility of modelling both cause-effect calculations (essential for performance simulations) and the standard effect-cause techniques to be implemented at a more empirical level.

Figure 2 - Reverse Calculation: Effect → Cause
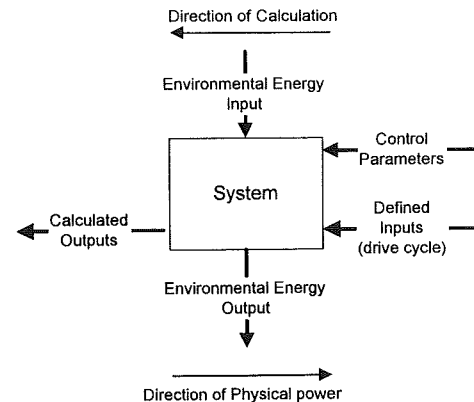
The normal physical outputs of a system, for example the vehicle velocity, are assumed to be defined (from a drive cycle), the results of a calculation from one sub-system then form the defined inputs to the adjoining system. Other control parameters are also considered including the environmental effects on a system and control parameters such as operating limits.

39

Figure 3 - Forward Calculation: Cause → Effect
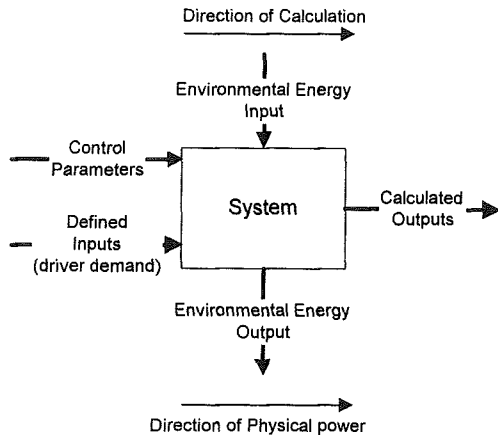
Forward calculation routines will be used primarily for performance tests including 0-60mph, ¼ mile sprint, gradeability tests and range prediction. The normal physical inputs of a system, particularly, driver accelerator pedal demand, are assumed to be defined (from a drive cycle) and the outputs calculated for each consecutive sub system. Using basic iterative calculation procedures, the forward calculation routines can predict a potential response to a given drive cycle.

This type of calculation has some inherent complexities involved with determining a solution, particularly the management of a closed loop control system per time increment. In addition limiting control factors such as, energy source capacity .v. driver demand and the matching of final vehicle speed to vehicle drive cycle speed within an acceptable error limit have to be accommodated within the calculation procedures.

Control Strategies

The majority of the control strategy options relate to hybrid powertrain configurations, in particular engine mode (i.e. off, idle, maximum power or maximum efficiency) and operation, for example power supplied by the engine and the working point (speed, torque) at which the engine will deliver this power. Also the battery models and vehicle dynamic model will account for the effects of regenerative braking. The parameters involved with control optimization include; ZEV area, vehicle charging, battery state of charge, driver demand and power required from the controller.

The major aim of control optimization is to avoid deep battery discharge in order to improve battery life and preserve vehicle range in electric mode. However the strategy employed has also to accommodate the capability of compromise, for example in extreme working conditions, when it may be necessary to provide high power rapidly to the electric motor (e.g. when overtaking).

In conclusion, the systems modelling phase of the project has documented over 40 detailed simulation

algorithms for each individual systems as well as the overall vehicle control strategies.

VMS SOFTWARE IMPLEMENTATION

This work package includes object oriented software analysis, design and implementation using the results of the systems modelling described above. All aspects of the software will be integrated including the relational database, simulation objects, user interface and reporting system. This task ends with a VMS which has been modeled and programmed using quality assurance procedures (version management) including validation of sub-systems and the total system, coupled with relevant user documentation. The core program architecture has now been developed together with a trial user interface and a basic selection of vehicle system models. The VMS software is being developed using state of the art development tools and object orientated methodologies which caters for:

• reusable components
• enforces modular design
• allows inherited functionality
• eases maintenance and debugging
• encapsulated functions and data forming an intuitive representation of real world objects

The simulation program is being developed to be flexible enough to model future technological advances in component design and to accommodate almost any advanced powertrain configuration (refer to Appendix 2 for VMS Class Hierarchy diagram). This has been achieved by coding each powertrain component as a self contained 'object' with its own functions and data variables encapsulated within a defined interface. This process allows objects to be; developed independently, later updated or even completely rewritten without affecting the rest of the software and validated separately.

Incremental development versions of the software have already been produced, incorporating features such as runtime graphing of data, intuitive data input interfaces (e.g. on-line help facilities) and, in the near future, test bench facilities for validation of individual software 'components' or powertrain systems. It is expected that later versions will be available for both user trials and demonstrations, prior to detailed validation work.

VEHICLE SIMULATION

The next step in validating the VMS tool developed above will be to use it to simulate the operation of a selected range of vehicles on specific routes (as defined in the data acquisition phase). The objective will be to correlate the simulation results to the data collected from on-vehicle measurements and determine the accuracy of the incorporated models. Investigation into potential sources error will also be carried out, particularly in three main areas:

40

(a) Experimental errors - equipment calibration
                                    - measurement procedures
(b) Modelling errors   - modeling algorithms
                                    - error propagation

(c) Simulation errors   - calculation routines
                                    - effects of time increment

Initially validation and accuracy prediction will be based on steady state driving conditions, with subsequent analysis being focused on transient drive cycle effects. The results from this phase of the project will provide a realistic evaluation and validation of the system with a representative group of users.

SYSTEM OPTIMISATION

Following the vehicle simulation phase of the project, the VMS tool will be used to optimize vehicle/route combinations and provide guidelines for users to achieve an optimum vehicle specification for each route. Following the optimization stage, a final release version of the VMS software will be produced, marking the end of the project. Through dissemination activities by all the contributing Project Partners, it is aimed that the VMS tool will establish itself as a standard tool for vehicle simulation which can be utilized by a wide range of users.

CONCLUSION

An increasing array of new technology solutions is now being developed that could potentially help reduce the environmental impact of urban transport systems. However, the increasing diversity and complexity of new technology systems requires new techniques to understand and assess their suitability for given applications and to optimize their performance. Also, these technologies must compete effectively in the market place against current technologies which have undergone decades of development, investment and cost reduction. Simulation tools have an important role to play in assisting these new technologies by:

- shortening the duration and reducing the cost of development
- improve understanding of their potential benefits
- helping users to gain confidence to purchase such vehicles

Overall, effective simulation tools will significantly assist in the introduction of low polluting transport systems based on these new technologies.

CONTACT

Jaimie Swann   BEng (Hons), CEng MIMechE

Research Department
Motor Industry Research Association (MIRA)
Watling Street, Nuneaton, CV10 0TU

e-mail: jaimie.swann@mira.co.uk
web: www.mira.co.uk

APPENDIX

1. Series Hybrid Layout
2. VMS Class Hierarchy Diagram

1. Series Hybrid Layout

Daylight | Head Wind Speed | Payload | Time Distance Velocity Head Wind Speed Gradient

Body / Chassis

Tractive Effort
Aerodynamic Drag
Rolling Resistance
Acceleration Resistance
Climbing Resistance

Mechanical Auxiliaries | Lights | Electrical Auxiliaries | Cargo

Wheel

Torque Speed

Fuel
Engine
Battery
Controller
Motor
Clutch
Gearbox

Initial Tank Volume

Fuel — Chemical Energy — Engine — Torque Speed — Generator — Voltage Current — Controller — Voltage Current — Motor — Torque Speed — Clutch — Torque Speed — Gearbox — Torque Speed — Propshaft — Torque Speed — Differential

Vehicle Controller | ZEV Area

Voltage Current | Voltage Current

Differential
Wheels
Cooling System
Lights
Mech Aux
Elec Aux
Interior
Air Con

Torque Speed | Temperature | Voltage Current

Air Conditioning | Cooling System | Battery | Occupants

Torque Speed

Temperature

Interior

Wheel

VEHICLE SYSTEM BOUNDARY

Desired Temperature Ambient Temperature | Initial Battery SOC Opportunity Charging Power | No. of Occupants

Tractive Effort
Aerodynamic Drag
Rolling Resistance
Acceleration Resistance
Climbing Resistance

Time Distance Velocity Head Wind Speed Gradient

2. VMS Class Hierarchy Diagram

TObject

TVMSApplication (abstract)

TThermAirConnection | TThermLiquidConnection
TChemConnection | TElecConnection | TMechConnection

TRequirement (abstract) | TSimulation (abstract) | TSystem (abstract) | TSystemComponent (abstract) | TExpertSystem | TInitialise (abstract)

TVehicleDriveCycle

TVehicleSimulation | TVehicle

TVehiclePerformanceTest

TPowertrain | TSpecificSystemComponentType

TPowertrainPerformanceTest

TPowertrainDriveCycle | TPowertrainSimulation

TChemPowertrainDriveCycle
TElecPowertrainDriveCycle
TMechPowertrainDriveCycle
TThermAirPowertrainDriveCycle
TThermLiquidPowertrainDriveCycle

TInitInitialCondidtions
TInitVehicleSimulation
TInitPowertrainSimulation
TInitVehicle
TInitPowertrain
TInitVehicleDriveCycle
TInitVehiclePerformanceTest
TInitPowertrainDriveCycle

TInitChemPowertrainDriveCycle
TInitElecPowertrainDriveCycle
TInitMechPowertrainDriveCycle
TInitThermAirPowertrainDriveCycle
TInitThermLiquidPowertrainDriveCycle

TInitPowertrainPerformanceTest
TInitSpecificSystemComponentType

42

Styling for a Small Electric City Car

T. G. Chondros, S. D. Panteliou, S. Pipano, D. Vergos, P. A. Dimarogonas, D. V. Spanos
University of Patras, Greece.

A. D. Dimarogonas
Washington University in St Louis, Mo.

ABSTRACT

Design of electric cars faces a significant growth all over the world. Powered by rechargeable batteries these vehicles can contribute significantly to the reduction of the big cities' pollution. The shape of a vehicle in our times is of major importance for the market and it represents the car's philosophy and character. Styling requires the definition of the general dimensions and layout of the car in advance. Computer aided techniques were developed to support a systematic design process of E-240, a 2400 mm long electric mini-car, developed at the University of Patras.

INTRODUCTION

It is expected that the use of electric vehicles shall have a significant contribution to the improvement of air quality in urban areas in the very near future [1-4]. Such a large scale introduction is both technically feasible and socially acceptable. For the solution of other, non-environmental problems associated with intensive road traffic, such as congestion, the use of scarce space, and road safety advocate the design of new and integrated transportation concepts, which owe to be based, for passenger transport, on a more balanced ratio of private as well as public vehicles use, public transportation facilities etc. Within such transportation systems, to facilitate the introduction of electric vehicles these have to be designed in such a way to perform specific tasks, for which they are suitably tailored, and considering the existing technical limitations [5]. Although the change of the public preferences and mentality is necessary, it is expected that electric cars will be used in the city traffic exclusively, and possibly they will have only two seats, with the smallest dimensions permitted by ample crash length.

Electric vehicles are not just concept cars, but they are going to become part of the cars of the future. Of course, the cost of an electric car can't be compared with the cost of a thermal vehicle. Thermal vehicles are in use for over 100 years, and therefore they have already paid-off development cost. The technological problems which are connected to the electric vehicles are expected to be solved in the near future because of the increasing investments for R&D. The global auto industry is today refining car design with terrifying speed, by the fusion of many new technologies, notably in advanced materials, computer - aided design and manufacturing, all reinforced by new manufacturing and marketing strategies and innovative public policies [6-8]. In the case of electric cars, new aspects must be integrated in the design process such as body design, motors, microelectronics, power electronics, electric storage devices, energy management software etc.

The shape of a vehicle in our times is of major importance for the customer and it represents the car's philosophy and character. Styling begins by considering the fundamental overall requirements of the project. These are determined from different factors which tend to change throughout the years, and are dictated by market demands and improved techniques. Besides, physiological and psychological requirements, safety, materials selection, economic factors, and the changing trends of public taste, make styling a delicate balance between philosophy and science [9 - 13]. Although car manufacturers and designers have devised the appropriate tools for car design, in most cases these tools, including the software, are sophisticated, expensive and in general proprietary.

Engineering design is a creative process and one is tempted to say that it appears to the designer by revelation. Since the times of Aristotle and Hero of Alexandria [14], however, knowledge in engineering design has been identified to be empirical in nature while such empirical knowledge can be further enhanced by reason, in other words by the application of the knowledge gained by natural science through mathematical processing. The latter is thought not in the Pythagorean sense, that is, numbers constitute the fundamental knowledge, but in the sense that mathematics is a means to quantify and organize empirical knowledge based on observation and experimentation.

Engineering design has evolved over the millennia having an ever changing balance between intuitive application of experience and mathematical modeling of it [15]. Ancient engineers could obtain results that are comparable with the contemporary ones obtained with the application of natural science, mathematics and intense numerical computation. As an example, sizes of mass-produced manufacturing products usually conform to the so-called "Renard Series", that is, each size is the previous one multiplied by the n-th root of 10, n usually selected in the range 2 to 10. It was found that the sizes of standardized balance weights found in the West House of Acrotiri (in the Aegean island of Thera) of about 1500 BC. closely conform to the Renard 7 series (n = 7) while the sizes of Roman lead pipes conform almost exactly to the same Renard 7 series!

By the Alexandrian times, we have the first mathematical expressions for design equations in parallel with a substantial number of intuitive design rules described by the Alexandian Engineers (Ctesibius, Philo and Hero) and Vitruvius. These rules were followed very closely for more than 1,500 years until the days of the industrial and the scientific revolutions.

Extensive mathematical implementation of the empirical knowledge related with engineering design was made possible with the advent of continuum mechanics of the great mechanicians of the 16-19th centuries. Though in clear contrast to the knowledge of the discrete nature of matter, even since the time of the Ionian philosophers (such as Anaxagoras and Heraclitus), continuum mechanics played an important role in the mathematical development of the engineering design knowledge, together with natural science and engineering.

In recent times, the advent of digital computers brings back the Pythagorean notion of the impossibility for the existence of non-commensurable numbers with enormous implications in engineering design: one can hardly find now an engineering design endeavor that cannot be fully described in mathematical terms, even intuitive truths.

The final philosophical question on engineering design is our ability to reach the ultimate design, the one that surpasses any other possible design. It is certain that we are very far from an exact mathematical description of nature and there are many mathematical games showing the impossibility of such undertaking. This has a direct implication on engineering design where all our mathematical descriptions are based on, often times crude, assumptions about the geometry, the properties and the service conditions. It is however very dangerous to rush in denying the future possibility of an ultimate design based on our experience of recent times that progress has surpassed many of the predictions of impossibility, for example, of the machine beating a human in a game of chess.

Engineering design satisfies the practical needs of man and is related to the mankind while art satisfies the need of man to express himself and communicate his feelings. On the other hands, the engineered artifact and the work of art have something important in common, the form. Some say that the dividing line is in the fact that in engineering design there is a "method" a well documented procedure that, if followed by the designer, it will lead to a "good" product.

Such method obviously does not exist in fine arts. This assertion is only partially true. There are methods and procedures that govern the design of the form of engineering designed products but there are not (at least, not as yet) methods and procedures available for the detailed design of the form. The proof is easy: manufacturers of the same kind of product, the mid-size passenger car, for example, have at their disposal the same procedures and methods, materials, analytical methods, mathematics, computer programs, etc. Why, then, all the mid-size passenger cars are not exactly the same? The answer can be found in the fact of the intuitive truths that are not the same in different manufacturers. Intuitive truths are not all based on experience, thus even if two designers could conceivably have the same experience they would not possess the same intuitive truths. A crude way to define talent is the ability to synthesize intuitive truths from other intuitive truths, related or unrelated. Thus experience and talent is what makes the difference in specific engineering design decisions, for even the managerial decisions are (supposed to be) based on experience and talent. Thus engineering design has substantial overlap with art and this is why many, and the authors, believe that engineering design cannot be fully machine-automated in the foreseeable future.

Car design requires the collaboration of experts from various fields. The contribution of specialists from different sectors and their integration is necessary for the success of the design. Car design has consolidated its own methodology consisting of the model creation, the prototypes, and testing, that sometimes have direct effects on the design. This type of design evolves continuously. Technology concerned with design and car manufacturing becomes obsolete and updating must be continuous. Today, most of the large car manufacturers offer electric vehicles for sale, and they have prototypes and small test fleet in operation. Minor automobile manufacturers or subcontractors offer electric vehicles for sale.

Most of the electric cars in production are at least as safe, and their cost comparable, to mass-production cars. But, detailed design is often neglected in order to reduce cost. In the frame of the aforementioned conditions, and expectations for the future of the electric vehicle, the capability for the design of these vehicles by small enterprises or research institutes is necessary, in order to support their successful first steps.

A project for the development of a small two-seater electric city car started at the University of

Patras in 1990. The intention of this attempt was to combine the design of a small electric city car with modern car-body, with the development of the necessary design tools. The objective was the creation of a functional, good-looking, easy to be manufactured with low cost and existing technology small electric car.

Figure 2 Closed body

-Comfortable space for two passengers.
-Small external dimensions.
-Simple and light construction.
-Mechanical parts available from existing passenger cars
-Sufficient safety, active and passive.
-Reliability and low servicing.
-Low production cost.
-Flexibility of the body design to be easily adapted for different uses.

Figure 1 Artist's free-hand sketches of an electric city car.

THE STYLING PROJECT

The words "styling" and "stylist" are common enough today, though the art of styling has existed from the earliest times. Leonardo da Vinci (1452-1519) a great artist-designer-craftsman, successfully combined pure art and science, thus becoming the founder of modern styling [14]. Industrial revolution gave rise to industrial design and the term styling associated with it. The general use of the term stylist, however, is quite recent; it was introduced into the automotive industry in the early 1920s to distinguish between its visual and mechanical designers, and has been retained ever since.

Styling commences with considering the fundamental requirements of the project. For the electric vehicle to be designed, the preliminary investigation determined that the car should satisfy the following requirements:

Fig. 3 Open body

The aforementioned requirements in combination with the mechanical and electrical parts selection and arrangement [16-19], gave way to the creation of freehand-sketches as shown in Figures 1,2 and 3. From freehand sketches of the many forms and vehicle variations, finally, the visuals shown in Figure 4 were investigated with a view to refining the details and ensuring their physical compatibility. The design of the E - 240 body had to adopt formal treatments not necessarily innovative, while preserving the modern conception of the electric vehicle. This task was facilitated after the decision for use of composite materials for the body construction. During the creative

and formal definition phases of the project different solutions were considered. The ergonomic study of the interior in conjunction with the electrical and mechanical parts arrangement defined that the monovolume concept was feasible [16].
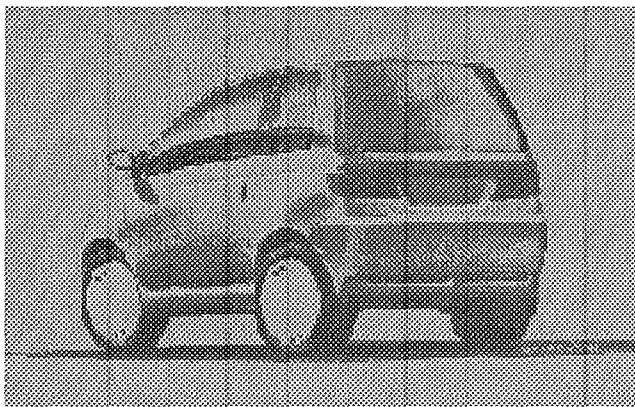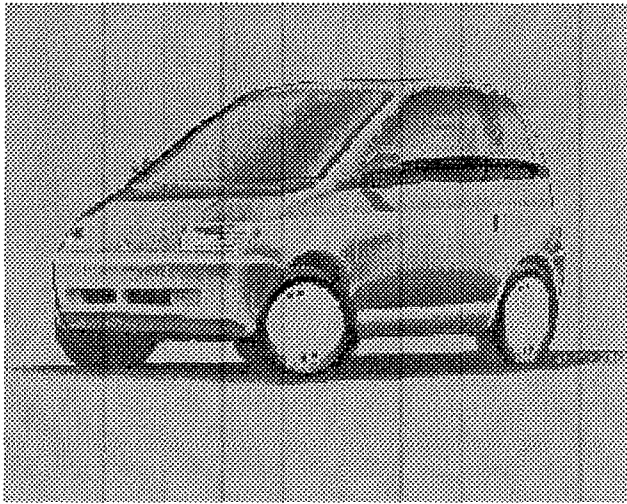
Figure 4. The visuals of the exterior form

In a typical production car moving on level urban roads, one third of the power supplied to its wheels beats the brakes, one third the air, and one third the tires and road. In highway driving, air resistance, rising as the square of speed, becomes a dominant 60-70% of wheel power [20]. Consequently, improvements in the field of electric cars include reducing vehicle weight, aerodynamic drag, tire rolling resistance, and bearings friction, and increasing the efficiency of the electric motor and its control electronics as well as regenerative braking. Aerodynamic drag is proportional to the product of drag coefficient, Cd, times effective frontal area, A. Both can be markedly reduced, and this is one of the principal tasks of the designer. The biggest Cd saving comes from simply making the bottom of the car as smooth as the top.

Low Cd is easier to obtain in a large than a small car because there is more room to avoid rear-end discontinuities, and the influence of the ground plane ranges from neutral to favorable with good design

(which must provide adequate ground clearance). The other aerodynamic drag factor, frontal area, is also reducible by better packaging and styling. More compact powertrain components permit steeply downsloping bonnets, which in turn permit more visibility with less glass, and hence less mass [21]. For the elimination of aerodynamic drag provisions were taken for use of existing technologies such as: optimization of airflow beneath the front hood and the side members, flush windows, bonding of the windshield, rear window and side window, and also the use of front and rear fairings, as well as the formation of an almost smooth bottom.

THE INTERIOR STYLING

Figures 5 and 6 show the range of typical habitable compartment dimensions for car design and driver's seat configuration [22]. A computer-aided design algorithm was developed for the selection of the interior main dimensions. A Quick Basic program is used to "discuss" with the designer the choice of the main dimensions of the car, such as, wheel-base, total length, height, width, and other dimensions necessary for the design process. The program offers extensive help both on car design general procedures and recommended practice, as well as to crucial dimensioning points i.e. the seating reference point (SRP), the hip point (H point) etc.
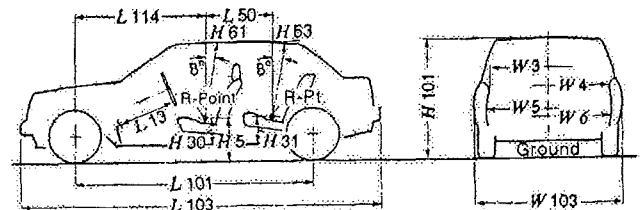
Dimension			Subcompact car mm		Long car mm
H	5	R-point to ground, front	460	to	510
H	30	R-point to accelerator heel point, front	240		300
H	31	R-point to accelerator heel point, rear	300		310
H	61	Effective headroom, front	940		980
H	63	Effective headroom, rear	920		950
H	101	Vehicle height	1360		1400
L	13	Steering wheel to brake pedal	480		630
L	50	R-point distance (front to rear seat)	710		830
L	101	Wheelbase	2430		2880
L	103	Vehicle length	3840		4930
L	114	Center of front wheel to R-point, front	1250		1590
W	3	Shoulder room, front	1310		1430
W	4	Shoulder room, rear	1290		1420
W	5	Hip room, front	1260		1430
W	6	Hip room, rear	1240		1470
W	103	Vehicle width, overall	1620		1820

Figure 5 Basic dimensions of the habitable compartment

46
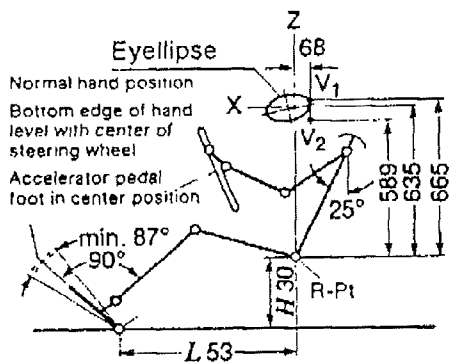
Figure 6 Driver's seat configuration

Once a set of values has been determined they are saved in a data bank and they are available for future projects. The screen before the conversion of the selected initial dimensions in a DXF file appears as in Figure 7. After the introduction of the main dimensions from the designer, the program determines the position of the basic mechanical parts of the car, and creates a drawing file defined as DXF.
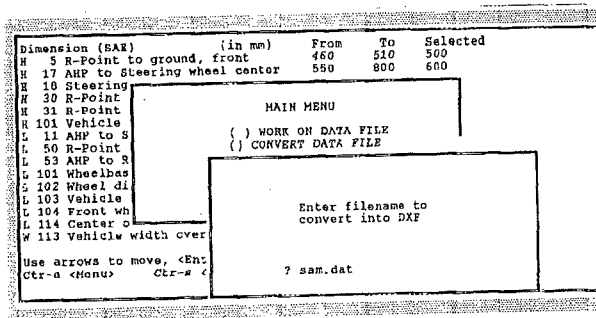
Figure 7 The working environment with full-screen editor

This file can be read, and therefore reproduced on screen, by most drawing packages. A drawings library contains wheels, floor, bumpers, windshields, steering wheel and passengers' body mannequins. By inserting the appropriate DXF file in the drawing package and selecting the option for a new drawing using the DXFIN command, the user creates a first approach of the car's layout. Figure 8 shows the result of this procedure for the general case of a four-seater car.

In the drawings database there are also available a motor, a transmission box and batteries. These elements can be manually inserted by the user at their desired positions and, furthermore, be scaled as shown in Figure 9 where the electric motor and controller was placed in the front and batteries in the front ant rear of the car.
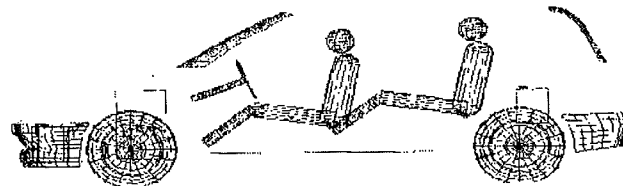
Figure 8 A first approach of the interior compartment arrangement.

From the combination of the information stored in the DXF file and the mechanical components drawing library, a first approach of the interior habitability of the car can be obtained. Also, the arrangement of the main mechanical and electrical components can be evaluated. Modifications in the main dimensions may be introduced, which imply the creation of a new DXF file. This is shown in Figure 9 where the initial overall length of the car was reduced to form a hatchback car, and the power and drive-train elements are positioned in place. This technique helps designing the car from the interior compartment.
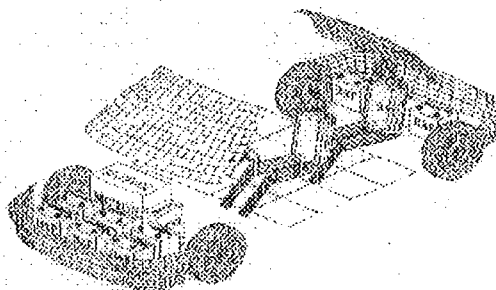
Figure 9 Arrangement of electrical and mechanical components

At this stage, the designer has an overview of the feasibility of the project. All the fundamental components - passengers, mechanical and electrical parts, windshields, bumpers, floor - are disposed in their positions. Modifications by the designer concerning the positioning of the batteries and mechanical components are easy to be made since this operation can be accomplished manually on the screen. After the determination of the desired layout, the DXF file used contains the basic points coordinates that must be used for the three-dimensional drawings of the car. The three basic views of the car body have to be adapted after the artist sketches on the views plotted from the existing DXF file and produce the orthographic drawings shown in Figure 10. These drawings will give an idea of the feasibility of the proposal and, furthermore will serve as a basis for the creation of the body wire-frame.
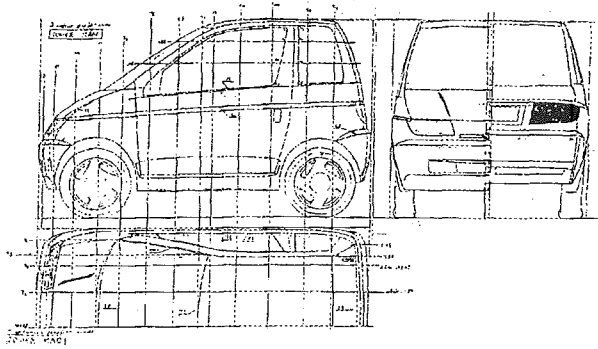
Figure 10 The orthographic drawings

The wire-frame model is shown in Figure 11. After the completion of the wire-frame model the "edgesurf" command is used to produce a surface model. Smoothing of the designed surfaces can be achieved with the aid of the appropriate functions available in the drawing software. Smoothing is a necessary step to optimize styling of the exterior form, and facilitate the manufacturing procedure for the body panels.
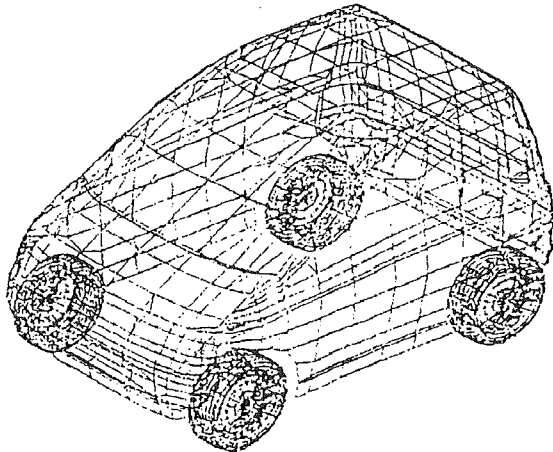
Figure 11 The wireframe

THE EXTERIOR FORM

From the artist's work, Figure 4, the creation of the drawings for the front view, side view and top view was achieved with the aid of the drawing software. These drawings were used for the generation of the external form model and also, to check the compatibility of the passengers' space dimensions with the aid of two-dimensional adult mannequins. The external form model was made of polystyrene cubes attached together with polyurethane and cut in shape by an electric wire. The surface was covered with plaster and rubbed until it became totally smooth. Finally, it was painted and some items such as mirrors, door handles, front and rear lights, trimming material and wheels were placed on it. A specially designed and constructed

measuring device helped to provide the required symmetry between the two sides of the model, Figure 12.
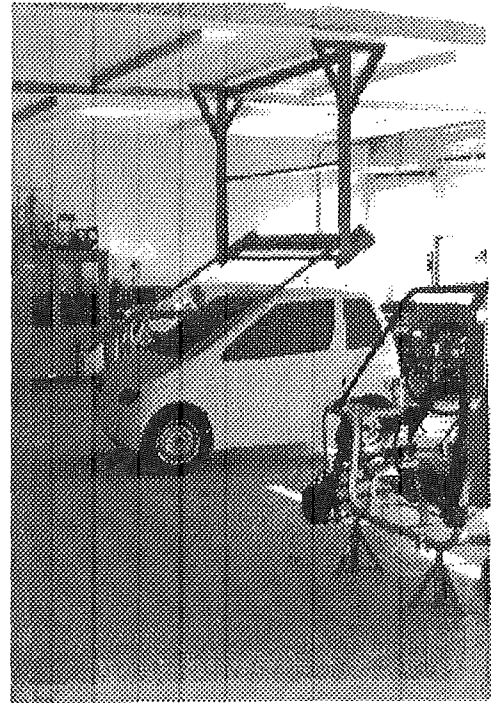
Figure 12 The pantograph

The completion of the design of the chassis and the body, gave way to two parallel processes:
   a. The creation of a full scale plaster model Figures 13 and 14.
   b. The construction of the chassis with an open-type steel body for the testings Figure 14.
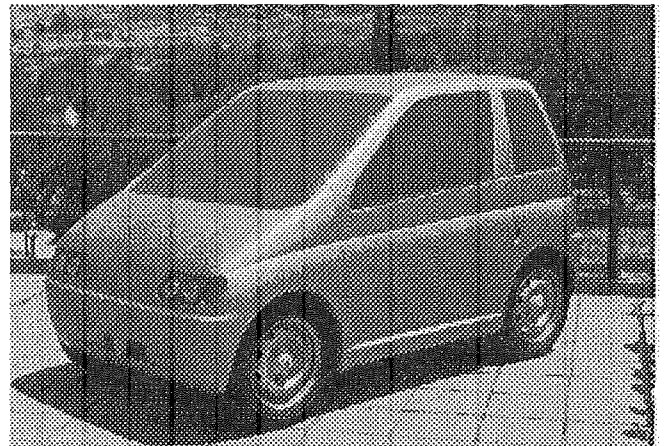
Figure 13 Full scale model of E-240, front view.

The design of a small car has to harmonize the normal compared to other vehicles' dimensions, height and width, with the small length. Simple and smooth lines forming rounded shapes were used throughout the design process to diminish the impression that the car looks like a cube. Also, rounded shape eliminates the static feeling coming from the big and vertical

48

passenger compartment. The absence of corners - a trend followed by almost all car designers - gives an impression of dynamism to the vehicle. The monovolume concept, preserved throughout the design process, asked for a shortened, steeply downsloping bonnet with the same inclination as that of the windshield, and wheels placed at the extremes of the bodywork. The windscreen is of fairly large dimensions permitting the positioning of one wiper, and all the glass elements are curved. The extension of the windshield towards the front contributes to a further increase of the cabin volume. The absence of the radiator grille accentuates the living space upwards. Headlamps consist of twin round-shaped lights with the direction indicator lights coming flush with the side of the fenders. Below the front bumper, on the lower fairing, two horizontal slits permit air flow for the ventilation of the electric motor and front batteries stack, as well as passing of the recharging spring-extended cable.

Figure 14 Full scale model of E-240, rear view.

One of the basic requirements of the external form was the reduction of the static feeling coming from the increased height of the car as compared with other dimensions and especially limited length. In order to preserve an image of dynamism a wedge shape was given to the belt-line. In this way, better visibility is achieved for the driver by releasing a larger area for the side mirrors, at the lower front end of the front windows. Raised belt-lines imply that the window areas are not overdone, thus eliminating solar radiation at the interior.

Below the belt-line another line starting from the headlamps and passing over the tail-lamps forms the lower edge of the tailgate. This peripheral line determines the beginning of a slight increase of the body width, to encompass the increased space requirements of the wheels arches, as well as to reinforce the doors and side panels. The lower part of the door is somehow hollowed, a trend starting to be followed in production cars. As it was identified after a detailed observation of different forms for the lower part of the body, this type of curvature change offers smooth transition from the edges of the body, where the wheels are placed, to the upper part of the body where the

glasses are placed.

The wraparound door, a technology adopted by almost all car manufacturers, closes flush with the gutterless roof thus eliminating the number of external panels and facilitating the assembly process. The necessity of obtaining the maximum space from the interior of the car asked for an almost vertical rear tailgate. This option did not give the dynamism shown in most small passenger cars, derived from a generous bend onto the side of the hatch, giving a sense of movement. Thus, the rear end of the second side window had to form a slanted thick C-pillar transmitting "thrust" to the whole body, eliminating the static feeling coming from the almost vertical tailgate. The tailgate consists mainly from the windshield, with its lower end coming flush with the tail-lights. Just below it, vertical tail-lights wrap around the corners without disturbing the peripheral line. Since batteries were to be put at the back of the car there wasn't the need for a flange to lower the tailgate between the tail-lights. Instead this flange forms an integrated part with the rear bumper thus permitting easy removal and positioning of the back batteries stack on the car.

Figure 15 The testing prototype.

The overall dimensions of the model are: 2440 mm length, 1410 mm width, and 1480 mm height. The wheelbase is 1660 mm long and the wheeltracks are 1250 mm front and 1180 mm rear. The ground clearance with normal loading conditions varies between 110 - 180 mm. For comparison, the corresponding dimensions of the FIAT Cinquecento utility car, one of the smaller cars in production, are: 3227 mm length, 1487 mm width, and 1435 mm height.

Since electric cars have to last for years, to be environmental friendly, their design must not follow fashion but rather design techniques that use the most suitable materials and commercially available software. Simplified design methodology is very important in order to provide flexibility to small companies and

preserve a continuous "dialogue" between engineers and stylists.

THE MANUFACTURING PROCESS

Electric cars must remain light while combining roomy interiors with ample crash lengths. Yet better materials and design can also substitute for crash length. Composites and other ultra strong net-shape materials will dominate in electric cars. They would bounce without damage in minor collisions. Under severe loading, composite structures fail very differently than metal. However, even under compressive loading - often considered composites' weak point - composite structural elements show high and in many cases better energy absorption performance than comparable metal structures. Extensive aerospace experience is available from aircraft composite structures. Painting - the costliest, hardest and most polluting step in carmaking, accounting for nearly 90% of some major automakers' hazardous toxic releases, and for almost half of assembly plants' capital cost and body parts' total cost - will be eliminated by the mould color technique already in use.

Bodywork is strictly related with the existing manufacturing technology. Economical design solutions require a reduction in the number of panels and assembly operations. The car may be considered as belonging to the super utility segment. To preserve flexibility of the manufacturing process the chassis (the under-frame) was constructed as a separate part from the body. With such an arrangement, it is possible to build cars with different types of bodies - one of the initial requirements - and simplify the assembly process [16]. This type of design for the body allows for a substantial reduction to the costs of restyling in case of different use of the car, since the main dimensions and shape of the lower part of the body are not going to be modified. The ladder type frame with the mechanical parts attached on it and independent sub-frames bearing the front and rear suspension with the wheels, provides additional flexibility to the assembly process.

Small cars produced in Japan and from some small firms in Europe are using miniaturized mechanical components, in order to reduce weight and space requirements. The initial requirement for use of available from normal cars mechanical parts, apart from the ease of availability, assures for the reliability and low cost of this equipment. Thus, 13 inches wheels diameter was selected in order to achieve an unlimited availability of front suspension struts with disc brakes assemblies, these components being used from all car manufacturers. The front suspension is of McPherson type, and the rear one consists of a transverse leaf-spring and vertical dampers and A-type wishbones. Both front and rear suspensions are mounted on auxiliary sub-frames that are anchored to the main frame by means of silent-blocks.

The two motors are placed transversely under the seats and the power is transmitted to each of the front wheels with the aid of transmission chains running inside the tunnel. The controller of the motors and the charger are located under the dashboard. Behind the front seats there is enough space for the position of a 3 kW portable generator (hybrid version). The conventional power unit compartment in front of the car is used for the location of 60% of the accumulators with the rest located over the rear axle. Testing and evaluation of the drive-train gave the necessary feedback to redesign various components of the body concerned with the suspension of the mechanical and electrical parts [23-24] .

The use of the individual frame makes possible the application of different bodies on the same chassis. This is an advantage for a flexible manufacturing procedure The floor panels from the rear bumper up to the airbox will be constructed as an integrated part which serves as a guide for the attachment of the side panels. The side panels with the doors are to be constructed separately and fastened on the truss frame. The bonnet with the front fenders is an integrated part with the front bumper which opens upwards, thus facilitating the removal of the front stack of batteries. An artist's conception for the assembly procedure [25] of the car is shown in Figure 16.
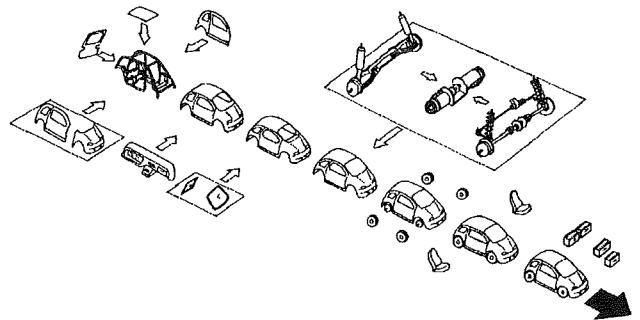
Figure 16 The assembly line.

CONCLUSIONS

The development trends for cars are determined, on one hand, by the expectations that politicians, ecologists and economists have, regarding future automobiles and, on the other hand, by emerging technologies contributing to new possibilities in car design. It is expected that environmental concerns and resulting legislative measures will have large influence on future car development. Electric car will play an important role in this direction. With the existing level of technology in accumulators the reduction of the passengers transportability and the dimensions of the electric car as compared to conventional cars is expected.

The main characteristics of the chosen design are the rounded one-box shape with extremely compact dimensions, very short overall length, excellent visibility and good entering and leaving characteristics, combined with good aerodynamics and unique design.

The body can be constructed by recycled composite light materials with good rigidity and strength characteristics. The mechanical parts have been chosen from normal cars, and arranged so that the minimum space is reserved. The short overall length, the long - associated to the overall length - wheelbase, and the roomy interior, generate a functional and maneuverable vehicle.

The outlined procedure provides an algorithm for styling and design of an electric city car. This methodology needs commercially available software drawing packages and can be easily adopted by small car manufacturers. The proposed algorithm provides the capability of modifications during the styling of the car, from conceptual design to detailed drawing, so that the end result - the aesthetics and the car function - are optimized to the benefit of its identity, personality and use.

CONTACT

Thomas G. Chondros, Assistant Professor, University of Patras, Department of Mechanical Engineering & Aeronautics, Patras, 265 00, Greece.
E-mail: chondros@mech.upatras.gr
Andrew D. Dimarogonas, W. Palm Professor of Mechanical Engineering Department, Washington University in St Louis. Campus Box 1185, 1 Brookings Drive, St. Louis, Missouri, 63130-4899. Email: add@mecf.wustl.edu.

REFERENCES

[1] Society of Automotive Engineers, Inc., 1992, *Electric and Hybrid Vehicle Technology*, SP-915, USA.

[2] Society of Automotive Engineers, Inc., 1991, *Electric Vehicle, Design and Development*, SP-862, USA.

[3] Bates, B., 1992, *Electric Vehicles: A Decade of transition*, Society of Automotive Engineers, Inc., PT-40, Warrendale, Pa.

[4] McCrea S., 1991, *Why Wait for Detroit? Drive the Car of the Future Today*, South Florida Electric Auto Association, Florida USA.

[5] Maggetto, G., 1992, *Advanced Electric Drive Systems to Reduce Pollution*, European Association of Electric Road Vehicles (AVERE).

[6] Kent Stiffler, A., 1992, *Design with Microprocessors for Mechanical Engineers*, McGraw-Hill, Inc.

[7] Dimarogonas A.D., 1988, *Computer Aided Machine Design*, Englewood Cliffs,N.J., Prentice-Hall.

[8] Dimarogonas A.D., 1992, *MELAB, Computer Programs for Mechanical Engineers*, Prentice - Hall, Englewood Cliffs, NJ 07632.

[9] Giles J.G., 1971, *Body Construction and Design*, Butterworth & Co Ltd, London.

[10] Society of Automotive Engineers, Inc., 1991, *Exterior Body Panels and Bumper Systems*, SP-859.

[11] Pawlowski J., 1969, *Vehicle Body Engineering*, Editor G. Tidbury, Business Book Limited, London.

[12] Maroselli J.C., 1958, *L' automobile et ses grands problemes*, Larousse, Paris.

[13] Seiffert U., P.Walzer, 1991, *Automobile Technology of the Future*, Society of Automotive Engineers, Inc.

[14] Dimarogonas A. D., 1986, *History of Technology*, Symmetry Publ., Athens, 3rd Edition.

[15] Dimarogonas, A.D., 1997, "Philosophical Issues in Engineering Design", Journal of Integrated Design and Process Control, Vol 1, No 1, pp 54-75.

[16] Chondros, T. G., Michalitsis S. M., Panteliou, S. D., Dimarogonas, A. D., 1994, "Chassis Design for a Small Electric City Car", SAE International Congress & Exposition, Detroit, MI, USA.

[17] Chondros T.G., P.A. Belokas, K. Vamvakeros and A.D. Dimarogonas, 1997, "Vehicle Dynamics Simulation and Suspension System Design", 96MJA508, SP-1223, SAE International Congress and Exposition, Detroit MI, USA.

[18] T. G. Chondros, D. Dokos, S. Tselepis, T. Romanos and P. Valachis, 1997, "Computer Aided Design and Monitoring of Drive Trains for Electric Cars", 1st European Conference on Clean Cars, National Technical University of Athens, Greece.

[19] T. G. Chondros, S.D. Panteliou, D. Dokos, S. Krouskas, and A. D Dimarogonas, 1997, "Computer Aided Design and Control by an Expert System of Drive Trains for Electric Cars", 30th ISATA Conference, Paper No 97AE031, Florence, Italy.

[20] Artamonov M.D., V.A. Ilarionov, M.M. Morin, 1976, *Motor Vehicles, Fundamentals and Design*, MIR Publishers, Moscow.

[21] Lukin P., G. Gasparyants, V. Rodionov, 1989, *Automobile Chassis, Desing and Calculations*, MIR Publishers, Moscow.

[22] Society of Automotive Engineers, Inc., 1991, *ON-Highway Vehicles & OFF-Highway Machinery*, HANDBOOK Volume 4.

[23] Chondros T.G., A. Papageorgiou, A. Georgacopoulos, P. Baltas, 1994, "Testing and Evaluation of a Mini Electric City Car", 27th ISATA International Symposium on Advanced Transportation Applications, Aachen, Germany, Proceedings p.p. 217 - 228.

[24] Chondros, T.G., A. Darzentas, T. Voutsinas, A. Georgacopoulos, and P. Baltas, 1994, "Performance Evaluation of EV Power Trains", 12th International Electric Vehicle Symposium (EVS 12), Anaheim, Ca, USA, Symposium Proceedings Vol. 2, p.p. 668 - 677.

[25] Chondros, T.G., 1996, "Design and Industrialization of Electric City Cars", Conference on Environment - Development - Civilization, University of Patras, Greece.

Patents and Alternatively Powered Vehicles

Rob Adams
Derwent Information, United Kingdom

ABSTRACT

This morning/afternoon I intend to look very briefly at the nature of patents and how they can be used as an integral part of the product development process. In particular I will look at three different forms of power and power storage currently being developed. These are lithium batteries, fuel cells and hybrid Vehicles.

Within this paper I have looked at these developments in electric vehicle technology by using patent abstracts from 40 different issuing authorities over a five year period. To do this I have searched on-line using Derwent's World Patent Index (DWPI), a collection of 16 million patents abstracts going back some 40 years, and have used the various statistical analysis tools that are available with the file. From this analysis I have identified which companies are the major players in the development of each of the technologies I have focused upon.

My conclusions will show that published patent applications are the largest available single source of technical information in the world, giving a comprehensive coverage of all technical areas, providing details of existing technology, thus saving money on repeated research, as well as giving a insight into the activities of your closest competitors, or equally as important companies who you didn't recognise as working in the same field of technology as you! In particular I believe that this analysis will show the strength of Japanese companies in the electric vehicle technology market.

INTRODUCTION

Before analysing the patent activities of the various companies working in electric vehicle development I would like to refresh your memory as to the nature of patents:

A patent is a bargain between the state and inventor, in which the inventor can obtain up to 20 years protection against unauthorised copying of his invention. In return for this the inventor must file a full and detailed disclosure of how the invention works.

In the engineering sense this means that the patent can be likened to a technical specification where someone skilled in the particular technology should be able to understand and recreate the device being patented. Obviously this can't be done on a commercial basis unless an agreement is made to license the technology from the inventor, or the patent has expired, or alternatively the original patentee has let the patent lapse before the end of it's term by not paying the yearly maintenance fees. Patents are also a valuable source of 'prior art', that is knowledge which already exists in form of past inventions. In fact a compulsory part of the patent examination process requires the gathering of prior art published world-wide.

In the right format patent information can detail a company's most valuable technologies or focus on a competitor's current R&D developments and as such is therefore useful in the process of product development, which should require you to have a full understanding of how technology is moving, who is at the forefront of technological developments and what opportunities there are available for licensing existing innovations.

MAIN FEATURE OF PATENTS

Currently there are 198 patent offices world-wide, which over the years have published over 40 million patents, an awful lot of information. An interesting point put forward recently in a report by the UK patent office shows that there is 1 new patent published in the world every minute of every day, with Japanese companies in the forefront. In fact Hitachi alone files on average about 5 new applications at the US Patent and Trademark office every day! On the Derwent system there are details of approximately 16 million patents stretching back over the last forty-five years.

FMC 1016

The main benefits to be gained from patent information are:

- They are often the first source of published information on new technology. This is the first time the invention has been made known in the public domain. To secure patent rights the details of the patent must be kept secret before the application is submitted. Most patents are published 18 months from filing.
- They are frequently the only source of information on a new invention. Studies have shown that 70% of the information in patents is never published elsewhere.
- Patents provide full and practical descriptions of the inventions. As I mentioned before in the introduction the text of the patent specification must have sufficient detail and include illustrations, so that an expert specialising in the field can recreate the invention.
- Patents offer comprehensive citation intelligence. Applications include search information that cites similar and other related literature on the subject matter of the invention. Such supplementary information provides a useful insight into the development of the particular technology.
- Standardised layout enables easy comparison of patent documents. Although there are exceptions, patent specifications have become standardised in their layout.
- Much of the information contained in patent specifications is freely available for public use, because the owner has not paid the renewal fees or the because the maximum 20 year term has expired.

These are the main benefits of patent information as an information use. I will now go on to briefly discuss how this information can be used in the business environment.

USES OF PATENT INFORMATION

As I mentioned before there is a vast amount of information available, but how can this be used as a tool in the product development process?

- Avoiding duplication of effort and infringement. searching world-wide patent literature should always be carried out at the start of any R&D programme, to avoid wasteful and costly duplication. The concept may already be protected by a patent, or perhaps patent protection has expired and the invention is freely available. A European report has been published which states that 30% of all R&D duplicates work already done - that is £50 million pounds every day in Europe alone!
- Current Awareness. Patents can be an invaluable source of up-to-date intelligence on upcoming technology in a particular technical field. In most cases patents are applied for in the early stages in the development of an invention and the eventual

product in the marketplace, so organisations who keep aware of developments may spot new ideas within their own industry early on. This may point to diversification or development in a different, more valuable direction.
- Licensing opportunities. Even if an invention is protected by a patent it may be possible to negotiate a licence for its use.
- Competitive Intelligence and technology trends. Monitoring of patent information increases the awareness of your competitors and the technologies that they are developing, and from a strategic point of view can be used to analyse the trend of patent applications by a particular company over a set time period, e.g. 5 or 10 years. I will use trend analysis in the next section of this paper to show companies researching and developing in the field of fuel cell technology. An increasing portfolio of patent applications on a particular topic could suggest a strong possibility that the company intends to release a product in that field in due course.
- Inspiration. Browsing through patents on a subject of interest can encourage the development of new ideas, particularly since some concepts are often transferable to unrelated industries.

Moving on to look at an analysis of the Electric Vehicle patenting. This analysis shows some interesting trends.

ELECTRIC VEHICLE PATENTS 1992 - 1996

Using Derwent's World Patents Index database I searched for patents published to companies, by year, between 1992 and 1996. I should remind you that the actual filing dates of these inventions will be approximately eighteen months before the publication. This enables patent applicants to take full advantage of international agreements allowing filings in other countries of commercial interest within one year of initial filing, while obtaining the same basic ('priority') date.

The search is restricted to patents related to electric propulsion and power supply for automobiles, for the 40 patent authorities covered by Derwent.

Table 1 - Electric Vehicle Patents 1992 - 1996

Electric Vehicle Patents

54
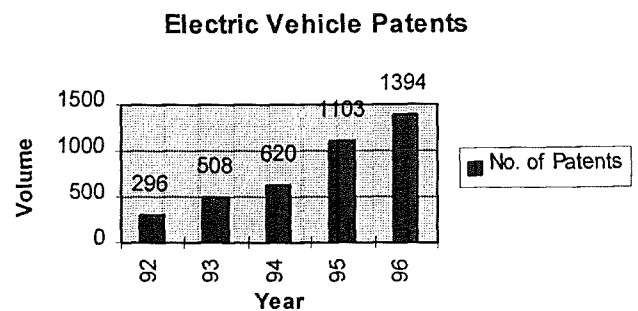
The chart shows that there has been a considerable increase in the amount of patenting activity in this field since 1992. By examining the priority countries, i.e. the countries in which the published patents were originally filed and, normally invented, we can see in which countries the bulk of the research is being performed.

This time I will look at the patents published between the years 1994 and 1996. That amounts to 3,117 patents, again from the 40 countries covered by DWPI.

Table 2 - Patent Publications by Priority Country 1994 - 1996

Patent Publications, By Priority Country
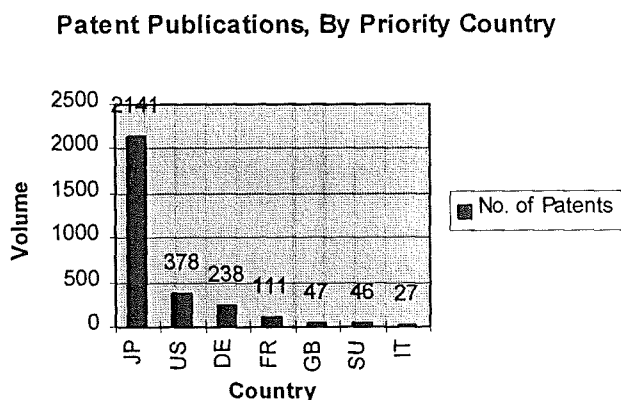
This table really is significant when you take into account that the priority country is generally the location where the research has taken place, i.e. where the invention has been made. Far in front are the Japanese, with over 2000 patents in a three year period relating to electric vehicle technology. Following the Japanese are the United States and then Germany. This, I believe, illustrates the importance of competitive intelligence with respect to Japanese companies in particular. By following the patenting activities of these companies you are better able to determine their research and development plans.

The previous tables show patenting activity generally in the field of electric vehicles. I would now like to look at three different technologies. For this paper I have chosen fuel cells, lithium batteries and hybrid vehicles.

CASE STUDY 1 - FUEL CELLS

This is a technology that was originally developed for the space sector in the 1960s. Fuel cells silently combine hydrogen and oxygen to create electricity and water, making them one of the most promising electric vehicle technologies. A wide variety of prototype systems are under development - while some car makers, for example, are storing compressed hydrogen and oxygen at normal temperatures on board, others take in air and store methane, using integrated 'reformers' to convert it into hydrogen.

Similar to the search I had prepared for the subject of electric vehicles, I again ran a search on DWPI over the time period 1992 to September 1997. This time the search was restricted to only those new inventions in the field of fuel cells. The results are shown in table 3. As you can see there has recently been a rise in the number of patents in this particular technology.

Table 3 - Fuel Cell patents 1992 - 1997

Fuel Cells
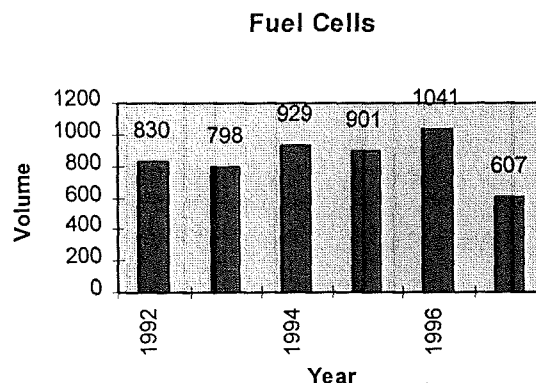
Another interesting analysis of the patents in this field can show which are the main countries of research. By looking at the priority countries for each of the patents we obtain the following results as shown in table 3.

Table 4 - Patent Publications by Priority Country 1992 - 1997

Priority Countries for Fuel Cells
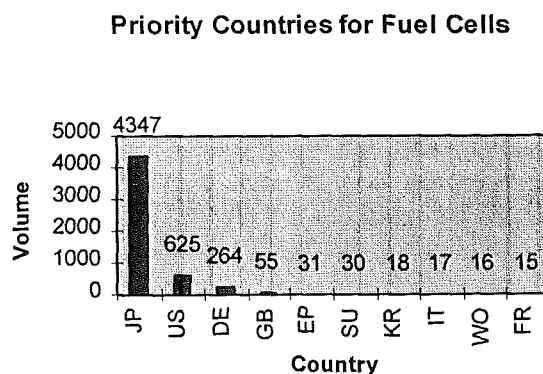
From table 3 it can be seen that Japan is at the forefront of technological development in the field of fuel cells. Normally the priority country is where the research has taken place. Taking this into account the number of Japanese patents by far exceeds those in the US.

Looking more closely at the companies applying for the patents I did an analysis of the top ten patenting companies in the field of fuel cells, applying for or being granted patents up until September of this year. The companies are ranked in descending order in table 4.

55

Table 5 - Top Ten Patenting Companies 1997

Company	Country
Fuji Electric	Japan
Toshiba	Japan
Mitsubishi Jukogyo	Japan
Tokyo Gas Co.	Japan
Sanyo Electric Co.	Japan
Osaka Gas Co.	Japan
Ishikawajima Harima Heavy	Japan
Nippon TT Corp	Japan
Siemens	Germany
Honda Motor Co.	Japan

Table 4 clearly shows the strength of the Japanese in this particular technology. Only one company out of the top ten patenting organisations in the field of fuel cells isn't Japanese, that company being Siemens of Germany.

If I move on to look at another area of technology of relevance to the automotive industry, I can again show the strength of Japan.

CASE STUDY 2 - LITHIUM BATTERIES

This is an interesting field of research currently being undertaken in the pursuit of a solution to the problem of providing power to an electric vehicle. Two areas of power storage technology exist in this field. These are lithium hydride batteries and more recently lithium ion batteries. The latter technology is currently used to power portable computers and cellular telephones. It is hoped this type of battery will solve the existing problem of providing a longer source of power.

I ran a search on DWPI, again over the years 1992 up to September 1997, and listed the total number of new inventions from the 40 authorities covered by Derwent. This search was restricted to only those patents related to the automotive industry. The results are listed in table 6.

Table 6 - Lithium Battery patents 1992 - 1997
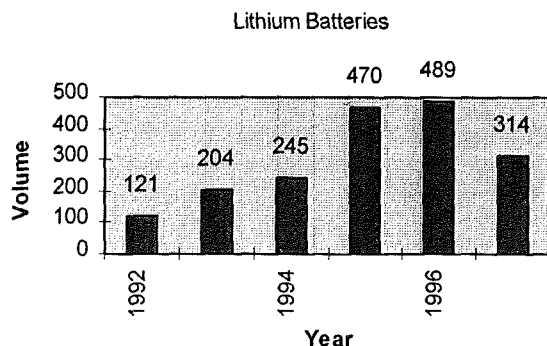
Lithium Batteries

As you can see the number of new inventions in this field of lithium batteries has risen from 121 in 1992 to a high of 489 in 1996. So far this year up until the start of September there has been 314 new inventions.

Turning now to analyse where the research for this technology is taking place, we can look at where the patent was first filed. As I had mentioned, generally this is a good indication of the country in which the research has taken place. The priorities are ranked by country in table 7.

Table 7 - Patent Publications by Priority Country 1992 - 1997

Priority Countries - Lithium Batteries
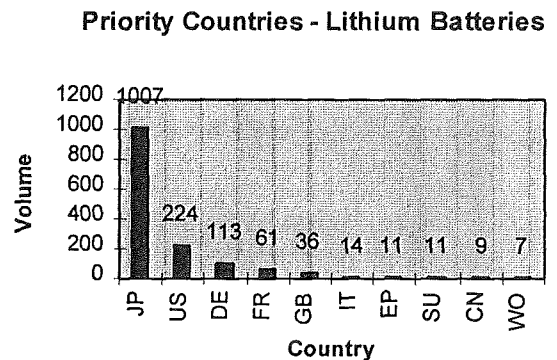
As before with the general analysis of electric vehicles we can see that the majority of the research is again taking place in Japan. Over the time period of the analysis over 1000 patents originated in Japan, while the US were second with 224 and Germany was third with 113 originating patents in the field of Lithium batteries.

To further emphasis the strength of Japan in this field, I have ranked the top ten companies holding patents in this technology. As you can see in table 8 the top ten companies patenting in the field of Lithium Batteries in 1997 are all Japanese.

Table 8 - Top Ten Companies in Lithium Battery Technology - based on 1997 new inventions

Company	Country
Nissan Motor Company	Japan
Mitsubishi Motor Company	Japan
Honda Motor Company	Japan
Toyota Motor Company	Japan
Hitachi	Japan
Sumitomo Denso	Japan
Yazaki	Japan
Matsushita Denki	Japan
Toyoda Automatic Loom Works	Japan
Yamaha Motor Company	Japan

56

Whilst we need to bear in mind that Japanese companies tend to patent more generally, it is still quite clear that they are at the forefront of research into lithium battery technology.

CASE 3 - HYBRID VEHICLES

For my final case I would like to look at the patenting activities as before, this time in relation to new inventions in the field of hybrid vehicles. Many engineers believe that the technology offers the best solution to the problem of developing an economically viable alternatively powered vehicle. I have used International Patent Classifications and Derwent's own internal classification system, as well as some keywords to determine which records should be retrieved in this field.

As with the case 1 and 2, I ran a search on DWPI to over the years 1992 up until September 1997. This search is limited to new inventions in the 40 authorities covered by Derwent. The results are shown in table 9, ranked by year.

Table 9 - Hybrid Vehicle Patents 1992 - 1997
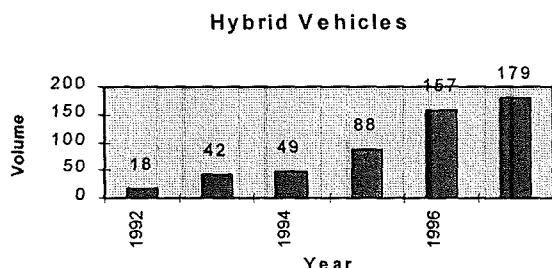
Hybrid Vehicles

As with fuel cells and lithium batteries, the number of new inventions in the field of hybrid vehicles has risen considerably over the years, from 18 in 1992 to 179 in September 1997.

By analysing the priority countries I can again show that Japan is again where the majority of the patented research is taking place. This is shown clearly in table 10.

Table 10 - Patent Publications by Priority Country

Hybrid Vehicles
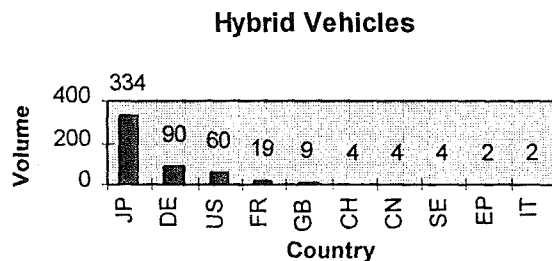
Germany is second to Japan in this particular technology, ahead of the US and France. An analysis of the German patents would show the top companies in this field. However in a bid to be consistent I have again chosen the patents published in 1997 to show the top ten companies in the field of hybrid technology. These are listed in table 11.

Table 11 - Top Ten Patenting Companies in Hybrid Technology 1997 (up to September)

Company	Country
Equos Research	Japan
Toyota Jidosha	Japan
Aisin AW Co	Japan
Mitsubishi Company	Japan
Nippondenso Company	Japan
General Motors	US
Honda Motors	Japan
Audi	Germany
Clouth Gummiwerke	Germany
Hino Motors	Japan

While the Japanese Companies do again dominate this list, there are two German companies and General Motors from the US in this list. Certainly the numbers of patent applications in this technology and indeed the other two technologies I looked at will rise over the coming years.

This has been a short introduction to the possible benefits and uses of patent information. I hope that this has provided you with some interesting facts on patents and in particular in relation to the electric vehicle industry. I believe that mass produced electric vehicles will be commonplace by the year 2005, although I wouldn't like to try and predict the power source. That is just left up to you the research, development and design engineers. We can arm you with the technical information that will enable you to stay ahead of your competitors, and equally as important stay abreast of the new technological advancements in your field.

I would like to finish with a quote from a source within the European Commission's department of technology transfer:

"one cannot refuse to invest in the future, and then be surprised that the future slips away"

CONCLUSIONS

My conclusions from this paper are really to reiterate the fact that patent information is comprehensive and valuable, covering all technical areas. It can provide savings on repeating research, to provide new ideas and impetus or to keep an eye on competitors' activity. Using patent effectively can enable a company to seize control over development initiatives and thus lay the bedrock for business success. I feel that in the field of electric vehicle

research it is essential to be aware of the development plans and activities of Japanese companies, as much of the research in this technology is taking place in Japan.

ACKNOWLEDGMENTS

REFERENCES

1. Derwent's World Patents Index On-line file, Derwent Information, London

58

FMC 1016

An Electric Vehicle with Racing Speeds

Edward Heil, Colin Jordan, Karim J. Nasr, Keith M. Plagens,
Massoud Tavakoli, Mark Thompson and Jeffrey T. Wolak
GMI Engineering & Management Institute

ABSTRACT

The Formula Lightning is an exciting part of GMI Engineering & Management Institute's motorsports program. This project is an excellent opportunity for students to apply and test their acquired classroom skills in practical applications. Competing in six race events annually, students are exposed to high caliber competitions in engineering design, combined with the thrill of racing.

The Formula Lightning is a unique high-speed electric vehicle. Most of the challenging engineering tasks lie within the drive train design and battery system efficiency. Part of the battery system design and development includes a quick and reliable technique for exchanging battery packs under race conditions. Designed and built by GMI students, this project encompasses all fields of engineering giving experience with mechanical and electrical design as well as project management and marketing.

INTRODUCTION

Formula Lightning Electric Vehicle racing was created as yet another step toward advancing Electric Vehicle technology. Through competition, college students at many universities are contributing to the advancement of electric vehicles.

GMI purchased a chassis in April 1995, to enter competition with other Lightning teams. Over the last year and a half, designs for electric propulsion systems have been developed. These designs were developed to have the capability of propelling the vehicle at speeds of 120 MPH. A battery system, which powers the drivetrain, was designed to allow a battery exchange within a 16-second pit stop.

FORMULA LIGHTNING HISTORY

Some major advances in harnessing electricity to power vehicles are being made by college students. They can race their Formula Lightning cars with a silence that seems out of place at a racetrack, but may become quite commonplace, in the near future. Formula Lightning Racing was developed by Solar and Electric Racing Association (SERA), in association with the Electric Vehicle Technology Competition (EVTC) in 1993, to aid in the advancement of technology used in the maintenance and operation of electric vehicles.

The races bring together some of the country's brightest college students, each seeking a way to optimize the performance of their school's entry into the electric race. All entries must use a standard chassis, with modifications occurring only in the battery exchange and drive system of the car. The cars are of open wheel design, allowing room on the sides for traction batteries, which provide energy for propulsion. Besides the benefit of participation in the advancement of electrically powered vehicles, the races bring about teamwork and application of learned engineering skills.
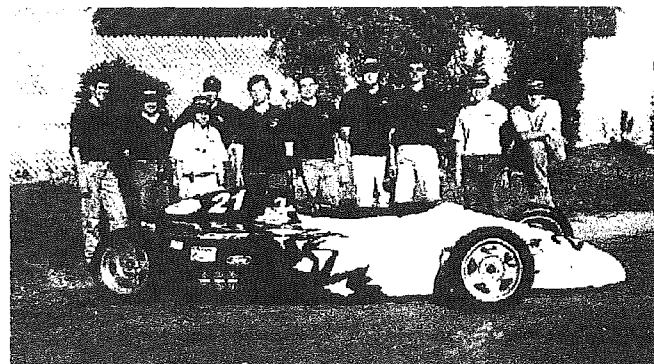
GMI Formula Lightning Team

GMI TEAM STRUCTURE

GMI first entered into competition in February of 1995. Many of the team members were familiar with the operation of electrically powered vehicles; most had participated in the development and success of the GMI hybrid electric vehicle (HEV), and were eager to approach a new challenge.

The GMI Lightning Team is one of the Institute's unique teams because it has both A-section and B-section students working on the same project. The A-Section student body attends school from January through March and again from July through September. During this time, the B-Section student body is working at a cooperative employer. It is at the end of these intervals that the student body exchanges roles. The B-Section population returns to school in April and October respectively, while the A-Section population works at their respective cooperative employer.

Because of this co-op arrangement, there is a great emphasis placed on the organization of the team. Strict documentation must be followed to inform the opposite section of developments with the vehicle. Checklists and master documents that record progress have been implemented to aid in this effort. Master documents are kept with the team's advisory board, and communication is established to assure efforts are not duplicated.

Leadership of the team has been broken down into several functions. Controlling the master documentation is the job of the team faculty advisors, representing both mechanical and electrical engineering. For each student team section, there is an appointed team leader. Beyond that, leadership is divided into several areas that govern component implementation and operation (i.e. battery team, drivetrain team, etc.). Weekly meetings are conducted to inform the on-campus team of latest events, work in progress, and to develop new ideas for team advancement. As a means of keeping the entire team informed of current events, an e-mail document containing the weekly meeting minutes is forwarded to both sections of the team.

SPONSORSHIP AND PUBLIC RELATIONS

One of the things quickly learned about racing is the fact that it takes a great deal of talent, but even more money. With an annual budget in excess of eighty thousand-dollars, skills in running a small business are definitely required. Immediately apparent was the need to raise money beyond the initial fifty thousand-dollar start-up grant from the General Motors branch of the United Auto Workers (UAW-GM).

Ideas were formulated about pursuing sponsorships, and it was immediately apparent that the alumni body of GMI could benefit the most from participation. Coincidentally, GMI was actively pursuing alumni events throughout the country to bring alumni together. When the ideas were meshed the Lightning team and the GMI alumni office combined efforts. A trial event in Phoenix, Arizona was conducted in March of 1997, to bring alumni in contact with current students. This synergistic effect led to the donation of funds that purchased the current drive system. This developing relationship has led to continuing support from alumni and corporations across the country. Geographically, the

team has utilized alumni in finding local event specific sponsorship. These sponsors benefit from increased local exposure the team can provide through vehicle display and media relations.

GMI has actively pursued media attention a means of public relations. A local newspaper distributed around the Detroit area publishes stories on our recent events as well as post race information and photographs. GMI's alumni newspaper has joined in and now dedicates a section to the Lightning. Television coverage has been sought actively as well. ESPN2 broadcasts one Lightning race annually, and local television is involved whenever a testing session is planned.

MECHANICAL

All of the Lightning teams start with a specified chassis and develop a drive train and battery system to propel it. Twelve hundred pounds of batteries are changed during a pit stop that lasts only sixteen seconds. Power from the electric motor is transferred through an aluminum-housed differential propelling the car to speeds over 120 miles per hour.

DRIVE TRAIN

The drive train consists of a motor coupling and a differential. A 120 kilowatt, nominal, 150 peak horse power, Advanced DC motor with an Electric Vehicle Components Ltd. (EVCL) "Godzilla" controller is used. This motor will only deliver 120 horsepower at the shaft due to internal resistance, and the inefficiency of power conversion for this motor, as with most DC motors; peak horsepower is attained at the motor's top speed of 7000 rpm and peak torque is at 0 rpm. A Magnaloy magnesium alloy coupling, rated at 550 foot pounds, is used to join the motor to the differential. The cast aluminum differential finds its origins in a Lincoln Mark VIII. It is equipped with limited slip and can be equipped with gearing ratios from 2.47:1 to 4.10:1 depending on track requirements. Testing has been conducted to optimize motor operating efficiency and life vs. expected racing conditions.
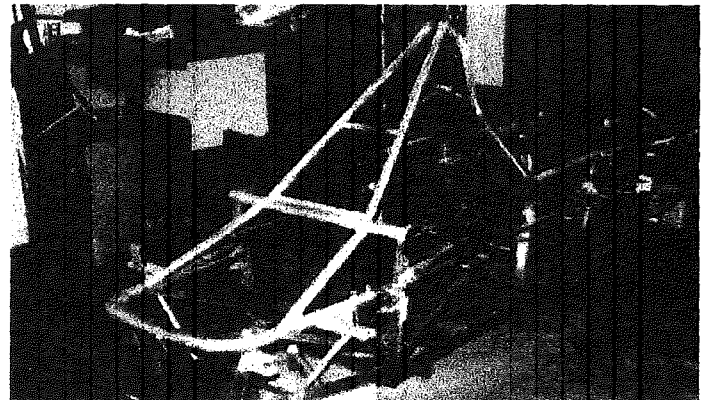
Figure 2: Formula Lightning Chassis

BATTERY EXCHANGE SYSTEM

The intent of the battery exchange system is to exchange the entire traction battery set with another in a minimum period of time. In the GMI system, forty-eight batteries weighing 24 pounds each need to be exchanged. GMI's solution is to separate the batteries into boxes, four batteries per box with six boxes on each side of the car. Forty-eight boxes have been built to provide four sets of batteries that will be used during competition. These packs provide a manageable means of moving the batteries and contain any fragments in case of an accident. The packs are made from aluminum angle bar that is TIG welded together (Figure 1). DuPont Lexan™ is used to form sides and fully encase the packs. When complete with wiring and plugs, the boxes weigh 102 pounds each. A series of rails designed to accept the boxes, were built into the side of the chassis. A two-terminal plug is used for the electrical connection, and a pin is used to guide the box into proper location. As the boxes are slid into place, the electrical connectors mate, completing the circuit. A steel bar has been molded to the body so when the battery door closes all the packs are secured (Figure 2). Latch handles are located in the rear wheel wells and are locked by bringing the lever over the center. When the side of the car closes, a handle is thrown and hooks are pulled over a bar that is attached to the body.

For visual verification of security, the handles have been oriented so the handle protrudes from the body envelope when unlatched. In the GMI team's last attempt, all of the batteries were successfully exchanged in a pit stop lasting less than 16 seconds.

ELECTRICAL

The electrical content of this paper describes the batteries, dashboard layout, the motor controller and the high voltage-wiring layout.

BATTERIES

The batteries used in the GMI Formula Lightning are made by Hawker Energy Products. The model used is a Genesis® sealed lead acid battery. This particular battery is effective for several reasons. Most important is the high energy density (28.7 Watt-hours per Kilogram). Another, the Genesis battery features a low internal resistance, which allows extreme current draw with little drop in pack voltage. The low internal resistance also supports fast recharging. Typically, 90% of the battery's energy can be replaced in less than one hour using the correct charging algorithm (discussed in a later section). Also, the battery is a robust enough to handle heavy current draw without gassing. Since the batteries are a sealed lead acid, and gassing is not significant, there is no required maintenance on the battery packs.

The 26 Ah Genesis battery was selected for electrical, as well as packaging concerns. The 26Ah battery weighs only 24 pounds and has a footprint measuring 6.5" X 6.9" and a height of 4.9". Due to its method of construction, it can be mounted in any position. These features offer great flexibility in pack configuration as will be discussed later.

PACK CONFIGURATION

The GMI Formula Lighting Battery System is responsible for holding 48 26 Ah Genesis® batteries. The battery pack consists of 12 boxes, each of which houses 4 batteries. The boxes are configured into 3 parallel strings of 4 boxes. Each of the 4 boxes in a string is wired in series to give a total of 192 Volts. Three strings of 4 boxes result in a combine output of 192 Volts with a 78 Ah capacity.

The main benefit of a parallel configuration includes reduced current draw and multiple current sources. This is important in reducing the effects of weak batteries in a series string. A high voltage string increases the number of batteries in series. A greater number of batteries will increase the probability of imbalance. Imbalance is the inequality of the relative capacity of each of the batteries in a series string. The weaker of the batteries in such a string will diminish overall capacity, but will not limit the current flow in the pack. As a result, the weaker batteries can be severely discharged well below the 100% depth of discharge mark of 10V. These undercharged batteries will get progressively worse and cause problems in other batteries during charging. Using more lesser voltage strings in parallel will help reduce the effects of a bad battery by masking it during discharge, and isolating it during charging.

The benefit of a series configuration is higher pack voltage. This is not beneficial in battery management, but is better in reducing I^2R losses in the drive system. At a higher voltage, less current will be drawn at a given power output. Less current results in higher efficiency.

With the current drive train, three 192Volt strings are the best compromise of voltage and capacity. The Advanced DC Motor is rated for a maximum of 192 Volts and testing has shown that high motor current coupled with voltages near 192 volts results in severe arcing. This arcing sets the upper voltage limit on the motor. By utilizing this highest pack voltage, current draw is reduced, lowering I^2R losses in the form of heat. It is also beneficial in achieving highest peak horsepower.

BATTERY CHARGING

The charging of the battery packs is accomplished using an adjustable DC power supply to implement a mixed charging algorithm. The charger is capable of supplying 6720 watts with a maximum of 28

amps on the primary or secondary of the autotransfomer. The GMI charger is setup to supply 28 Amps at 240 Volts on the output. This limitation in current requires the batteries to be charged with a constant current at the start of charge, and a constant voltage at the conclusion of the cycle. Each string of 192 Volts is charged separately.

With the lead acid battery, 15% more energy than drawn out must be replaced. The low internal resistance of the battery allows large initial charging currents to be accepted, and must be limited to protect the charger. This is accomplished by reducing the output voltage of the charger to maintain 28 Amps. The voltage can then be raised as the battery takes on a charge to maintain 28 Amps. This is done until 240 Volts is reached (15 volts per battery). At this point, a constant voltage is maintained until the current drops down to zero.

Typically, 90% of the energy is replaced in about 50 minutes. At this point the current draws is usually 5 amps or less. This trickle charge is then continued for several hours to restore the remaining 10% of capacity.

DASHBOARD WIRING AND CONTROLS

There are a total of 4 switches for the driver to operate. A master power switch controls the CRM (Master Control Relay). This switch activates the 12-Volt power and begins pre-charging the controller. The next switch energizes the main contactor to power up the controller, the controller cooling system, and removes a short across the two speed pot wires. This short provides assurance the car will not move off the capacitor charge even if the accelerator is depressed. Additional switches are used to control a emergency taillight and motor cooling fan. A large E-Stop style button is used to setoff the Halon fire suppression system.

A mixture of analog, and digital meters are used to monitor vehicle systems. The batteries are monitored with the use of a Cruising Equipment E-Meter. This meter utilizes a voltmeter and ammeter to monitor battery status. Voltage is input through a voltage pre-scalar to lower the voltage level into the meter. Current is measured across a 500 Amp 50 mV shunt. The meter is programmable to accept the Peukert exponent describing the battery. Peukert's equation is as follows: $C_P = I^n t$ where C_P = Peukert Capacity in Amp Hours, I = current in Amperes, t = time in hours, and n=(log t_2 – log t_1)/(log I_1 – log I_2). The constant n is determined experimentally by running two discharge tests at different currents.

By using this exponent and the logarithmic Peukert equation, battery capacity can be more accurately approximated. An RS-232 serial port allows data to be dumped into a memory module or computer for later use.

A J-type thermocouple is used to monitor motor brush temperature. A small hole is bored into the center brush and the thermocouple is secured using an epoxy type adhesive. This data is displayed on an analog gage in the dash panel.

Motor Current is measures across a 1000A 50mV shunt. This is read on an analog meter. Using an analog meter is necessary to capture a true RMS measurement on the motor current. The signal from the shunt is superimposed with a great deal of noise from the pulse-width-modulated controller. The analog meter is better able to handle this noise, as well as being easier to read while the current changes.

Motor RPM is read through a standard automotive tachometer. The tachometer is setup for a four-cylinder engine, which would fire two pulses per revolution. These pulses are developed off of an encoder wheel on the output shaft of the motor and picked up using a DC proximity switch.

MOTOR CONTROLLER

Supplying power to the motor is accomplished through the use of a motor control system. Currently, the GMI utilizes a "Godzilla" DC motor controller from Electric Vehicle Components Ltd. (EVCL). This unit utilizes microprocessor controlled insulated gate bipolar transistors (IGBT's) to limit the flow of power to the motor. Specifically designed for electric vehicle racing, the "Godzilla" unit is capable of carrying up to 336volts and 1200amps. In racing conditions the microprocessor control allows the user to limit battery and motor supply currents. With a supply voltage of 192volts, limits had to be obtained for current at the nominal voltage. Limits for the Advanced DC motor combination were established experimentally. Temperature is the largest obstacle in increasing power delivered to the motor. Recording temperature data from the motor, while running it on a water-brake dynamometer established a constant current motor limit of 600amps. This limit is subject to the availability of adequate forced air-cooling.

HIGH VOLTAGE WIRING

The high voltage wiring utilizes a 1/0 and 2/0 welding cable grade wire. The connection to the batteries is accomplished through an Anderson Carbolon SB175 Connector. The connector is a three-piece unit: a plastic housing and two silver-plated contacts. The contacts have the capability of handling 175 Amps, and can accommodate a 1/0 cable.

The negative side of each of the three192 V strings is wired to include a Bussman® FWX-250A semiconductor fuse in series. The fused negatives are then routed to a Kilovac® Bubba contactor. From the contactor, a 2/0 cable is used to the motor controller. The positives are switched through two Flaming River Emergency disconnects. From the main disconnects a 2/0 cable is used to connect to the motor controller.

A pre-charge circuit is used to provide a controlled method of charging the capacitors in the motor controller. This is necessary to prevent a large inrush of current when the car is powered up. A time constant of 4 seconds is used for the EVCL Godzilla controller. As an additional safety feature, a discharge circuit is included.

HAZARDS AND SAFETY CONSIDERATIONS

Formula Lightning racing has many possible hazards related to both the actual racing of the vehicle, as well as to the basic maintenance. With regards to the Formula Lightning, hazards of major concern are stopping the car, securing the valve regulated lead-acid batteries used to power the car, and controlling fire onboard, if it does occur. Because the management of these hazards is so critical, not only for the sake of the individual driver, but also for the other participants with which the car is competing, EVTC has issued, in the specifications, rules regarding safety.

Stopping the car quickly requires that the brakes be able to lock all four tires at any speed. Lightning vehicles are capable of speeds in excess of 140 MPH, therefore braking is a major factor. In order to meet this requirement, the team has implemented four-wheel disc brakes with carbon-metallic linings. Stopping takes on another meaning for the Formula Lightning because it is an electric vehicle. A vehicle developing an electrical fault or overload must employ some method of being disabled. A master disconnect switch is included for this purpose.

The master disconnect disconnects all main battery powered equipment including the motor and related gauges. This switch is for use during times when no driver is in the car, i.e. during maintenance or repair periods. This switch is located on the outside of the vehicle. There is also an emergency disconnect switch on the instrument panel of the vehicle which will, when actuated, disconnect power to the controller and to the Kilovacs. The need to secure the batteries is crucial for two reasons. The first reason is that the batteries contain a sulfuric-acid mixture, which is highly corrosive. If they should fall out during a race or an accident, the result would be a very dangerous situation. The second is that the car contains around twelve hundred pounds of batteries. If the batteries should suddenly shift or fall out of the car, the risk of accident and injury to the drivers becomes very large.

It is for the safety of the driver and other participants that EVTC has also set rules for the battery support structure in addition to battery enclosures. In order to fulfill these requirements, the team has designed as system whereby the main batteries, numbering 48, are divided into boxes of four batteries each. These boxes are made of an aluminum frame with Lexan on all six sides. These boxes not only protect the batteries and serve to contain spills if they occur, but also ease in the exchange operation during pit stops. As far as securing the battery boxes, the battery exchange system described earlier provides the necessary support and locking capabilities required by the vehicle specifications.

A halon type fire suppression system is used in the car. This system is controlled by a single switch on the vehicle's instrument panel and is designed to extinguish fire in either of the battery pods on the sides of the car or in the motor compartment to the rear of vehicle.

Safety requirements designed into the car are as follow: A break-away cockpit engineered to separate from the car in a serious collision. Five-point driver restraints, as well as arm restraints, keep the driver within the vehicle's envelope. Crushable aluminum honeycomb structure in the front of the car acts as a sacrificial energy absorber in a front-end collision. All electrical components are isolated to reduce the risk of electric shock and short circuits. Cockpit controls are flat black in color to reduce driver glare and eyestrain. Also, an onboard communication system was implemented to maintain communication with the pit area.
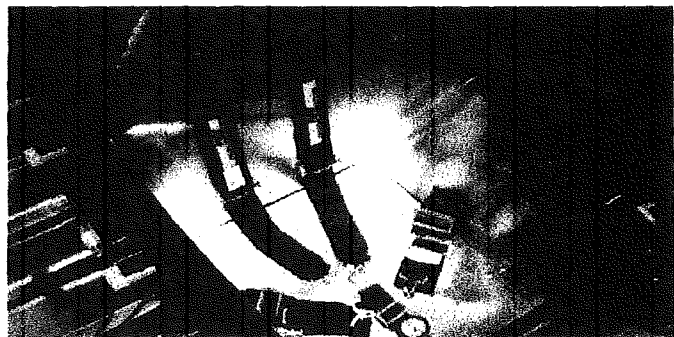
Figure 3: Vehicle cockpit with driver restraints

When students are working with an electric vehicle, the hazards are present not only for the drivers during the races but also for the supporting team members. Electric shock and burns are always a possibility when working with high current batteries. Due to the high voltages used, special care must be taken when servicing the vehicle. Team members are required to take a class, outside of school, regarding basic circuits and battery safety. Safety goggles and acid proof gloves are required when handling the batteries. Also all tools that are used on the batteries are insulated. A buddy system has been implemented when work is being done on the car to reduce the chance of human error leading to accidents.

Racing the Formula Lightning can be fun, but special care must be taken to keep it safe. The team has taken many steps to maintain safety at all times, both during the race and during maintenance. The safety of each team member comes first.

CONCLUSIONS

The emergence of Formula Lightning racing was due to the increased concern toward electric vehicle technology. The GMI team has worked diligently to make GMI a contender in the Formula Lightning races. They built upon their experience with the HEV design, and dealt with the mechanical, electrical, and safety aspects of the project. As with many GMI students, their time was occupied with their studies, but they still managed to develop the Formula Lightning vehicle. The new challenges that were imposed upon the team were overcome with a swift and focused approach.

REFERENCES

1. Electric Vehicle Technology Competitions, Ltd. *Vehicle Specifications.* January 1, 1996.

2. Hawker Energy Products Inc. *Genesis Application Manual.* Second Edition. March 1996.

64

FMC 1016

Battery State Control Techniques for

Charge Sustaining Applications

Herman L.N. Wiegman
University of Wisconsin - Madison

A. J. A. Vandenput
Technical University of Eindhoven

ABSTRACT

A foundation of battery normalizations, modeling and control techniques is presented for charge sustaining HEV applications. Charge and voltage based battery state observers and controllers are compared. The voltage based technique is shown to provide robust state control, as it directly constrains terminal voltage. Additionally, it provides good power cycle efficiency, and is insensitive to the initialization and drift problems characteristic of charge based controllers. Special attention is given to VRLA batteries, and dynamic loads from typical driving cycles. Future work is introduced which identifies battery power capability and efficiency as possible state control variables.

INTRODUCTION

Electric Vehicle (EV) based battery models and monitors have focused on predicting the State-of-Charge (SOC), or State of Energy (SOE). These methods have normally been based on Amp-hour integrators which are modified by rate and temperature information.[1, 6, 11] The monitors focus on giving the user "effective" or "useable" charge remaining information. The 3 disadvantages of these empirically based SOC/SOE monitors are;

- a priori empirical data required to modify estimate based on current rate, direction and temperature

- difficulty in initializing charge state value

- integrator drift and errors over long driving cycles

These weakness are minimized for short term discharge applications (EV's), where a slightly pessimistic end-of-charge estimate is acceptable. Acceptable battery monitoring results have been obtained.

Other empirical battery models are based on the terminal voltage behavior as a function of discharge current and stored charge. Shepherd's model requires similar empirical a priori knowledge before accurate results about battery state can be obtained.[2] Burke (1986) introduced a similar method for determining relative battery state from voltage drop information.[5] These references formalized the concept of loaded voltage as an end-of-charge indicator for EV's.

Hybrid Electric Vehicles (HEV's) employing electrochemical energy storage require new methodologies of battery state monitoring and control. Battery charge control divides HEV's into two broad groups; Charge Depleting (CD-HEV), and Charge Sustaining (CS-HEV).[14] CD-HEV's operate the battery as a pseudo fuel tank, much in the same way as EV's. CD-HEV's are often able to use EV type battery state monitors to help determine engine operating modes.

CS-HEV's actively control the battery state's operating range and operate the battery as a Load Leveling Device (LLD). The battery tends to be smaller than those in EV's or CD-HEV's, hence the relative current and power stresses are much higher. These high stresses and continuous cyclic power flow make charge remaining algorithms impractical. The distinctly different nature of LLD's and probable lack of over-night charging, requires a new approach for successful battery state control for CS-HEV's.

It is the aim of this paper to compare charge and voltage based control techniques for CS-HEV's battery state regulation. Special attention is given to Valve Regulated Lead-Acid (VRLA) batteries and dynamic driving cycles. The robustness of the different battery state control schemes will be discussed.

SYSTEM OF NORMALIZATIONS

The fields of Electro-Chemistry, System Design, and Electrical Engineering all use incomplete and sometimes arbitrary systems of normalizations to describe battery parameters. Table 1 shows a comprehensive set of electrical normalizations for batteries which was initiated by reference [4]. Typical per unit (pu) value ranges specific to CS-HEVs are also given in Table 1. The subscript "n" is reserved for the normalizing base quantities.

Table 1. System of Electrical Normalizations

Parameter	Base Quantity	Units	Range
Charge	Q_n = Rat. Capacity	A-h	0.1~1 pu
Voltage	V_n = Nom. Voltage	Volts	0.8~1.2 pu
Energy	$E_n = Q_n V_n$	W-h	< 1 pu
Time	$t_n = 1$ h	Hours	0.1~5 pu
Current	$I_n = Q_n / t_n$	Amps	+/- 5 pu
Power	$P_n = V_n I_n$	Watts	+/- 5 pu
Impedance	$Z_n = V_n / I_n$	Ohms	.02~.1 pu

The system of normalizations used in this paper does not use standard MKS units for Charge, Energy and Time. The units of A-h, W-h and hours instead of Coulombs, Joules and seconds were chosen for simplicity and due to industry practice. Some comments on the system are listed below.

- It is recommended that Q_n be defined at the 20 hour rate, or as the ideal Faradic Charge of the active mass.

- The V_n base quantity is defined at the 100% SOC, open circuit voltage at rated temperature, which adjusts to both acid concentrations and chemistries.

- The above base quantities can be applied on a cell, module, string, or complete system level. It is also chemistry independent.

All battery parameters in the follow plots are normalized. Time is not normalized in the plots or equations out of convenience for the reader.

BATTERY MODELING

An electrical equivalent circuit model of an electro chemical cell is presented which features conservation of charge and energy, and includes a gassing circuit. The objective of the simple physical model is to avoid the weaknesses of previous empirical models while providing sufficient complexity to provide an adequate backbone for charge, energy, voltage and power based battery state estimation and control techniques.

ELECTRICAL MODEL

Schöner (1988) introduced a battery model with a gassing circuit, which is essentially reproduced here in Figure 1.[7] The model's main feature is the separation of
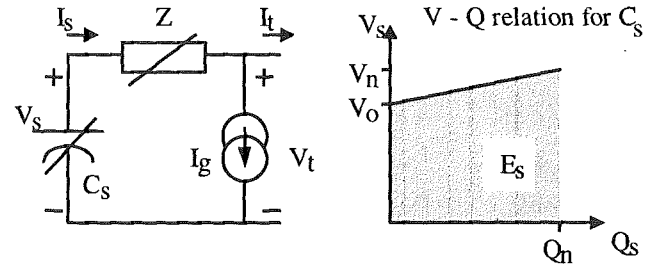
Figure 1: Electrical equivalent circuit model used for battery state controllers. The model obeys conservation of charge and energy, and includes a gassing circuit. The plot of V_s vs. Q_s shows the open circuit voltage relation, while the shaded area represents stored energy.

parallel processes in the electrochemical cell. This is vital for accurate charge estimation required by charge sustaining applications. The two circuits of the model are the *redox circuit* (Z, C_s), and the *gassing circuit* (I_g). The gassing current, I_g, is an exponential function of the terminal voltage and linear function of temperature. The Tafel relationship for a typical VRLA battery is included in the Appendix and is extractable experimentally.[7] The gassing relationship is also known to be age insensitive.

The series impedance element, Z, is represented as a single, non-linear, lumped element. This element represents the three components of the Randles-Ershler impedance model; diffusion, double-layer (charge transfer) and electrolyte components, which can be characterized over temperature, rate, and SOC.[9, 12] The Z element is assumed to be primarily resistive in the range of 0.01 to 0.1 Hz which is the range of concern in many CS-HEV's applications which can avoid significant diffusion resistance effects by charge cycling the battery on a moderate time scale (< 5 minutes).

MATHMATICAL RELATIONS

The mathematical relations of the above model are given below. Subscript "g" is reserved for the *gassing* circuit variables, subscript "s" is reserved for charge *storage* variables, and the "t" subscript is reserved for *terminal* quantities.

The mathematical relations for State of Charge (SOC) estimation, terminal voltage behavior and efficiency performance are given below. Additional relations are included in the appendix for completeness.

Equations 1 through 4 establish the basis for charge estimation in the battery model. Equation 1 defines the gassing circuit current as a function of temperature and terminal voltage. A more complete description of the Tafel gassing relation is given in the Appendix.

$$I_g = f(V_t, \text{Temp}) \qquad \text{[A]} \qquad (1)$$

$$I_s = I_g + I_t \qquad \text{[A]} \qquad (2)$$

66

where $I_g \geq 0$, and I_s & I_t are bi-directional.

$$Q_s = Q_0 - \int I_s \cdot dt \qquad \text{[A-h]} \qquad (3)$$

$$SOC = \frac{Q_s}{Q_n} \qquad \text{[pu]} \qquad (4)$$

The initial charge in the capacitor, Q_0, must be know to obtain an accurate estimate the battery charge content. In this paper, no further Peukert style modifications are applied to the definition of SOC. Separating the gassing current from the redox current allows for accurate (<1% error) SOC estimation.

Equations 5 and 6 describe the voltage behavior of the model. Equation 5 defines the charge storage voltage, V_s, as a function of the actual (not estimated) stored charge, Q_s. Both the nominal voltage, V_n, and the offset voltage, V_0, must be experimentally measured at 100% and ~0% SOC respectively. For lead-acid systems, these two voltages are assumed to be temperature independent and the relationship is assumed to be linear over stored charge.[3] The resistance term R is assumed to be the dominant Real term of Z.

$$V_s = V_0 + (V_n - V_0) \cdot \frac{Q_s}{Q_n} \qquad \text{[V]} \qquad (5)$$

$$V_t = V_s - I_s \cdot R \qquad \text{[V]} \qquad (6)$$

The instantaneous power efficiency of the battery model is defined in Equation 7. The power efficiency is a function of current rate, SOC, and temperature. The Power Cycle Efficiency is defined in Equation 8 as the product of charging and discharging power efficiencies. This can be evaluated at some nominal current rate, and it will then be a function of SOC and temperature.

$$\eta_{pow} = \left[1 - \frac{I_s \cdot R}{V_s}\right]^k \qquad \text{[pu]} \qquad (7)$$

$$\text{where,} \quad k = \begin{cases} +1, & I_s > 0, \text{ Discharging} \\ -1, & I_s < 0, \text{ Charging} \end{cases}$$

$$\eta_{cycle} = \eta_{charge} \cdot \eta_{discharge} \qquad \text{[pu]} \qquad (8)$$

LLD SPECIFICATION

The fundamental requirements of the battery in a CS-HEV is to provide temporary energy storage. The battery acts as an LLD and should provide a high overall power cycle efficiency, and as stiff a voltage profile as possible. An example LLD specification for a typical CS-HEV (as found in reference [13]) is given in Table 2.

The Power Cycle Efficiency of the battery must be as high as possible. Large variations in terminal voltage ($I \cdot R$ drops, Equ 7) while under load automatically represent low power processing efficiencies. A stiff voltage characteristic (low series impedance) from an electro-

Table 2. Typical CS-HEV LLD Specification

Description	per unit Requirement
Pow. Cycle Efficiency	> 85 % (at nominal rates)
Power Processing	> +/- 4 pu (intermittent) ~ +/- 2 pu (nominal)
Term. Voltage Variation	< +/- 0.15 pu variation from nominal voltage.
Min. Energy Storage	>> ΔE_s of any 1 event.

chemical battery is seen as desirable.

BATTERY STATE DESCRIPTORS

This section classifies battery state descriptors based on importance to the CS-HEV LLD specification. The battery "state" is often described by the relative amount of stored charge in the electrolyte (SOC). Other ways to describe the batter "state" are via electrolyte temperature, terminal voltage behavior, stored energy, short term power delivery capability, etc. These descriptions of the battery can be divided into two groups based on the importance of the state descriptor to the function of the battery as an LLD.

PRIMARY STATES

Optimal control of LLD's require knowledge about the power processing capability and power cycle efficiency performance. Indirectly, terminal voltage variation under load gives power cycle efficiency information, as shown by the $I_s \cdot R$ term in Equation 7. Power Cycle Efficiency, Power Capability, and Terminal Voltage are fundamental to LLD operation and are classified as *Primary States* of the battery. These state descriptors are highly dependent upon the series impedance, and temperature of the battery and must comply with the LLD specification on a continual basis.

SECONDARY STATES

Battery properties of less concern to the LLD specification are actual stored charge, stored energy, and electrolyte temperature. As long as the battery is performing well with respect to the immediate needs of the specification, stored charge, stored energy and cell temperature are free to change. These battery state descriptors are defined as *Secondary States* for LLD devices. The first two descriptors of charge and energy content are weakly related to the series impedance of the battery. All are slowly changing in time.

It is interesting to note the above LLD state descriptor groupings also apply to the batteries of EV's. If the EV battery can not meet the short term power demands (or voltage limits) set forth by the driving cycle (or electric motor), then the secondary goal of predicting stored charge or useful vehicle range is a mute point. It has been the goal of many SOC monitors to predict when a *primary state* of the battery would falter (terminal voltage), by monitoring an empirically modified
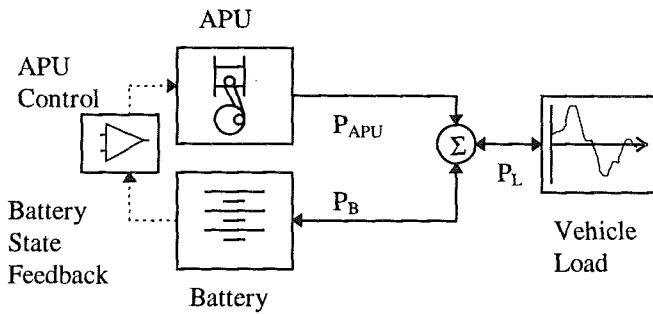
Figure 2: Example HEV power flow diagram. APU power is modulated in a switched mode manner. The battery state feedback determines when the APU is turned on or off.

secondary state (Peukert modified SOC).

CHARGE vs. VOLTAGE CONTROL

This section experimentally compares State of Charge (SOC) and State of Voltage (SOV) control techniques in a series hybrid with switched mode (thermostat) APU operation.[13] The APU is assumed to operate under constant power mode, and is cycled on and off to maintain the battery state description within hysteresis band limits.

The general power flow diagram of the example Series CS-HEV configuration is shown in Figure 2. The energy efficiency of the battery in Figure 2 is defined in Equation 9. For the purpose of comparing battery control techniques, the vehicle load and APU powers are assumed to be measurable before the summing junction, and there are no power processing equipment between the summing junction and battery terminals.

$$\eta_{Bat} = \frac{E_L}{E_{APU} - \Delta E_s} \qquad [pu] \qquad (9)$$

where E_L is the net energy required by the vehicle load, E_{APU} is the net energy delivered to the summing junction, and ΔE_s is the change in battery stored energy over the test.

EXPERIMENTAL CONFIGURATION

A small scale laboratory test bench was assembled to experiment with charge and voltage based control techniques for a series hybrid with switched-mode APU operation. The small scale tests were implemented with bi-directional power source, a computer controller/data logger, and a string of three test modules. Figure 3 shows a diagram of the test set-up with bi-directional power source, current regulator, computer controller, and DUT.
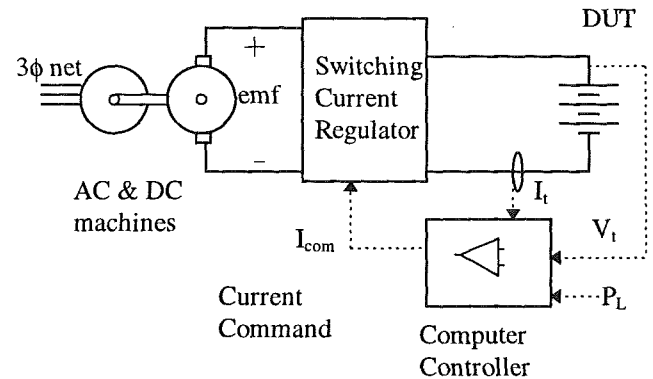
Figure 3: Connection diagram of the small scale (400 Watt) battery test set-up. A seamless bi-directional power source was realized by a combination of electric machines and a bi-directional current regulator.

The computer controller implemented a software APU and the battery current command was calculated from the battery power demand and the known terminal voltage. The operation of the APU was based on hysterisis control limits applied to the battery state descriptor (voltage or charge based). Figure 4 shows how the computer controlled battery power flow by monitoring terminal voltage and current, and by applying error correction to the commanded battery current.

The scaled experiments applied true power control to the battery, unlike the simplified battery current controller found in reference [8]. The experimental test bench featured an ample 50 Hz current regulation bandwidth and the experiments were run with a 4 Hz sample frequency.

CONSTANT LOAD EXAMPLE

A constant vehicle load example is used to compare the battery state controllers. A constant vehicle load of 0.5 per unit power is assumed along with thermostat control of an APU capable of producing 1.0 per unit power. This example is analogous to a 1590kg CS-HEV, driving at a constant 50 kph (~3.9kW load), while the APU (~7.7kW) is thermostatically switched on and off to maintain the
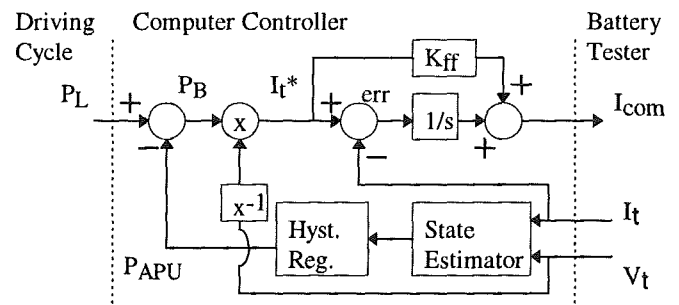
Figure 4: Control block diagram for the software implemented APU in the scaled test bench. Load power demand, and terminal quantities are inputs, and current command is the output. The software APU power is modulated on/off by hysterisis control applied to the battery state descriptor.

SOC Control: Vt, It, SOC estimate and APU power vs. Time

Terminal Voltage vs. SOC (Control Variable)

solid = Trajectory

dash = Control Limits

dashdot = Ideal V–Q Relation

X = Begin
O = End

Figure 5: Terminal Voltage, Current, SOC estimate and APU Power vs. Time for the SOC controlled constant load example. Note the on/off control of the APU based on the SOC hysterisis band control limits [0.63~0.70]. Initial SOC was 0.83 pu.

Figure 6: Terminal Voltage vs. SOC estimate for the constant load experiment under SOC control. The trajectory begins on the ideal V-Q relation, and then traverses a cyclic pattern within the control bands. The voltage trajectory drifts upwards ~1% indicating possible drift in the SOC estimate.

state of the battery within a set of hysterisis band limits.

SOC CONTROL

The performance of the gassing current compensated SOC regulator in a Switched Mode APU example is presented. The terminal voltage characteristic of the battery under SOC control is examined, while the SOC is regulated within a window of 0.63 to 0.70 pu.

Figure 5 shows how the battery terminal quantities, SOC estimate and APU reacted over the 100 minutes of the constant load example. The SOC began the test at an initial value of 0.83 pu and the SOC estimate was successfully regulated. The SOC estimate was calculated using equations 1-4 (gassing current compensated, redox current integrator).

Closer examination of the experiment emphasizes the short comings of charge based state control as listed in Section 1. The initial SOC for the control algorithm was determined from the open circuit voltage of the battery, after 12 hours of rest. Initializing the SOC value will always be a challenge. If a stable open circuit voltage reading is not available, the algorithm may need to begin with the last estimated SOC value which may harbor previously accumulated errors. Drift in the SOC estimate due to current measurement errors can also become significant over longer driving cycles. A V-Q plane plot is presented to show this phenomena.

Figure 6 shows the terminal voltage vs. SOC estimate. The voltage trace is seen to drift slightly upward as the test progresses, thus indicating either a long term stabilization in the diffusion of the acid or a drift/error in the estimation of SOC. Similar problems will exist for energy based battery controllers. The fundamental short

coming is that the terminal voltage is not directly observed or bounded by the SOC controller.

Additional information can be extracted from Figure 6. The trapezoidal trajectory is not centered about the ideal V-Q relation due to the I_s·R voltage drops (Equation 6). The constant load experiment applied about equal charge and discharge currents to the battery, hence the charging resistance of the battery can be estimated to be about 2.5 times the discharge resistance in the 65% SOC range. This unbalance can be expected at higher states of charge, when the acid concentration is high. Operating the battery in a lower SOC region will help to equalize the ratio of charge/discharge resistance's, and will help to improve the power cycle efficiency performance. Unfortunately, the optimal operating range for SOC will vary as a function of the ratio between charging and discharging currents and resistances. To obtain good power cycle efficiency over a wide range of events, the controller must continually adjust the control limits applied to the SOC estimate based on a priori experiments.

SOV CONTROL

A terminal voltage hysterisis regulator example is shown. The estimated SOC trajectory is examined, while the terminal voltage is bounded in the 1.04 ~ 0.92 pu range (+/- 0.06 pu variation).

Figure 7 shows how the terminal quantities (V_t, I_t), SOC estimate and APU reacted during the 100 minutes of the constant load example under SOV control. The terminal voltage control limits were intentionally set to mimic the SOC control example in Figure 5. Both SOV and SOC

SOV Control: Vt, It, SOC estimate and APU power vs. Time
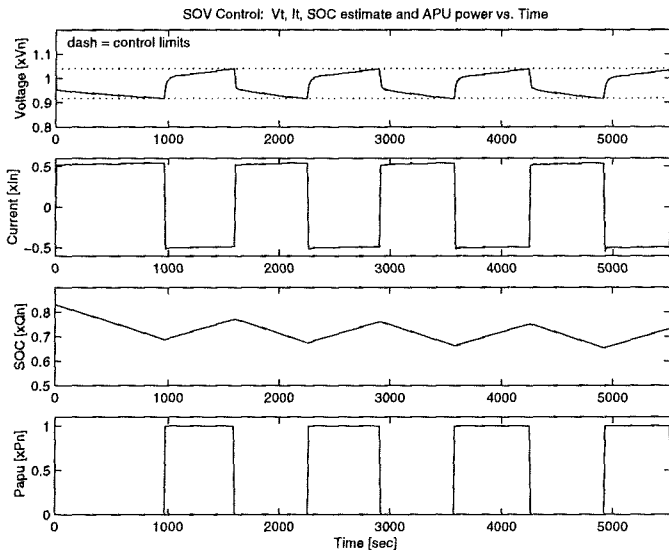
Figure 7: Terminal Voltage, Current, SOC estimate and APU Power vs. Time for the SOV controlled constant load example. The terminal voltage was regulated in the 0.92 ~ 1.04 pu range. Initial SOC was 0.83 pu.

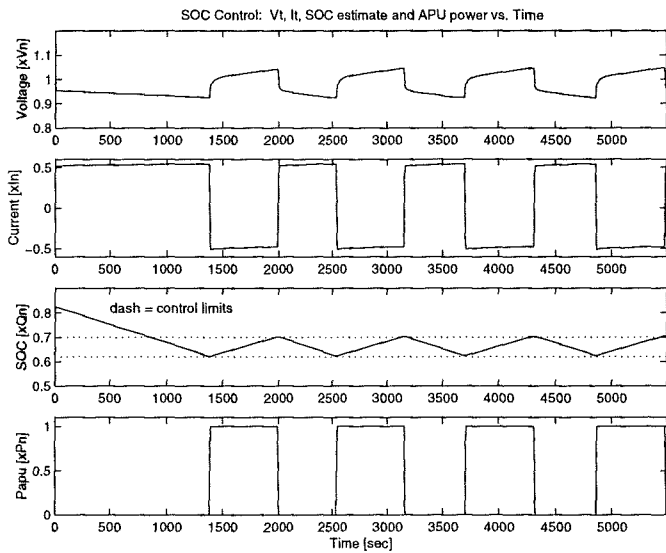examples delivered net energy efficiencies (Equ 9) of 93.8%. The results were understandably similar due to the similar operating conditions, but a fundamental difference is seen in how the battery state is controlled.

Figure 8 shows how the SOC estimate responded relative to controlled terminal voltage. The voltage controlled battery allows the SOC (estimate) to drift downward before it establishes a steady state level. SOV control is naturally stable, because the ideal Q_s-V_s relation is a diagonal line. This diagonal relationship forces the actual (not estimated) SOC to a region where the voltage control limits are near equi-distant from the operating point on the diagonal relationship.

The exact distances between the voltage control limits and the settling point on the Q_s-V_s relationship are determined by the ratio of the charge and discharge I_s·R voltage drops. SOV control allows the voltage drop ratio to determine the operating range of the SOC. This key characteristic automatically adjusts the SOC range to favor higher energy efficiencies. The charging to discharging impedance drop ratio tends to push the SOC towards lower values when charging impedance drops are dominant. Similarly the SOC is forced towards higher levels when discharging drops are dominant. Thus moving the SOC operating range in the desired direction.

The voltage control variable is not an estimated state of the battery as is the SOC variable. The terminal voltage is directly measurable, and no integration is used to process the signal. This provides robust control of the terminal voltage, and when coupled with the diagonal, temperature independent, Q-V relationship of Figures 1 & 8, it also bounds the range of SOC operation over wide operating conditions and temperature.

SOC vs. Terminal Voltage (Control Variable)
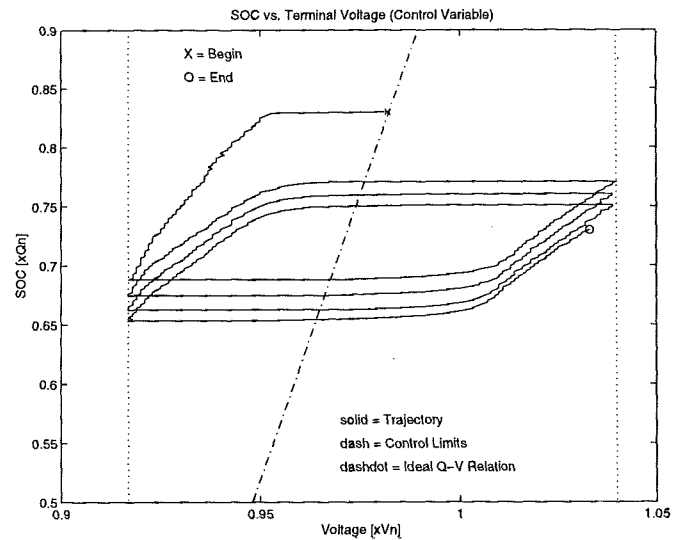
Figure 8: SOC vs. Terminal Voltage for the experiment in Figure 7. The ideal relation between SOC and V_S is also shown. The voltage control limits [0.92~1.04] loosely bound SOC, which is allowed to drift towards a steady state value (~0.7 pu.).

CONTROL WITH DYNAMIC LOADS

The above constant vehicle load examples do not address many of the challenges present in typical driving cycles. This section first quantifies the power spectrum experienced by HEV batteries, and then provides a control methodology for voltage based techniques.

Typical driving cycles exhibit broadband power spectrums. The average, and low frequency power demand is supplied by the APU, so the battery must supply the mid to high frequency power components. Special attention must be given to high frequency components in the terminal voltage when if it is used as a control variable.

Harmonic Spectrum of Power Demand vs. Frequency

Typical 1590kg vehicle

Bag 1&2 of FTP-75

0dB = 2.2kW

Figure 9: Vehicle power spectrum of the FUDS driving cycle for a typical 1590 kg vehicle. The 0dB level is equivalent to ~2.2 kW. The corner frequency is ~0.02 Hz and there is an attenuation of 30dB/decade.

70

An example 1590 kg vehicle was simulated in several driving cycles and the vehicle power spectrums were obtained. The resulting power spectrums [$10\log(P_L / P_{avg})$ vs. log frequency] were all similar. Figure 9 shows the power spectrum for the FUDS. All three driving cycles featured a corner frequency of approximately 0.02 Hz, and natural attenuation on the order of ~30 dB/decade. The SFUDS driving cycle did not reproduce the broadband spectral content as shown in Figure 9, hence it was not used to dynamically test the battery state control techniques. The computer controlled test bench enabled the use of realistic driving cycles.

2-D VOLTAGE CONTROL

The high frequency power spectrum which the battery must process causes dynamic swings in the terminal voltage. Terminal voltage control techniques as used in the constant load example are still applicable, but the control limits must be broadened to avoid premature APU state changes. Practically, the terminal voltage control limits should be extended to the maximum allowed by the LLD specification (Table 2). These broad limits generally satisfy APU control requirements for dynamic loads but have two drawbacks;

- Broad terminal voltage control limits do not sufficiently constrain SOC for non-dynamic loads. The SOC will drift to one extreme or the other before a wide terminal voltage limit is reached.
- Broad voltage control limits do not encourage small impedance drops necessary for good power efficiency during nominal loading conditions.

To overcome these two deficiencies, a 2-dimensional voltage control algorithm is introduced. Besides the dynamic terminal voltage events being monitored, a trend in terminal voltage is also monitored and constrained. The voltage trend is derived from a Low-Pass-Filter (LPF) applied to the terminal voltage. The control limits applied to the filtered voltage are much tighter than the broad limits applied to the instantaneous terminal voltage. With the addition of the voltage trend control, the two above drawbacks are avoided.

LPF Corner Frequency

The trend voltage corner frequency and control limits are derived from the typical driving cycle power spectrum and ideal V_s-Q_s relationship respectively. The LPF corner frequency should be placed below the natural corner frequency encountered in the driving cycle (0.02Hz). The LPF will then attenuate the high frequency content in the trend voltage indicator, resulting in a low noise state feedback signal.

The LPF corner frequency should not be set too low, thus causing significant delay in the trend indicator. Reference 13 introduced a practical lower limit on the LPF, based on worse case loading. The equations defining the trend voltage and LPF corner frequency are

shown in Equations 10 & 11.

$$V_{trend} = LPF(V_t) \qquad [V] \qquad (10)$$

$$\frac{P_B}{2\pi \cdot 3600 \cdot E_S \cdot \Delta SOC} < f_{xLPF} < f_{xDrvCycle} \qquad [Hz] \qquad (11)$$

where P_B is the maximum prolonged battery power event in Watts, E_s is the energy storage of the battery in W-h, ΔSOC is the maximum allowed change in charge content (%) before APU action is desired. The HEV in reference 13 had a lower LPF limit of 0.001 Hz. A first order LPF with a corner frequency of 0.0026 Hz (60 second, first order time constant) was successfully used and is also used in the below experiments.
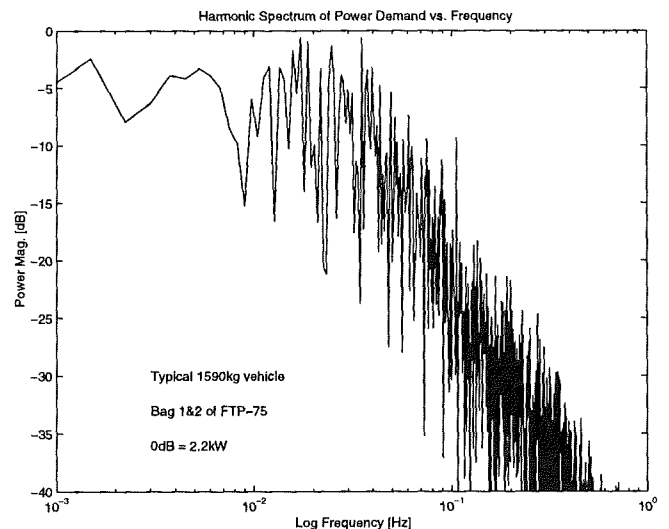
Control Limits

The control limits for the voltage trend indicator should be set close to the limits of the diagonal V_S-Q_S relationship (values of V_n and V_o). This will insure that the SOC always finds a steady state operating region before drifting too closely to an extreme (0 or 100%). The terminal voltage limits are set to the max allowed by the LLD specification.

Figure 10 shows an example of the two voltage signals vs. time. The terminal voltage behaves dynamically within wide control limits. The filtered terminal voltage behaves slowly within tighter control limits. The two upper control limits dictate when the APU should be turned off in order to reduce the voltage states, and the two lower limits determine when the APU should be turned on in order to increase the voltage states. Either of the two voltage signals can cause the APU state to change.

A 2-dimensional hysterisis control box is presented which shows how the two voltage indicators influence the APU state. Figure 11 shows a plot of terminal voltage vs. trend voltage. The steady state relation between the two is a unity slope line. The diagonal nature of the unity slope line insures that the voltage trajectory will move between APU off and on bounds.
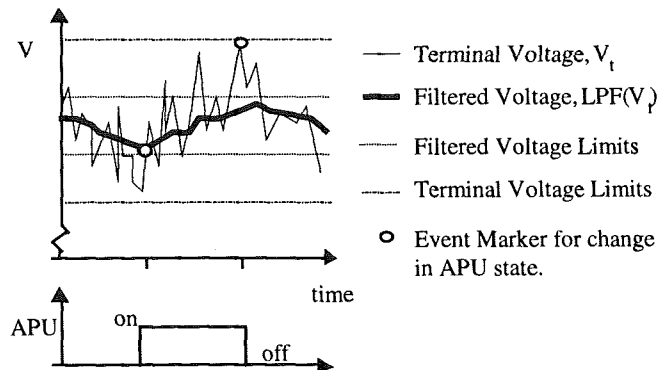
Figure 10: Two voltage signal control example with event markers. The on/off state of the APU is directed by either the trerminal or filtered battery voltage and respective control limits.
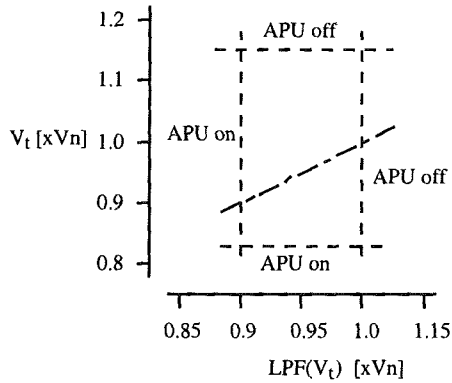
Figure 11: 2-D normalized voltage control box (terminal voltage vs. filtered voltage) features two APU turn-off bounds and two turn-on bounds. The unity relation (dash dot) is also shown.

DYNAMIC LOAD EXAMPLE

The first 505 seconds of the FUDS cycle was selected as a the seed for the dynamic load experiments. The power demand for 1590 kg vehicle was scaled to +/- 3 pu. peak power stresses and used as an input Load Power, P_L, for the scaled test bench. The APU power level was then set to 1.0 pu. in order to mimic the stresses present in the example HEV. Twelve driving cycles were repeated sequentially, elongating the test to 6060 seconds. The experiments were carried out in a temperature controlled oven at 30°C.

SOC CONTROL

The battery traces from the SOC controlled dynamic load example are shown in Figure 12. The SOC was regulated within the range of 0.40~0.45 pu. (empirically determined to produce acceptable voltage results). The terminal voltage responded within the min and max allowed limits (0.83-1.15 pu.). The net battery energy efficiency over the test was 84.0% and an 8°C temperature rise was witnessed. Once initiated, the APU operated with an approximate duty cycle of ~39% and with a period of ~640 seconds.

The APU operating period is determined by the average power demand, SOC control limits, and energy content of the battery. The period is inversely proportional to the left hand side of Equation 11. The SOC estimate is based on the time integral of the dynamic current, thus resulting in a slowly moving control variable which predictably moves between the hysterisis control limits.

Figure 13 shows the Terminal Voltage vs. SOC estimate plane for the experiment in Figure 12. The SOC estimate is seen to be well regulated, and the voltage is well behaved. The target of ~43% SOC was selected after some trial and error. The V-Q trajectory of Figure 13 provided a way to evaluate an appropriate range for the SOC level; terminal voltage responds in an acceptable manner (within min/max limits).
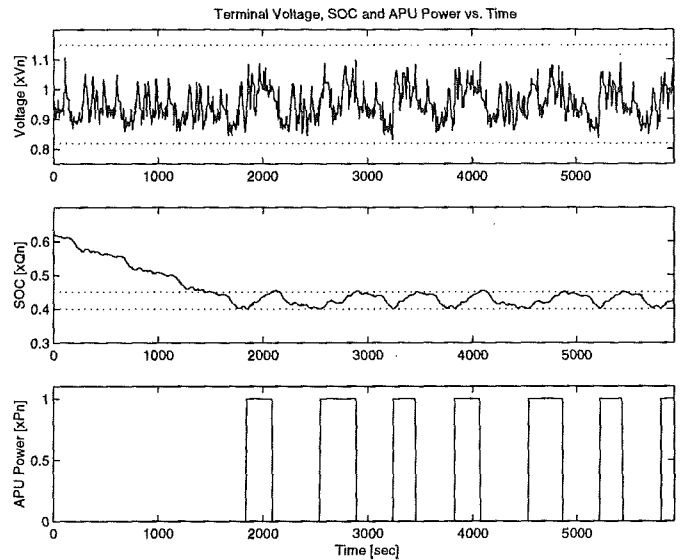
Figure 12: Terminal voltage, SOC and APU power vs. time for the dynamic load example. The SOC was controlled within the range 0.40 ~ 0.45pu. This control range was experimentally determined to provide acceptable terminal voltage behavior [0.82~1.15 pu].

SOV CONTROL

The experiment was reapplied under 2-dimensional SOV control with the following limits: trend voltage control limits of 0.9 ~ 1.0 pu., and terminal voltage control limits of 0.83 ~ 1.15 pu. The SOV technique achieved a power cycle efficiency of 85.1% and the battery experienced only a 7°C temperature rise. The APU operated with an approximate duty cycle of ~38% and with an average period of ~500 seconds.

The APU operating period is a function of the voltage control limits, internal impedance, the magnitude of the dynamic load events in the driving cycle and the LPF of
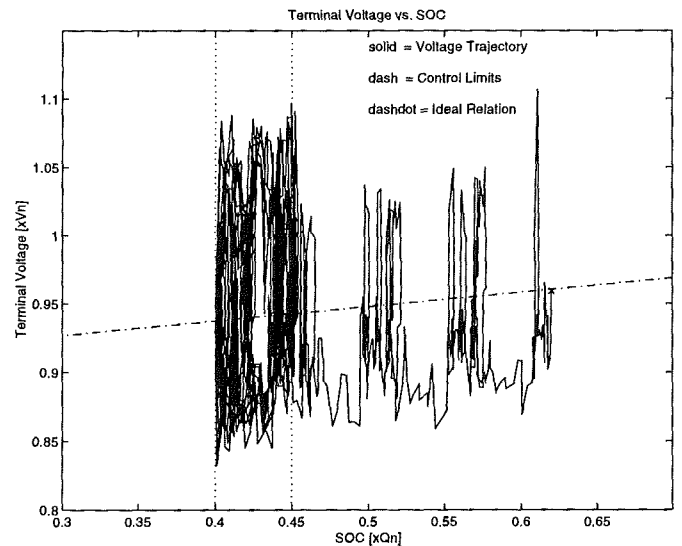
Figure 13: Terminal Voltage vs. SOC plane for the dynamic load example of Figure 12. The terminal voltage behaved within acceptable limits while the battery SOC was controlled in the 0.43 pu range.

72
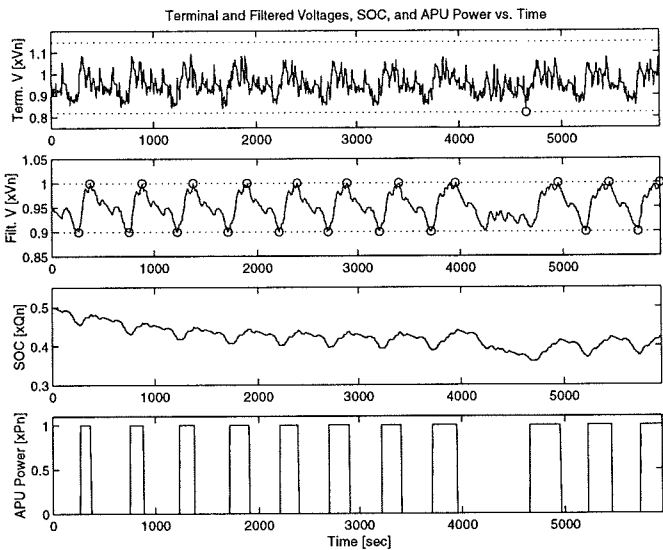
Figure 14: Terminal voltage, filtered voltage, SOC estimate and APU power vs. time for the dynamic load example under 2D-SOV control. Circles mark the voltage events which controlled APU operation.

the trend voltage. Slower filters and less dynamic events tend to increase APU operating periods. The battery quantities under SOV control are shown in Figure 14 and the events which changed the APU state are shown with circles.

Figure 14 shows how the SOV control allowed the SOC to vary in a steady state operating region. Figure 15 shows the test's 2-D voltage control box. The trajectory shows how both trend and instantaneous voltage signals are well contained inside the control limits.

COLD TEMPERATURE OPERATION

The SOV technique works well under cold operating conditions. The same control limits can be used in VRLA systems, independent of temperature. The APU operating periods are generally shorter for cold operation. The trend and dynamic voltage control limits are easily reached due to elevated series impedances in the battery, but the battery terminal voltage is always well constrained (SOC control does not control terminal voltage under cold operation). An example of low temperature (0° C) operation is shown in Figure 16. The battery began the test at 0°C (ice water bath) and experienced a 15°C rise internal to the modules. The net energy efficiency of the battery over the test was 83%. The SOC eventually drifted to the same range as Figure 14, but was initially at ~47% while the battery was cold. Allowing the SOC to find an operating range which satisfies the primary voltage constraints is a great benefit to the voltage based state controller.
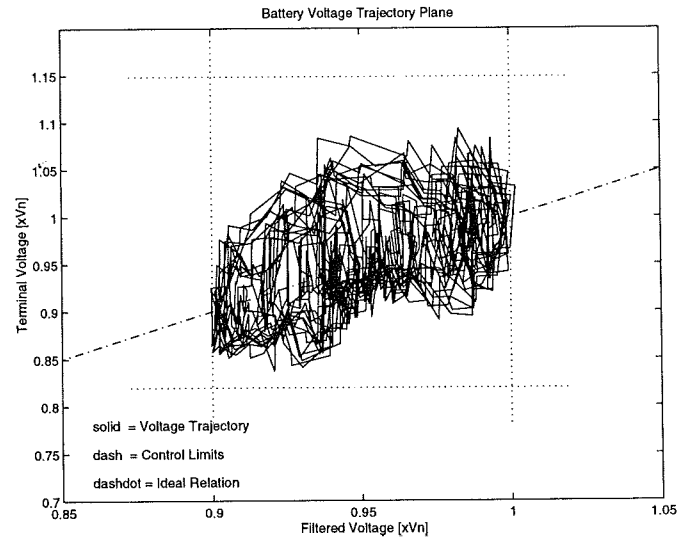
Figure 15: 2-dimensional voltage control box for the dynamic load experiment of Figure 14. Both trend and dynamic voltage events are well bounded and the voltage trend indicator dictated almost all of the APU events.

FUTURE WORK

An LLD controller should ideally move the device (battery) towards higher power cycle efficiencies. This type of controller requires information about the series impedance elements of the battery model. Some initial work in this area was presented in reference [10]. Identifying the impedance on-line will lead to better LLD utilization and higher overall system efficiencies. Future work at UW-Madison will focus on identifying the non-linear Randles-Ershler model components.
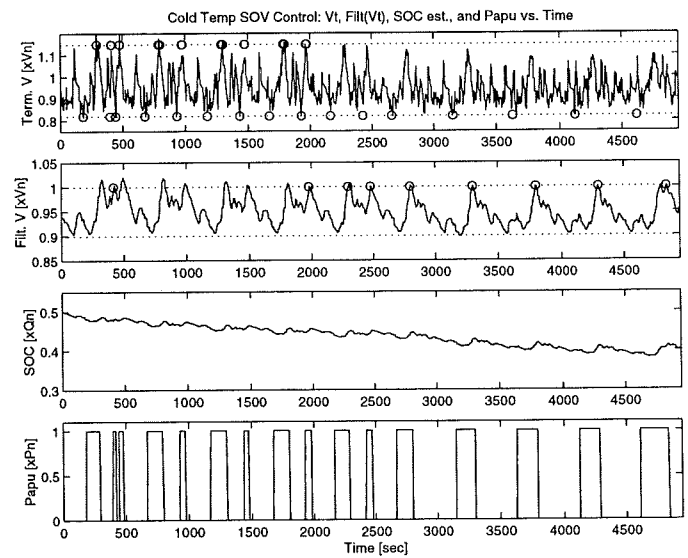
Figure 16: Terminal voltage, filtered voltage, SOC estimate and APU power vs. time for low temperature test. The SOV control technique kept the voltage well bounded and produced an overall 83.1% power cycle efficiency while in the 0 ~ 15°C operating range.

73

CONCLUSIONS

Several conclusions can be made from the discussions and experiments made in this paper. The paper was specially focused on CS-HEV's with switched mode APU control and VRLA batteries. Some caution must be applied when extending the below statements beyond these contexts.

- Battery power capability, cycle efficiency and terminal voltage are primary indicators of the battery state for CS-HEV's. Charge and Energy storage are secondary indicators.
- SOC based control of the battery state does not directly control terminal voltage, which is free to vary with dynamical loading and series impedance. SOC control limits must be a priori experimentally determined over rate and temperature.
- SOV based control techniques constrain terminal voltage and loosely bound SOC. The I-R voltage drops tend to move the SOC in favorable directions which improve power cycle efficiency.
- SOV battery state control has no initialization problems, and provides robust performance even under low temperature operating conditions.

ACKNOWLEDGMENTS

CONTACT

Mr. Wiegman is a Ph.D. candidate at UW-Madison. He can be reached at 1415 Engineering Dr., Madison, WI 53706 or by wiegman@cae.wisc.edu. Mr. Wiegman earned his BSEE at Worcester Polytechnic Institute in 1988 and his MSEE at UW-Madison in 1991. He spent three years on the staff of GE's Corporate R&D Center transitioning power processing solutions to several businesses before returning to pursue Ph.D. studies at UW-Madison. He recently spent a year in Eindhoven, the Netherlands after receiving a Netherland-America Foundation Fellowship. Mr. Wiegman has been an active member of UW-Madison's Hybrid Electric Vehicle team for several years.

REFERENCES

[1] Peukert, W., "Uber die Abhangigkeit der Kapazitat von der Entladestromstarke bei Bleiakkumulatorn." Electrotech. Z., vol 18, 1897, pp 287-288.

[2] Shepherd, C.M., "Design of Primary and Secondary Cells, II. An Equation Describing Battery Discharge," J. Electrochemical Soc., Vol. 112, #7, 1965, pp 657-664

[3] Bode, H., Lead-Acid Batteries , Wiley Int., Princeton, NJ, 1977, ISBN 0-471-08455-7

[4] Schleuter, W., Skudelny, H.C., "The Electrical Behavior of Lead-Acid and Nickel Iron Batteries," IEEE Ind. Appl. Soc. (IAS), 1983, pp 363-369

[5] Burke, A., "An Adaptive Battery State of Charge Indicator (ASCI) for Urban Driving," 8th Int. Elect. Veh. Sym. (EVS-8), 1986, pp 350-

[6] Kaushik, R., Mawston, I., "Discharge Characterization of Lead/Acid Batteries," J. of Pow. Sources, v.28, 1989, pp 161-169

[7] Schöner, H.P., "Electrical Behaviour of Lead/Acid Batteries During Charge, Overcharge, and Open Circuit," 9th Elect. Veh. Sym. (EVS-9), 1988, #063

[8] Brandt, D., "Driving cycle testing of electric vehicle batteries and systems," J. of Pow. Sources, Vol. 40, 1992, pp 73-79

[9] Noviello, E.I., Plaitano, Tortora, "Battery Diagnostics and Performance Prediction: Computational vs. Expert System Based Approach," IEEE-INTELEC, V1, 1993, pp 460-468

[10] Kopf, C., "Adaptive Control of an EV Drive System to Account for Time-Varying Battery Parameters," EVS-12, EVAA, Vol. 2, 1994, pp 1-10

[11] Song, S., Kim, K., Oh, S., "A Dynamic State-of-Charge Model for Electric Vehcle Batteries," EVS-12, EVAA, 1994, pp 519-527

[12] Mauracher, P., Karden, E., "Dynamic Modelling of Lead-Acid Batteries Using Impedance Spectroscopy for Parameter Identification," 5th ELBC, Barcelona, (J. of Pow. Sources, V 67, pp 69-84),1996

[13] Hochgraf, C., Ryan, M., Wiegman, H., "Engine Control Strategy for a Series Hybrid Electric Vehicle Incorporating Load-Leveling and Computer Controlled Energy Managment," SAE Publ. 960230, or SP-1156, 1996, ISBN 1-56091-786-5, pp 11-24

[14] An, F.,Frank, A., Ross, M. ,"Meeting Both ZEV and PNGV Goals with a Hybrid Electric Vehicle - An Exploration," SAE Publ. 961718, or SP-1189, 1996, ISBN 1-56091-840-3, pp 17-32

APPENDIX

All experimental results shown in this paper were derived from a sample of three Yuasa NP4-12 modules. The normalization values for these typical 12 Volt, 4 Ah, VRLA modules are shown below.

V_n 2.17 V/cell = 13.04 V/module (100% SOC)

Q_n 4.0 Ah = 14,400 Coulombs   (C/20 rate)

E_n 8.68 Wh/cell = 31,250 J/cell

T_n 1 h = 3600 s

I_n 4.0 A   (modules rated to 3 pu discharge)

P_n 8.68 W/cell

Z_n 0.543 Ω/cell

Other Characteristics:

V_o 1.95 V/cell ....(~0% SOC, 25°C)

R discharge 0.03 Ω /cell ..... (50% SOC, 30°C)

     charge 0.05 Ω /cell ....(50% SOC, 30°C)

C_θ 1250 J/°K , ... thermal capacity

τ_θ 1 hour , ...thermal time constant (in air)

M 1.7 kg , ...12V module mass

ADDITIONAL MODEL RELATIONS

The stored energy relation for the model is based on charged stored in the non-linear capacitor, C_S. It is defined in Equation 12 and is expanded in Equation 13 for the temperature independent and straight line V-Q relation of Figure 1.

$$E_s = \int_0^{Q_s} V_s(q) \cdot dq \qquad \text{[J]} \qquad (12)$$

$$E_s = V_o \cdot Q_s + \frac{V_n - V_o}{2 \cdot Q_n} \cdot Q_s^2 \qquad \text{[J]} \qquad (13)$$

Short term (~10 sec) power capability is defined in Equations 14 and 15, where R is assumed to be the dominant element of Z in the ~0.1 Hz region, and R may be some function of rate, temperature and current direction.

$$P_{max} = \frac{V_s \cdot V_{\lim} - V_{\lim}^2}{R} \qquad \text{[W]} \qquad (14)$$

$$V_{\lim} = \begin{cases} V_{max} & \text{Charging Power Capblty.} \\ V_{min} & \text{Discharging Power Capblty.} \end{cases} \qquad \text{[W]} \qquad (15)$$

GASSING CURRENT COMPENSATION

The SOC estimates used in this paper accounted for charge loss to gassing currents. The gassing phenomena was characterized over temperature for the Yuasa NP4-

12 modules under test. The Tafel Current vs. Terminal Voltage relationship is shown in Figure 17. The resulting fitted normalized gassing current model as a function of temperature is given in Equations 16 and 17.

$$\ln\left(\frac{I_g}{I_n}\right) = 8.0 \cdot \left(\frac{V_t}{V_n} - 1\right) + B_g \qquad \text{[pu]} \qquad (16)$$

$$B_g = 0.038 \cdot (T + 273) - 16.3 \qquad \text{[pu]} \qquad (17)$$

Where B_g is a temperature dependent offset term, T is in degrees Celsius, V_t and I_g are converted to per unit form. The gassing model is valid over: $1.0 \le V_t \le 1.15$ for the example battery.
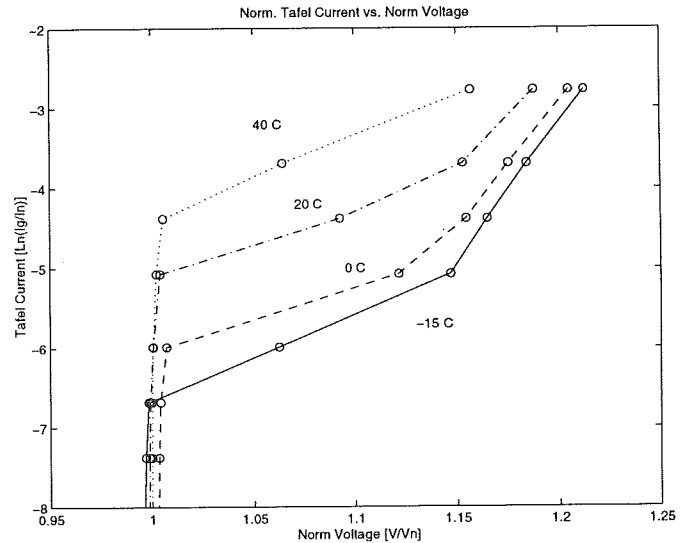
Figure 17: Normalized Tafel current as a function of per unit terminal voltage for 4 temperatures. The gassing relationship is modeled over the middle region, which is the range of typical over-voltages.

DEFINITIONS, ACRONYMS, ABBREVIATIONS

Most variables listed below are plotted in normalized form (per unit system) in this paper.

E_s Stored Energy in the cell/battery........... [Wh]

I_{com} Current command to experiment .... [A]

I_t^* Reference terminal current command .... [A]

η_{cycle} Net LLD Energy Efficiency (@ some rate) [-]

η_{Pow} Power Efficiency (direction dependent) .... [-]

P_B Battery power delivery (bi-directional)..... [W]

P_L Vehicle power demand (bi-directional).... [W]

P_{APU} APU power delivery (uni-directional)....... [W]

Q_o Initial Charge at start-up .... [A-h]

R Resistive portion of Z at ~ 0.01 Hz................ typically Electrolyte and Double Layer.....[Ω]

T Temperature internal to cell ....[Celsius]

V_o Offset voltage (obtained at 0% SOC) ...... [V]

Load Leveling Device Selection for Hybrid Electric Vehicles

Paul B. Koeneman and Daniel A. McAdams
The University of Texas at Austin

ABSTRACT

An important component in many hybrid electric vehicle (HEV) concepts is the load leveling device (LLD). The best type of LLD for HEVs is under debate. This paper identifies the important concept selection criteria for the three leading types of LLDs being considered for use in HEVs. The performance of electrochemical batteries, ultracapacitors, and flywheels is compared using these criteria. The concept selection methodology indicates that at the present time flywheels show the most promise for development for use in a hybrid electric vehicle. The use of this type of selection methodology is a powerful tool in identifying concepts worthy of development as well as determining performance criteria in need of improvement within each concept.

INTRODUCTION

The motivation for the development of hybrid electric vehicles (HEVs) comes from multiple sources. First, there are the state governments. In 1990, the California Air Resource Board passed legislation imposing strict ultralow emission standards [23]. Consumers also motivate the automakers to pursue hybrid vehicle technology by urging industries to produce more environmentally friendly products. Another influence is the federal government. The Partnership for a New Generation of Vehicles (PNGV) is a cooperative between the Big Three automakers and several federal government agencies. It has set goals for the next generation of vehicles. One goal is that new vehicles achieve three times the fuel economy of current vehicles with no loss of vehicle performance. This objective is equivalent to a fuel economy of 34km/l. The PNGV wants these new vehicles to have the same performance and price as current vehicles, and it wants the production prototypes ready by the year 2004 [17].

Currently, the most promising way to accomplish the PNGV objectives is with HEVs. HEVs have a fuel consuming engine to supply average power and an energy storage device to supply peak power [5]. This configuration means the engine only needs to be sized to meet average power demand rather than the peak power demand. In a high-performance vehicle, the ratio of peak power to average power can be as high as 16 to 1 [2]. In a HEV with a series configuration, the fuel consuming engine drives a generator which charges the energy storage device. Also, a regenerative braking system reclaims some of the vehicle's kinetic energy during braking and charges the energy storage device. The energy is used to drive one or more electric motors connected to the wheels.

The energy storage device essentially acts as an energy buffer. It discharges during high power demand and charges during low power demand, thus allowing the fuel consuming engine to ideally operate at one most efficient speed [15]. Because of this intended operation, the energy storage device is sometimes referred to as the load leveling device (LLD). The three LLDs most widely researched are electrochemical batteries, ultracapacitors, and flywheels.

There is currently some debate over which type of LLD is the best choice for use in HEVs. This paper compares the performance of the different types of LLDs that could be used in hybrid electric vehicles and attempts to determine which concept is the best investment of development effort. This paper does not attempt to design a specific vehicle. A design approach is used to compare and select LLDs for development for HEVs and to prioritize the focus of research into LLDs.

DESIGN APPROACH

LLD selection is posed as a design problem for two distinct and complementary reasons. Choosing a LLD for a HEV is a design decision, made at the conceptual stage of design. Also, though research into any LLD will improve LLD and HEV performance, posing LLD selection as a design problem directly links LLD research to the needs of the final customer, the consumer. For application oriented research, knowledge of the customer needs is crucial for resource allocation as well as for provision of a competitive edge as innovations move from the laboratory to the showroom.

As the goal here is the comparison and selection for development of a LLD for a HEV, the usage of the methodology will not be presented in complete detail. Also, as this paper concludes with the selection of the LLD, the methodology will not be presented to completion. For context, a general overview of a design method is presented to clearly put the selection in the context of design. Figure 1 shows a general product design methodology. This approach is consistent with

those proposed in Ulrich and Eppinger [24] and Pahl and Beitz [19] as well as those used in industry.

The identified design problem is a hybrid power source for a consumer automobile. Although HEVs are a research topic, their feasibility has been proven with operational prototypes. For the purposes of discussion, a family sized car with a series configuration under urban usage is assumed for a consistent basis of comparison throughout this paper. This usage assumption reduces the customer audience and has implications on customer needs, as applied to a power source. Reducing these customer needs, however, to engineering criteria yields a small set of important design criteria that clearly have impact on many types of automobiles. The conceptual configurations used for comparison is the same for each LLD, as this interchangeability is one of the goals for a HEV.
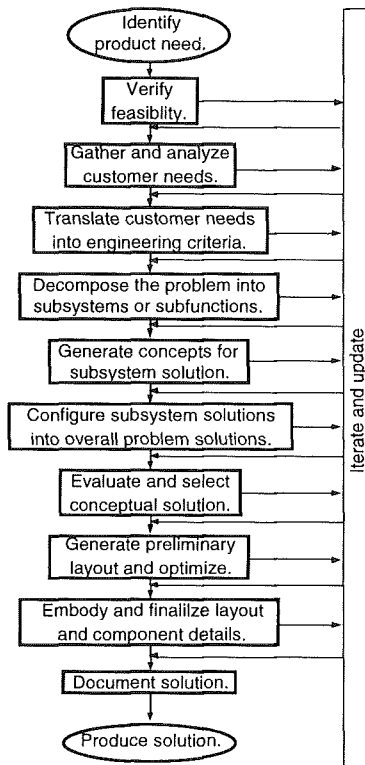
Figure 1. A general design methodology.

SELECTION CRITERIA

The primary traits a consumer looks for in a vehicle that are affected by the LLD include: acceleration rate, fuel economy, level of maintenance, safety, and cost. When these customer demands are translated into engineering requirements and some production considerations are added, the following list of concept selection criteria for an LLD results: specific energy, specific power, efficiency, lifetime, cost, self-discharge, safety, sensitivity to ambient conditions, environmental impact, low maintenance, regulation complexity, and potential for growth.

This list of requirements agrees closely with those proposed by other authors [4,13]. The remainder of this section briefly describes the requirements.

The energy requirement for a HEV is determined by the need to climb hills, pass other vehicles, and operate against headwinds. The energy storage requirements reported in the literature ranges from 0.6-2 kWh [14,7]. It takes about 0.5 kWh to accelerate a family sized car up to highway speeds [14]. Allowing for hills, passing, and headwinds makes the proposed range of values reasonable. The desired point in that range for a given vehicle is determined by the control strategy used by the engine-LLD combination.

The PNGV goal that the acceleration rate of current cars must be maintained in future vehicles establishes the peak output power requirement for the LLD. The use of regenerative braking establishes the peak input power requirement. The range of values proposed for the output power requirement in HEVs is 60-100 kW [14,3]. The precise point in the range is determined by the desired acceleration time and the mass of the vehicle. The input power from the regenerative braking system is approximately the same magnitude as the peak output power. The LLD could be required to accept short duration input currents as high as 20 amps [8].

In the interest of good fuel economy the efficiencies of each component of the power train should be optimized. This supposition includes maximizing the power transfer efficiency, the ratio of input energy to useful output energy, of the LLD. Low self-discharge also contributes to fuel economy. While the LLD only handles transient energy, it would be nice to not have to completely recharge the LLD every time the vehicle is started. The LLD must be able to hold a charge over periods of nonuse.

Long lifetime and low maintenance both contribute to the reliability of the vehicle. One of the failings of current electric vehicles is the need to replace the entire battery pack every few years. Ideally, the LLD would last the entire life of the vehicle and require no maintenance.

Low cost is a desired trait in almost all designs. Another failing of current electric vehicles is their high purchase price. The PNGV set a goal that the next generation of vehicles have comparable costs to current vehicles.

The LLD should also be safe to humans and the environment. The primary safety concerns for the LLD are failures caused by internal factors and by collisions. The safety of the environment involves any toxicity of components and recyclability. Another PNGV goal is that 80% of a vehicle be recyclable.

Since HEVs have to operate in a variety of environments, LLDs must function under a range of ambient conditions. The primary conditions of interest

are the temperatures, mechanical shocks, and vibrations experienced in a vehicle.

The power that the LLD supplies must be regulated. The power will need to be conditioned to drive the electric motors which drive the wheels. The complexity of the power flow controller is a factor in selecting an LLD.

The last desirable characteristic is potential for growth. Implementing any of the three types of LLDs requires a considerable investment in a mass production system. That investment is best applied to a technology that will not become obsolete in the near future. The future performance of the concepts must be anticipated based on current research.

After an initial comparison it was found that the requirements that most distinguish between the different LLD concepts are specific energy, specific power, efficiency, life, and cost. These criteria are emphasized during the final evaluation.

LOAD LEVELING DEVICES

Currently, there are three types of LLDs seriously being considered for use in hybrid electric vehicles. These are electrochemical batteries, ultracapacitors, and flywheels. This section presents the performance characteristics of each of the LLD types.

ELECTROCHEMICAL BATTERIES

Electrochemical batteries are the traditional choice for storing energy in vehicles. This fact is primarily due to the decades of experience at using batteries in automobiles. There are at least a dozen types of batteries currently being developed for use in electric and hybrid electric vehicles. Presently, one battery type which seems well suited for use as a LLD is the bipolar lead-acid electrochemical cell.

Specific energy – The strength of batteries is their high specific energies. There are bipolar lead-acid batteries available that have a specific energy of 55 Wh/kg [11].

Specific power – Bipolar lead-acid batteries can have a specific power as high as 830 W/kg [16]. This power is an order of magnitude higher than most other battery types. As a comparison, nickel-cadmium cells have specific powers on the order of 80 W/kg and specific energies of 55 Wh/kg [21].

Efficiency -- Because of the high internal resistances of batteries, all battery types possess efficiencies no greater than 75% [22]. The actual efficiency for a battery serving as an LLD will be much less than the value in the vendor data. The capacity and efficiency of electrochemical cells are rate sensitive. Standard battery tests discharge at a rate of C/3, where C is the rate that will fully discharge the battery in one hour. LLD batteries in hybrid electric vehicles have demonstrated discharge rates as high as 30C.

Lifetime --The short cycle life of batteries is a major concern for their use in hybrid vehicles. Bipolar lead-acid batteries that have undergone cycle testing have managed 15,000 shallow discharges [17]. For light vehicle use, this quantity of discharge should result in a battery life of about five years.

Cost --The initial cost of polar lead-acid batteries is about $72/kWh [22]. Distributing this cost over the expected life of the battery yields $14.40/kWh-year of service.

Safety -- The safety concerns for lead-acid batteries are overcharging and acid spills. If a lead acid battery is overcharged, explosive gases can build up. Also, if acid leaks from the battery, care must be taken during clean up.

Environmental impact – Lead-acid batteries contain some toxic chemicals; however, the batteries are almost completely recyclable. In addition, since lead-acid batteries are widely used today, the recycling systems are already in place.

Sensitivity to ambient conditions -- Compared to other types of batteries, lead-acid cells have good low temperature characteristics; however, they still experience significant loss of capacity during cold weather and a shortened cycle life in hot weather [6]. Mechanical vibrations and shocks should not affect the performance of the lead-acid cells.

Level of maintenance -- The current trend in batteries is towards "maintenance-free," sealed batteries. These batteries require no care other than to be switched out at the end of their life.

Self-discharge – Over short durations electrochemical cells experience only small amounts of self-discharge. Around 1% per day is typical [22].

Ease of regulation – Electrochemical batteries can be difficult to regulate. As mentioned previously, it is dangerous to overcharge a battery cell. A number of lead-acid cells in series and parallel will be necessary to achieve the power system voltage. It is difficult to evenly charge such a stack of batteries. Some cells will receive more charge than others and overcharging can occur [9]. Safe charging requires monitoring of the individual cells.

Potential for growth --There are two other battery types that hold promise for the future. Nickel-metal hydride batteries that have been optimized for specific power are predicted to reach 800-1000 W/kg and have a specific energy of 50 Wh/kg [17]. Initial experimentation with lithium-polymer test cells has demonstrated a specific energy of 250 Wh/kg and peak specific power between 1-2 kW/kg for short durations.

ULTRACAPACITORS

Ultracapacitors, also called double layer capacitors, have developed considerably over the last few years with the advent of new electrode materials to become well suited for use in hybrid electric vehicles.

Ultracapacitors store energy in a polarized liquid layer which forms when a potential exists between two electrodes immersed in electrolyte. The electrodes are composed of materials which exhibit large surface areas per gram of material. Some materials have specific surface areas of 400 to 1500 square meters per kilogram [23]. Some electrodes consist of carbon and metal fibers bonded into a composite fabric.

Specific energy – Prototype ultracapacitors with carbon-metal composite electrodes and an organic electrolyte have exhibited specific energy values as high as 7 Wh/kg [2].

Specific power -- The primary appeal of ultracapacitors is their high specific power. Specific powers greater than 1600 W/kg have been demonstrated [10].

Efficiency -- The very low internal resistance, around 0.2-2 ohms per square centimeter [2], of ultracapacitors gives them a very high cycle efficiency. The energy transfer efficiency is between 92-98% [7].

Lifetime -- Ultracapacitors have been tested to 500,000 cycles and experienced only a 20% loss in capacity. This high cycle life means an ultracapacitor LLD should last the entire life of a vehicle.

Cost – Once in mass production, ultracapacitors are expected to cost around $500/kWh [10]. Assuming the life of a vehicle is 15 years, distributing the initial cost over the lifetime of the LLD yields $33.33/kWh-year.

Safety -- The only safety concern for ultracapacitors is accidentally coming in contact with the output terminals. The low internal resistance can result in large output currents. The terminals will need to be insulated to prevent accidental contact.

Environmental impact -- The only environmental concern is that the composite electrodes may be difficult to recycle.

Sensitivity to ambient conditions – Ultracapacitors are only very slightly sensitive to temperature and not sensitive to mechanical shock and vibration.

Level of maintenance – There should be no maintenance required over the life of the vehicle.

Self-discharge -- There is no information about the self-discharge of ultracapacitors in the literature; however, it was never mentioned as a weakness. Ordinary capacitors can be constructed so as to have very small leakage currents, on the order of picoamps.

Ease of regulation – Care must be taken when charging so as to not to cause a breakdown of the electrolyte. The electrolytes currently used in ultracapacitors have breakdown voltages around 1-3 volts [2].

Potential for growth -- Ultracapacitors show considerable promise for the future. There is still much material science research to be done on electrode and electrolyte materials [17]. The specific energy and specific power for ultracapacitors is expected to triple in the long term [11].

FLYWHEELS

Storing energy with flywheels is an old idea that has recently received renewed interest. Much research on flywheels was conducted during the 1970's, but that research was all but abandoned during the 1980's. The recent resurgence of interest in flywheels is largely due to the advent of filament wound composite rotors [1] and high magnetic field permanent magnets [21]. Composite rotors can rotate faster than the old steel rotors because of their increased strength to weight ratio.

Specific energy -- The specific energy values for current flywheel energy storage systems range between 28-50 Wh/kg [11,20,25]. The Lawrence Livermore National Laboratory (LLNL) has developed an flywheel battery system for use with hybrid vehicles that stores 1 kWh with a specific energy of 50 Wh/kg [20].

Specific power -- The LLNL flywheel battery can deliver 200 kW with a specific power of 10 kW/kg of system mass [20].

Efficiency – With the flywheel rotating in a vacuum on magnetic bearings, very high efficiencies can be achieved. The energy recovery efficiencies for electromechanical batteries range from 95-98% [17].

Lifetime -- Since the rotor is the only moving part and it has little to no contact with anything else, the flywheel system should have a long service life and be able to withstand a virtually unlimited number of deep-discharge cycles [20].

Cost – Cost estimates for automotive flywheel systems are hard to come by since none have been mass produced. One estimate suggests a 4.1 kWh flywheel system can be mass produced for $800 per unit [12]. This estimate corresponds to $495/kWh. The flywheel should last the entire life of the automobile. When the cost is distributed over a 15 year life of a vehicle, the yearly cost is $13/kWh-year.

Safety -- The big safety concern with flywheel systems is the possibility of rotor failure. Fortunately, experiments indicate that when a composite fiber rotor fails it turns into a corrosive cloud of hot fibers and small pieces, not ballistically penetrating fragments. Flywheel systems have metal/fiber composite containment vessels which can contain the rotor fibers [20]. DARPA has funded the Flywheel Safety Project to design safe rotors and containment vessels.

Environmental impact -- The only environmental concern for a flywheel system is the difficulty in recycling the composite rotor.

Sensitivity to ambient conditions – A flywheel energy storage system is not sensitive to temperature and vibration. The rotor will have backup ceramic bearings to

	Batteries	Ultracapacitors	Flywheels
Specific Energy(Wh/kg)	55±20	7±1	50±20
Specific Power (W/kg)	830±80	1600±600	10,000±2000
Efficiency (%)	75±5	95±3	96.5±2
Life (cycles)	15,000±0	45,000±0	45,000±0
Cost ($/kWh-year)	14±6	33±6	13±6

Table 1. LLD Concept Characteristics.

prevent damage to the system in the advent of severe mechanical shock loads.

Level of maintenance -- The flywheel should require no maintenance over the life of the vehicle.

Self-discharge – The magnetic bearings and vacuum give flywheels a low self-discharge rate, about 1% per day. The LLNL flywheel takes over two months to spin down on its own [20].

Ease of regulation – A flywheel battery is an AC machine. The motor driving the vehicle's wheels will most likely be an AC machine. This similarity simplifies the power conditioning. Also, steps must be taken to not overcharge the flywheel. If the rotor is driven too fast, the rim the rotor will expand to the point where it touches the containment vessel.

Potential for growth – The primary focus for future development is in reducing the cost of production. New simpler and less expensive magnetic bearings are being developed. Less expensive fiber winding methods and materials for use in the rotor are also being developed.

CONCEPT COMPARISON

The selection of the preferred LLD concept is done using a selection matrix approach, similar to that proposed by Otto and Wood [18]. In this method, the selection criteria that most distinguish between the concepts are weighted relative to each other. Then, a reference concept is selected (in this case, the battery). The concepts are rated against the reference concept using the values in Table 1. An important feature of this selection methodology is that it accounts for uncertainty in both the performance of the concepts and uncertainty in the criteria weighting. The ranks are expressed as a nominal value and a tolerance. In addition, a confidence value is determined. Additional details about this methodology along with the associated mathematics can be found in Otto and Wood[18].

Every engineer will assign different weights to the various criteria. This selection methodology allows for uncertainty in the weighting factors. The weighting factors and their uncertainty are shown in Table 2. The criteria are weighted fairly evenly. The specific power is weighted slightly more because supplying peak power is the primary function of the LLD. Life is weighted slightly less because, since cost is a separate issue, the predictable replacement of the LLD unit is merely an inconvenience.

A fairly large uncertainty of ±5 is assigned to the first four criteria to accommodate designer discretion. A larger uncertainty of ±10 is assigned to cost because the importance of cost may change as the development process continues.

The lead-acid battery is selected as the reference concept since it is currently the industry standard for use in HEVs. The other concepts are scored based on the data in Table 1. The values and their tolerances were obtained through a survey of the relevant literature. The life estimates for the ultracapacitor and flywheel concepts are listed as 45,000 cycles because this is the assumed number of cycles a vehicle will experience in its lifetime, and the value of surviving beyond this number is debatable. Table 2 shows the concept scoring matrix with the total scores for each concept, the tolerance on each score, and the confidence levels of the results.

The confidence level is a measure of the degree of belief in the results of the scoring matrix. Table 2 shows that the greater specific power, efficiency, and lifetime of flywheels give them the highest score. The confidence level in the battery column is 0.96. This value means that it is 96% certain that the choice of flywheels over batteries is correct. In the same manner, it is 92% certain that flywheels are a better choice that ultracapacitors. Table 2 also shows that the weaknesses of batteries are specific power, efficiency, and lifetime, and the weaknesses of ultracapacitors are specific

		Load Leveling Device Concepts					
		Batteries		Ultracapacitors		Flywheels	
Selection Criteria	Weight	Rating	Weighted Score	Rating	Weighted Score	Rating	Weighted Score
Specific energy	20±5	100	20.0	76.0	15.2	97.5	19.5
Specific power	25±5	100	25.0	164.2	41.1	864.2	216.1
Efficiency	20±5	100	20.0	120.0	24.0	121.5	24.3
Lifetime	15±5	100	15.0	150.0	22.5	150.0	22.5
Cost	20±10	100	20.0	86.5	17.3	100.7	20.2
Total Score		100.0±15.3		120.1±30.9		302.5±278.3	
Confidence		0.96		0.92		N/A	

Table 2. Concept Scoring Matrix.

81

FMC 1016

energy and specific power

To demonstrate the capabilities of the three LLD concepts and reinforce the results of the scoring matrix, Table 3 shows the mass of a LLD unit necessary to meet the energy and power requirements of a HEV. The mass of the LLD is an important parameter because reducing the mass of the vehicle improves the fuel economy. One kWh and 100 kW are chosen as the energy and power demand, respectively, of a representative HEV.

Table 3 shows that the mass of a lead-acid battery pack is determined by the peak power requirement, and 120 kg of lead-acid batteries is needed to meet the power demand. Slightly more mass is needed with ultracapacitors. They are, however, constrained by the energy storage requirement, and an ultracapacitor with a mass of 142 kg is required to meet this requirement. The flywheel LLD is by far the lightest concept. The flywheel is limited by the energy requirement, and the necessary mass is only 20 kg.

Criteria	Battery Mass, (kg)	Ultracapacitor Mass, (kg)	Flywheel Mass, (kg)
Energy Requirement	18	142	20
Power Requirement	120	63	10

Table 3. Necessary LLD Concept Mass.

CONCLUSION

The use of a design methodology for concept selection in this paper provides a clear link between customer needs, design criteria, and research and development needs. In this case, the results indicate a research focus into flywheel LLDs. In a general case, using a customer motivated design approach in this way allows research and development to be focused on results that will have an impact on customer satisfaction, and in turn product and company success, as the research matures.

The performance capabilities of all the LLD concepts are expected to increased as the concepts are developed. For this reason research should be continued on all the concepts. In particular, the specific power of batteries needs to be increased. The specific energy and cost of ultracapacitors needs to be increased, and mass production methods for flywheel batteries need to be developed so that flywheel cost is reduced.

CONTACT

Paul B. Koeneman
The University of Texas at Austin
Department of Mechanical Engineering
C2200
Austin, TX 78712
(512)471-4772
koeneman@mail.utexas.edu

REFERENCES

1. Ashley, Steven, "Flywheels Put a New Spin on Electric Vehicles," *Mechanical Engineering*, October 1993.
2. Ashley, Steven, "Surging Ahead with Ultracapacitors," *Mechanical Engineering*, vol. 117, no. 2, pp 76-79, 1995.
3. Bates, Bradford, "Getting a Ford HEV on the Road," *IEEE Spectrum*, vol. 32, no. 7, pp 22-25, 1995.
4. Braess, Hans-Hermann and Regar, Karl-Nikolaus, "Electrically Propelled Vehicles at BMW -- Experience to Date and Development Trends," *Electric Vehicle Design and Development SAE Special Publication SP-862*, pp 53-62, 1991.
5. Burke, A.F., "Hybrid/Electric Vehicle Design Options and Evaluations," *Electric and Hybrid Vehicle Technology SAE Special Publication SP-915*, pp 53-77, 1992
6. Burke, A.F., "Cycle Life Considerations for Batteries in Electric and Hybrid Vehicles," *Electric and Hybrid Vehicles -- Implementation of Technology SAE Special Publication SP-1105*, pp 163-173, 1995.
7. Burke, Andrew F., "Electric/Hybrid Super Car Designs using Ultracapacitors," *Proceedings of the Intersociety Energy Conversion Engineering Conference*, vol. 2, pp 89-95, 1995.
8. Davis, Gregory W., "The Effect of a Regenerative Braking System in the Amphibian Hybrid Electric Vehicle," *Proceedings of the Intersociety Energy Conversion Engineering Conference*, vol. 3, pp 1430-1435, 1994.
9. Dickinson, Blake E. and Swan, David H., EV Battery Pack Life: Pack Degradation and Solutions," *Electric and Hybrid Vehicles -- Implementation of Technology SAE Special Publication SP-1105*, pp 145-154, 1995.
10. Dowgiallo, Edward J. and Hardin, Jasper E., "Perspective on Ultracapacitors for Electric Vehicles," *IEEE Aerospace and Electronic Systems Magazine*, vol.10, no.8, pp 26-31, 1995.
11. Heitner, Kenneth L., "Energy Storage Requirements and Optimization of Sustaining Power Source for Hybrid Vehicles," *Proceedings of the Intersociety Energy Conversion Engineering Conference*, vol. 3, pp 1387-1392, 1994.
12. Hively, Will, "Reinventing the Wheel," *Discover*, vol.17, no.8, pp 58-68, 1996.
13. Hoolboom, Gerard J. and Szabados, Barna, "Nonpolluting Automobiles," *IEEE Transactions on Vehicular Technology*, vol.43, no.4, pp 1136-1144, 1994.
14. Hunt, Gary L., Sutula, Raymond A., and Heitner, Kenneth L., "Energy Storage Requirements and Testing for Hybrid Electric Vehicles," *Proceedings of the Intersociety Energy Conversion Engineering Conference*, vol. 2, pp 97-102, 1995.
15. Kalberlah, A., "Electric Hybrid Drive Systems for Passenger Cars and Taxis," *Electric Vehicle Design and Development SAE Special Publication SP-862*, pp 69-78, 1991.
16. Merry, Glen W., "Zinc-air Batteries for Electric Vehicles," *Electric Vehicle R&D SAE Special Publications SP-880*, pp11-16, 1991.
17. Moore, Timothy C. and Lovins, Amory B., "Vehicle Design Strategies to Meet and Exceed PNGV Goals," *Electric and Hybrid Vehicles -- Implementation of Technology SAE Special Publication SP-1105*, pp 79-121, 1995.
18. Otto, K.N. and Wood, K.L., "Estimating Errors in Concept Selection," *1995 Design Engineering Technical Conferences*, vol. 2, pp 397-411, 1995.
19. Pahl, G. and Beitz, W., *Engineering Design: A Systematic Approach*, Springer Verlag, London, 1984.
20. Post, Richard F., Bender, Donald A., and Merritt, Bernard T., "Electromechanical Battery Program at the Lawerence Livermore National Laboratory," *Proceedings of the*

Intersociety Energy Conversion Engineering Conference, vol. 3, pp 1367-1373, 1994.

21. Schaible, Uwe and Szabados, Barna, "A Torque Controlled High Speed Flywheel Energy Storage System for Peak Power Transfer in Electric Vehicles," *Conference Record -- IAS Annual Meeting*, vol.1, pp 435-442, 1994.

22. Steeg, Helga, *Electric Vehicles: Technology, Performance, and Potential*, OECD/IEA, 1993.

23. Trippe, Anthony P., Burke, Andrew F., and Blank, Edward, "Improved Electric Vehicle Performance with Pulsed Power Capacitors," *Electric and Hybrid Vehicle Advancements SAE Special Publications SP-969*, pp89-94, 1993.

24. Ulrich, Karl T. and Eppinger, Steven D., *Product Design and Development*, McGraw-Hill, 1995.

25. Wells, Stephen P., Pang, Da-Chen, and Kirk, James A., "The Design, Manufacture, and Testing of a Composite Flywheel for Energy Storage," *Mechanics in Materials Processing and Manufacturing*, vol.194, pp 397-404, 1994.

Simulation of Hybrid Electric Vehicles with Emphasis on Fuel Economy Estimation

Erbis L. Biscarri and M. A. Tamor
Ford Motor Company

Syed Murtuza
University of Michigan

ABSTRACT

This paper describes SHEV, a computer program created to simulate hybrid electric vehicles. SHEV employs the time-stepping technique in order to evaluate energy flow in series hybrids, and makes use of a unique method in order to speed up the fuel economy estimation. This estimation method is a refinement of the "state of charge matching" method and is explained in detail.

The graphic user interfaces employed in SHEV make it easy to use and give it a look similar to regular Windows® applications. This paper also gives some examples of the screens created by the program, depicts its main flowchart, and describes a battery model optimized for this application.

INTRODUCTION

This paper describes SHEV, a program for Simulation of Hybrid Electric Vehicles. SHEV has a focus on fuel economy estimation and details will be given on its unique estimation method.

Fuel Economy (FE) is one of the more important figures of merit for a Hybrid Electric Vehicle (HEV) and thus one of the relevant outcomes of simulation programs used in their development. Moreover, sensitivity analyses are usually performed, in order to identify which parameters affect FE the most [1], [2]. These require running a simulation program many times to obtain an estimate of the FE for each value of the parameter, a very time consuming task. SHEV estimates the FE with a new method, in order to reduce the total simulation time.

HEV BLOCK DIAGRAM

SHEV assumes the *series* hybrid configuration as depicted in Fig. 1. The main subsystems are:

- Fuel Tank
- Hybrid Power Unit
- Auxiliary Modules
- Energy Storage Subsystem
- Traction Inverter Module
- Traction Motor

The Hybrid Power Unit (HPU) is composed of a fuel powered engine, an alternator and associated rectifier/controller. It is sometimes called Auxiliary Power Unit or APU in the literature.
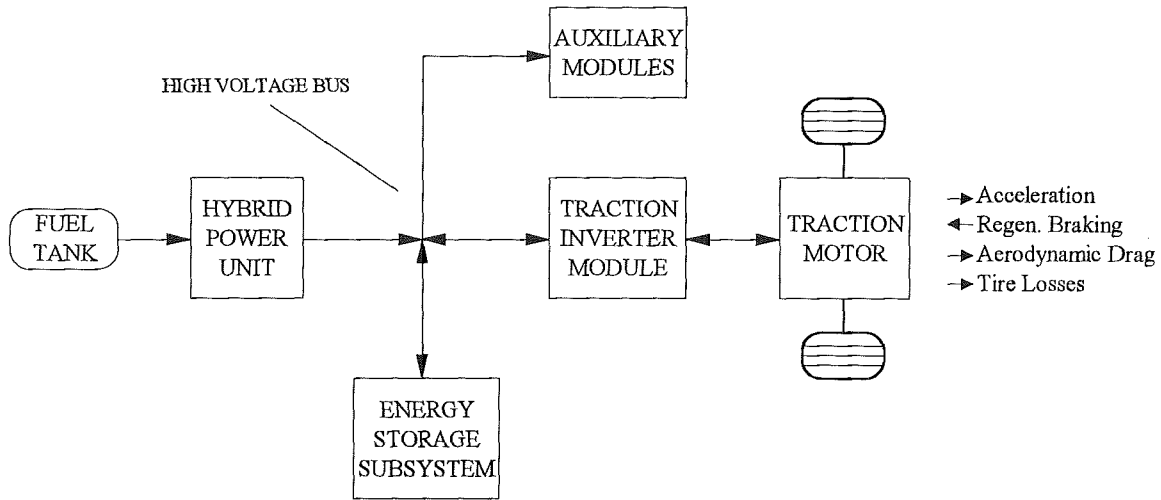
Fig. 1: Series Hybrid Electric Vehicle - Simplified Block Diagram and Energy Flow

The Auxiliary Modules (AM) block represents the general purpose electric loads, like air conditioner, lighting, and radio system. The Energy Storage Subsystem (ESS) can be a battery, flywheel, ultracapacitor, or a combination of these. The efficiencies of the Traction Inverter Module (TIM) and Traction Motor (TM) can be accounted individually or combined in the TM efficiency definition (efficiency map).

The simulation assumes a fixed transmission ratio to avoid the need of a separate transmission/transaxle block. This is a reasonable simplification, since many HEV prototypes (like Dodge Intrepid ESX [3]) and also some Electric Vehicles (like GM's EV1 [4], [5], and Ford's Ecostar [6]) employ a fixed transmission ratio. The transmission losses are accounted in the TM efficiency.

This paper also assumes a simple ON/OFF strategy (the so called 'thermostatic' operation) to control the status of the HPU [7]. An additional assumption is the use of Regenerative Braking (Regen for short) [8], [9]. Regen recovers part of the kinetic energy of the vehicle during deceleration and stores it in the ESS.

The arrows in Fig. 1 indicate the possible directions of the energy transfer between each block. When the vehicle is accelerating and the HPU is on, it converts the chemical energy from the fuel into electric energy. This energy is used by the auxiliary loads and Traction Inverter Module, as required in order to feed the TM. Depending on the energy balance at the High Voltage Bus, the storage subsystem can either receive energy from (ESS under charge) or provide energy to (discharge) the bus. The inverse arrows in the path High Voltage Bus - TIM - TM

represent the energy flow during regenerative braking.

The small arrows on the right hand side of the diagram show the energy flow at the wheels, during Acceleration (vehicle increasing its kinetic energy), during Regenerative Braking (deceleration), and also the energy drags caused by the Aerodynamic force and Tire Losses.

SHEV's initial screen displays a simplified version of this block diagram (see Fig. 2), as a handy reminder of the topology used and names of each of the subsystems.
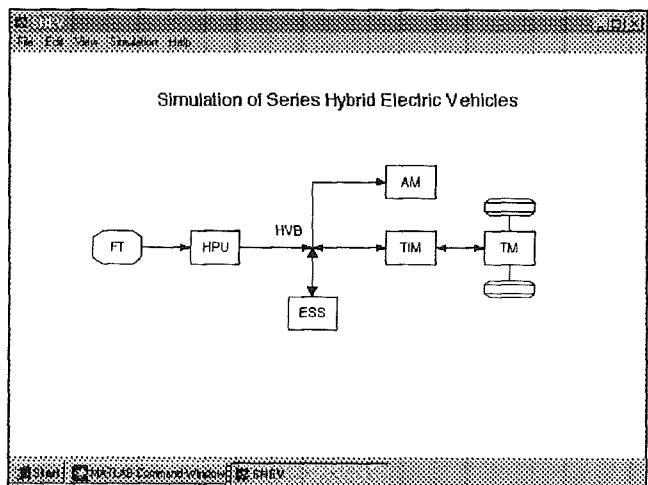
Fig. 2: SHEV's Initial Screen

BATTERY MODEL

The battery model is of special importance. It is relatively simple, in the sense that it simulates pseudo-static conditions, but takes into account

some of the non-linearities present in a real battery. We felt it was adequate to model the battery by using the equivalent circuit shown in Fig. 3. SHEV makes use of this model only to evaluate instantaneous voltage and current. The calculations used to estimate the SOC are described later on.
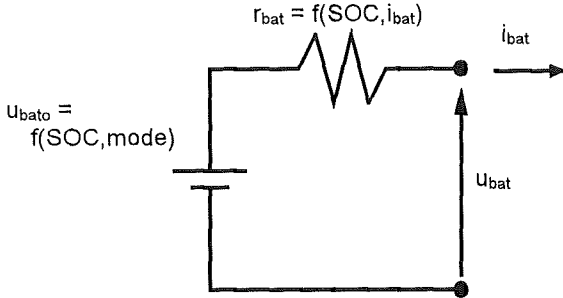
Fig. 3: Battery Model

The associated variables are:

u_{bato} = open circuit voltage, in V
r_{bat} = equivalent internal resistance, in Ohm
SOC = state of charge, in %
i_{bat} = current sourced by the battery, in A
u_{bat} = voltage across battery terminals, in V
mode = charge or discharge

At a first glance it may seem sufficient to make u_{bato} dependent of SOC only (since the regular definition of the open circuit voltage implies in zero current through the battery). But SHEV's battery model extends the meaning of u_{bato}, making it reflect two different conditions: charge and discharge. This substantially improved the fit obtained by using linear regression.

The relationship between the variables of Fig. 3 in a real battery is very complex. It depends not only on its basic materials (lead - acid or nickel - metal hydride for instance), but also on its internal construction (plate, tubular, dimensions of each component, etc.). Keeping in mind that in a HEV the usual range for SOC is short, say between 40% and 80%, then a linear approximation of the open circuit voltage against SOC seems reasonable.

In summary, we can apply the following formulas to simulate u_{bato}:

$$u_{bato} = k_{vd0} + k_{vd1} \cdot SOC \quad if \quad i_{bat} \geq 0$$

$$u_{bato} = k_{vc0} + k_{vc1} \cdot SOC \quad if \quad i_{bat} < 0$$

where:

k_{vd0}, k_{vd1}, k_{vc0} and k_{vc1} are arbitrary linearization

coefficients

While the equations used to simulate r_{bat} are:

$$r_{bat} = k_{d0} + k_{d1} \cdot SOC + k_{d2} \cdot i_{bat} \quad if \quad i_{bat} \geq 0$$

$$r_{bat} = k_{c0} + k_{c1} \cdot SOC + k_{c2} \cdot i_{bat} \quad if \quad i_{bat} < 0$$

where:

k_{d0}, k_{d1}, k_{d2}, k_{c0}, k_{c1}, and k_{c2} are arbitrary linearization coefficients

Fig. 4 shows the match obtained between the typical battery behavior (continuous lines) and the emulation calculated from the formulas presented (dotted lines). The chart shows a nice fit except for small discharge currents.
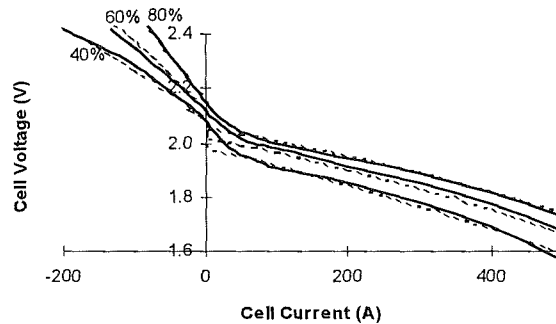
Fig. 4 Typical and Emulated Cell Voltage Versus Current at Various SOC

The linearization formulas presented provide a good approximation for the open circuit voltage and series resistance, and are used in SHEV in order to calculate instantaneous voltage and current at the battery terminals. The model presented so far simulates the ohmic losses inside the battery with a reasonable approximation.

If we try to extend the usage of this model to obtain the changes in the SOC the result will not be satisfactory, though. Other significant loss mechanisms would be neglected and the efficiency of the charge and discharge processes would be overestimated.

Peukert's equation is usually adapted to calculate the SOC [10-13]. The energy capacity of a battery is measured in Ah and is highly dependent on the discharge current. This phenomenon is described by:

$$I^n \cdot t = C$$

where:

I = discharge current, in A
n = exponential constant, usually around 1.35 for lead-acid batteries
t = discharge time, in h
C = capacity constant, in Ah

The formula expresses the experimental experience that the capacity drops more rapidly as the current increases, and is valid only for a certain range. For very low values of discharge current we can assume a constant capacity instead, as exemplified in Fig. 5.
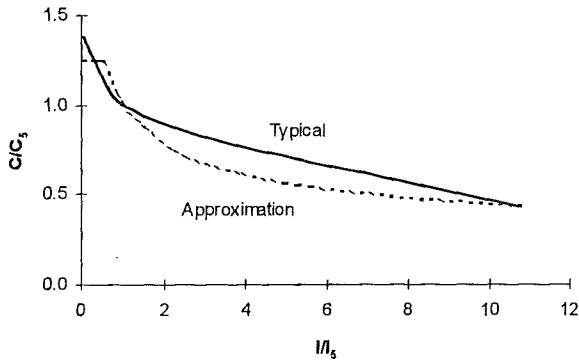
Fig. 5: Battery Capacity Versus Discharge Current

Limiting the maximum value of C to 1.25 * C5, the change in SOC during a given time interval is calculated by:

$$\Delta SOC(i) = \frac{-i_{avg} \cdot \Delta t}{36 \cdot C_5 \cdot \left(\dfrac{i_{avg}}{I_5} \right)^{-0.35}} \quad \text{if} \quad i_{avg} \geq 0.529 \cdot I_5$$

$$\Delta SOC(i) = \frac{-i_{avg} \cdot \Delta t}{45 \cdot C_5} \quad \text{if} \quad 0 \leq i_{avg} \leq 0.529 \cdot I_5$$

where:

$\Delta SOC(i)$ = change in the state of charge of the battery at instant i, in %
i_{avg} = [$i_{bat}(i)$ + $i_{bat}(i-1)$] / 2 , in A
Δt = t(i) - t(i-1), in seconds
C_5 = battery capacity at a 5h discharge rate, in Ah
I_5 = discharge current that depletes the battery in a 5h interval, in A

During the charging process, a constant efficiency is typically assumed (as in [10] and [11]), and the change in SOC can be calculated by:

$$\Delta SOC(i) = \frac{-i_{avg} \cdot \Delta t \cdot n_{chr}}{3,600 \cdot C_5} \quad \text{if} \quad i_{avg} < 0$$

where:

n_{chr} = battery charging efficiency, in %

DRIVING SCHEDULES

Estimation of FE requires specific driving schedules, like the one defined by the Environmental Protection Agency (EPA) for US highway driving conditions [14], seen in Fig. 6. Most driving schedules establish a target speed for the vehicle at 1 second time increments, but SHEV accommodates schedules with fixed or variable time increments. SHEV assumes a constant acceleration or deceleration between each point in the schedule, in order to simplify the calculations.
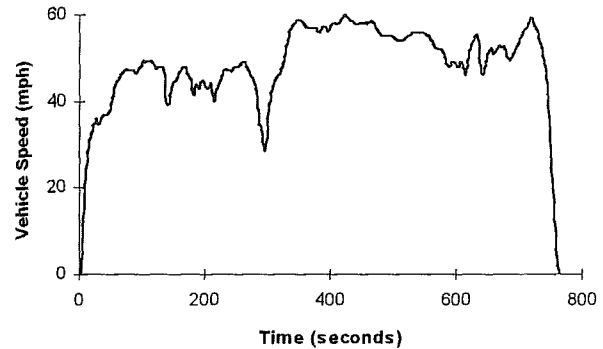
Fig. 6: EPA Highway Driving Schedule

SIMULATION PROGRAM

A time stepping simulation program was developed, using Matlab® as a convenient software platform [15]. The basic vehicle dynamics models are taken from Gillespie [16] and Sovran and Bohn [17]. Papers on similar programs were also used as references ([10], [11] and [18-24]).

Fig. 7 illustrates SHEV's main flowchart. At each time step, the program calculates the power required to meet the schedule, assuming a constant acceleration or deceleration during each step interval. The power required at the wheels is reflected into power requirements at the traction motor and traction inverter module. The vehicle control strategies will define if the HPU will be on or off, depending on the state of charge of the battery and the power required from the high voltage bus. As a result, the battery will experience a charge or a discharge, and its SOC will increase or decrease.
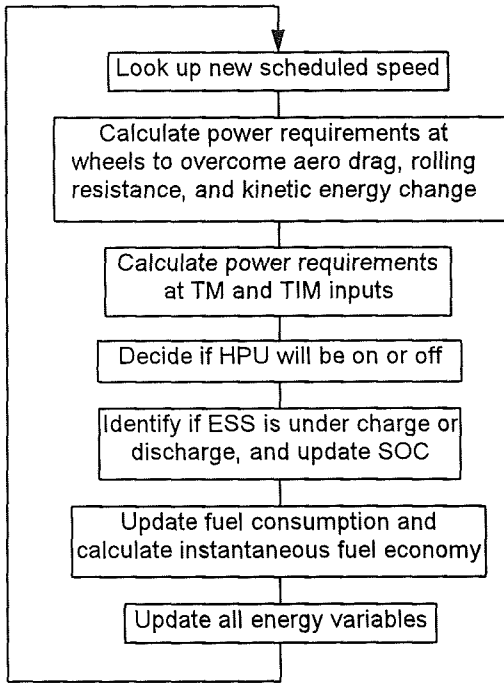
Fig. 7: Main Flowchart of the Simulation Program

During these calculations, the program takes into account physical constraints of the subsystems (e.g., maximum torque of the motor), and warning or error messages are displayed when applicable. The program converts the power requirements into energy needs from the HPU, and calculates the fuel consumption and instantaneous fuel economy. SHEV repeats this process for each discrete time instant, and uses a supervisory loop to control the overall simulation.

SHEV was developed to allow the simulation of the energy requirements of a typical HEV, with enough flexibility to permit evaluation of different FE estimation algorithms. It should be emphasized that SHEV's objective was not the perfect simulation of the behavior of a specific HEV.

The graphic user interface capabilities of the software platform have been exploited in order to create an easy to use, interactive, program. The user can select many simulation parameters by mouse navigation, and type constants in self-explanatory boxes. The pop-up menus available at the top of the screen resemble the familiar sequence File/Edit.../Help available in most Windows® applications.

After the end of the simulation, the user can view a summary of the vehicle behavior, or select charts of many variables to be displayed on the screen. Fig. 8 and Fig. 9 illustrate more examples of the look of the screens created by SHEV.
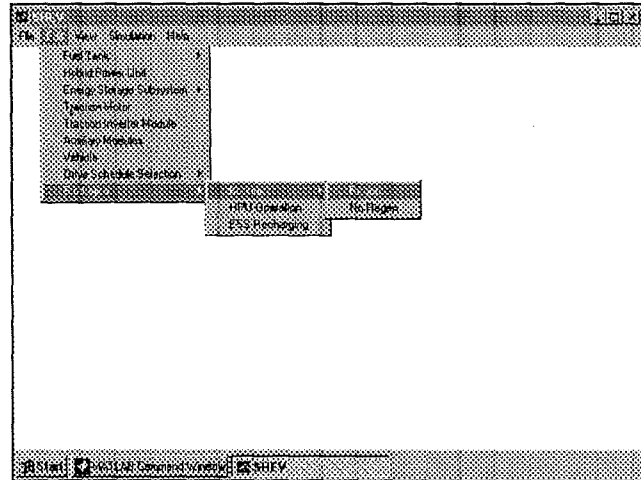
Fig. 8: Example of SHEV Screen (Selection of Regenerative Braking)
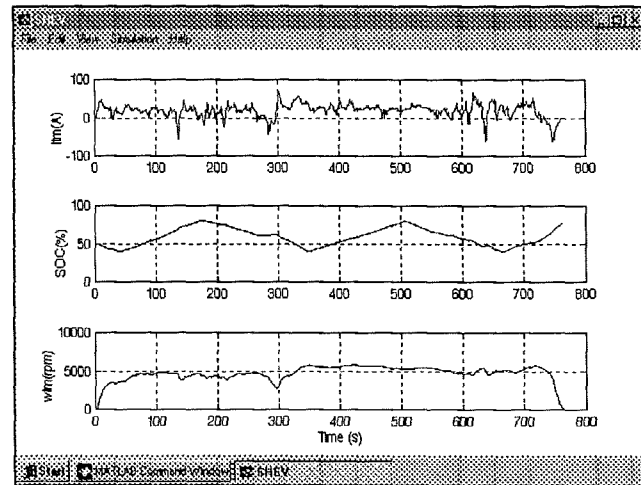
Fig. 9: Example of SHEV Screen (Some of the Charts that can be Displayed)

FUEL ECONOMY ESTIMATION

For vehicles propelled by an internal combustion engine alone, the FE is given by:

$$FE = \frac{D}{FC}$$

where:

FE = fuel economy, in miles per gallon
D = total traveled Distance, in miles
FC = total Fuel Consumed, in gallons

The same approach does not hold for vehicles that have a substantial energy storage element (usually a large battery), like the HEV [25], [26].

The first reason is that the fuel consumption is not strictly dictated by the energy required to meet the speeds defined in the schedule. On one hand, the battery can experience a net increase in its state of charge (SOC) along the schedule, which will increase the fuel consumption. On the other hand, the battery can experience a net discharge, providing some energy to the traction motor (and thus less fuel will be necessary to overcome the schedule requirements).

A second and more subtle reason is that a single run of the schedule may not be representative of the vehicle behavior. The initial state of the vehicle (i.e., its initial SOC), as well as its operational strategies, affect the FE estimate. In other words, the results of a single run may differ from another one starting with a different SOC. Also, some strategies are adaptive, changing over time, and thus changing the FE. For those situations, an average behavior is more useful.

In summary, additional processing is required in order to account for the existence of the storage element. In order to compare different estimation methods, during the development of SHEV we used a vehicle with the characteristics listed in Table 1[1].

Table 1: Base Vehicle Used for Simulation

Frontal Area: 2 m^2	ESS Charging Efficiency: 85%
Aerod. Drag Coeff.: 0.20	ESS Discharging Efficiency: 85%
Tire Loss Coefficient: 0.005	ESS Energy Capacity: 1.0 kWh
Vehicle Test Mass: 1100 kg	ESS Initial State of Charge: 50%
Regenerative Braking	ESS Lower Threshold: 40%
Fuel: gasoline	ESS Higher Threshold: 80%
HPU Power: 20 kW	TM Field-weakened Perm. Magnet
HPU Efficiency: 35%	TM Power: 50 kW
HPU Strategy: Thermost.	TM Max. Torque: 220 N-m
AM Load: 1.0 kW	TM Max. Shaft Speed: 7500 rpm
Transmission Ratio: 7.0	TM Efficiency: mapped
Tire Radius: 12 inches	TIM Efficiency: 96%

The simulation was initially run for an extremely high number of passes (1000), where all multiple-run methods converge to about the same FE estimate[2]. This estimate was then considered the "true" FE for the given vehicle configuration and driving schedule.

The simulation was run again, using fewer passes of the schedule, and the estimation errors were

---

[1]A simple battery model (fixed charging and discharging efficiencies and constant energy capacity) was used during the evaluation of the FE estimation methods.

[2]This statement may not be correct for all situations. There might be cases where a "phase lock" condition exists between the on/off cycles of the HPU and their relative positions along the driving schedule. This can cause the FE to be abnormally high/low when the HPU is mostly on/off for regions with high energy demand. This situation by itself would deserve a dedicated study and is beyond the scope of the current paper.

calculated by:

$$\%Error = \frac{\overline{FE} - FE}{FE} \cdot 100\%$$

where:

$\overline{FE}$ = fuel economy estimate, in mpg
FE = "true" fuel economy, in mpg

BASIC SOC MATCHING METHOD

This method tries to reduce the effect of the change in the SOC by running a second, partial, pass, until the instantaneous SOC matches its initial value. The *instantaneous* fuel economy at this moment (distance divided by the fuel consumed) is then picked as the FE estimate. In other words, given the instant t_m that equates:

$$SOC(t_m) = SOC_i$$

then:

$$\overline{FE} = \frac{D(t_m)}{FC(t_m)}$$

where:

tm = instant where the SOC match occurs, in seconds
$SOC(t_m)$ = SOC at time t_m, in %
SOC_i = initial SOC, in %
$D(t_m)$ = total distance traveled until time t_m, in miles
$FC(t_m)$ = total fuel consumed until time t_m, in gallons

Fig. 10 provides a graphical example. Note that SOC is higher than SOC_i at the end of the first pass (at 764 seconds). A second pass is started, and stopped only when SOC reaches 50%. This happens at 966 seconds, and the instantaneous fuel economy at this point is used as the FE estimate.

In this method, SOC_i has to be in a range that will be crossed through the simulation, i.e., it has to be between SOC_L and SOC_H limits. SOC_L and SOC_H are the lower and higher SOC thresholds, respectively, and are used by the thermostatic strategy to define when to turn on and off the HPU.

Eventually, it may take more than two passes until the instantaneous SOC matches SOC_i. This may happen for vehicles with a large ESS, for instance.
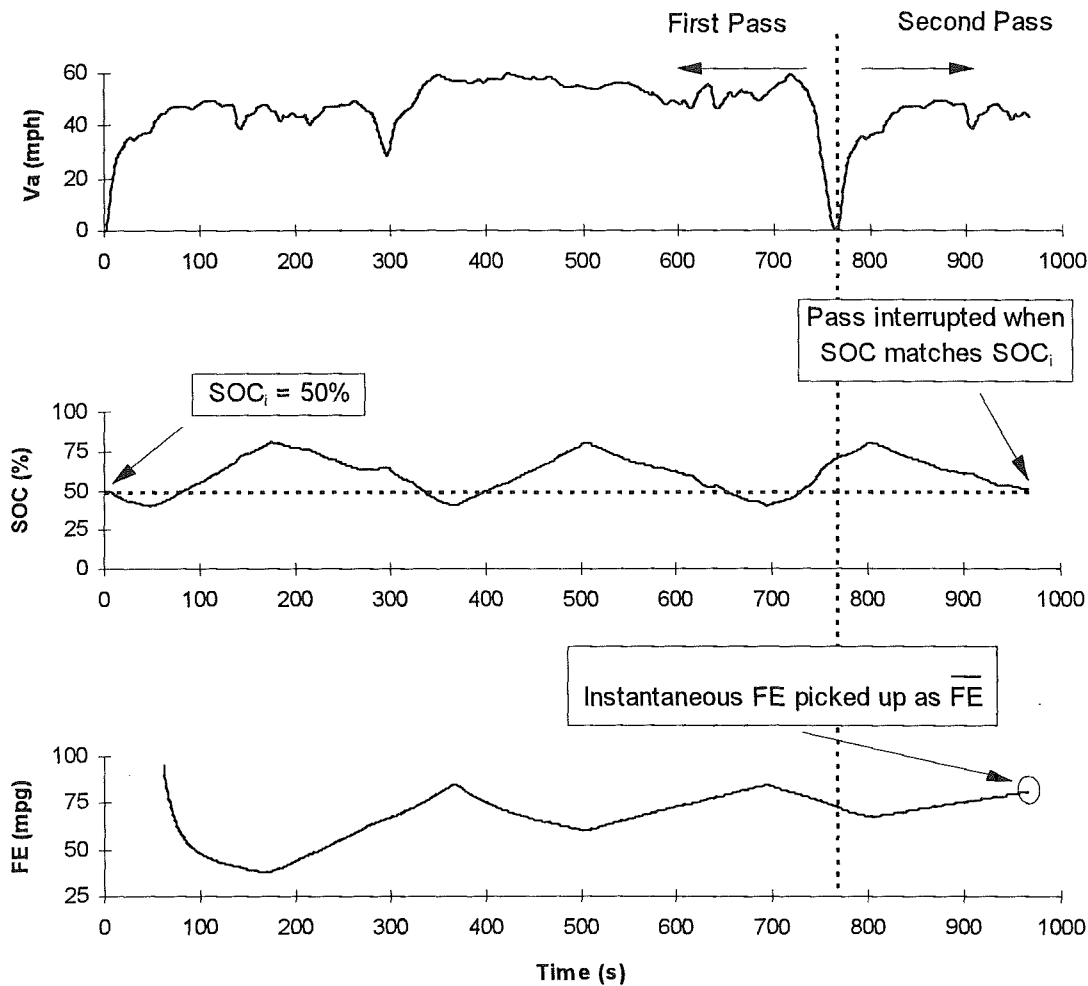
Fig. 10: SOC Matching Method

A source of error in the FE estimate is that the schedule does not demand the same energy from the TM at each instant. If t_m (instant where the matching occurs) is in a region where the schedule has a small energy demand (low speed and/or low acceleration), then FE will most likely be overestimated. If t_m is in a region with high energy demand, then FE will probably be underestimated. Errors in the range of 4% were found during the evaluations of this method.

MULTIPLE RUNS WITH SOC MATCHING

This is an extension of the basic SOC matching method, with many complete passes run before starting the partial pass. The intent is to benefit from the natural averaging of many successive runs.

A similar procedure is found in Aceves and Smith [19]. Instead of fixing the number of runs, they set a minimum distance to be traveled before the program searches for a SOC matching.

Although the estimation error generally reduces as the number of simulation passes increases, it is difficult to define a stop criterion since the convergence is not monotonic, as illustrated in Fig. 11. A relatively large number of passes has to be used, in order to guarantee a small error.
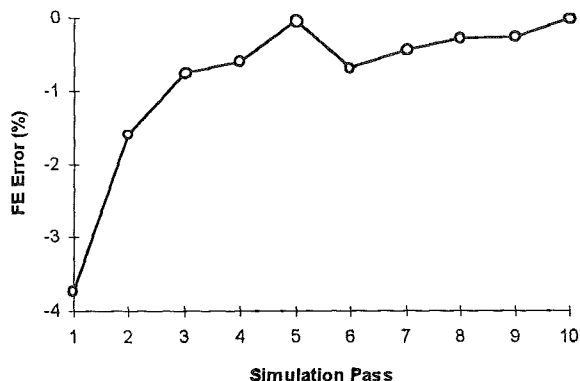
Fig. 11: Example of Estimation Error Evolution for SOC Matching Method

SHEV'S METHOD

SHEV uses the multiple runs with SOC matching method, with some refinement. It can be demonstrated that the estimation error in the FE depends on the instant where the SOC matching occurs. Large estimation errors are usually associated with large values of the variable ΔE_m defined by:

$$\Delta E_m = \frac{\Delta E_{LOAD}}{E_{Lm}} \cdot 100\%$$

where:

ΔE_m = relative energy change for the SOC-matching method, in %

ΔE_{LOAD} = change in E_{LOAD}, since the last complete pass until the SOC match, in kWh

E_{Lm} = E_{LOAD} value when the SOC match happens, in kWh

E_{LOAD} = total energy load, in kWh

While E_{LOAD} is given by the formula:

$$E_{LOAD} = E_{TIM} + E_{AMT}$$

where:

E_{TIM} = total energy required at TIM input, in kWh

E_{AMT} = total energy required by the AM block, in kWh

ΔEm translates how far (in terms of energy spent) the SOC matching point is from the last complete pass. If ΔE_m is small, this means that the SOC match happened right after the beginning of a new pass, or after many complete passes were run. In any case, we are close to an ideal situation (i.e., the match happening right at the end of the last pass) and the effect of the difference in the energy stored in the ESS will be small. Thus, the instantaneous fuel economy obtained at this point is very close to the real FE value.

The scatter chart in Fig. 12 illustrates the results for the same base vehicle, using the highway schedule. Each point indicates the error obtained with a different number of passes.

Large estimation errors are associated with high values of the relative energy change. We can now use the ΔE_m variable as a stop criterion: if we run the multiple simulations and stop the program only when the magnitude of ΔE_m is below 0.2%, we should achieve a FE estimate within ±0.5% of the true value.

In the simulations run with this method, typically half the number of passes was enough to achieve the FE estimate. The comparison was made with the regular "multiple runs with SOC matching" method, under the highway schedule, to obtain less than 0.5% error.
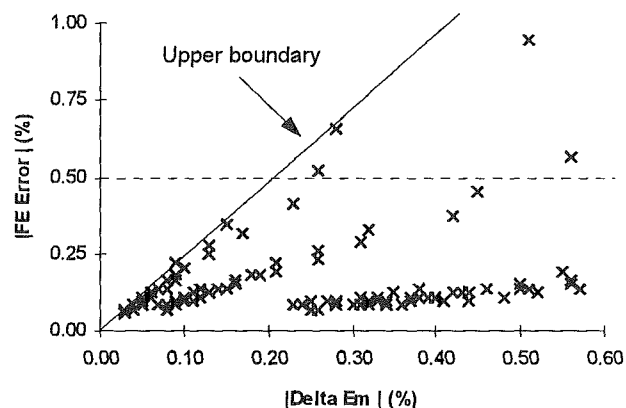
Fig. 12: Scatter Chart of Estimation Error Versus Relative Energy Change, Highway

CONCLUSION

This paper provided an overview of SHEV, a simulation program focused on fuel economy estimation for series hybrid electric vehicles. SHEV employs the time-stepping technique to calculate powerflows in the vehicle, and makes use of convenient graphic interfaces to access and display vehicle data.

The paper also described in detail the linearized battery model which was optimized for the operating conditions of the simulation. Finally, it presented SHEV's fuel economy estimation method. This method is an evolution of the "state of charge matching" method, and allows shorter estimation times.

ACKNOWLEDGMENTS

REFERENCES

1. D. Busse and C. Braun, " Hybrid-electric-vehicle sensitivity analysis", *Automotive Engineering*, February 1997.
2. K. Yamaguchi et al., "Development of a New Hybrid System - Dual system", *Strategies in Electric and Hybrid Vehicle Design*, SAE SP-1156, 1996.
3. K. Jost, "Chrysler's Hybrid Concept", *Automotive Engineering*, May 1996.
4. K. Buchholz, "Electric Vehicle for the Masses: GM's EV1", *Automotive Engineering*, April 1996.
5. F. A. Wyczalek, "GM Electric Vehicle Technology in the 1990's", *Proceedings of the 26th IECEC*, vol. 4, 1991.
6. K. Cook, "Behind the Scenes of a Near Productionised Fast Electric Vehicle", *Automotive Engineer*, vol. 20, No. 4, August/September 1995.
7. C. G. Hochgraf et al., "Engine Control Strategy for a Series Hybrid Electric Vehicle Incorporating Load-Leveling and Computer Controlled Energy Management", *Strategies in Electric and Hybrid Vehicle Design*, SAE SP-1156, 1996.
8. S. R. Cikanek and K. E. Bailey, "Energy Recovery Comparison Between Series and Parallel Braking Systems for Electric Vehicles Using Various Driving Cycles", *Fifth AME Symposium on Advanced Automotive Technologies of the 1995 ASME International Congress and Exposition*, San Francisco, CA, November 12, 1995.
9. F. A. Wyczalek and T. C. Wang, "Regenerative Braking Concepts for Electric Vehicles - A Primer", *SAE Technical Paper Series 920648*, 1992.
10. K. E. White, "A Digital Computer Program For Simulating Electric Vehicle Performance", SAE 780216, SAE Congress and Exposition, Detroit, 1978.
11. J. R. Bumby et al., "Computer modeling of the automotive energy requirements for internal combustion engine and battery electric-powered vehicles", *IEE Proceedings*, vol. 132, Pt. A, No. 5, September 1985.
12. R. Kiessling, "Modeling of Lead-Acid Batteries for EV Fuel Gauge and Similar Applications", 26th ISATA (International Symposium on Automotive Technology and Automation) - Dedicated Conference on Electric, Hybrid and Alternative Fuel Vehicles: Progress in Technology & Infrastructure, Aachen, Germany, Sep. 1993.
13. H. Bode, *Lead-Acid Batteries*, John Wiley & Sons, 1977.
14. ----, "EPA Highway Fuel Economy Driving Schedule", Environmental Protection Agency, *Code of Federal Regulations*, vol. 40, Special Edition of the Federal Register, July 1, 1994.
15. *Matlab: Version 4.0: User's Guide*, The Mathworks Inc, Prentice-Hall, 1995.
16. T. D. Gillespie, *Fundamentals of Vehicle Dynamics*, Published by SAE, 1992.
17. G. Sovran and M. S. Bohn, "Formulae for the Tractive-Energy Requirements of Vehicles Driving the EPA Schedules", *SAE Technical Paper Series 810184*, 1981.
18. M. C. Chang, "Computer Simulation of an Advanced Hybrid Electric-Powered Vehicle", *SAE Technical Paper Series 780217*, 1978.
19. S. M. Aceves and J. R. Smith, "A Hybrid Vehicle Evaluation Code and its Application to Vehicle Design", *Design Innovations in Electric and Hybrid Electric Vehicles*, SAE SP-1089, 1995.
20. J. Schreiber et al., "Electric and Hybrid Electric Vehicle Study Utilizing a Time-Stepping Simulation", *Proceedings of the 27th IECEC*, vol. 1, 1992.
21. R. Slusser, "ELVEC - An Electric / Hybrid Vehicle Performance Simulation Computer Program", *EVC EXPO 80 Conference Proceedings*, 1980.
22. F. E. Wicks and D. Marchionne, "Development of a Model to Predict Electric Vehicle Performance Over a Variety of Driving Conditions", *Proceedings of the 27th IECEC*, vol. 1, 1992.
23. L. E. Unnewehr and C. W. Knoop, "Electrical Component Modeling and Sizing for EV Simulation", *SAE Transactions*, vol. 87, 1978.
24. G. H. Cole, *Simplev: A Simple Electric Vehicle Simulation Program - Version 2.0*, Idaho National Engineering Laboratory, April 1993.
25. M. Duoba and R. Larsen, "HEV Dynamometre Testing with State-of-Charge Corrections in the 1995 HEV Challenge", SAE 960740, SAE International Congress & Exposition, Detroit, MI, Feb 26-29, 1996.

ABOUT THE MAIN AUTHOR

Erbis L. Biscarri received the B.S. degree in electronic engineering from the University of Sao Paulo, Brazil in 1983, where he also specialized in industrial administration. He is currently pursuing the M.S. degree in manufacturing systems engineering at the University of Michigan, while developing a thesis on simulation of hybrid electric vehicles.

His work experience includes design of analog instrumentation, switched mode supplies, and audio products. He is currently working as a senior product design engineer with Ford Electronics, developing entertainment products for automotive applications. His interests comprise electric and hybrid vehicles, high speed flywheels, analog design, and lean manufacturing.

Validation of ADVISOR as a Simulation Tool for a Series Hybrid Electric Vehicle

Randall D. Senger, Matthew A. Merkle, and Douglas J. Nelson
Virginia Polytechnic Institute and State University

ABSTRACT

One of the most widely used computer simulation tools for hybrid electric vehicles (HEVs) is the ADvanced VehIcle SimulatOR (ADVISOR) developed by the National Renewable Energy Laboratory. The capability to quickly perform parametric and sensitivity studies for specific vehicles is a unique and invaluable feature of ADVISOR. However, no simulation tool is complete without being validated against measured vehicle data to insure the reliability of its predictions. This paper details the validation of ADVISOR using data from the Virginia Tech FutureCar Challenge Lumina, a series HEV. The modeling process is discussed in detail for each of the major components of the hybrid system: transmission; electric motor and inverter; auxiliary power unit (fuel and emissions); batteries; and miscellaneous vehicle parameters. The integration of these components into the overall ADVISOR model is also described.

The results of the ADVISOR simulations are then explained. These results are compared to measured vehicle data on energy use, fuel efficiency, emissions output, and control strategy function for a variety of driving cycles and test procedures. Uncertainties in the measured data are discussed. Finally, the discrepancies between predicted and actual behavior are analyzed. This validation process shows that ADVISOR has extensive value as a simulation tool for HEVs. The existing limitations of the program are also discussed, with recommendations for improvement.

INTRODUCTION

Hybrid vehicles provide some of the most promising designs with the capability of meeting the goals of the Partnership for a New Generation of Vehicles (PNGV). Ideally, these vehicles will achieve three times the current fuel economy while drastically lowering emissions levels, and without sacrificing the features, comfort, and performance of current conventional automobiles. However, the development of these vehicles will require accurate, flexible simulation tools. Such a simulation program is necessary to quickly narrow the technology focus of the PNGV to those configurations and components that are best suited for these goals. Therefore, the simulation must be flexible enough to encompass the wide variety of components that could possibly be utilized. Finally, it must be able to assist vehicle designers in making specific decisions in building and testing prototype automobiles.

With the existing technology, the most common form of hybrid passenger vehicles is that of a hybrid electric vehicle (HEV). Most existing HEVs utilize batteries for electrical energy storage, which is converted to mechanical work at the wheels of the vehicle. Fuel is also stored on-board and is usually converted through an internal combustion engine (ICE) to produce mechanical work, which can be used to drive the wheels of the vehicle or can be further converted to electrical energy.

HEVs provide the benefits of both electric vehicles (EVs) and traditional ICE vehicles, while minimizing the limitations of each. They utilize the high efficiencies and low emissions of pure electric vehicles with the range and quick refueling capabilities of ICE vehicles. The basic design of a HEV generally falls into one of two categories: parallel or series.

Parallel HEVs are configured such that both the electric motor and the ICE are mechanically coupled to the drive wheels of the vehicle. This design offers the advantage of drive system redundancy. If either of the drive systems should fail, the other system would still be available to move the vehicle for service. A parallel hybrid usually provides better highway fuel economy and less mass than its series counterpart. It also provides the ability to withstand long uphill grades. The design often allows for a pure electric vehicle, or zero emissions vehicle (ZEV), mode. However, the parallel design does not allow for full vehicle power when
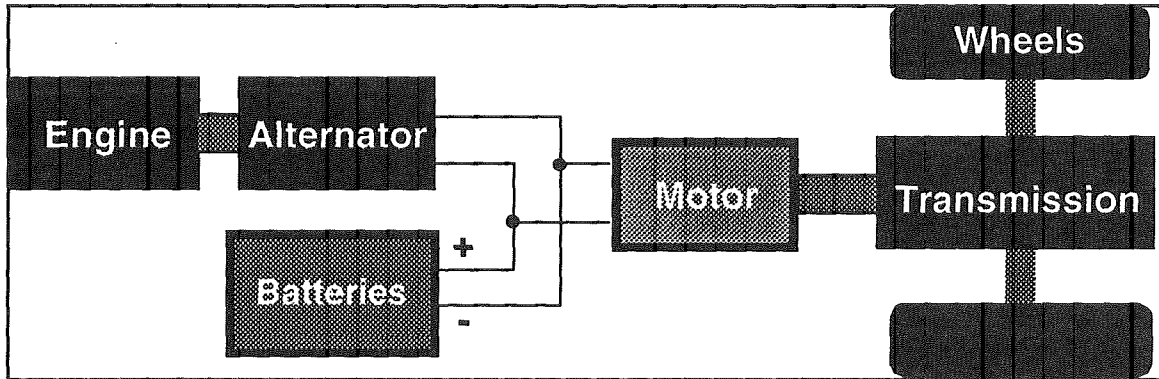
95

Figure 1. Series HEV Schematic

operating in ZEV mode. The mechanical coupling of the motor, engine, and wheels can also be complex, often times requiring a multi-speed transmission. The direct mechanical connection between the engine and the wheels also makes engine tuning more difficult, since the engine must operate over a fairly large range of speeds and loads.

Series HEVs are similar to pure EVs in that only the electric motor is mechanically coupled to the drive wheels of the vehicle as shown in Figure 1. The ICE is used only to drive an alternator to generate electrical energy, which can be used to power the electric motor or to recharge the batteries. The entire assembly, from the fuel input to the electrical output, is known as the auxiliary power unit (APU). This design results in a simpler mechanical connection to the wheels than parallel hybrids, which, in turn, allows more freedom in component placement. The electric motor can be sized such that only a single-speed transmission is required. Full power is available at all times, even when operating in ZEV mode. Since the ICE is not mechanically coupled to the wheels, isolation of the engine load from that of the vehicle is simplified, and this provides excellent city fuel economy. The design also lends itself well to future improvements in battery technology. As the energy storage capability of batteries improve, a series vehicle can simply use the ICE less and less, moving toward a pure EV design. However, there is no redundancy in the drive system, so a failure in the electric drive system renders the vehicle undriveable (similar to an ICE failure in a typical vehicle). The ability of a series HEV to sustain a long uphill grade at a given speed is determined by the size of the battery pack, and may not be acceptable under extreme conditions. Finally, series hybrids are usually slightly heavier than a comparable parallel HEV.

In order to realize the benefits of HEVs, the designs must be refined and put into production before improved emissions and fuel economy can occur on a large scale. This will require accurate, flexible simulation tools, which will expedite the design processes for HEVs. This will enable engineers to predict the relative performance of one design to another and concentrate on the best designs.

This paper begins with a discussion of the available tools for performing HEV simulations, and compares their features and abilities. It then studies in more detail the operation of one simulation tool, which is used throughout this work, ADVISOR. The basics of ADVISOR are explained, including the information required for simulating a series HEV. The necessary data includes general vehicle parameters and models for each major component of the vehicle: APU, motor/inverter, transmission, and batteries.

Each component of the Virginia Tech FutureCar is described in detail. The testing procedures for each component and the integration of the test data into the ADVISOR model are described. This test data is displayed for each component.

The modifications to the ADVISOR code itself which were necessary to accurately reflect the operation of the Virginia Tech vehicle and the effects of these changes are discussed. A number of simulations are subsequently performed to test the validity of ADVISOR under a broad spectrum of operating conditions. The accuracy of the ADVISOR predictions are described and contrasted with measured test data at various intermediate points, including vehicle road load, electric drivetrain energy use on standard driving cycles, and APU/battery energy use on standard driving cycles. The final measure of the simulation is the comparison of the vehicle's city fuel economy, highway fuel economy, and emissions, which are presented and explained.

From the results of these simulations, some conclusions are drawn. The details of the discrepancies and uncertainties in the ADVISOR code, the component models, and the measured data are discussed. The validity of ADVISOR as a simulation tool for this vehicle and similar vehicles is evaluated and recommendations for reliable use are listed.

REVIEW OF LITERATURE

A search of the recent literature reveals a number of computer software simulations are available specifically for HEVs. These simulation tools have varying abilities to predict vehicle performance in one or more areas, such as fuel economy, emissions, acceleration, and grade sustainability. Some of the more prominent tools are reviewed here with their capabilities and features.

SIMPLEV

SIMPLEV, A Simple Electric Vehicle Simulation Program, Version 2.0 (Cole, 1993) is a computer software program developed at Idaho National Engineering Laboratory for modeling EVs and series HEVs. Its interactive, menu-driven interface allows the selection of a particular vehicle, individual components (batteries, motor, inverter, transmission, engine, generator, and catalysts), and a specific standard driving cycle. It is limited by the fact that it does not have the ability to simulate either parallel HEVs or conventional ICE vehicles. Also, the operation of the series HEV provides an initial estimate of the APU contributions, but does not model the exact behavior of the Virginia Tech vehicle. Due to the nature of the source code for SIMPLEV, implementing changes to model other series and parallel control strategies would be very difficult.

The general simulation theory is similar to all of the simulation programs described here. The vehicle power at the wheels required to meet the driving cycle is calculated, and the power required from the bus is determined using the individual component efficiencies. It has the capability for plotting output data or saving the data at each time step of the simulation. SIMPLEV can report vehicle fuel economy, energy usage, emissions (HC, CO, NO_x) and a number of other vehicle variables.

The energy use predictions of SIMPLEV (using version 3.0) were compared against measured data by the National Renewable Energy Laboratory (NREL) (Cuddy, 1995). The measured data was obtained from the 1994 Hybrid Electric Vehicle Challenge entries of Pennsylvania State University and California State Polytechnic University-Pomona. However, the measurements contained quite a bit of total uncertainty (50%). This analysis showed the SIMPLEV model accurately predicted the actual vehicle energy use (to within the uncertainty) for a 200 m (1/8 mi) acceleration test and a 58 km (36 mi) range test.

CarSim

CarSim 2.5.4 is simulation tool developed by AeroVironment, Inc. with essentially the same capabilities and limitations as SIMPLEV. This code was also included in the NREL study (Cuddy, 1995) discussed above. The results of the CarSim simulation were compared to measured data from both vehicles and to the SIMPLEV results. CarSim agreed with SIMPLEV to within 5% for the acceleration test and the range test. It also correctly reflected the actual energy use to within the uncertainty of the test measurements.

HVEC

A Hybrid Vehicle Evaluation Code (HVEC) was developed by Lawrence Livermore National Laboratory (Aceves, 1995) to simulate only pure EVs and series HEVs. This menu-driven code does have existing models for a number of unique components not available to the previously mentioned simulations. Fuel cells may be used in place of ICEs as an APU, a flywheel may be chosen as the energy storage device instead of batteries, and a number of alternative fuels (such as hydrogen and compressed natural gas) can be used instead of gasoline. The code has the ability to model the overall vehicle fuel economy, emissions, and performance characteristics. Once again, the flexibility of HVEC as a simulation tool is limited due to its fixed structure.

CSM HEV

CSM HEV is simulation tool developed by the Colorado School of Mines to predict the behaviors of HEVs (Braun, 1996). This code operates in the user-friendly environment of MATLAB/SIMULINK, which allows for easier configuration changes than for any of the tools discussed previously. The program also allows for parametric analysis of the sensitivity of various HEV designs to changes in input parameters. However, the literature admits that the code was still very much under development and not ready to be validated against actual measured data at that time.

V-Elph

V-Elph, or Versatile-Elph, is an extension of the Electrically-Peaking Hybrid (ELPH) simulation code developed at Texas A&M University (Butler, 1997). The originial ELPH code was limited to one particular HEV control strategy, but V-Elph expands the capabilities to any general series and hybrid HEV. The code is based in MATLAB/SIMULINK and can be more easily modified to reflect the operation of real-world HEVs. This code is considerably simpler than the others mentioned because the dynamic interactions between vehicle components are easily visualized with intuitive subsets of blocks and connecting lines instead of many complicated, difficult-to-comprehend equations. This block diagram system model represent a major improvement in the usefulness of a single simulation tool to a wide range of users.

The code utilizes a standard data flow for all component models which allows easy transitions to unique components, fuels, and control strategies. It is unclear from the literature whether the current version of V-Elph has the ability to predict emissions output, but the flexibilty of the code would allow this feature to be

added. Custom fuel economy and performance data can also be easily plotted using V-Elph.

ADVISOR

The Advanced Vehicle Simulator (ADVISOR) developed by the National Renewable Energy Laboratory represents the best of the HEV simulation tools available at this time, and the particular tool used in this analysis of the Virginia Tech FutureCar. The code, like V-Elph, operates in the MATLAB/SIMULINK visual block diagram programming environment. It contains the wide range of features and broad flexibility necessary to model any type of HEV or ICE vehicle, with a minimum of change.

As with many of the simulations mentioned previously, it can utilize a variety of custom and standard driving cycles. However, unlike any of the other tools, it also easily generates results from batches of cycles, including the most recent draft SAE test procedures for HEVs (SAE, 1997), with state-of-charge corrections and vehicle soak periods. It can predict the fuel economy, emissions, acceleration, and gradability of a given vehicle and plot or data log any number of intermediate and final values. Another particularly convenient feature unique to ADVISOR is the well-refined graphical user interface (GUI) which allows the user to easily select from a list of custom or pre-defined base vehicles, interchangeable components, driving cycles, and outputs. Finally, the components and control strategy can be run through the standard MATLAB optimization routines to determine the ideal operating conditions for a particular configuration.

ADVISOR has been a primary tool used by the PNGV as it narrows the technology focus in attempt to meet its goals. A study conducted by NREL utilized ADVISOR to analyze various theoretical vehicle configurations (Wipke, 1996), which is one of the primary uses of this simulation tool. The vehicles studied were three ultra-lightweight chassis, one each with a parallel HEV, series HEV, and ICE drivetrains, and two vehicles with 1996-weight chassises, one a parallel HEV and the other an ICE drivetrain.

The sensitivity of each of fuel economy of each of these vehicles to certain vehicle parameters was the first item studied. This type of analysis helps to show the strengths and weakness of different configurations in a short amount of time and with minimal expended effort—the value of such a simulation tool. It also highlights areas of concentration necessary to meet the desired fuel economy goal of 34 km/l (80 mpg). One interesting result of this study was that both parallel and series HEV configurations showed approximately the same sensitivity to all parameters, with the exception of electric drivetrain and battery efficiencies. The fuel economy of the lightweight series vehicles tended to be 2-3 times as sensitive to these efficiencies as their parallel counterparts. This sensitivity can be a major

advantage or disadvantage to a series HEV: relatively low efficiencies would discredit the plausibility of series vehicles, while high efficiencies would demonstrate excellent fuel economy.

This same study also examined the possible design spaces for the same vehicle configurations. To reach the 34 km/l (80 mpg) goal with a parallel HEV, one of the most likely designs would require an average APU efficiency of 35% with a vehicle mass of 1000 kg (2200 lb). This represents a weight savings of 50% over current conventional vehicles and the very best of current ICE technology.

Finally, the study concluded that the 1996-weight hybrid vehicles would result in nearly 20% fuel economy improvement over the current ICE vehicles, and a 25% in comparing lightweight vehicles. Both series and parallel designs demonstrated similar potential in achieving these goals.

Another study, also conducted by NREL, examined the differences between the parallel and series configurations in more detail than before, even allowing for different control strategies within each configuration (Wipke, 1997). This is an excellent example of using the simulation tool to determine the best vehicle configurations, saving valuable time, effort, and expense. It was concluded that parallel HEVs could expect a 24% improvement in fuel economy over ICE vehicles when both use the best available technology and low road load designs. The parallel design was also shown to have a 4% improvement over a similarly-designed series HEV.

In order to have faith in the predictions produced by ADVISOR, it must first be shown to provide data which accurately reflect the as-built behavior of current HEVs. This thesis will study the validity of the ADVISOR simulation tool in modeling the Virginia Tech FutureCar, which is a fully operational series HEV developed for competition in the 1996-1997 FutureCar Challenges. This validation, in conjunction with other such studies, will provide a solid background for future ADVISOR theoretical simulations.

VEHICLE MODELING

Basic ADVISOR Operation

All vehicle modeling, whether for conventional ICE vehicles, EVs, or HEVs, is derived from the basic equation of solid-body motion (Newton's Second Law), as given in Equation 1 in its scalar form.

$$F = ma \qquad \text{Equation 1}$$

This equation can be modified with the specific forces that typically act on vehicles and can be rearranged into the form of Equation 2.

98

$$F = mgC_{rr} + \frac{1}{2}\rho C_D Av^2 + ma + mg\sin(\theta)$$

Equation 2

F force required at the wheels of the vehicle
m mass of the vehicle
C_{rr} coefficient of rolling resistance between the tires and the road surface
ρ density of the ambient air
C_D coefficient of drag of the vehicle in the direction of travel
A cross-sectional area of the vehicle
v magnitude of the velocity (i.e., speed) of the vehicle in the direction of travel
a acceleration of the vehicle
g local acceleration of gravity
θ angle of inclination of the road surface upon which the vehicle is traveling

This simple modeling equation provides an accurate method for describing the straight-line motions of an automobile. The first term indicates the force required to overcome the rolling resistance of the vehicle. Note that this force is constant regardless of the speed of the vehicle and tends to dominate at relatively low speeds. The second term represents the drag force that the vehicle must overcome at a certain speed. This term is proportional to the square of the speed of the vehicle and, therefore, tends to be small at low speeds, but increases rapidly with velocity. The mass inertia of the vehicle is shown in the third term of this equation. It is non-zero only when the vehicle is accelerated or decelerated and has no effect under constant-speed cruising conditions. Finally, the force required to propel the vehicle on a non-zero grade is accounted for in the last term of the equation.

Although this equation uses only the first-order approximations for each term, it is accurate enough for most analyses, and it is the basis for almost all vehicle simulation tools, including ADVISOR.

ADVISOR uses a quasi-steady approximation approach to vehicle modeling for parallel and series HEVs, pure EVs, or ICE vehicles. At each discrete time step, ADVISOR calculates the required energy at the wheels of the vehicle using a pre-determined vehicle velocity profile. It then determines the amount of energy required into each component to meet the energy requirement at the wheels. The structure used for series HEV modeling is shown in block diagram form, Figure 2.

At each discrete time step, ADVISOR first determines the desired vehicle speed from the desired trip profile, which is often a standard driving cycle. It then uses vehicle parameters such as vehicle mass, coefficient of drag, frontal area, and rolling resistance in Equation 2 to compute the vehicle road load (force required at wheels). This allows the calculation of the required torque at the wheels using Equation 3, and the required angular velocity of the wheels using Equation 4.

$$T = Fr_r \qquad \text{Equation 3}$$

$$\omega = \frac{v}{r_r} \qquad \text{Equation 4}$$

The input angular velocity of the transmission is calculated using the overall reduction ratio of the transmission in Equation 5. Compensating for the transmission efficiency as a function of input speed and torque, the input torque can be computed with Equation 6.

$$\omega_{in} = \omega_{out} R_{trans} \qquad \text{Equation 5}$$

$$T_{in} = T_{out} \frac{1}{R_{trans}} \eta_{trans}(T_{out}, \omega_{out}) \qquad \text{Equation 6}$$
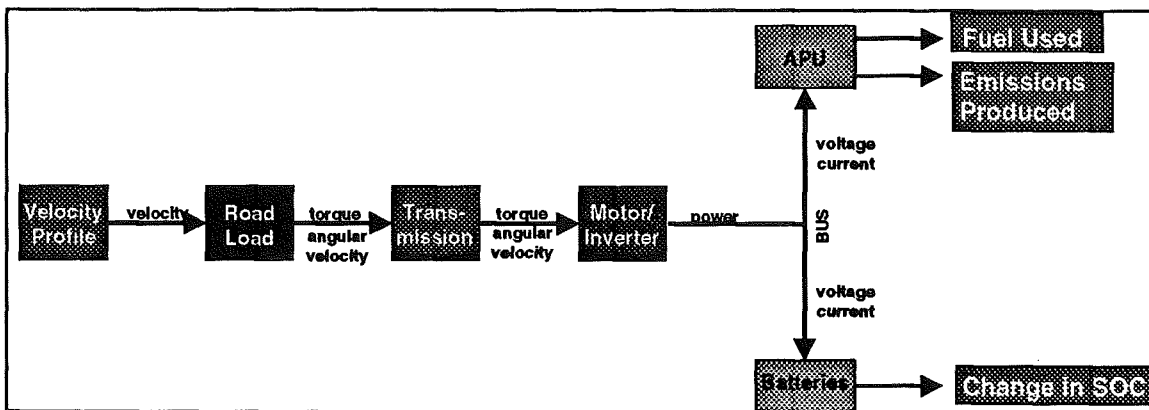

Figure 2. ADVISOR Series HEV Data Flow

Similarly, using the efficiency of the motor/inverter at that particular speed and torque, the input power required from the vehicle's high-voltage bus is determined, as in Equation 7.

$$P_{bus} = \frac{T_{out}\omega_{out}}{\eta_{mot}(T_{out},\omega_{out})\eta_{inv}(T_{out},\omega_{out})}$$

Equation 7

The power from the bus is supplied either by the batteries exclusively (APU off), or by a combination of the batteries and the APU (APU on). The relative amount of power contributed by each source is dependent upon the equivalent internal resistances of the APU alternator and the batteries. Once this power distribution has been calculated, ADVISOR updates the battery state of charge (SOC), fuel used, and emissions produced based on this information, and then proceeds to the next time step.

Component Modeling

The accuracy of the simulation is largely dependent upon the accuracy of the various component models and parameters which ADVISOR requires: APU, motor/inverter, transmission, batteries, and general vehicle parameters. It is imperative, therefore, that these component models be carefully determined to best represent the actual performance of that component within the system as a whole. This is

especially true of the APU model, since it directly determines the fuel usage and emissions produced. This is not always straightforward, because in order to test individual components, that device must often be removed from the system. This may lead to a different behavior than when incorporated in the rest of the system, thereby skewing the results of the entire simulation.

In order to accurately model a series HEV, it is first necessary to understand the operation of the individual components in that system, the interactions between components, and, finally, the behavior of the system as a whole. The actual vehicle used for validation of the ADVISOR simulation was the Virginia Tech entry in the 1996 FutureCar Challenge (FCC). A 1996 Chevrolet Lumina was converted to series HEV operation as shown in Figure 3.

The Virginia Tech FutureCar is a classic range-extending series HEV. The vehicle typically operates as a pure EV with an on-board generator (the APU), which maintains the batteries at an acceptable SOC. Under normal operation, when the APU controller senses a low battery SOC, it executes a start-up procedure for the engine and maintains the engine speed at the proper level to produce power until the batteries reach a high SOC. It then shuts down the engine and continues to monitor battery SOC. The packaging of the various components can also have a significant effect on the operation of the system. Temperature, vibration, and orientation can drastically affect the operation of the
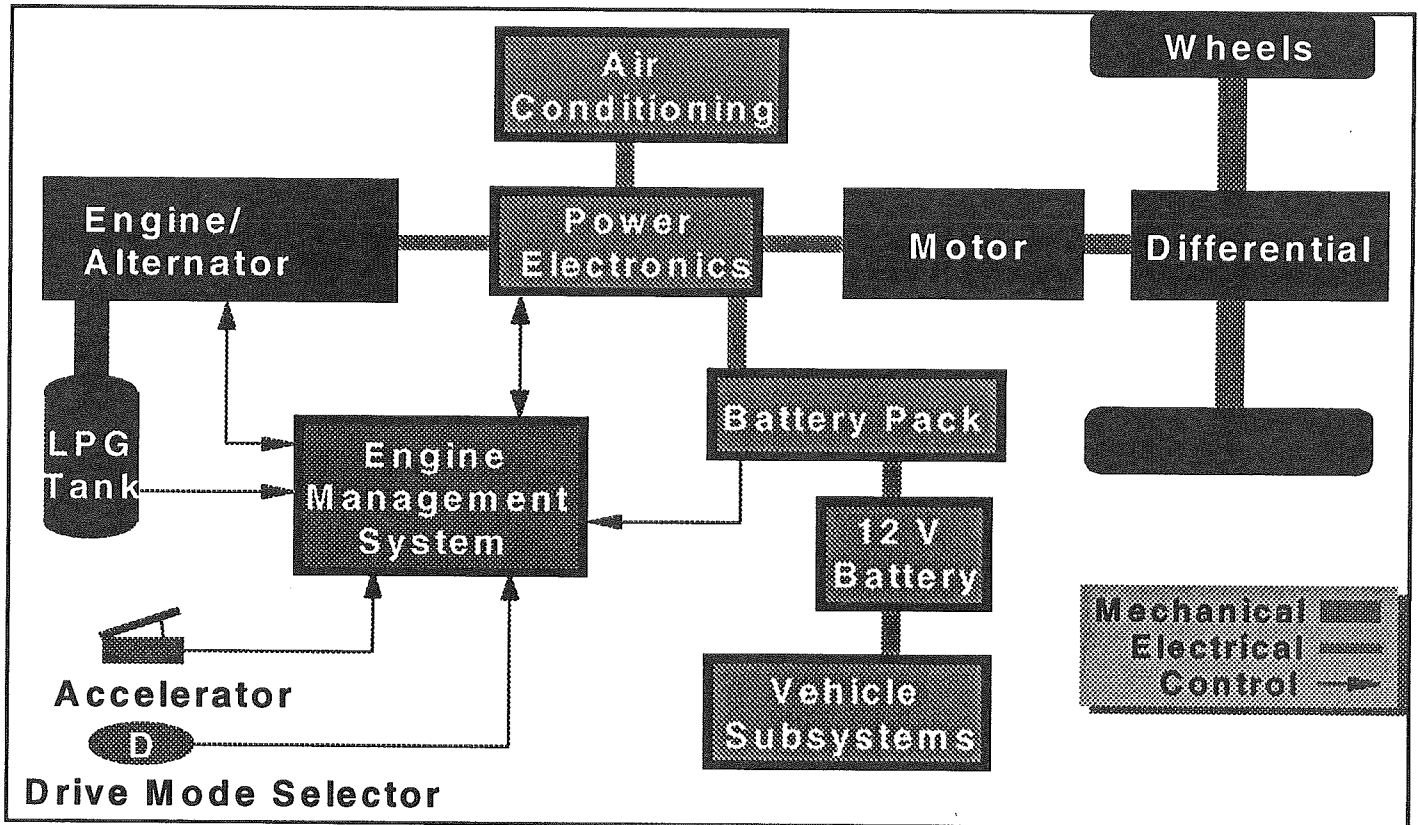

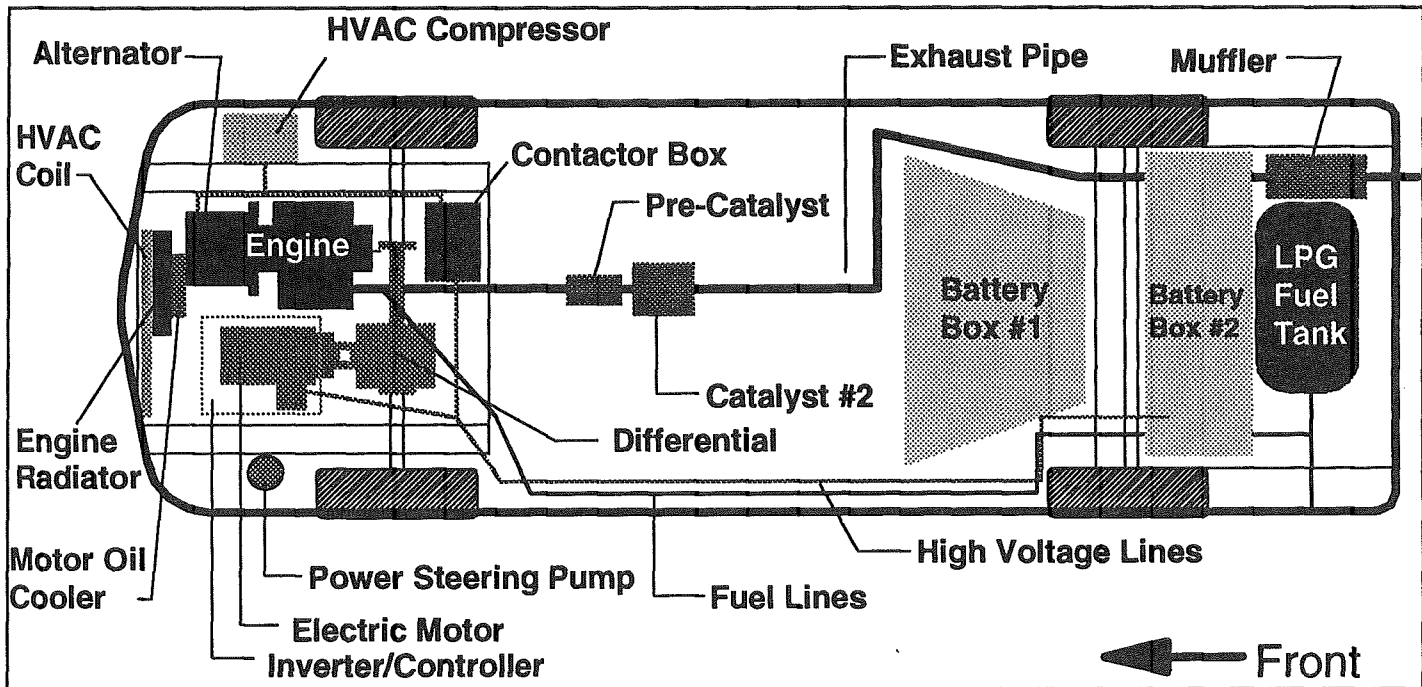Figure 3. Virginia Tech FutureCar System Schematic

100

Figure 4. Virginia Tech FutureCar Component Packaging Diagram

individual HEV components. The location of the components in the 1996 FutureCar Challenge entry is shown in Figure 4.

Each major component is described in detail below. The required information for each component is unique, and, therefore, each has its own procedures for testing. During all testing, care was taken to insure that the measurements represented the actual operation of the component as it operates in the system and to insure that each measurement was as accurate and certain as possible. Many of the components are described by efficiency or performance maps that are best represented by color contour maps that do not reproduce well in a black-and-white publication. The reader is referred to Senger (1997) (which is available in an online archive) for these figures.

Auxiliary Power Unit (APU)

The design considerations for the Virginia Tech FutureCar APU were a small, quiet, lightweight ICE, preferably from a production automobile with existing emissions control devices, with the capability to produce the average highway power required (approximately 20 kW) for extended periods of time. The APU chosen to meet these goals is a Suzuki three-cylinder, 1.0 liter (61 in^3), spark-ignited internal combustion engine, which is normally used in Geo Metro automobiles. It is rated with a peak power of 41 kW (55 hp) at 5700 rpm and peak torque of 79 Nm (58 ft-lbf) at 3300 rpm using the stock engine control unit (ECU) operating on gasoline at the stock compression ratio of 9.5:1.

The engine was modified to operate on liquefied petroleum gas (LPG, or propane). A programmable GFI Controls throttle-body injection system was used for fuel control, with a programmable Electromotive TEC-II unit used for spark advance control.

The APU includes a Fisher three-phase, permanent magnet alternator rated nominally at 18 kW (24 hp) at 2800 rpm. The alternator is permanently mounted to the engine and is driven directly by the engine crankshaft.

The APU, as defined for these simulations, encompasses all components which convert the fuel energy of the LPG entering the system to mechanical work to AC electrical energy to DC electrical energy leaving the system. In addition to the components listed above, the APU also includes wiring, fuses, connectors, and a bridge rectifier.

In order to satisfy the ADVISOR requirements for APU component mapping, a number of different parameters were measured. Each of the APU maps was determined as a function of bus voltage and APU output current. All measurements were taken at steady-state conditions to satisfy the quasi-steady assumptions used by ADVISOR. The APU was mounted normally in the vehicle, with the complete fuel and exhaust systems, while tested. However, the DC output was disconnected from the vehicle bus and attached to an artificial electrical resistance load bank, which allowed for easier mapping. DC output voltage was measured across the load with a standard multimeter and DC output current

was measured with a standard multimeter using a precision shunt on the positive leg of the load. The uncertainty in the electrical measurements was determined to be less than 1%. Fuel mass flow was measured using the GFI monitoring software designed for use with the fuel system. The accuracy of this method was tested using a known mass of fuel and compared to the measurements given by the software. Under standard operating conditions for the APU, the variance between the two measurements was less than 5%. All emissions levels were measured using a calibrated OTC 5-gas exhaust analyzer.

Fuel efficiency was defined as the fuel energy flow into the system divided by the electrical energy flow out of the system. This was determined by measuring the mass flow of fuel into the engine and the DC voltage and current out of the APU over the entire operating range of the APU. The efficiency was then expressed in terms of grams of fuel in per kilowatt-hour (kWh) of DC energy out.

Three categories of vehicle emissions are of particular importance to study because they are regulated by the federal government in the Clean Air Act Amendments of 1990 : hydrocarbons (HC), carbon monoxide (CO), and oxides of nitrogen (NO$_x$). Engine-out emissions levels were reported in parts per million (ppm) of the total exhaust gas flow. For each emission (HC, CO, and NO$_x$), the values were then converted to grams of emission per kWh of DC energy out using Equation 8. The molecular weight of CO is 44 g/mole; for NO$_x$, all of the oxides were assumed to be in the form of NO, which

has a molecular weight of 30 g/mole; and for HC, the majority of the species was assumed to be in the form of propane, C$_3$H$_8$, with a molecular weight of 44 g/mole.

$$M_{emiss} = \frac{(25.8)(PPM)(10^{-6})(MW_{emiss})}{44}(\dot{W}_{out})(\dot{m}_{fuel})$$

Equation 8

The engine-out emissions levels as functions of engine speed and load (APU voltage and current) are then used to model the emissions in ADVISOR.

Steady state catalyst reduction efficiencies as functions of speed and load were determined by simultaneously measuring before and after catalyst emissions levels for HC, CO, and NO$_x$. The catalyst reduction efficiency for HC is then given by Equation 9, with similar equations for CO and NO$_x$.

$$\eta_{HC} = \frac{HC_{in} - HC_{out}}{HC_{in}}$$

Equation 9

Finally, the warm-up efficiency of the catalysts from a "cold" (APU at ambient temperature) start for each species of emission was determined as a function of temperature. These are reported as the percentage of the full efficiency of the catalyst at steady state conditions in Figure 5.
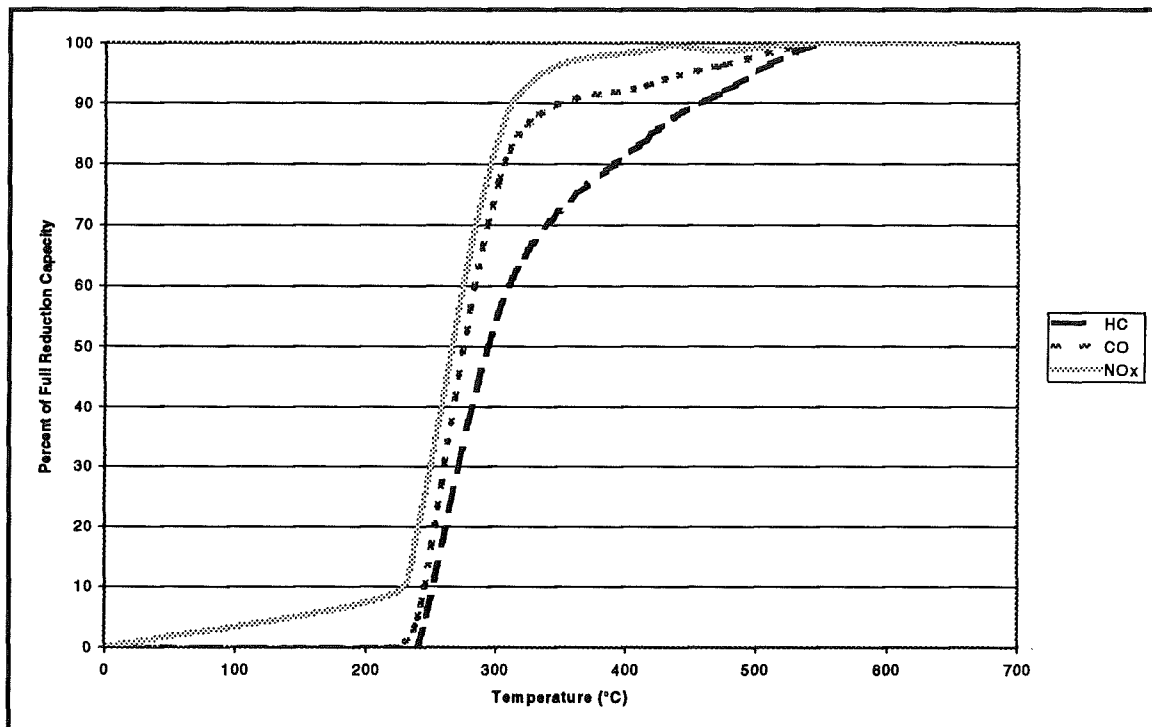

Figure 5. APU Catalyst Warm-Up Efficiency

These measurements provide the necessary data for the APU component model in ADVISOR. Once the above values were entered into the proper ADVISOR format, the APU model was complete.

Motor/Inverter

The design of the Virginia Tech FutureCar utilizes a General Electric EV2000 prototype electric vehicle drive system. This system is ideal for a series HEV because it was originally designed as a pure EV drivetrain. The electric motor is a three-phase, AC induction motor rated at 80 kW (107 hp) continuous and 100 kW (135 hp) peak. The graph of the maximum continuous motor power and torque at the rotor is given in Figure 6, with a peak torque of 190 Nm (140 ft-lbf) occurring at 0 rpm. The rotor speed is reduced from a maximum 13,500 rpm by an integral 4.29:1 planetary gear set such that the maximum output shaft speed is 3150 rpm. The motor is cooled and its gearset lubricated by lightweight synthetic oil.

The DC-to-AC inverter is based on insulated gate bipolar transistor (IGBT) power switching devices. The inverter can withstand input voltages from 200 VDC to 400 VDC and input currents of up to 400 A. The variable frequency AC output is used to control motor speed. It is mounted on an air-cooled heatsink. The inverter (and motor) support regenerative braking, which

effectively turns the electric motor into a generator that allows recharging of the batteries. This provides improved braking performance and recaptures some of the vehicle kinetic energy that would typically be dissipated as heat. A large number of driveability factors can be customized through a PC-based software interface. The inverter control contains many self-protection routines, which help avoid damage resulting from high voltages, excessive currents, motor overspeed, etc.

The motor and inverter efficiency maps were obtained from personal communication with General Electric and with the consent of Virginia Power Technologies (Boothe, 1997). The maps are separated into a motor efficiency map and an inverter efficiency map. The motor map consists of the efficiency of the motor, from electrical energy in to mechanical energy out, as a function of output speed and output torque. Regenerative braking consists of merely operating the motor at a negative torque value; therefore, the regenerative braking map is simply the mirror image of the motive map. The inverter efficiency, from DC electrical energy in to AC electrical energy out, is also given as a function of motor output speed and torque. Again, the regenerative braking inverter map is merely the mirror image of the motive map.
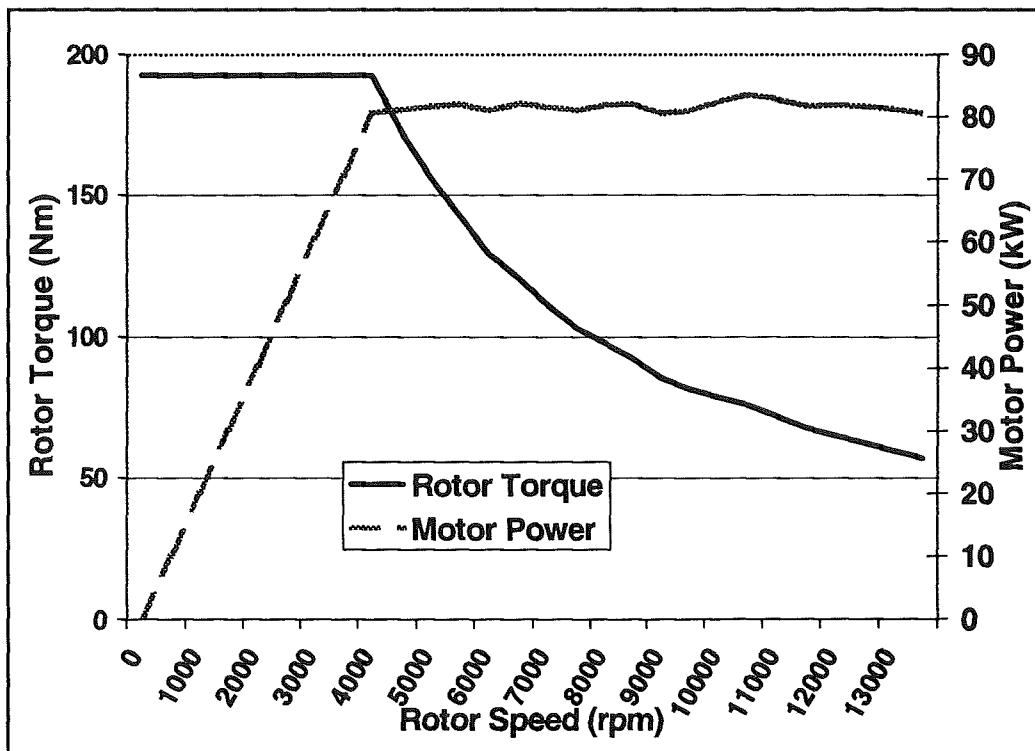

Figure. 6. Maximum Continuous Motor Torque and Power

Transmission

The transmission is needed only to couple the output of the electric motor to the front wheels of the vehicle. Because the electric motor provided enough torque to adequately power the vehicle over its entire operating range, a single-speed transmissions was desired for its low size and weight. However, to improve component packaging, it was determined that a right-angle drive was preferred. The lightest, smallest, unit found was the front differential used in a four-wheel-drive Chevrolet S-10. This oil-lubricated transmission provides an acceptable 3.41:1 gear reduction, with a torque rating to handle the output of the motor.

No facilities were available on-site which would allow for accurately determining a transmission efficiency map as a function of speed and torque over the operating range. It was decided that an engineering estimate using established data was more desirable than inaccurate test data. The MEV-75 single-speed transmission map used with the SIMPLEV simulation (Cole, 1993) was adapted for use with ADVISOR. This transmission was integrated with a similar motor/inverter combination in the Ford Ecostar electric minivan, and should therefore provide a reasonably accurate approximation for the Virginia Tech FutureCar transmission.

Batteries

The batteries used in the Virginia Tech FutureCar were valve-regulated, non-spillable, sealed lead-acid modules manufactured by Hawker Energy Products under the model name of Genesis. The nominal 12 VDC modules were rated at 26 Ah at the c/10 rate, with a mass of 11 kg (24 lbm) per module. Twenty-seven modules were connected in series to form a nominal 324 VDC battery pack with 7.1 kWh of energy storage at the c/3 rate and 6.1 kWh at the c/1 rate (Hawker, 1996).

The testing procedures and considerations for battery testing are not covered in this paper, but the results of that testing are presented for completeness. The battery model requires the determination of a number of parameters as functions of SOC. First, the internal resistance of each module (including interconnects) was computed as a function of SOC. Open-circuit voltage of a module was also given as a function of SOC (Hawker, 1996). Both the internal resistance and open-circuit voltage functions (Merkle, 1997) are shown in Figure 7.

The "round-trip" charging efficiency, defined as the output capacity of the battery divided by the capacity input to the battery, was set at 90%. Finally, the useable capacity of the batteries was required, and was determined to be 20 Ah at the C/1 rate.
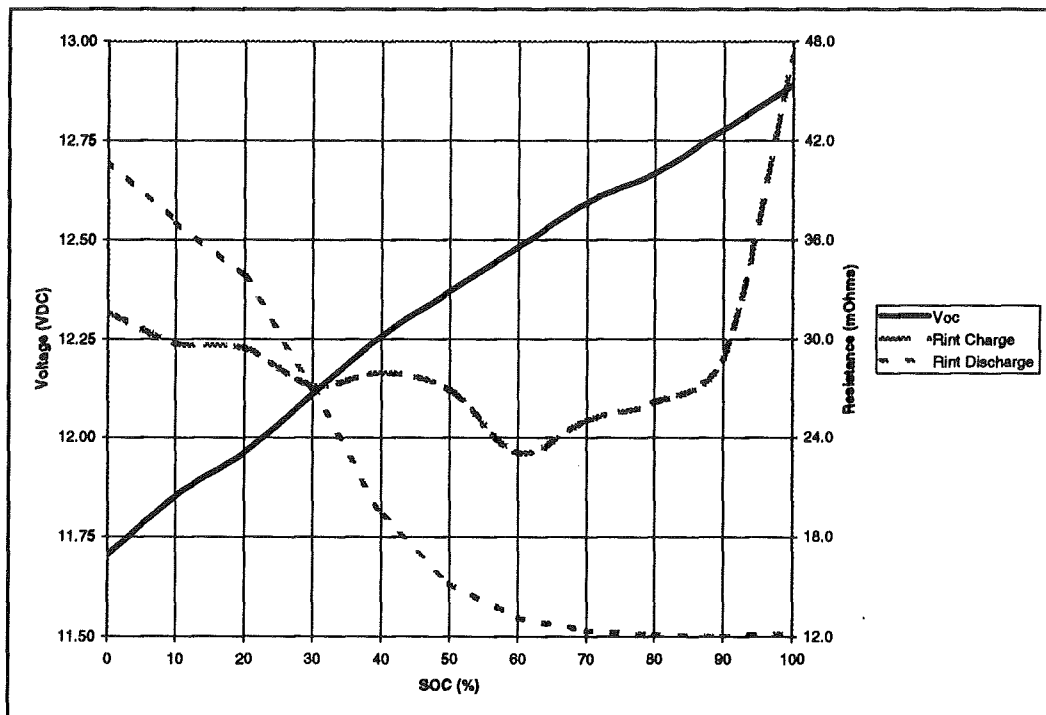

Figure 7. Battery Module Internal Resistance and Open-Circuit Voltage

Miscellaneous Vehicle Parameters

ADVISOR also requires a number of miscellaneous parameters to describe the vehicle as a whole. These parameters are quite important to an accurate simulation of the vehicle, since an error in these will propagate throughout the rest of the model. Many of these parameters are difficult to measure with the desired accuracy, so in many cases a good engineering estimate provides a better value.

The first parameters are used to determine the road load of the vehicle at a given speed. The same road load information was required to properly set the dynamometer at the 1996 FutureCar Challenge, that data was already available. The road load of the Virginia Tech FutureCar was measured on Ford's Dearborn Proving Grounds in Dearborn, MI. The rolling resistance of the vehicle and the drag product (product of the coefficient of drag and frontal area) can be determined by fitting the measured road load curve with Equation 2. Using the frontal area provided by General Motors for a 1996 Chevrolet Lumina (the aerodynamics of the Virginia Tech Lumina were essentially unmodified), the coefficient of drag can be determined.

The weight of the vehicle was also measured at the 1996 FCC. The regenerative braking fraction (fraction of total energy expended which is recaptured by regen) was calculated using data acquired during dynamometer testing at the 1996 FCC, which was performed at the Environmental Protection Agency in Ann Arbor, MI. Representative fuel energy and fuel density properties were determined by a laboratory analysis of the LPG. Accessory loads are the estimated average of all vehicle subsystems required to operate the vehicle in its different modes, such as ZEV mode versus APU-On mode. Standard temperature and pressure ambient conditions were assumed for all testing and simulation, since a large portion of the testing was performed indoors with climate control, and no better values were available.

Table 1. Miscellaneous Vehicle Parameter Summary

Parameter	Value	Units
Coefficient of drag	0.325	
Frontal area	2.04	m^2
Rolling resistance	0.005	
Rolling radius	0.323	m
Mass	2000	kg
Front weight fraction	0.53	
Regenerative fraction	0.5	
Accessory load	500	W
Fuel specific energy (LHV)	47.3	MJ/kg
Fuel density (STP)	1.92	kg/m^3
Fuel density (liq.)	498	kg/m^3
Ambient air density	1.2	kg/m^3
Local acceleration of gravity	9.81	m/s^2

A summary of the miscellaneous vehicle parameters used in the simulations is given in Table 1.

SIMULATION RESULTS

Modifications to original ADVISOR code

Accurate system simulation requires that models of individual components be representative of component performance when assembled into a system. To accurately simulate the Virginia Tech FutureCar using ADVISOR, a number of changes were implemented into the code. The most significant change was made to the APU loading calculation. ADVISOR originally determined the load on the APU using a single, pre-defined operating speed and torque. This operating point did not vary under any circumstances, producing a constant power when on. This type of operation is the ideal "single operating point" type of series HEV. However, the Virginia Tech APU functions more as a "load following" type of series HEV, where the APU speed is regulated to a specific speed. The APU controller actuates the throttle position to maintain constant speed under the different torques required by the vehicle bus.

The changes in the ADVISOR code were confined mostly to the "Engergy Storage" subsystem, with a few changes to the "APU" subsystem. An iteration was introduced into the Energy Storage block diagram which used battery SOC and the required power from the bus to determine the proper bus voltage and the correct current flows from the batteries and APU respectively (Merkle, 1997). The APU block diagram was then changed, such that its look-up tables (for fuel economy, emissions, etc.) were functions of its voltage and current instead of its speed and torque.

With these modifications in place, the results from the simulation were taken step-by-step and compared to the actual measured data and checked for accuracy before moving on to the next step. The comparisons for each step are detailed below.

Road Load Comparison

The first major calculation performed by ADVISOR during a simulation is that of the vehicle road load from miscellaneous vehicle parameters. Measured road load data for the Virginia Tech FutureCar was available for constant speeds on a zero grade; therefore, this was used as the standard for determining the accuracy of the ADVISOR road load predictions. This data was collected at the 1996 FutureCar Challenge during coastdown testing, which was used to set the road load for the subsequent dynamometer testing. The measured and predicted curves are given in Figure 8.
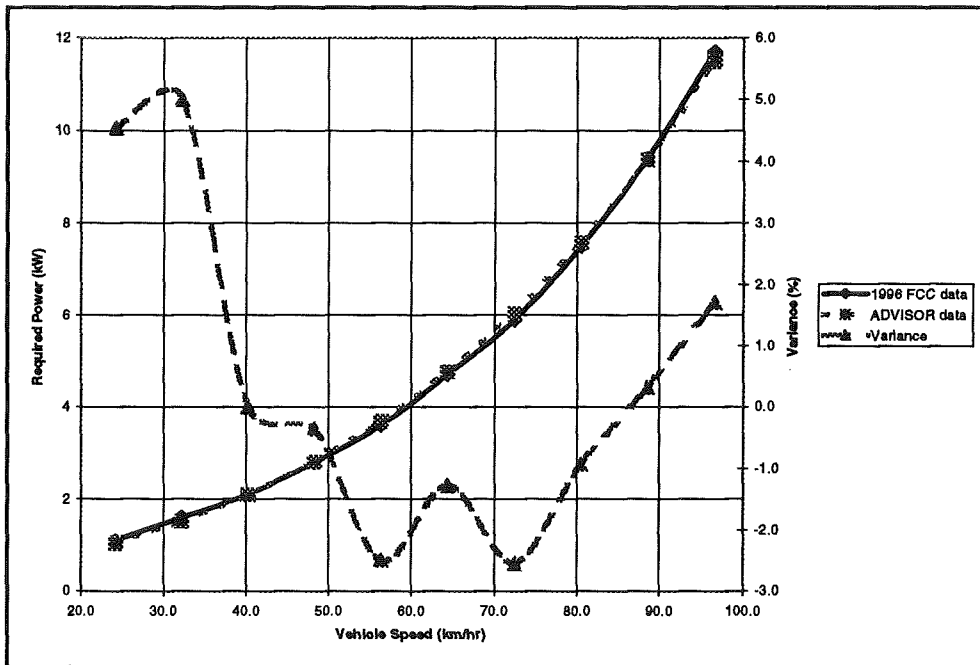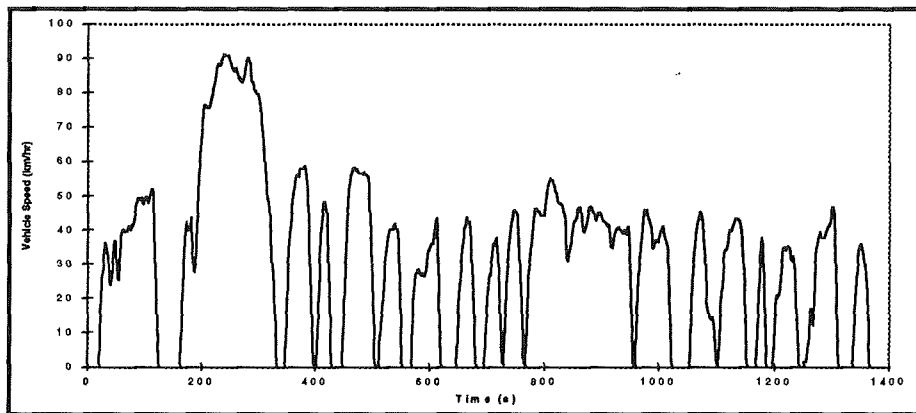
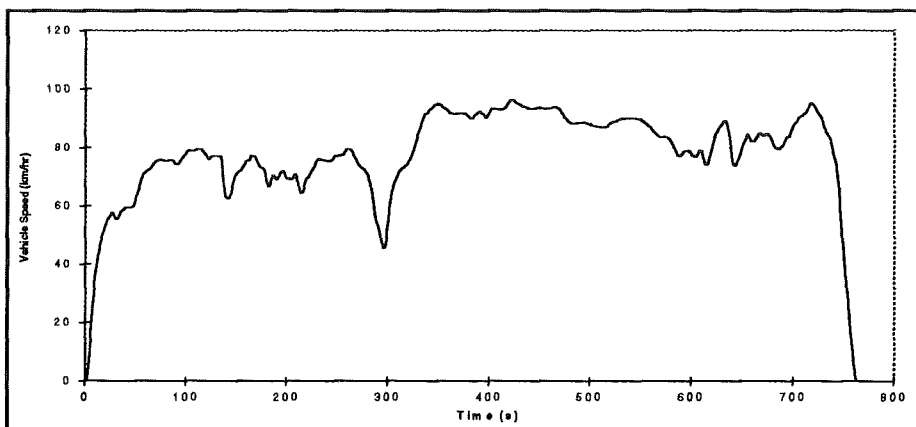Figure 8. Road Load Curve Comparison

Figure 9. FUDS Driving Trace

Figure 10. FHDS Driving Trace

106

The variance between the actual and predicted values is less than 3% at speeds above 35 km/hr (22 mph). Only at very low speeds, where the power requirements are very low and the effect on overall energy usage is small, does the discrepancy approach 5%. This excellent agreement between the values is quite necessary for an accurate simulation since these power requirements will be used to determine other vehicle energy use.

Standard Driving Cycles

Industry standard methods of comparison were used to evaluate the effectiveness of ADVISOR as a simulation tool for series HEVs. The large portion of the comparisons were performed using the standard driving cycles. The Federal Urban Driving Schedule (FUDS) is the current federal government cycle which is used to represent typical city driving . The Federal Highway Driving Schedule (FHDS) is used to imitate typical highway driving. These cycles were created in 1970s. Most people agree that these tests reflect more conservative driving behaviors than those typical of most Americans. Both the FUDS and FHDS are defined by speed versus time traces on a zero grade which are shown in Figures 9 and 10, respectively.

The FUDS is 1371 seconds in length and covers a distance of 12.0 km (7.5 mi). The average vehicle speed for the test is 31.5 km/hr (19.6 mph) with a maximum speed of 91.2 km/hr (56.7 mph) and quite a few complete stops.

The FHDS is 765 seconds long and covers a distance of 16.5 km (10.3 mi). The average speed during the test is 77.7 km/hr (48.3 mph) with a maximum of 96.4 km/hr (59.9 mph) with no stopping required until the end of the test.

Electric Drivetrain Energy Usage Comparisons

The electric drivetrain of the vehicle, defined here as the components which take electrical energy from the bus and transform it into the mechanical energy necessary to meet the road load, consists of the transmission, electric motor, and inverter. A simulation tool must accurately describe the energy use of these components as a system in order for the simulation to accurately predict vehicle fuel economy and emissions. This electric drivetrain system can be isolated and studied by operating the vehicle in ZEV mode, which does not allow the APU to operate. By isolating the electric drivetrain from the APU, the APU-related effects and battery efficiencies are eliminated, leaving only a true picture of the electric drivetrain energy efficiency. For the 1996 Virginia Tech FutureCar, the only ZEV test for which data was measured under controlled dynamometer conditions was a FUDS cycle, starting at a high SOC (HSOC), defined by the upper limit of the vehicle's control strategy. Table 2 and Figure 11 give comparisons of the ADVISOR predictions and the actual measured data from this test.

ADVISOR did an excellent job of simulating the energy use of the vehicle and the change in battery capacity over this driving cycle, resulting in less than 2% error in both cases. This level of accuracy is necessary if the simulation tool is to be used for obtaining absolute numbers and not just relative comparisons.

Table 2. ZEV-mode FUDS (HSOC) Energy Use Comparison

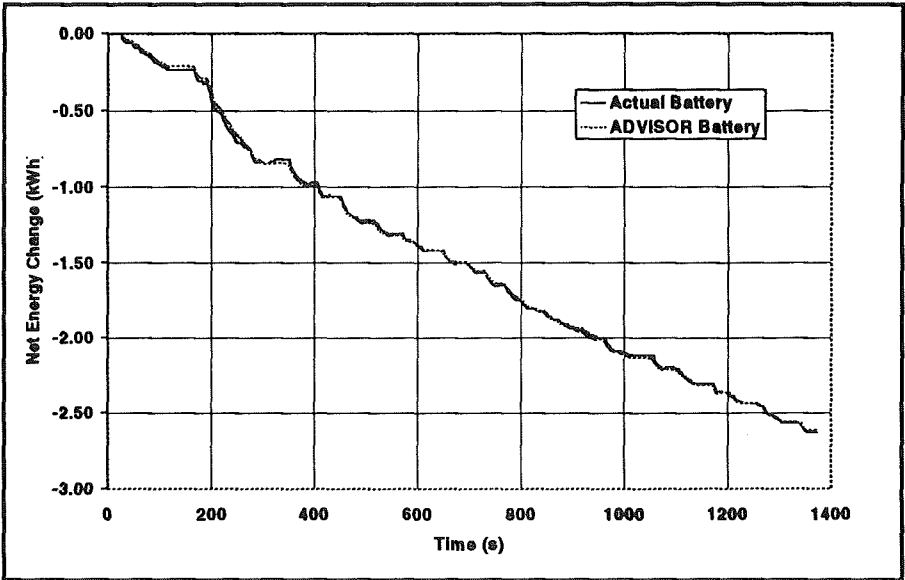| Cycle	Actual		ADVISOR		Difference	
	Energy (kWh)	Capacity (Ah)	Energy (kWh)	Capacity (Ah)	Energy (%)	Capacity (%)
FUDS (HSOC)	2.63	8.2	2.63	8.1	0.0	-1.2

Figure 11. ZEV FUDS (HSOC) Comparison

FMC 1016

APU/Battery Energy Usage Comparisons

Once APU operation is allowed during a driving cycle, the complexity of the system increases and makes an accurate simulation more difficult to achieve. However, data comparisons can then be made using not only electric drivetrain energy use, but also the relative battery and APU energy use required over a given driving cycle. Comparisons of this energy split are given in Table 3 for the totals and as a function of time in Figure 12 for an urban driving cycle pair (two consecutive cycles) with a low initial SOC (LSOC).

Table 3. FUDS Pair (LSOC) Energy Use Comparison

Cycle	Actual		ADVISOR		Difference	
	Energy (kWh)	Capacity (Ah)	Energy (kWh)	Capacity (Ah)	Energy (%)	Capacity (%)
Batteries	-0.15	-1.3	-0.30	-1.7	-100.0	-30.8
APU	5.28	15.8	4.95	15.4	6.3	2.5
Total	5.43	17.1	5.25	17.1	3.3	0.0

In this case the simulation appears to be quite inaccurate at modeling the relative contributions of the batteries to the overall vehicle energy requirements, with a difference of 100% in energy use and an energy use curve with a totally different shape. However, notes from the 1996 FutureCar Challenge indicate that the test may have been skewed. During this test, the APU speed control operated erratically, with frequent swings from low speed to high speed. At too low a speed, the APU output voltage is lower than the bus voltage of the vehicle, and no current is produced; at too high a speed, the APU output current becomes much higher than anticipated. These conditions can be seen in the data: from 0-400 seconds, the APU seemed to produce less power than expected; form 400-1600 seconds, more power than expected; from 1600-2000 seconds, about the correct amount of power; and again, less power than expected from 2000 seconds until the end of the test.

In order to accurately model the overall energy use over the entire FUDS pair, a nominal value of 3450 rpm was used for average engine speed, which was lower than the setpoint of the engine speed controller, but likely more indicative of the actual average speed of the engine during the FUDS pair.

Table 4 and Figure 13 show the same types of comparisons for the urban driving cycle pair with a high initial SOC.

Table 4. FUDS Pair (HSOC) Energy Use Comparison

Cycle	Actual		ADVISOR		Difference	
	Energy (kWh)	Capacity (Ah)	Energy (kWh)	Capacity (Ah)	Energy (%)	Capacity (%)
Batteries	-2.02	-6.7	-1.93	-6.8	4.5	-1.5
APU	3.42	10.0	3.31	10.2	3.2	-2.0
Total	5.44	16.7	5.24	17.0	3.7	-1.8

During this test at the 1996 FCC, the problems with the APU speed control had been corrected as witnessed by the much smoother APU operation. The LSOC limit (APU turn on point) of the control strategy was lowered from its normal value of 40% to 27% in order to better match the test data. This could have been due to inconsistencies in the vehicle's SOC-determination or by a driver-selected APU-off selection until the beginning of the second cycle of the FUDS pair (at approximately 1400 seconds). Also for this simulation, the average engine speed set in ADVISOR was a more realistic 3600 rpm. As a result, this study shows a much more reasonable agreement between the actual test data and the ADVISOR predictions, with less than 5% error at any time during the test and an almost exact match between the shapes of the energy curves.

A final example is given in Table 5 and Figure 14 for a single highway driving cycle beginning at a high SOC.

Table 5. FHDS (HSOC) Energy Use Comparison

Cycle	Actual		ADVISOR		Difference	
	Energy (kWh)	Capacity (Ah)	Energy (kWh)	Capacity (Ah)	Energy (%)	Capacity (%)
Batteries	-0.92	-2.9	-0.98	-3.1	-6.5	-6.9
APU	1.86	5.7	1.89	5.7	-1.6	0.0
Total	2.78	8.6	2.87	8.8	-3.2	-2.3

For this cycle, the average APU speed was raised slightly from 3600 rpm on the FUDS cycle to about 3700 rpm, since the engine tends to run somewhat faster on the more steady FHDS cycle. At the 1996 FCC, the APU was manually shifted on to ensure that the test would work out such that a highway fuel economy value could be easily determined. According to the test data, this APU-on occurred at a SOC of 64%, so the ADVISOR value LSOC limit was set accordingly. Once again, the ADVISOR predictions track the actual data with good accuracy, with the energy comparison graphs taking on nearly identical shapes, and with less than 10% discrepancy at any point during the test.

HEV Test Procedures

Although energy use comparisons can be convenient for analyzing specific cases of HEV operation, a measure of the vehicle's overall efficiency for a broad spectrum of operating conditions is needed. This categorization should also allow for easy comparison to other HEVs, EVs, and ICE vehicles. For conventional ICE vehicles, the standard test procedure consists of a cold (i. e., ambient temperature) start FUDS, followed by a 10-minute ambient temperature soak, followed by the first 505 seconds of another FUDS. This procedure determines the vehicle's city fuel economy and emissions level. An FHDS is then performed for which no data is taken, followed immediately by another FHDS for which vehicle fuel economy is obtained.
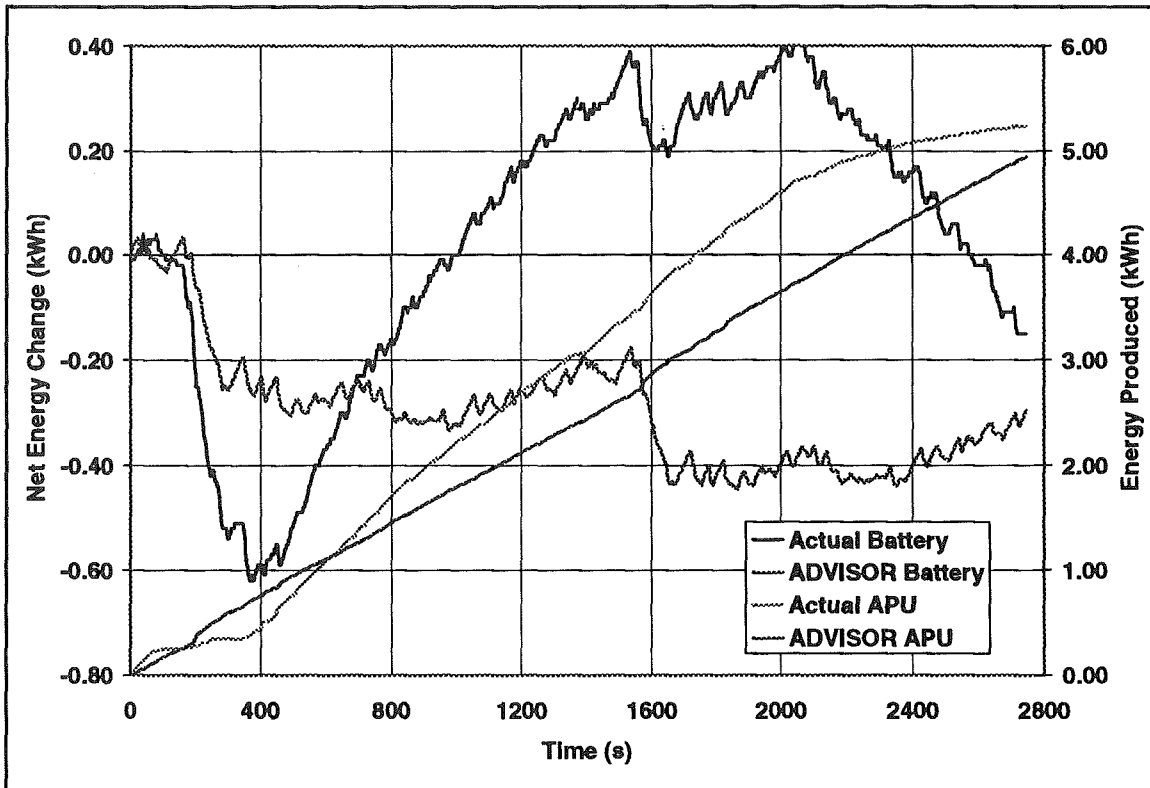
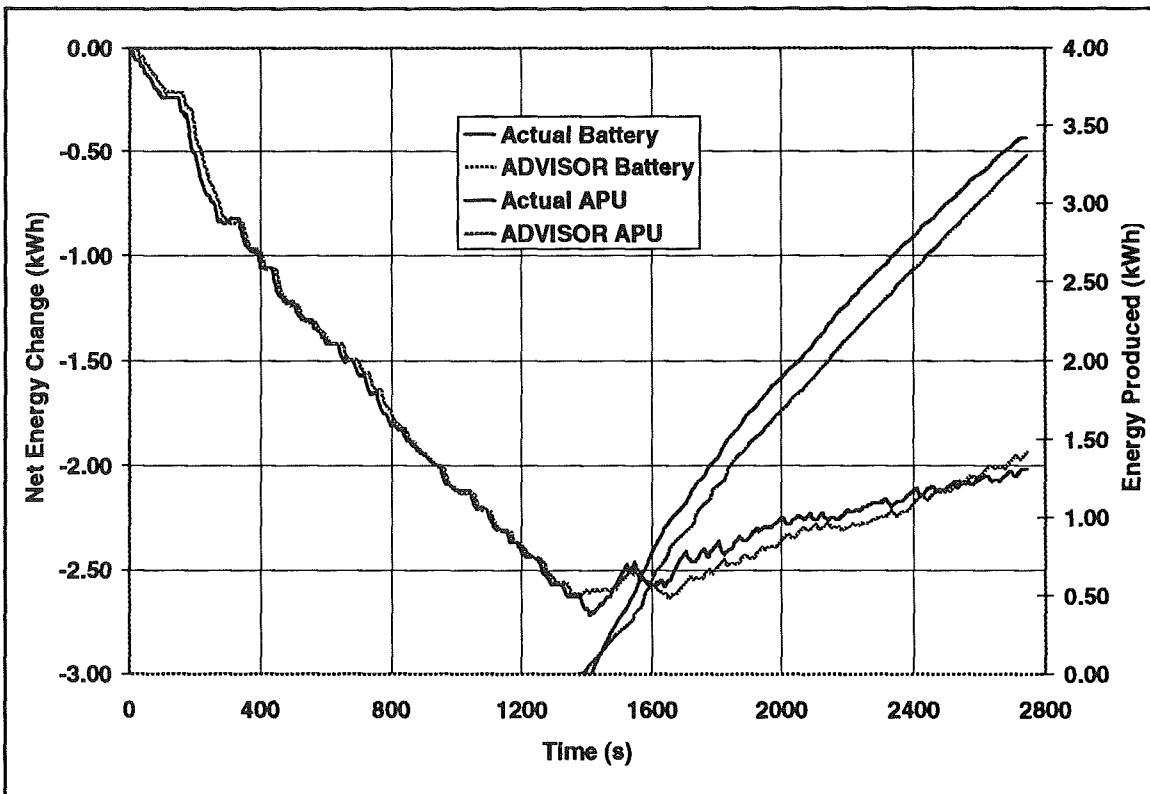Figure 12. FUDS Pair (LSOC) Energy Comparison
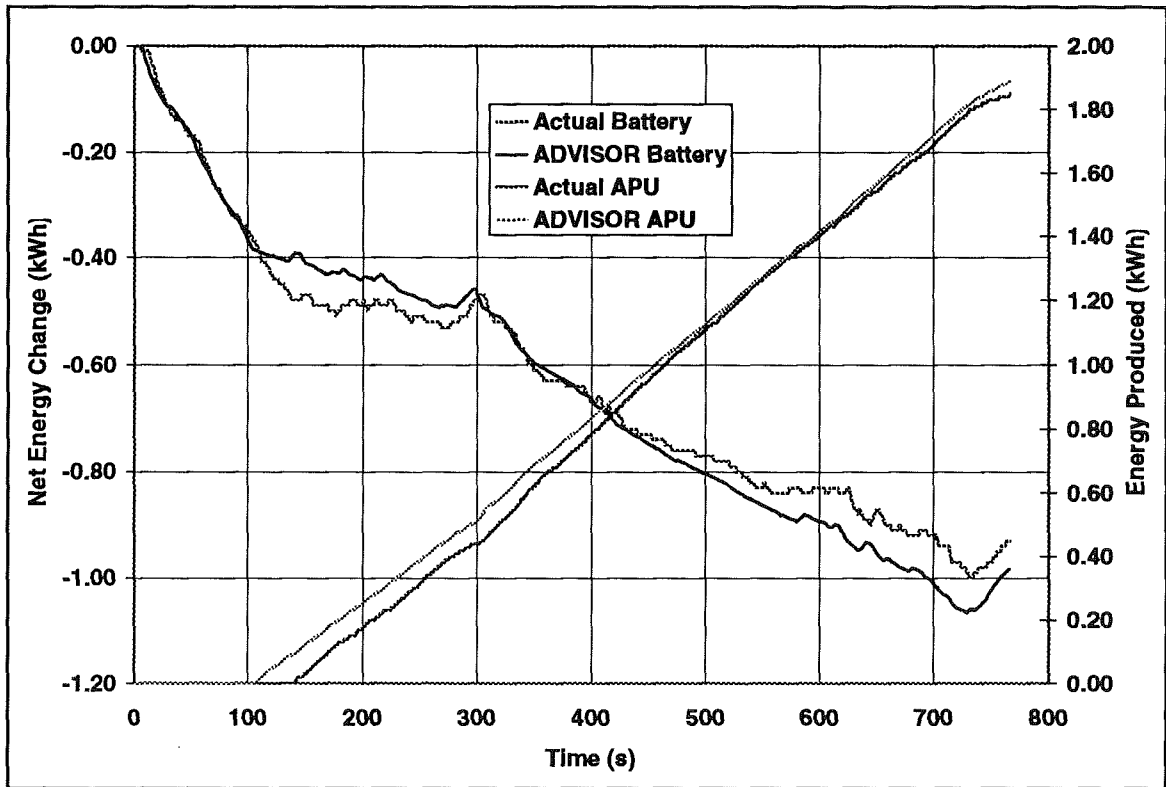

Figure 13. FUDS Pair (HSOC) Energy Comparison

FMC 1016

Figure 14. FHDS (HSOC) Energy Comparison .

For series and parallel HEVs, however, the procedure is much more complex. This is due to the fact that HEVs not only have the ability to store energy in the form of an expendable fuel (always decreasing), but also in the form of a battery pack which can be charged and depleted. This results in a vehicle whose behavior (specifically, fuel economy and emissions) is based upon the amount of energy stored in the batteries at the onset and conclusion of the testing.

In order to arrive at a fair and reasonable test for which HEVs could be accurately compared to each other and to conventional vehicles, the Society of Automotive Engineers (SAE) established the Hybrid-Electric Vehicle Test Procedure Task Force. The HEV testing procedures have yet to be finalized, but the current draft of the procedure (known as SAE Recommended Practice J1711) from this committee (SAE, 1997) was used as the basis for the actual vehicle dynamometer testing and for the simulation modeling.

The procedure called for in SAE J1711 depends heavily upon the configuration and design strategy of the particular vehicle in question. The Virginia Tech FutureCar was designed to be a charge-sustaining, series HEV for both the city and highway cycles, which is defined as the ability to maintain a given battery SOC over the cycles. SAE J1711 calls for pairs of FUDS cycles to be run; each pair consists of one FUDS cycle followed by a 10-minute ambient soak, followed by another FUDS cycle. The vehicle tests also require that

the high and low battery SOC points (HSOC and LSOC, respectively) be known for the vehicle under normal operating conditions. For this type of vehicle, the SAE test procedure is as follows:

Test 1: One cold (ambient) start FUDS pair starting at the LSOC; change (increase) in SOC, fuel use, and emissions are recorded.

Test 2: Two consecutive FHDSs (no soak) starting at the LSOC point (data is taken only for the second test); change (increase) in SOC and fuel use are recorded.

Conditioning: Vehicle is soaked at ambient conditions for 12 hours.

Test 3: One cold (ambient) start FUDS pair starting at the HSOC; change (decrease) in SOC, fuel use, and emissions are recorded.

Test 4: Two consecutive FHDSs (no soak) starting at the HSOC point (data is taken only for the second test); change (decrease) in SOC and fuel use are recorded.

If this testing does indeed result in one test where SOC increases and one test where SOC decreases, then a SOC interpolation is possible. The recorded fuel use and emissions values for the city tests are linearly interpolated between the amount of charge gained during the LSOC test and the amount of charge used

110

during the HSOC test to obtain a value for zero net change in SOC. An example of this procedure, called SOC correction, is shown in Figure 15.
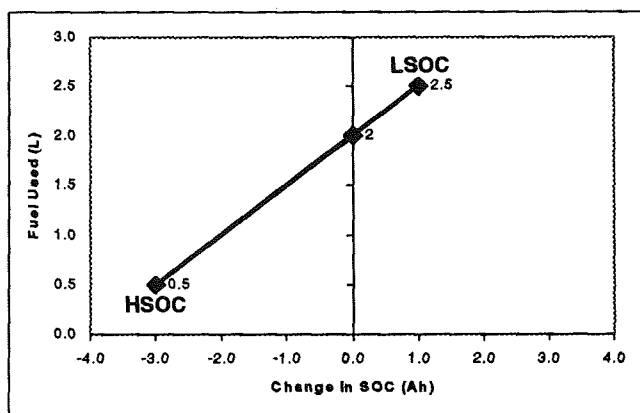

Figure 15. SOC Correction Example

Say, for example, that the measured fuel usage during the LSOC and HSOC FUDS pairs is interpolated to obtain a value of 2.0 liters (0.53 gal) of fuel used for no net change in SOC. Over the 24.0 km (14.9 mi) distance of the FUDS pair, this translates to a fuel economy of 12.0 km/l (28.2 mpg). A similar procedure is used for the emissions on the city cycle. The highway fuel usage is also computed similarly.

However, if for some reason (such as charge-depletion on both HSOC and LSOC tests), a SOC interpolation is not possible, another method is used to obtain fuel economy and emissions numbers which reflect the vehicle's behavior under the condition of zero net change in SOC. This is done using a value for the electrical energy which can be obtained from gasoline through the efficiency of an average power plant in the United States. The 1996 FCC value used to compensate for electrical energy usage was 0.321x9.69 kWh/l (0.321x36.66 kWh/gal) (Duoba, 1996).

Another important concept used in testing alternative fuel vehicles to insure fair comparisons is fuel energy equivalency. For non-gasoline fuels, the reported fuel economy values are often translated into "gasoline-equivalent" numbers for easier comparison of different vehicles. This is done as shown in Equation 10 using the lower heating values (LHV) of the fuel with respect to that of gasoline.

$$ FE_{eqiv} = FE_{fuel}\left(\frac{E_{RFG}}{E_{fuel}}\right) \qquad \text{Equation 10} $$

Since the Virginia Tech FutureCar used propane fuel, Equation 10 translates 10.0 km/l (or 10.0 mpg) of propane to 13.7 km/l (13.7 mpg) of gasoline equivalent, denoted as km/l$_e$ (mpg$_e$).

SOC-Corrected Fuel Economy Comparisons

The fuel economy results from the 1996 FutureCar Challenge were obtained primarily by using the electrical energy equivalency method outlined above. Since the Virginia Tech vehicle showed slight charge-depleting properties, a true SOC interpolation was not possible. Therefore, the fuel use from the LSOC test (on a gasoline equivalent basis) was added to the amount of gasoline necessary to replenish the electrical energy used during the test. This total fuel use was then divided into the distance traveled during the test to arrive at the city fuel economy value. The corrected city fuel economy was estimated to be 10.5 km/le (24.6 mpge). This value will be taken as the actual value for purposes of comparison in this study, and is verified from results for the 1997 FutureCar Challenge for the updated Virginia Tech vehicle.

The method used to obtain the highway fuel economy was similar to the city cycle. In this case, only a single FHDS cycle was run (from a HSOC), and the standard electrical energy conversion was used to determine the highway value. The actual value from the 1996 FCC is 17.1 km/le (40.2 mpge). Only the final fuel economy numbers are available from the 1996 FutureCar Challenge, preventing the comparison of the measured fuel use on the individual cycles with the predicted fuel use from ADVISOR. A comparison of the final fuel economy values is given in Figure 16.

ADVISOR was forced to determine the fuel economy values in the same manner as at the 1996 FutureCar Challenge for the sake of comparison. A FUDS LSOC pair was performed, with the results given in Table 6. A FHDS HSOC cycle was also executed, with the results also in Table 6.

Table 6. ADVISOR Fuel Economy Calculation

Cycle	Quantity	Value	Gasoline Equivalent
FUDS	Actual fuel use	3.44 liters LPG	2.51 liters
	Net battery energy change	-0.30 kWh	0.097 liters
	Total equivalent fuel use		2.61 liters
	Cycle distance	24.0 km	
	Fuel Economy		9.2 km/l
FHDS	Actual fuel use	1.20 liters LPG	0.88 liters
	Net battery energy change	-0.98 kWh	0.32 liters
	Total equivalent fuel use		1.20 liters
	Cycle distance	16.5 km	
	Fuel Economy		13.8 km/l

The ADVISOR predictions differ from the measured values by 12.2% and 19.2% for the city and highway, respectively. Especially with the uncertainty surrounding the 1996 FCC fuel economy numbers, these numbers show the reasonable accuracy of ADVISOR at predicting SOC-corrected fuel economy.
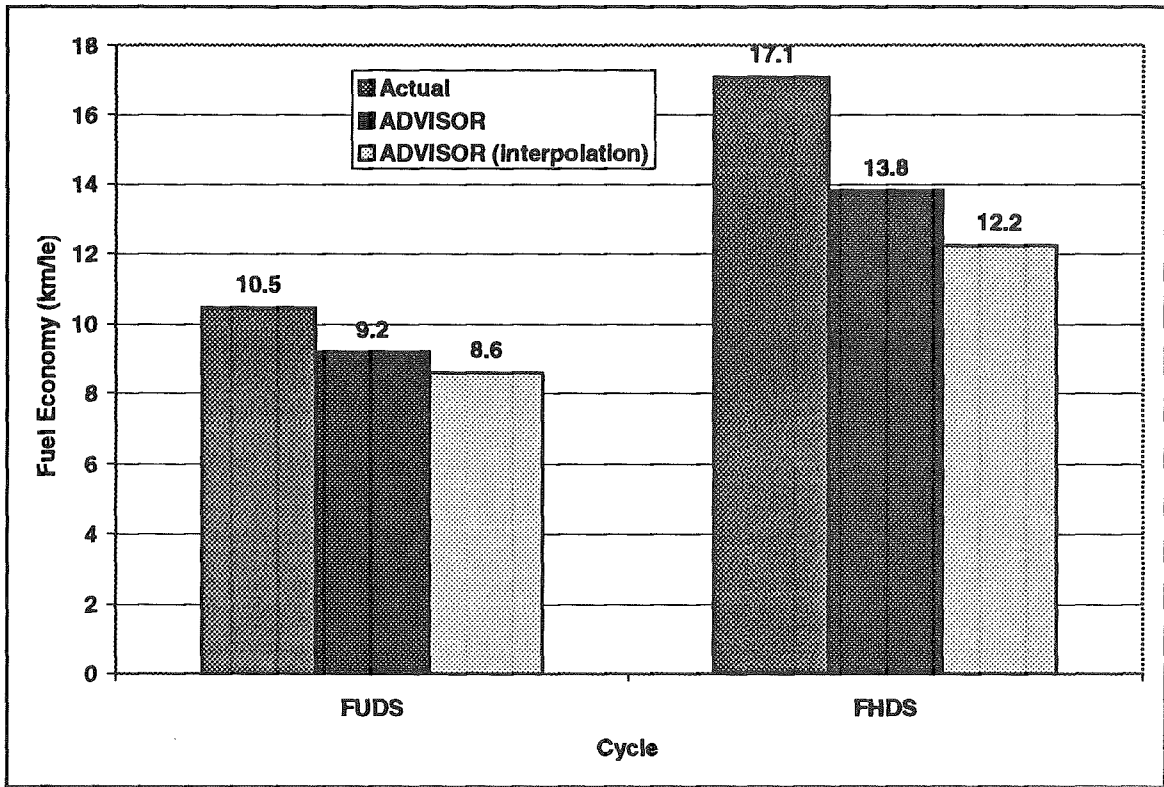
111

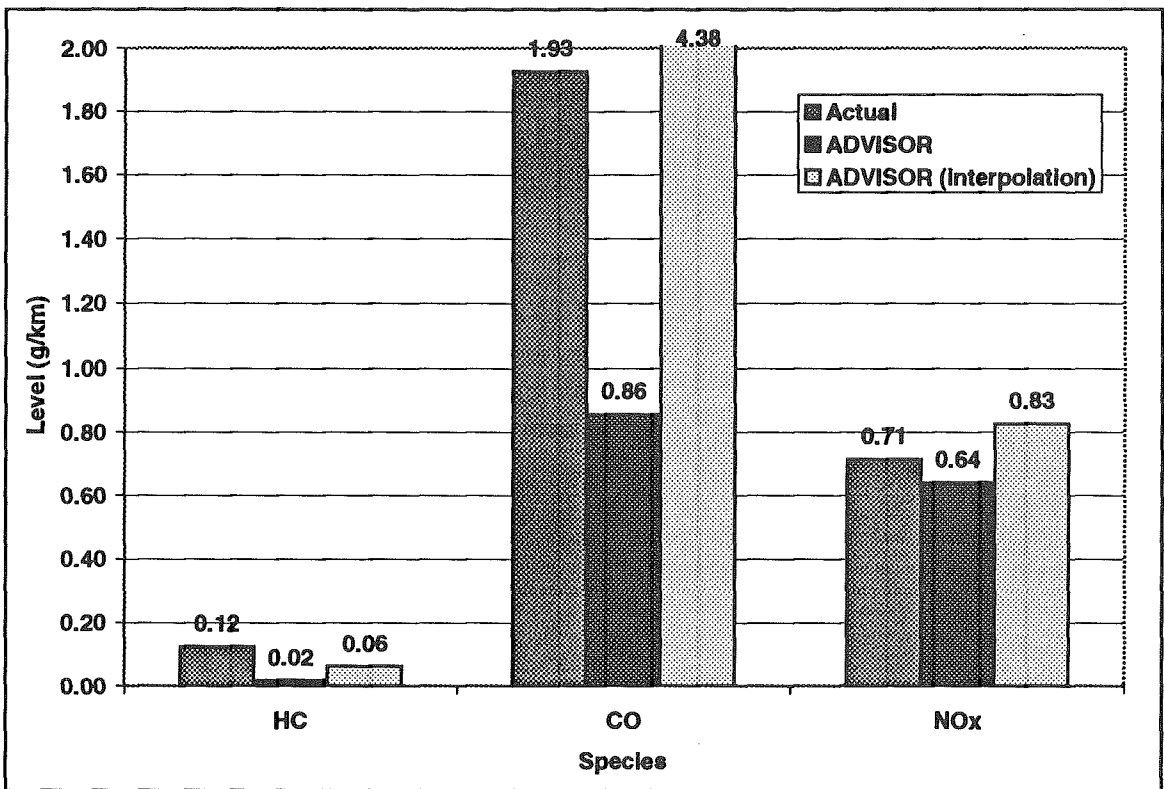Figure 16. SOC-Corrected Fuel Economy Comparison

Figure 17. SOC-Corrected FUDS Emissions Comparison

112

SOC-Corrected Emissions Comparisons

The 1996 FutureCar Challenge SOC-corrected FUDS cycles emissions numbers are the only emissions results available for the Virginia Tech vehicle. A comparison of this data with the ADVISOR predictions is shown in Figure 17. Emissions values from ADVISOR were calculated similarly to the city fuel economy number using standard emissions equivalency factors for the amount of electrical energy used (HC: 0.016 g/kWh; CO: 0.117 g/kWh; NOx: 1.25 g/kWh). The ADVISOR values are lower than the measured values by 86.0%, 55.5%, and 10.4% for HC, CO, and NOx, respectively. These numbers do not show that ADVISOR, in combination with the APU model, can accurately predict emissions values, although its NOx prediction is quite close to the actual value, and its values are generally of the same order of magnitude of the actual values.

The ADVISOR code was also utilized to predict the operation of the Virginia Tech vehicle when tested following the SAE J1711 interpolation procedure, instead of attempting to match the procedures performed at the 1996 FutureCar Challenge. The fuel economy and emissions results of the SAE J1711 predictions are given in Figures 16 and 17 respectively. The fuel economy numbers under SAE J1711 are lower than the actual values and the predicted values using the FCC test procedures. The FUDS emissions values under SAE J1711 are generally higher than the actual values and the ADVISOR values using the FCC procedures. Both the fuel economy and emissions discrepancies are the result of using standard fuel use and emissions production values for an equivalent amount of electrical energy usage. These standard values do not necessarily reflect the actual operation of the Virginia Tech FutureCar, and, consequently, the use of these values would not result in accurate simulation results.

The various standards used here to test the validity of the ADVISOR simulations represent a fairly thorough evaluation of the ADVISOR code and the Virginia Tech FutureCar component models. This assessment should be adequate to allow for some conclusions to be drawn about the accuracy specific to the Virginia Tech model, the general accuracy of ADVISOR, its strengths and weaknesses, and other potential uses as a simulation tool for HEVs.

CONCLUSIONS AND RECOMMENDATIONS

Many aspects of the validation process are prone to misinterpretation, uncertainty, and mistakes. These can drastically alter the results of the simulation and therefore their effects must be carefully considered and accounted for in making conclusions about the usefulness of a particular simulation tool. With the proper understanding of the causes of discrepancies and the limitations of the program, a simulation can be quite useful even when the data may not exactly predict the

actual values. The major influences on the ADVISOR predictions are discussed below with a proposed method of limiting its adverse effects or eliminating them altogether.

Measured Data and Test Procedures

A number of problems with the procedures of collecting data and uncertainties in the measurement of the data on the Virginia Tech FutureCar and its components may have caused difficulties in testing the accuracy of ADVISOR. In fact, the measured data were the single most significant source of uncertainty in the entire validation process.

Some measurement problems were caused by the vehicle itself not performing as desired. During the FUDS LSOC test, the engine speed control, designed to hold a constant speed, oscillated wildly during most of the test. This chaotic behavior is nearly impossible to model, and is consequently a source of much uncertainty. Repeated attempts to start the engine during a test also occurred on at least one occasion, causing a difficult modeling problem. These problems could be corrected by more extensive vehicle testing and tuning to ensure reliable operation before recording data.

The actual electrical behavior of the vehicle as a function of time was recorded during all testing at the 1996 FutureCar Challenge. Careful study of this data allowed a number of possible discrepancies to be fixed in the simulations. However, this type of data is not available for the actual vehicle speed, fuel use, or emissions production. The lack of intermediate data from the dynamometer testing prevents the reconciliation of other possible discrepancies in the simulation. Given the proper resources, this data would greatly help to verify proper operation of the simulation throughout the process, from road load calculation to SOC-corrections.

Differences in test procedure must be closely monitored and repeated if accurate simulations are to be performed. Even a slight difference in a test (vehicle preconditioning process, the catalyst temperature at the start of a test, the amount of soak time between tests, and the ambient temperature during engine testing are common examples) can cause large variations in the results. Every effort was made here to replicate the testing as performed at the 1996 FutureCar Challenge in the ADVISOR simulations, but small errors are likely, introducing a level of uncertainty. For this reason, detailed logs should be made during data collection which will allow the conditions of the actual test to be reproduced as closely as possible by the simulation.

In order to determine the APU model for ADVISOR, fuel efficiency, emissions, and catalyst efficiency maps were generated from extensive testing. However, the data for these values are extremely sensitive to the air/fuel ratio

of the engine. On the Virginia Tech APU, this air/fuel ratio was controlled by a commercial closed-loop fuel controller, which oscillated about a stoichiometric ratio. Merely operating 1% on the lean side of a stoichiometric mixture results in drastically different emissions levels (high NOx) than operating 1% on the rich side (high HC and CO). Significant changes in the emissions levels then cause significant changes in the catalyst efficiencies. As a result, large uncertainties are present in the measured APU and dynamometer data due to the inability to maintain a constant air/fuel ratio.

During all dynamometer testing, the speed of the vehicle was controlled manually. Therefore, there is inherent human error in the actual vehicle speed. This error, when taken to extremes by some of the less meticulous operators, can result in significant differences in vehicle operation. Simply using as much care as possible in driving the trace should significantly reduce this source of error.

ADVISOR

Some discrepancies in the simulation may result from the structure of the simulation itself. If the simulation code does not attempt to exactly reproduce the major features of actual vehicle operation (such as the vehicle control strategy), there is little hope for an accurate simulation. The constant engine speed with varying load based on bus voltage feature of the Virginia Tech control strategy was implemented in the ADVISOR code at the start of the validation process. This routine seemed to work well at modeling the true behavior of the vehicle as shown by the accurate results of the APU/battery energy comparisons.

Another feature that could have been introduced, but was not, is the concept that the engine speed on the Virginia Tech vehicle was not truly constant. The extremely high loads caused by hard accelerations cause the engine speed to slow down somewhat due to the limited torque capacity of the engine. This changes the effective open-circuit voltage of the alternator (now set in ADVISOR as a constant). However, relatively few high loads occur during the standard driving cycles, and the effect of these speed changes is small. Therefore, it was decided that a routine to vary engine speed according to torque limitation was unnecessarily complex.

One feature of ADVISOR, which is inherent to its nature as a computer simulation, is its quasi-steady assumption. This type of model requires that all events occur in small steady-state steps. However, real systems do not behave as steady-state systems; rather, they consist of many transient phenomena often occurring simultaneously. Many of a vehicle's transients can be accurately modeled in a quasi-steady environment using a sufficiently small timestep. However, all transient events cannot be accurately predicted by a quasi-steady model, regardless of timestep size, thereby introducing some error.

One of the most important of these to the ADVISOR simulation is the operation of the engine, which can be extremely nonlinear and is therefore not modeled well by the linear assumption of the quasi-steady approach. For example, the engine may need 1 g/s of fuel at 1000 rpm at a given load during one timestep, and 2 g/s of fuel at 1100 rpm at the same load during the next timestep, but it may actually require 3 g/s (and not 1.5 g/s) of fuel to accelerate from the first timestep to the next. If one adds in the effects of changing loads and the continuous variations in air/fuel ratio, the engine may not be modeled with sufficient accuracy. Predicting emissions is even less linear than fuel use. One possible solution to this problem would be to use a nonlinear modeling technique, such as a neural network, to represent the operation of the APU, with the remainder of the simulation operating in the traditional quasi-steady environment. This type of complexity may be excessive for ADVISOR, but it is likely necessary if accurate modeling of transient phenomena, such as emissions, is desired.

Validity of ADVISOR as a Simulation Tool

These results show ADVISOR to be a valid simulation tool, particular for series HEVs and the Virginia Tech FutureCar. Its predictions of the vehicle behavior are consistently within the bounds of uncertainty for each step of the simulation process.

Even as a generally valid simulation tool, ADVISOR has particular strengths and weaknesses that limit it use. It appears to be accurate enough for use in predicting the absolute values of particular vehicle attributes and not only as a tool for comparing the relative values of different vehicles. It seems to provide very accurate predictions of the energy use of a vehicle, and only slightly less accurate predictions of vehicle fuel economy over the standard driving cycles using standard test procedures. The simulation itself is quite stable and is not overly sensitive to variations in components and conditions.

The quasi-steady simulations would likely be the most accurate for pure EVs, since the transient effects of an electric drivetrain are fairly small and would not introduce errors as discussed previously. Series HEVs, having the next most-steady operating characteristics, appear to be nearly as accurately modeled. Parallel HEVs may also be modeled with a fair degree of accuracy since their electric drivetrains behave primarily in a steady manner. The accuracy would be inversely proportional to the extent to which transient effects of the ICE are allowed to vary—small engine variations could probably be modeled with high accuracy, while the fuel use and emissions effects of large engine variations would likely be underestimated.

ADVISOR is limited by the fact that it requires a large amount of accurate component testing (particularly of the APU) in order to arrive at accurate results, although this is inherent to all modeling. Its abilities to model emissions production are not highly accurate, although it is probably as accurate as many of the emission testing procedures. Its quasi-steady nature reduces its ability to accurately model certain items, such as the APU operation.

Despite its few limitations, ADVISOR proved itself to be a valuable simulation tool for modeling the behavior of HEVs in general, and the Virginia Tech FutureCar in particular. ADVISOR can be used with a great degree of confidence in predicting future behavior and making informed design decisions with a minimal amount of additional testing

ACKNOWLEDGMENTS

REFERENCES

Aceves, Salvador M., and Smith, J. Ray, February 1995, "A Hybrid Vehicle Evaluation Code and Its Application to Vehicle Design," Society of Automotive Engineers Publication SP 1089, Design Innovations in Electric and Hybrid Vehicles, pp. 43-52, SAE Paper 950491.

Aldrich, Bob, 1996, "ABCs of AFVs - A Guide to Alternative Fuel Vehicles," California Energy Commission.

Boothe, Richard, 1997, personal communication of data.

Braun, Christopher G., and Busse, David, August 1996, "A Modular Simulink Model for Hybrid Electric Vehicles," Society of Automotive Engineers Publication SP-1189, Technical Solutions to Alternative Transportation Problems, pp. 43 - 48, SAE Paper 961659.

Butler, K. L., Stevens, K. M., and Ehsani, M., February 1997, "A Versatile Computer Simulation Tool for Design and Analysis of Electric and Hybrid Drive Trains," Society of Automotive Engineers Publication SP 1243, Electric and Hybrid Vehicle Design Studies, pp. 19 -25, SAE Paper 970199.

Cuddy, Matthew, February 1995, "A Comparison of Modeled and Measured Energy Use in Hybrid Electric Vehicles," Society of Automotive Engineers Publication SP 1089, Design Innovations in Electric and Hybrid Vehicles, pp. 119 -128, SAE Paper 950959.

Cole, G. H., 1993, "SIMPLEV: A Simple Electric Vehicle Simulation Program, Version 2.0 User's Guide," USDOE Publication ID-10293-2, pp. 1 - 30.

Duoba, Michael, 1995, "The 1996 FutureCar Challenge Final Rules and Regulations," Section E-11.3.3, pg. 55.

Hawker Energy Products, Inc., 1996, Hawker Genesis Specifications.

Merkle, Matthew A., 1997, "Variable Bus Voltage Modeling for Series Hybrid Electric Vehicle Simulation", Master of Science Thesis, Department of Electrical Engineering, Virginia Tech, Blacksburg, Virginia.

Riley, Robert Q., 1994, "Alternative Cars in the 21st Century - A New Personal Transportation Paradigm," Society of Automotive Engineers, pp. 6 - 12.

Society of Automotive Engineers (SAE), February 26, 1997, "Draft SAE J1711: Recommended Practice for Measuring the Exhaust Emissions and Fuel Economy of Hybrid-Electric Vehicles," Society of Automotive Engineers Hybrid-Electric Vehicle Test Procedure Task Force.

Senger, Randall D., 1997, "Validation of ADVISOR as a Simulation Tool for a Series Hybrid Electric Vehicle Using the Virginia Tech FutureCar Lumina", Master of Science Thesis, Department of Mechanical Engineering, Virginia Tech, Blacksburg, Virginia. Available online at http://scholar.lib.vt.edu/theses/public/etd-91797-74847/etd-title.html

Senger, Randall D., Merkle, Matthew A., Nelson, Douglas J., February 1997, "Design of the 1996 Virginia Tech FutureCar," Society of Automotive Engineers Publication SP 1234, The 1996 FutureCar Challenge, pp. 101 - 112.

Senger, Randall D., Merkle, Matthew A., Nelson, Douglas J., June 1997, "Design and Performance of the Virginia Tech Hybrid Electric FutureCar," design paper submitted for the 1997 FutureCar Challenge, to be published by Society of Automotive Engineers.

Stinnett, W. A., Katsis, D. C., and Nelson, D. J., 1996, "Design of The 1995 Virginia Tech Hybrid Electric Neon," Society of Automotive Engineers Publication SP 1170, The 1995 HEV Challenge, pp. 215 - 229.

Wipke, Keith B., and Cuddy, Matthew R., 1996, "Using an Advanced Vehicle Simulator (ADVISOR) to Guide Hybrid Vehicle Propulsion System Development," presented at the Northeast Sustainable Energy Association 1996 Sustainable Transportation Conference, New York, NY.

Wipke, Keith B., and Cuddy, Matthew R., 1997, "Analysis of the Fuel Economy Benefit of Drivetrain Hybridization," Society of Automotive Engineers Publication SP 1243, Electric and Hybrid Vehicle Design Studies, pp. 101 - 109, SAE Paper 970289.

The Electric Automobile

E. Larrodé, L. Castejón, A. Miravete and J. Cuartero
University of Zaragoza

ABSTRACT

In this paper, the prototypes of electric cars done by the Engineering & Infrastructure Transportation Area in the Department of Mechanical Engineering of the University of Zaragoza is presented. The project started in 1993, the initial stage started doing calculation and construction of prototype I which was used as a technological demonstrator. The prototype I, was a very simplified electric vehicle with particular performance qualities. Prototype II has the features of an urban car comparable to the current combustion cars for urban purposes. A program of testing will be done in order to find problems that can be corrected for the prototype III, in which all the parameters analyzed will be corrected for a serial manufacture.

1. INTRODUCTION

The Electric Vehicle is presented in last years as the future alternative in urban transport. The comparisons between this one and the major competitor, the combustion automobile are always better for the last one due to economic reasons and for its capabilities and infrastructure facilities. However, the development and investigation of electric vehicles it is justified nowadays. All main automotive companies are involved in new prototypes of electric vehicles as an alternative of the problems that the present automobile have.

In order to know in detail the subject, we are going to evaluate the parameters that justify the use of electric vehicles.

1.1. ENVIRONMENTAL REASONS.

The first favorable consequence of the electric car is its low or zero direct contamination or contamination during its use. The difference with the combustion cars is mainly that those burn organic fuels giving as a consequence the emission of CO to the environment of the cities which cause the greenhouse gas effect. The electric car do not produce this effect in a direct form, so it is possible its control. However, in order to be able to compare in correct form the emissions of vehicles, it is necessary evaluate the full cycle of emissions, that is to say, from the obtention of primary energy to its use by the car. Thus, for example, if the electric energy that it is used to charge the batteries of the electric car is obtained by means power stations, a percentage of emissions to the environment can be attributed to electric cars. But, in the other hand, those emissions can be controlled and reduced then. Next table shows the comparison between the level of contaminant emissions for each type of vehicle ; gasoline, diesel and electric vehicles, in mg/Km.

Table 1. Comparison of contaminate levels for each type of vehicle.

	Gasoline	Diesel	Electric
Dust	15	135	26
SO_2	100	220	630
NOx	880	840	276
HC	310	300	16
CO	2150	2140	27
CO_2	234	214	126

In order to achieve that those results being comparable it is necessary to establish a standard cycle of driving, in this case it is showed a urban cycle for European drivers done in Belgium and called ECE-15. The consumption of each type of vehicle were compared and can be seen in the following lines.

- Diesel motorization :   6,5 l in 100 Km
- Gasoline motorization: 8,5 l in 100 Km
- Electric motorization :   28 Kwh in 100 Km

In this study, it was taking into account the full cycle of emission that includes the direct consumption of the primary energy, the production of electricity, and the distribution and transport of fuel. Results of contaminant emissions in Kg per 100 Km were the next :

Table 2. Contaminants emissions in Kg. per 100 Km for each type of vehicle.

	Gasoline	Diesel	Electric
Dust	-	0.019	0.0043
SO_2	0.005	0.027	0.04
NOx + HC	0.098	0.098	0.026
CO	0.27	0.27	0.0025
CO_2	25.8	19.8	10

117

Another source of environmental contamination is the acoustic, where in big cities, where the combustion car is mainly employed, could reach values of about 70 dB. This factor disappear by means the use of electric cars which are extremely silent.

1.2. PRESENT AVAILABILITY.

As it is known, one of the most important limitations in the current electric cars in comparison to the combustion cars, is its autonomy and its capacity of energy storage. Both parameters come from the absence of an optimum energy storage system, because the current systems are limited in its capacity and have a high weight and volume. Moreover, the time employed during the charge of those systems are very high (more than 6 hours for a full charge), while the consumption is done in less than 1 hour. However, some studies have been done respect to the type of driving in big cities, analyzing the following parameters :

- Number of kilometers done per day
- Number of travels done per day and per person.
- Medium velocity during the displacement.
- Number of passengers during each displacement
- Baggage carried per displacement.

General conclusions obtained in medium values are outstanding due to the number of kilometers done daily are directly related with the number of displacements done daily and per day, being 40 Km the mean value at a medium velocity of 50 Km/h, and being the medium number of passengers two with a 30% of the volume of the baggage occupied. This means that the 90% of the travels done in one year, could be done by means a small vehicle with an autonomy less than 80 Km, so, this travels will be specially recommended for electric vehicles, which satisfy all conditions named before, but with a lower level of consumption than the conventional cars, obtaining this way a very high energy saving. The rest·of the travels (10%) correspond to travels to the periphery of the big cities, travels of long distances, travels on holidays and weekends.

1.3. INFRASTRUCTURES.

One of the most important difficulties for the development of electric cars is, the absence of the necessary infrastructures for the maintenance of this types of vehicles. In comparison with combustion cars, it takes several hours to achieve a full charge of the energy storage system (batteries) of the electric cars, against few minutes to fill the tank of gasoline. The introduction of electric cars in big cities will involve conditioning of places for battery recharge, as well as the recondition of housing garages and car repair shops. All this things, will rise the electric energy consumption, so it will be necessary the creation of new auxiliary power stations, moreover it will be necessary a readjustment of the

energy supply, because the electric energy consumption, will raise during nights, due to the recharge of electric's cars will take place during this hours mainly.

1.4. WEIGHT AND PERFORMANCE QUALITIES.

Nowadays two important parameters limit the success of the electric car in the market, the first one is the ratio : weight of energy storage / total weight, which is extremely favorable for combustion cars (a few litters against more than 300 Kg), and the second one is the performances qualities like acceleration, autonomy, maximum velocity, etc.

In a combustion car, the fuel tank represent a 5% of the total weight of the car, however in a electric car the weight of batteries represent a 40%. As can be seen, with these data in our hands, it is very easy to see that the weight in a electric car is a decisive factor if it is compared to the combustion car. The load capacity in electric cars is far away from the same in combustion cars, that is the reason because, there is no development of systems where the load capacity is determinant, as trucks or coaches.

The second inconvenient, can be explained with the classification that has been done with this type of vehicles : urban cars, because for urban cycles of driving, the performance qualities of an automobile are not as important as other types of cycles of driving, as a road cycle of driving for example. For urban cycles of driving it is no necessary high performances qualities as high accelerations, or high maximum velocities than can be given by combustion cars, due to the limitations in maximum velocities and the dense road traffic of big cities. The great difference between the performance qualities of electric and combustion cars lie in the current motors, the energetic power obtained in combustion motors by organic combustibles is greater than the obtained in electric motors by using electric energy for the same relations in weight and size.

1.5. CONCLUSIONS

⇓ The relationship between the weight of the energy storage system (batteries) and the weight of the rest of the vehicle is unfavorable for electric cars, as a consequence there are no vehicles for mass transportation due to the limitation in the load capacity.
⇓ The quality performances are higher in the combustion car than in the electric car.
⇓ The autonomy of combustion cars is higher than the electric cars.
⇓ There are no infrastructure for maintenance of electric vehicles yet.
⇑ The level of contamination is very low though depending on the origin of the energy supply.

In order to have a serious alternative to the present car, it is necessary to search the adequate properties and a competitive design, because the electric car has more inconvenience than the combustion car as we have mentioned before. That is the reason because the electric car is restricted to uses as urban car, with reduced dimensions, easy way of driving, low levels of consumption and an enough autonomy for daily use for two people in the city.

2. DESCRIPTION OF THE PROJECT.

In this paper is presented the prototypes of electric cars done by the Engineering & Infrastructure Transportation Area in the Department of Mechanical Engineering of the University of Zaragoza.

The project starts in 1993, the stage 1 starts doing calculation and construction of prototype I which is used as an technological demonstrator. The prototype I, was a very simplified electric vehicle with particular performance qualities. Thus, it would be possible evaluate and make improvements for the next prototype of high features. At the same time, a grant given by CONSID from the Government of Aragón is obtained, in order to carry out the expenses. The title of the project is : "Design, Analysis, Optimization and Manufacture of a prototype of Electric Vehicle". Ref.: PIT0894. During this period of time, a direct collaboration between The University of Zaragoza and the Sociedad Española del Acumulador TUDOR S.A., in the Laboratory de Investigation de Azuqueca de Henares in Guadalajara, as well as in the factory of La Cartuja in Zaragoza. The collaboration consist in the support of traction batteries specially designed for electric in order to be implemented in the vehicle constructed by the University of Zaragoza and to make dynamic testing to obtain their behavior in real conditions. Once the design and manufacturing of the prototype I was finished, starts the stage 2, in which the prototype II is designed and manufactured. This prototype has the features of an urban car comparable to the current combustion cars for urban purposes. In this prototype are taking into account the experience of the first prototype, as well as the problems encountered during the analysis and manufacture.
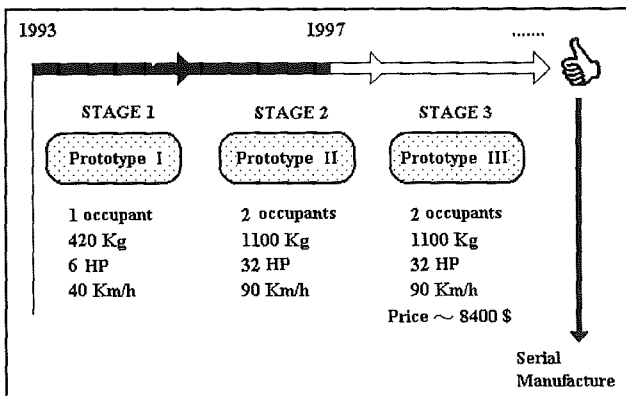

Figure 1. Description of the stages of the project.

The design and analysis of prototype II is at this moment finished, and it is the beginning of the manufacture. Once this prototype is constructed, a program of testing will be done in order to find problems that can be corrected for the third stage, the construction of prototype III, in which all the parameters analyzed will be corrected for a serial manufacture. The objective of prototype III is to improve and optimize all the parameters referring to the manufacture and assembly process, as well as the supply of components parts and maintenance, in such a way that this prototype being economical available for its serial manufacture. For this task, the prototype will have to be competitive and that means that the final price to public being very low because of the type of vehicle, small, and restricted to urban uses. So the final price will not higher than 8400 American dollars.

3. PROTOTYPE I.

The developing of prototype I, starts at the end of 1993, in order to obtain a technological demonstrator which gave us availability of the whole project as well as the establishment of the investigation line related to electric vehicles at the Department of Engineering and Infrastructure of Transportation. Due to carry out with own resources and at the beginning without any grant, the main components parts of the vehicle were simplified extremely, and the dimensions were reduced at minimum. The final cost of the prototype was approximately 5.500 American dollars. In the figure 2 it can be seen a photograph of the first prototype.

Main characteristics of prototype I are following :

Dimensions:
- Maximum height: 1.210 m
- Maximum width: 1.230 m
- Length: 2.040 m
- Wheelbase: 1.330 m

General Characteristics:

- Weight: 420 Kg.
- Structure: Steel box beams
- Bodywork: E-Glass fiber and polyester resin
- Steering: Rack
- Brakes: Rear brake disk
- Tires: 120/85 R 8
- Transmission: By chain

Performance qualities:

- Power: 6 HP
- Maximum Velocity: 45 Km./h.
- Acceleration from 0 to 45 Km./h: 12 s
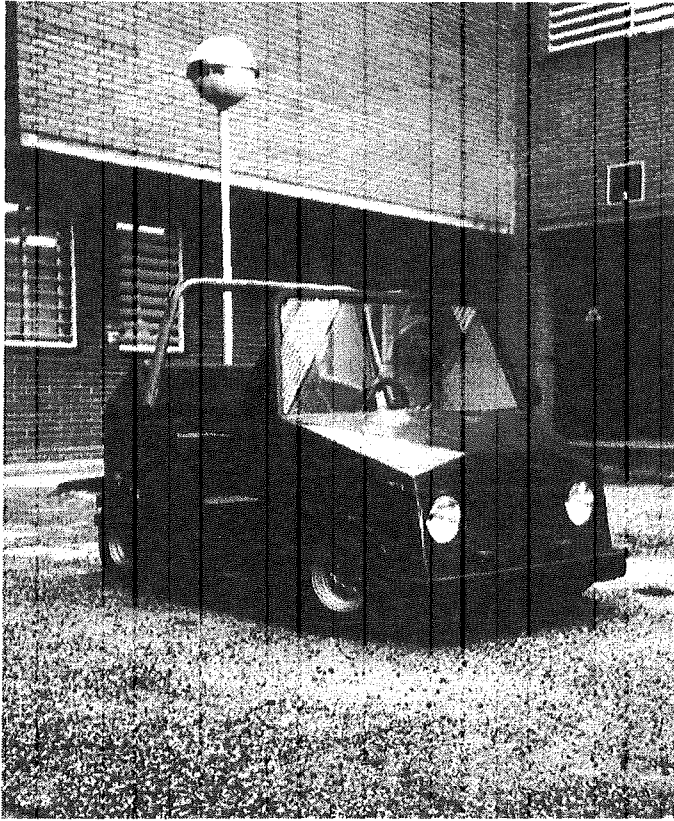- Autonomy at 30 Km./h: 80 Km

Figure 2. Photograph of prototype I.

The motorization system is composed by a direct current motor and independent excitation, at 24 V, with a nominal power of 6 HP, which lead us to reach velocities of about 45 Km/h. The selection of this type of motor is because its low weight, close to 20 Kg, its easy way of working, toughness and because its characteristics are similar to the DC Brushless motor, which is studied for the prototype II. Thus it can be analyzed in detail in order to obtain experimental results for later be applied to future prototypes.

The control, regulate the well working of the motorization system of the vehicle, so that, at each time the intensity given by the batteries to the motor is controlled, obtaining this way a Moment control. The power stage is composed by MOSFET's and the control stage by a microprocessor that is used to for protection and security purposes.

For the energy supply system, a set of 6 lead-batteries (Type L-3), given by S.E. Acumulador Tudor S.A. of 12 V and 60 Ah, were used. Those batteries which were tested by Tudor giving more than 400 cycles of life for a urban cycle (36.000 Km), gave a good response during the experimental training of the vehicle. Their main advantage is its toughness and security, due to this type of battery is closed and its density of energy.

As mentioned before, prototype I, is only for one occupant and its weight it is about 450 Kg., it contains 6 traction batteries of 12 V and 60 Ah of capacity. The

charger developed for the charge of those batteries has a power of 720 W, and introduce to the batteries a curve I-U with constant intensity at the beginning and later constant tension. The charger designed is a conmuted supply whose power circuit it works as follow: firstly the monofasic current is rectified by means a bridge of diodes and filtered later by means a group of condensers. From the level of high tension not regulated, it is obtained a level of tension and intensity regulated, determined by the curves I-U recommended by the manufacturer, by means a converter of high frequency using a configuration of H-bridge with a high frequency transformer.

4. PROTOTYPE II.

The prototype II is defined as an automobile of reduced dimensions for two occupants and with a 1100 Kg of total weight, designed specially for urban use and its energy supply is a set of 16 traction batteries of 12 V each one, which produce a tension supply of 192 V. The power established get 32 HP which with it is possible to reach a maximum velocity of 90 Km/h.

The design of the prototype II has been full up, making the calculations and design for all following systems:

- Components of Transmission
- Components of Translation
- Motorization
- Energy supply
- Structure
- Bodywork

Establishment of initial hypothesis.

- Gear box with two gears
- Maximum velocity of 90 Km/h at high gear and of 50 Km/h at low gear.
- Slope to overcome at high gear of 5% and at 50 Km/h of 15%.
- Reduced gauge and wheelbase.
- The mechanical reverse gear of the vehicle is rejected because is obtained making the electric motor spinning at reverse sense.
- The second shaft works at the same time as crankshaft
- The differential with planet, satellites, pinion and crown
- The drive axles get the moment from differential to the drive wheels
- Drive wheels generate in the contact with the ground the reaction forces necessary to achieve the movement of the vehicle.

4.1. GENERAL CHARACTERISTICS.

Characteristics of the design of Prototype II for electric car are resumed in next list :

120

- Aerodynamic coefficient : 0.45
- Maximum height : 1.435 m
- Maximum width : 1.487 m
- Aerodynamic height : 0.730 m
- Gravity center height g.c.h.: 0.550 m
- Gauge : 1.264 m
- Wheelbase : 2.200 m
- Distance front wheels to g.c.h. : 1.150 m
- Distance rear wheels to g.c.h. : 1.050 m
- Maximum slope at high gear : 4 %
- Maximum slope at low gear : 15 %
- Number of occupants : 2
- Weight by occupants : 75 Kg.
- Baggage weight : 50 Kg.
- Vehicle weight : 900 Kg.
- Driving weight : 1100 Kg.
- Gear box efficiency: 0.96
- Universal joint efficiency: 0.98
- Conical group efficiency : 0.98
- Tire (145/70 R13") : c.d.r. 1.725 m
- High ratio: 0.675
- Low ratio: 1.310
- Conical group ratio: 3.053
- Maximum power: 32 HP
- Revolutions at maximum power : 1790 r.p.m.
- Maximum moment : 125.475 Nm
- Maximum velocity at high : 90.924 Km/h
- Maximum velocity at low : 45.750 Km/h
- Friction coefficient : 0.013
- S.A.E. Friction coefficient : 0.016
  - Pump pressure front wheels : 2 Kg/cm^2
  - Pump pressure rear wheels : 2 Kg/cm^2
  - S.A.E. coefficient: 1
  - Static friction coefficient : 0.012

4.2. MECHANICAL COMPONENTS.

4.2.1. Performance qualities

Performance qualities of the vehicle are given by the acceleration capability, maximum velocity of the vehicle, and maximum slope that can be overcome as well as other parameter of less importance. Those characteristics are very influenced for the next parameters.

- Road holding qualities between tyres and ground
- The aerodynamic of the vehicle
- The motorization
- The design of the transmission chain.

4.2.2. Optimum position of the mechanical components.

In a car, the mechanical elements that carry out the transmission of the moment from the motor to the wheels, are grouped in a set called transmission chain or drive line of the vehicle. The design of this set have influence on the behavior and qualities performances of the vehicle. Four possibilities of construction of the transmission chain depending on the position of main mechanical elements, can be analyzed:

1. Front motor and front-wheel drive
2. Rear motor and rear-wheel drive
3. Front motor and rear-wheel drive
4. Rear motor and front-wheel drive.

The optimum position of the components part in an electric vehicle it is very important. The main problem is the position of the group of batteries which have a high volume and weight. All those configurations which need a high crankshaft are rejected for its worse efficiency and for the space necessary to put in. So, options 3) and 4) are rejected. It is recommended to put the motor in transversal place, thus avoiding to introduce a differential with conical gear.

For the other configurations, due to road holding reasons, it would be better to select option 2), because, when taking a ramp, the driving axle it is being overloading, thus obtaining profitable results due to have higher reaction forces on the driving axle, depending on the ground conditions of course.

However, we should not forget, that a 25% of the total weight, must be over front axle, in order to avoid loss of road-holding qualities in these wheels, that could cause an instability in the vehicle and a bad working of the steering which is placed in this axle. That is the reason because it is necessary to do a preliminary study of the distribution weights of each part of the vehicle, in order to get its optimum position in the vehicle.

Starting with the following hypothesis, taking into account the weight of next main part components:

- Occupants load : 150 Kg.
- Baggage load : 50 Kg.
- Structure and mech. components weight: 400 Kg
- Batteries load: 400 Kg.
- Motorization : 100 Kg.

We need also to establish the following hypothesis and restrictions:

- For security reasons, electric vehicles standards do not recommend to put batteries group in the front part of the vehicle, due to danger in case of frontal crash impact.

- The structure weight is uniformly distributed over front and rear axle

As the rear axle will support more load than the the front axle, it is better to put the motor into the front part of the vehicle, as well as the traction. So, we can assure a reaction force of more than 25% of the total weight over this axle, obtaining more freedom to distribute the rest of the components. So, option 1) is selected as the best.

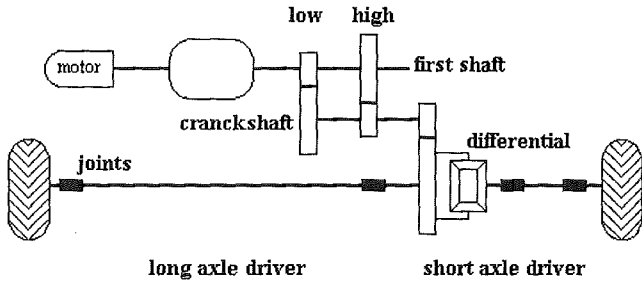The definitive scheme of the transmission chain and for the first shaft can be seen in the next figure:

Figure 3. Definitive scheme of the transmission chain.

4.3. MOTORIZACIÓN Y CONTROL.

The type of motor selected for prototype II is a DC Brushless, because is a silent machine and due to its toughness and strength, its high efficiency and low weight, being one of the best options for the range of power that the car needs. The power of the motor it will be 24 Kw and will be supplied with 192 V, which led us to reach velocities of 90 Km/h. A scheme of working can be see in next figure.
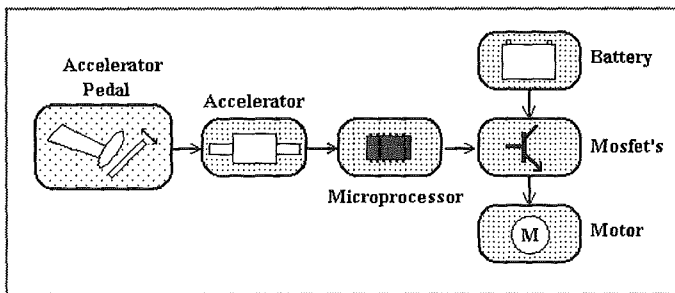

Figure 4. Scheme of the control, motorization and energy supply systems.

The control will follow the same criteria that prototype I, that is to say, we will control the moment. The regulation consist in the control of the intensity that batteries give to the motor, that will be which generate the moment of the motor. Or this purpose, the microprocessor will pick up the reference signal from the lineal accelerator (accelerator pedal) and will work over the Mosfet's in a specific way. The system has implemented the protections and security systems needed for a high efficiency and reliability.

4.4. ENERGY SUPPLY AND MAINTENANCE.

As mentioned before, prototype II has bigger dimensions than prototype I, and it contains 16 traction batteries of 12 V and 60 Ah of capacity. The design of the charger done for the maximum power for the charger of this batteries is 3456 W, which consist of a conmutation supply that by means a bridge of diodes and a battery of

condensers, rectify and filter the energy of the network, passing from this level of high tension not regulated to the required one (curves I-U), for the charge of the battery by means a configuration of H-bridge of high frequency. The block circuit for power is the next :
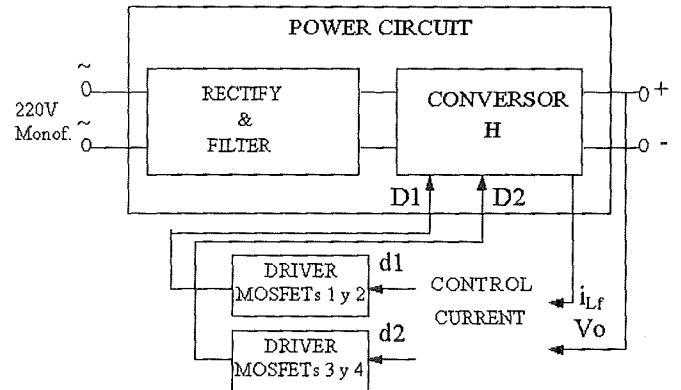

Figure 5. Scheme of the charger.

4.5. STRUCTURE AND BODYWORK

The structure of Prototype II, as well as Prototype I, it is composed by metallic box beams welded in order to achieve the requeriments of the dimensions given by the design of mechanical components of transmission and translation systems. The bodywork has been designed with composite materials laminates.

4.5.1 Calculation and design of the support structure.

Calculation and design was done by means a finite elements code ABAQUS/Standard version 5.6. Rigidity and strength calculations were done for two main static load cases (flexural and torsion load cases), enough to simulate the dynamic behavior of the vehicle.
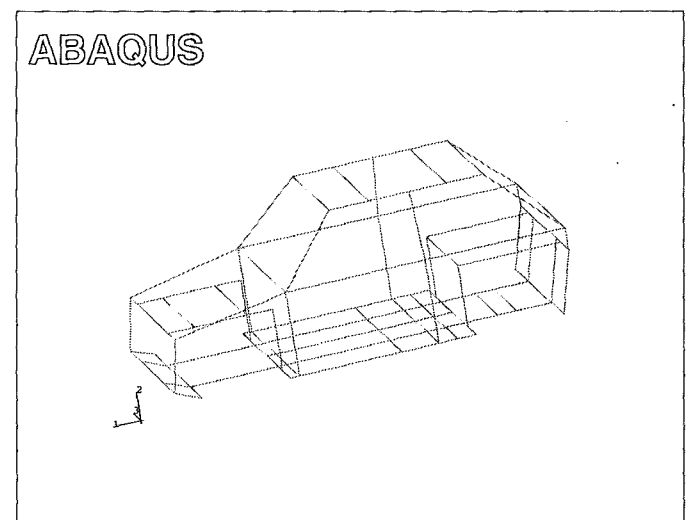

Figure 6. Numerical model in finite elements for the calculation of the structure.

The position of main components weight over the automobile structure are showed in next figure :
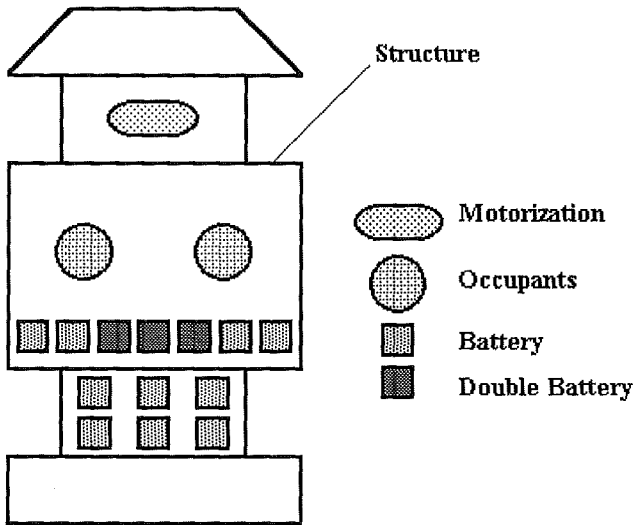
Figure 7.Weight disposition in the structure of the automobile.

Loads applied during the numerical calculation correspond to the weight of the next components :

Motorization (motor + control)   100 daN
Energy supply (battery + charger)   400 daN
Occupants load (occupants + baggage)   200 daN
Rest (struct. + bodywork + mech. compts.)   400 daN

Flexural calculation. Introduce loads that the car suffer during the longitudinal an transversal movements of the car driving due to the weight of its components. The simplified model can be seen in next figure :
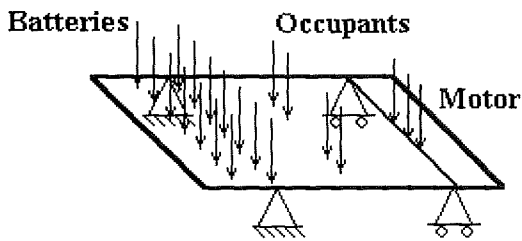
Figure 8. Simplified schema of the flexural calculation.

Torsion calculation. Introduce dynamic loads that the vehicle suffer due to an instability in one of its wheels, as well as the overturn moment when driving taking a curve The simplified model can be seen in next figure .
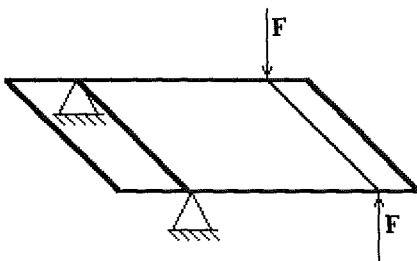
Figure 9. Simplified schema of the torsion calculation.

The results obtained gave good conclusions about the design of the structure done, so, the values of displacements and security coefficients were acceptable. Next figures show results of the numerical calculations of rigidity and strength done for both load cases.
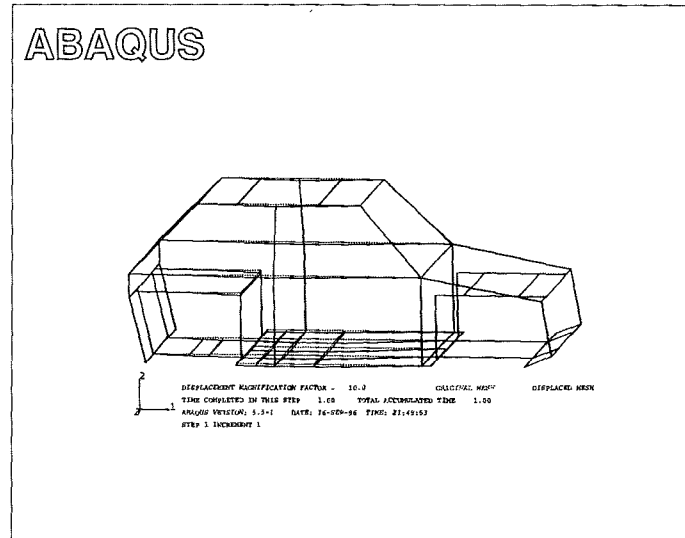
Figure 10. Deformed shape obtained during the flexural calculation.
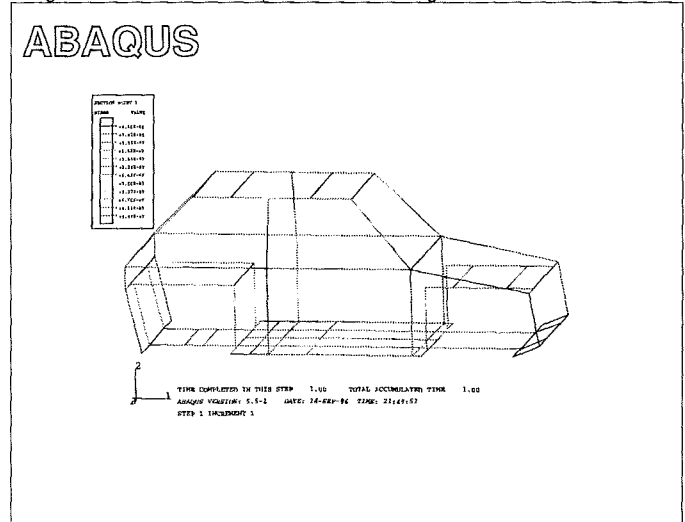
Figure 11. Maximum stresses obtained during the flexural calculation.
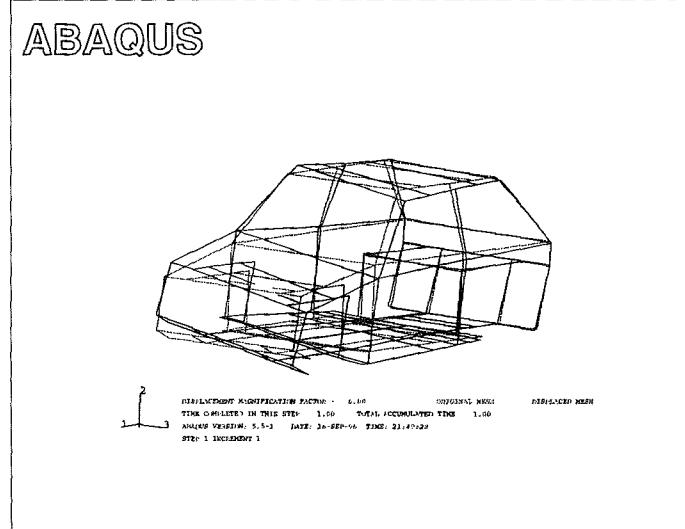
Figure 12. Deformed shape obtained during the torsion calculation.

Figure 13. Maximum stresses obtained during the torsion calculation.

4.5.2. Design of the bodywork.

The bodywork has been fully designed in composite materials, using E-Glass fiber and polyester resin. Joints between parts have been carefully studied and calculated in order to assemble each part in its appropriate place over the structure, calculated before, in an easy way. Thus, we achieve a simple design, very easy and fast to manufacture and to assemble.

The design of the bodywork has been done by means graphic design programs (ABAQUS/Standard Preprocessor), looking for two objectives : to obtain component parts easy to manufacture, and at the same time a design of components parts that show the last trends in the design of automobiles. The next figures show some views of the components parts, as well as the assembled structure over the main metallic structure

Figure 15. Exploded perspective of the component parts.

Figure 14. Lateral, frontal, rear and floor views of the design.

Figure 16. Assembled structure view.

5. CONCLUSIONS

The prototypes of electric vehicles presented in this paper are prototypes fully carried out by the Department of Engineering & Infrastructure of Transportation at the University of Zaragoza.

Prototype I, now finished, showed the capabilities of this University to carry out an Electric Vehicle with specific performance qualities, being the first step for future prototypes.

Prototype II, now in construction, have got the characteristics needed to become an urban car for multiple purposes, able to compete in performance qualities with current combustion vehicles. Due to its simplicity in the concept of electric vehicles, for its easy use, appropriate small dimensions for the present urban traffic, slow weight and manufacture costs plus its reduced consumption and maintenance.

The objective consist on the realization of prototype III, which will have the same characteristics that prototype II, but improving performance qualities and solving all the problems that could appear in the previous prototypes. Moreover, manufacture cost will be optimized in order to achieve a price lower than 8400 American dollars. Once this objective can be achieved we will be able to present a real alternative to the present urban combustion cars, obtaining this way an improvement in the quality of life in big cities referred to the reduction of noise and CO emissions.

6. ACKNOWLEDGMENTS

Acknowledge to all members of the Department of Engineering & Infrastructure of transportation in the University of Zaragoza for the collaboration during the realization of the project and specially to the group of Electric Vehicles.

Acknowledge to the Laboratory of Investigation of S.E. Acumulador Tudor S.A. in Azuqueca de Henares as well as the Factory of Tudor La Cartuja in Zaragoza for the collaboration during the realization of the project.

For last, acknowledge to the Government of Aragón and the University of Zaragoza for the economical support and the sponsorship of this project.

7. CONTACT

Emilio Larrodé.
Department of Mechanical Engineering
UNIVERSITY OF ZARAGOZA

c/ María de Luna 3, 50015 ZARAGOZA (SPAIN)
Phone. +34 76 761 888 - Fax +34 76 761 861

8. REFERENCES

1. Design for crashworthiness of light electric vehicles
   R. Kaeser, ETH Zurich
   EVS-11, Florence, 1992
2. Analysis of distribution, training and information infrastructures which are required for the use of electric and hybrid cars in town traffic.
   H. Van Muylem, Ph Lataire, VUB, 1992
   EDS report P-018, supported by the European Community
3. Electric vehicles of the future.
   NUTEK, Stockolm, 1992
4. Community regulations on electric vehicles
   AVERE, Brussels, 1980
5. EVA Manual : good practice in the use of battery powered vehicles, industrial trucks and specialized equipment.
   Electric Vehicle Association of Great Britain, London, 1989.
6. Infrastructure constraints on meeting the market potential of electric vehicles in European cities.
   P. Van der Bossche, H. Van Muylem, G. Maggetto.
   OECD/IEA seminar "The urban Electric Vehicle", Stockholm, 1992.
7. Concepts and models for the introduction of battery charging stations for electric vehicles in centers of big cities.
   D. Naunin, TU Berlin, 1992
   EDS report P-002, supported by the European Community.
8. New proposals for traffic pollution : The electric vehicle project.
   Consorzio MIP-Politecnico di Milano, 1992
9. COST 302 ; Technical and economical conditions for the use of electric road vehicles.
   CEC, Luxembourg, 1992
10. CITELEC- News nº 3, 4, CITELEC, Brussels, 1991, 1992.
11. STANDARDS : IEC, ISO, ISO/DIS, BS, DIN/VDE, CEN/TC150/WG4n75, prEN, EEC.

The Capstone MicroTurbine™ as a Hybrid Vehicle Energy Source

Howard Longee
Capstone Turbine Corporation

ABSTRACT

The 30 kW MicroTurbine developed by Capstone Turbine Corporation is currently being used in commercial service in a hybrid bus in Chattanooga, Tennessee. This program resulted from a joint program with the bus manufacturer, Advanced Vehicle Systems; the bus operator Chattanooga Area Regional Transportation Authority; and partial funding from CALSTART/ DARPA.

The MicroTurbine has been integrated into a purpose built electric bus used in daily service as part of a fleet of electric buses serving downtown Chattanooga. Over 300 hours and 500 starts have been accumulated. The bus manufacturer and the bus operator are very pleased with the performance and in particular the lack of vibration and quiet performance. Riders are unaware of any difference between the hybrid and pure electric buses. The noise level in the bus is only one dbA above the background. The conversion from battery only to hybrid operation has allowed addition of air-conditioning and provides for increased range. Extended service routes using MicroTurbine hybrid buses are being considered by CARTA.

A description of the system components, performance and lessons learned and future potential are discussed.

INTRODUCTION

SAE papers [1][2][3][4] have described the concept and early development of the Capstone MicroTurbine™ concept and development. This effort has evolved a machine currently in production for stationary power. The MicroTurbine is also being developed for hybrid vehicle applications. This paper describes the integration of the MicroTurbine with an electric bus.

SYSTEM DESCRIPTION

Capstone has integrated a Capstone MicroTurbine™, consisting of a turbogenerator and controller, and an independent data acquisition system into an electric bus. Photographs of the bus and the MicroTurbine installation are provided as Figures 1 and 2. The major suppliers and elements of the bus are:

- Capstone MicroTurbine™: 30 kW (ISO 59°F) turbogenerator and controller
- AVS: 22' electric bus
- Natural Gas Vehicle Systems Inc. : 1443 scf natural gas fuel system
- Solectria Drive System: Two 70 kW AC motors and controllers
- Fulmen: 192 amp-hr, 324 volt lead acid batteries
- Nartron: Two 18,000 BTU/hr electric air conditioners

Figure 1
Hybrid Electric Bus In Service At Chattanooga

The hybrid bus is part of a fleet of 15 electric buses operated in downtown Chattanooga Tennessee by the Chattanooga Area Regional Transportation Authority. The United Nations recognized Chattanooga for their cleanup initiatives and identified the electric bus system as a significant factor. The hybrid bus will allow expanding the electric service to areas beyond the range of the battery only busses.

127

Figure 2
Microturbine Installed In Hybrid Electric Bus
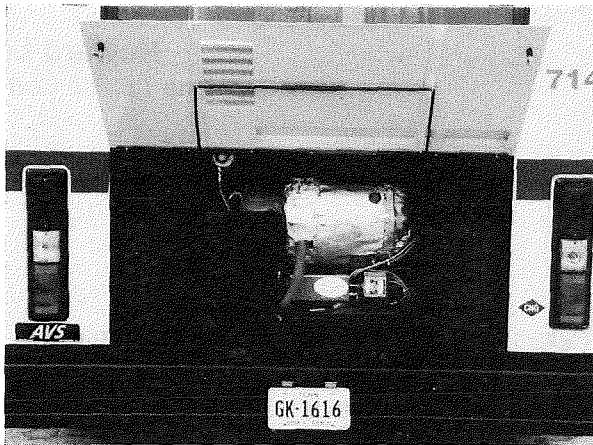
For the Chattanooga route, the MicroTurbine operates on compressed natural gas (CNG). Although the current fuel tanks are small, equivalent to 12.5 gallons of gasoline, the MicroTurbine doubles the bus range. This allows operation for an entire day with a single battery charge instead of two and permits adding air conditioning. Operating on longer, hilly routes are now being considered. The MicroTurbine is described as "quiet, no vibration, no smoke, and no smell".

The bus without the MicroTurbine has a range of 35 to 50 miles. The range with the MicroTurbine is extended to 90 to 100 miles. The average power required without air conditioning is 7 to 10 kW. The bus requires as much as 90 kW of power during acceleration or operation on hills. The MicroTurbine is able to supply the entire average demand of the vehicle which means that range is only limited by the fuel capacity. Initial testing with the AVS bus indicates that the average power demand is less than 10 kW. The air condition-ing system is expected to add about 5 kW to the load when operating. This leaves a significant margin to keep the battery charged as long as fuel is available.

The MicroTurbine controller has a battery management algorithm that tracks power into and out of the battery and assesses state of charge. The data acquisition system monitors the operation of the controller and tracks power in and out of the battery. This information is used for optimizing the battery management algorithm and allows evaluation of reduced capacity battery systems.

SYSTEM OPERATION

The vehicle operator controls the turbogenerator via a three position switch as shown on Figure 3. The three operating modes are OFF, CHARGE and AUTO. The CHARGE mode is used to charge the batteries when the bus is stationary and utility power is not available. The CHARGE mode is disabled when the drive system is activated. As the battery reaches full charge the turbogenerator power will taper off and the system will automatically enter cooldown.

Figure 3
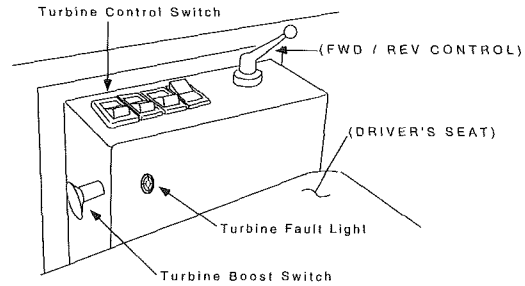
When in the AUTO mode, the MicroTurbine provides power in parallel with the battery. The MicroTurbine power is used to meet the average demand; the battery power is used to meet peak power requirements and to absorb regenerative braking energy. The MicroTurbine maintains the battery at essentially a constant State-of-Charge, thus limiting battery cycles and improving battery life. This control concept also reduces start/stops of the MicroTurbine which reduces loss of energy from the recuperator and reduces thermal cycles for improved efficiency and extended life. The controller monitors the battery state of charge (SOC) and automatically starts the turbogenerator when the SOC charge is below 75%. The output of the MicroTurbine has been limited to 20 kW as the average power required by the bus is less than 10 kW without air-conditioning and less than 15 kW with air-conditioning. The MicroTurbine output is reduced to a minimum of 6 kW if the SOC exceeds 75%. If the average load is less than 6 kW, the SOC will increase. The MicroTurbine automatically goes to cooldown if the SOC reaches 80%. This operation continues as long as the fuel supply is available. When the control switch is in the OFF position, the turbogenerator will automatically begin the shut down sequence. A boost mode switch allows the driver to obtain full MicroTurbine power in anticipation of a large load or passing.

A fault light indicates a system failure. Fault codes may be read from a display located in the controller compartment accessed from the outside of the bus.

Figure 4
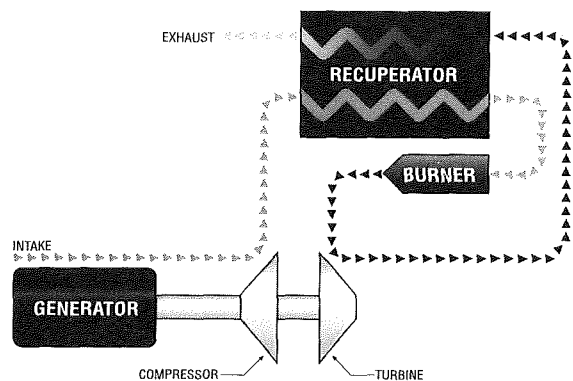
THE CAPSTONE MICROTURBINE™

The MicroTurbine is a compact, 165 pound electric power source. The heart of the unit is an efficient, high speed gas turbine driven generator. The permanent magnet generator is on a common shaft with the compressor and turbine wheels. This single rotating group is supported on air bearings so no lubrication system is required. As the unit is air cooled, maintenance is limited to infrequent cleaning of the inlet air and fuel filters. A unique circumferential recuperator is used to recover exhaust heat and increase the peak operating efficiency while maintaining a very compact package. The MicroTurbine may be operated with a variety of fuels including CNG, LNG, propane, diesel, ethanol, methanol and gasoline. Figure 4 shows typical production engine cycle flow, pressures and temperatures. Figure 5 shows the efficiency and power versus speed at 1100 ∞F for production engines. The turbogenerator is housed in a compartment in the rear of the bus and is accessible through a rear access door.

Figure 5

Thermal Efficiency vs. Generator Output Power
(ISO Standard Day)
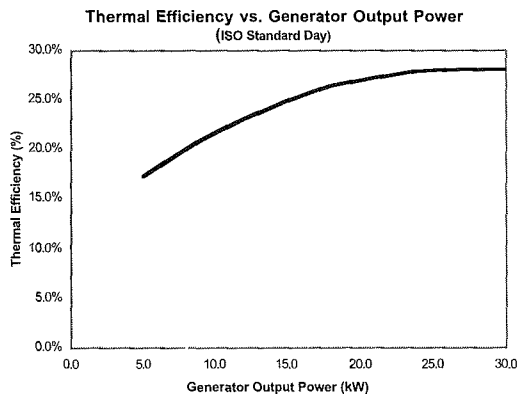
The 30 kW Capstone MicroTurbine™ is currently operating in a number of applications. Over 60,000 hours and 7,000 starts of field service experience have been used to refine the production design. A 60 kW (ISO 15 ∞C) MicroTurbine is currently in development testing.

Current engines operating on natural gas have a tailpipe emission signature of less than 4 parts per million by volume (ppmV) of NOx, CO and HC. Table I provides a comparison of the Capstone MicroTurbine™ emissions, as measured with production engines, and the California Air Resources Board limits for diesel buses and Ultra Low Emission Vehicles. The MicroTurbine™ emissions in Table I are corrected to 15% oxygen and are higher than expected tailpipe emissions.

A catalytic combustion system designed to achieve emission levels of less than 0.1 ULEV is currently under development.

The Capstone MicroTurbine is expected to be a major factor in the rapidly expanding hybrid vehicle market.

Table I
REPRESENTATIVE MIDRANGE EMISSIONS

EMISSION PRODUCTS*	MicroTurbine W/ Diesel Fuel (Steady State)	MicroTurbine w/ CNG (Steady State)	DIESEL ICE[2] (Urban Drive Cycle)	ULEV (Urban Drive Cycle)
NOx (ppmV)	<25[1]	<9[1]	1,266	
(gm/kW-Hr)	0.575	0.21	5.38	0.83
(gm/hp-Hr)	0.43	0.16	4.01	
CO (ppmV)	<10[1]	<9[1]	4,900	
(gm/kW-Hr)	0.14	0.13	20.86	7.1
(gm/hp-Hr)	0.1	0.1	15.56	
HC's (ppmV)	<10[1]	<9[1]	411	
(gm/kW-Hr)	0.08	0.07	1.75	0.17
(gm/hp-Hr)	0.06	0.05	1.31	
Particulates (ppmV)			16	
(gm/kW-Hr)	Negligible[3]	Negligible[3]	0.07	Negligible[3]
(gm/hp-Hr)			0.05	

[1] ppmV values have been corrected to 15% Oxygen; Actual tailpipe emissions are lower (4% each for NOx, CO & HC)
[2] Diesel engine values reflect 1995 California emission standards for diesel bus and urban drive cycle buses.
[3] Low level of smoke possible at start-up and shutdown.

MICROTURBINE CONTROLLER

The controller utilizes an inverter that can supply or extract power to and from the MicroTurbine. The inverter provides power to the PMG (permanent magnet generator) for starting and cooldown. During generator operation, PMG power is controlled to provide regulated DC power to the battery. The controller has significant flexibility for control. In addition to the basic engine control and power conditioning, analog inputs provide input to support the battery management system.

The controller is mounted on a vertical slide in the rear of the passenger compartment. A controller display panel is accessible via the door on the driver's side of at the rear of the vehicle. This display panel provides real time performance data as well as operating and fault history. The turbogenerator controller includes built-in diagnostics. In the event of a fault, the fault light on the operators console will illuminate and the turbogenerator will enter the cooldown mode. If the fault is temporary, the condition may be cleared by turning the turbine control switch to the off position and then returning to the auto mode. If the fault persists, the display panel in the left rear compartment should be queried when convenient to determine the cause of the fault. The bus may continue to be operated as long as sufficient battery charge is available.

PERFORMANCE

The bus has now accumulated MicroTurbine operation of over 500 starts and 300 hours producing power while traveling a total of nearly 6000 miles. Typical Chattanooga service consists of charging the batteries overnight, traveling 10 miles to the fueling station, charging the CNG tanks to about 2700 psig and returning to the station to begin passenger service. The route is 3 miles round-trip and requires about 20 minutes. The MicroTurbine starts automatically when the SOC drops to 75% which occurs shortly after refueling.

The data acquisition system was used to collect battery and MicroTurbine currents and bus voltage during regular operation. Efficiency was calculated based upon actual power delivered by the MicroTurbine™ controller to the battery bus and 1000 BTU/scf of CNG. Regenerative braking and battery recharging energy are excluded. Performance data is averaged and summarized in Table 1.

Table II	
PERFORMANCE DATA	
Mileage	
Battery Only - 80% DOD	41 miles
With MicroTurbine & 80% DOD	84 miles
(assuming 80% of fuel capacity used)	
Energy Usage	
Battery	1.17 kW-hr/mile
MicroTurbine	63 kW-hrs/1000 scf CNG
(at 10 kW average Power)	
Efficiency	21.7%

Table III illustrates the emission achieved with the MicroTurbine versus typical diesel and CNG buses. The MicroTurbine emission levels are calculated based upon 1.3 kW-hrs per mile and the emissions tabulated in Table I. The diesel and CNG emissions are from New York Department of Environmental Protection emission tests in 1990.

Table III			
TYPICAL EMISSIONS			
COMPONENT	MicroTurbine w/CNG	Standard CNG Bus	Standard Diesel Bus
NOx gms/mile	0.273000001	13.354	44.171
CO gms/mile	0.169	2.749000001	2.968999999
Non-Methane HC gms/mile	0.091	0.385000001	2.467000001
Particulates	Negligible	0.13	0.686000001

Figures 6 a and 6b show typical current and voltage transients with and without regenerative braking. Figure 7 illustrates power transients. These transients are under maximum load conditions with the air-conditioning operating and illustrate the ability of the management system to accommodate transients with and without regenerative braking.
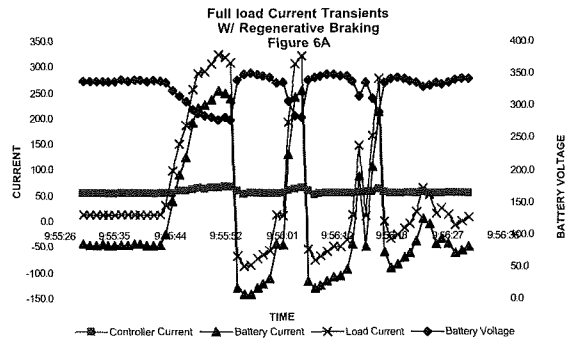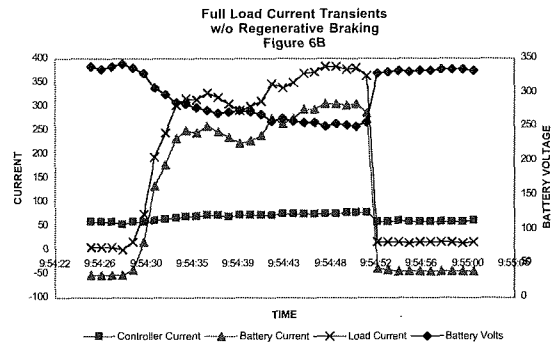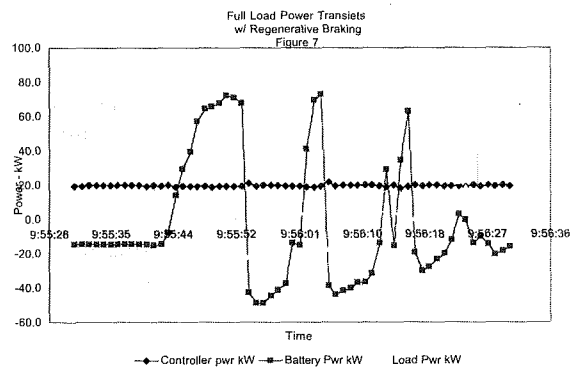
Figure 6a

Figure 6b

Figure 7

LESSONS LEARNED

Although the integration of the MicroTurbine with the electric bus and air-conditioning systems has proven to be very satisfactory, several lessons have been learned:

- Emergency disconnects - The initial emergency disconnect system consisted of four single pole contactors with small bootstrap fuses for coil power. Unnecessary trips resulted in over-voltage spikes that caused failures in the MicroTurbine and drive system power supplies. The contactors and shunt fuses were replaced with circuit breakers with shunt trips to eliminate the problem.

- Regenerative braking shudder - The MicroTurbine control algorithm was originally set to control at 90% SOC. This resulted in a shudder when the regenerative braking was applied. The regenerative braking gain was reduced and the SOC control point was reduced to 75% to eliminate the problem.

- Fuel system cleanliness - The major cause of downtime has been the fuel delivery system. The initial problem was a faulty high pressure regulator. Residue from the regulator and/or from replacing the regulator resulted in clogging the fuel control inlet filter. A larger inlet filter was installed which introduced contamination into the fuel metering valve. The system is fine as long as it is sealed.

- Fueling - The lack of CNG fueling facilities near the operating route has been a major drawback. Fueling the bus requires nearly two hours and 20 miles of range is used before the bus is returned to service. A CNG fueling station is to be installed at the maintenance facility in December 1997.

THE FUTURE

A hybrid bus with a liquid fueled MicroTurbine is planned to replace a diesel bus in the outer loop. Operation of this bus is scheduled to begin in the first half of 1998. A follow-on bus with a catalytic combustor is being considered.

A 45 kW MicroTurbine designed to provide high efficiency over a broad operating range is currently under development testing at Capstone. This engine will allow application of the MicroTurbine to bigger busses on more demanding routes.

CONCLUSIONS

Integration of the Capstone MicroTurbine™ into the electric bus has been very successful. Range and air-conditioning limitations of the battery powered bus have been overcome while maintaining the quiet and clean characteristics that make electric transportation so desirable.

The program has been very successful as evidenced by a number of manufacturers and operators who are planning procurement of hybrid buses with the Capstone MicroTurbine™.

REFERENCES

[1] MACKAY, R., "GAS TURBINE GENERATOR SET FOR HYBRID VEHICLES," 92-0441,SOCIETY OF AUTOMOTIVE ENGINEERS, INC., WARRENDALE, PA, 1992.

[2] MACKAY, R., "HYBRID VEHICLE GAS TURBINES," 93-0044, SOCIETY OF AUTOMOTIVE ENGINEERS, INC., WARRENDALE, PA, 1993.

[3] MACKAY, R., "DEVELOPMENT OF A 24KW GAS TURBINE-DRIVEN GENERATOR SET FOR HYBRID VEHICLES," 94-0510, SOCIETY OF AUTOMOTIVE ENGINEERS, INC., WARRENDALE, PA, 1994

[4] CRAIG, P., "THE CAPSTONE TURBOGENERATOR AS AN ALTERNATIVE POWER SOURCE ," SP-1243, THE ENGINEERING SOCIETY FOR ADVANCING MOBILITY LAND SEA AIR AND SPACE, WARRENDALE, PA, 1997

The Mercedes-Benz C-Class Series Hybrid

Joerg O. Abthoff, Peter Antony, and Michael Krämer and Jakob Seiler

Daimler-Benz AG

ABSTRACT

The Series Hybrid project is described concerning the scenario, technical data of vehicle and components and operating strategy. The two prototype cars offer an attractive driveability. Test results show high potential on emission reduction without increasing the consumption.

SCENARIO FOR THE SERIES HYBRID DRIVE

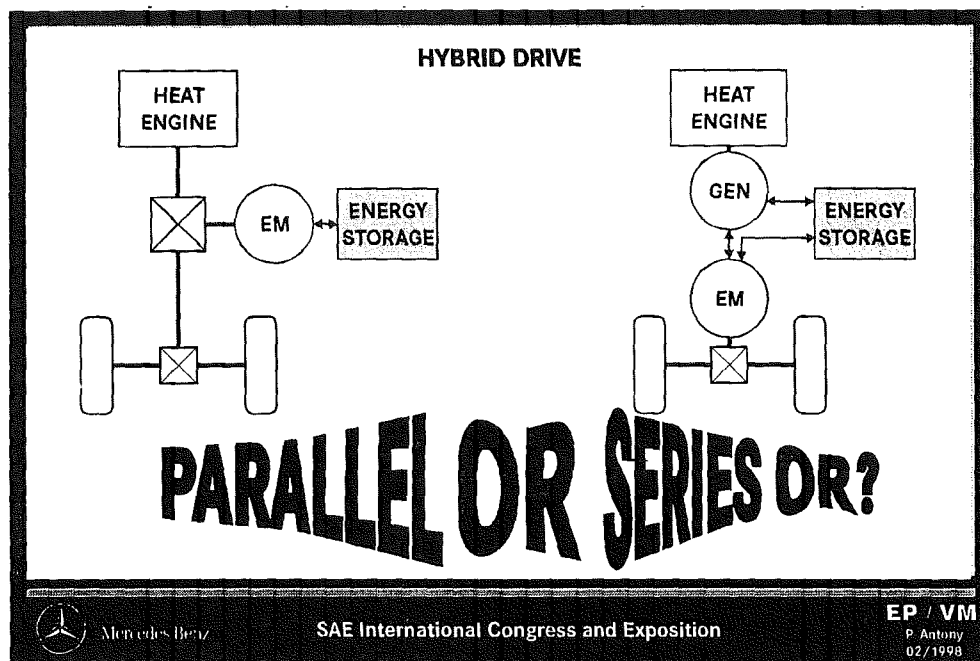The basic hybrid concepts of the parallel and series hybrid are sufficiently well known.

Figure 1.   Parallel and series hybrid concept

The question is frequently asked as to which concept is the best. It is not so easy to answer this question. It can only mean: which concept is the best for a given application?

In our opinion parallel hybrids make sense where a vehicle is required to be driven both conventionally and with electric drive only, e.g. conurbation scenario, driving and delivering in sensitive areas.

In terms of weight, packaging and costs, a realization is much easier if electric-only propulsion is only required for a limited performance and range.

Through the potential of driving in a combined mode, parallel hybrids provide the option of designing a smaller combustion engine and of reducing emissions (warm-up).

By completely decoupling the combustion engine from the wheels, series hybrids provide the facility of generating the drive current on board with optimized efficiency and emissions.

They are therefore preferably suitable for use with more stringent exhaust emission regulations with a lower fuel consumption potential at the same time.

Such a approach is given by the Californian EZEV legislation proposal:

Legislation of Emissions

		Emissions [g/m]				ZEV credit
		PM	CO	NMOG	NOx	
Sep. 1990	ARB passed the LEV legislation incl. ZEV-mandat					
1993	HEV Type A : Electric range 60 miles B : " " 40-59 miles C : " " 0-39 miles		0,01	0,005	0,004	full credit for typa A + B
Apr. 1995	HEV´s with APU HEV´s with ULEV-APU, intermittently			0,001	0,01	full credit partial
Jul. 1995	EZEV HEV type 1 : ULEV with techn. safeguards incl. evaporation + fuel cycle emissions 2 : ULEV incl. evaporation + fuel cycle emissions 3 : LEV, TLEV, ULEV	0,004	0,17	0,004	0,02	full credit 1: partial 2: partial 3: no credit
Jun. 1996	EZEV, sum of exhaust, refueling and evaporative emissions	0,004	0,17	0,004	0,02	full credit

EP / VM
P. Antony
02/1998

Mercedes Benz — SAE International Congress and Exposition

Figure 2. History of the EZEV legislation

Unfortunately, continuing discussion about legislation means that we developers have to aim at a moving target. In our series hybrid drive project, the attempt should now be made to show such low emission values with no negative effect on consumption using gasoline due to the existing infrastructure.

VEHICLE DESCRIPTION AND TECHNICAL DATA

As a prototype test vehicle we chose our smallest class at the time, the C class, since this choice has no relevance whatsoever with regard to a potential series production.

The vehicle was equipped with an electric drive to the rear axle. A tandem motor arrangement was chosen for packaging reasons. The combustion engine is located in its usual place and, - in conjunction with the directly flanged-on alternator, only acts as a power generator. The batteries together with the battery controller and the power electronics of the electrical machines are located in the trunk. In addition, there is an onboard charger, DC/DC converter and the central control unit which coordinates all the drive components according to higher strategies.

SYSTEMS OF HYBRID DRIVE

EP / VM
P. Antony
07/1998

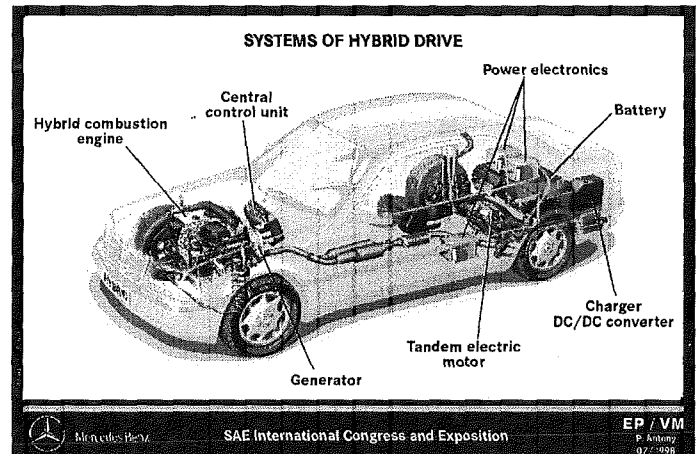Mercedes Benz — SAE International Congress and Exposition

Figure 3. The C-Class series Hybrid

Concerning the power conception we started up with the assumption, that hybrid vehicles are primarily first or only cars unlike electric vehicles , which due to their limited range are typical second cars. So we decided that the hybrid vehicle should accelerate better than the lowest powered series version of the C class and the maximum speed should be more than 150km/h.

TECHNICAL DATA

⊃ COMBUSTION ENGINE
- 1,8 l, 4 Cyl. Gasoline engine
- Optimized for hybrid use,
  65 kW/4000 rpm

⊃ VEHICLE
- Weight :1758 kg (+408)
- 0-60 mph : 13,7 sec
- Max. speed > 150 km/h

⊃ BATTERY
- NI/MH
- Power 34 kW
- Weight 255 kg

⊃ GENERATOR
- Permanent magnet
  synchronous generator
- Power 60 kW

⊃ ELECTRIC DRIVE
- Tandem motor
- Permanent magnet
  synchronous motors
- Power 2x 35 kW

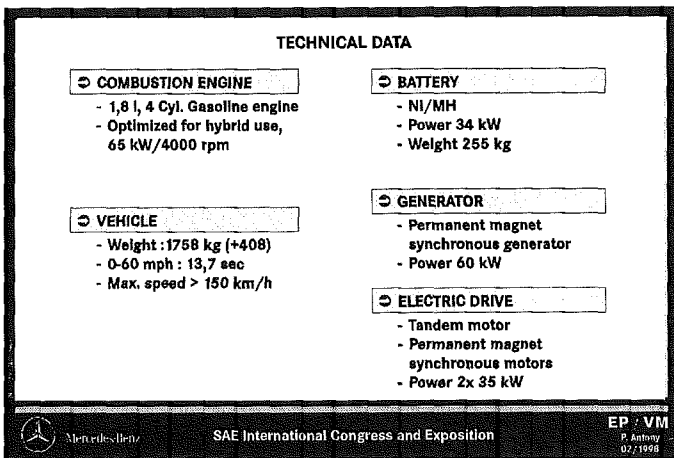Mercedes-Benz | SAE International Congress and Exposition | EP / VM | P. Antony 02/1998

Figure 4. Technical data

It was possible to meet the set targets satisfactorily with the following power rating:

Combustion engine: 65 kW

Generator: 60 kW

Electric motors: 2x35 kW

The acceleration is around 14 seconds from 1-100km/h and the maximum speed is 170 km/h.

The battery was also determined via power to permit the vehicle to follow the FTP cycle in each case, even if the generator temporarily does not supply any power. This means that it must be able to deliver a short-term output of 55 kW.

The problem was that such power peaks mean a thermal time response and this is only described poorly for most batteries.

With the above layout , two prototype cars have been built up.

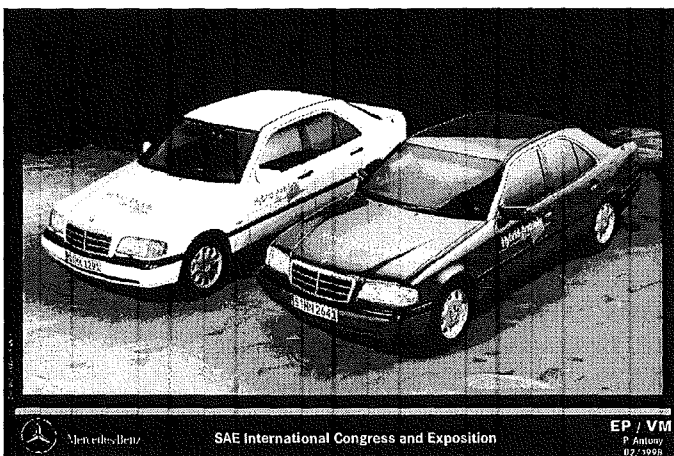Mercedes-Benz | SAE International Congress and Exposition | EP / VM | P. Antony 02/1998

Figure 5. The C-Class Series Hybrid

First, the vehicles were optimized for driveability. The response to the demonstration drives was quite positive although the optimization efforts for handling , noise and comfort have been far below production level at that time.

COMPONENT SELECTION

Combustion engine including exhaust gas aftertreatment

By completely decoupling the combustion engine from the wheels, and hereby offering more flexibility in the operating strategy, series hybrids are open for a wider range of heat engines.

COMPARISON OF HEATENGINES FOR SERIES HYBRID DRIVES

	Gasoline engine	Diesel engine	Gasturbine	Stirling engine
Fuel economy	◎	⊕	⊖	⊕⊕
Emissions	◎	⊖	⊕	⊕
Noise	⊕	⊖	◎	⊕
Vibration	⊕	◎	⊕⊕	⊕
Availability	⊕⊕	⊕⊕	⊖	⊖⊖
Costs	⊕	◎	⊖	⊖⊖

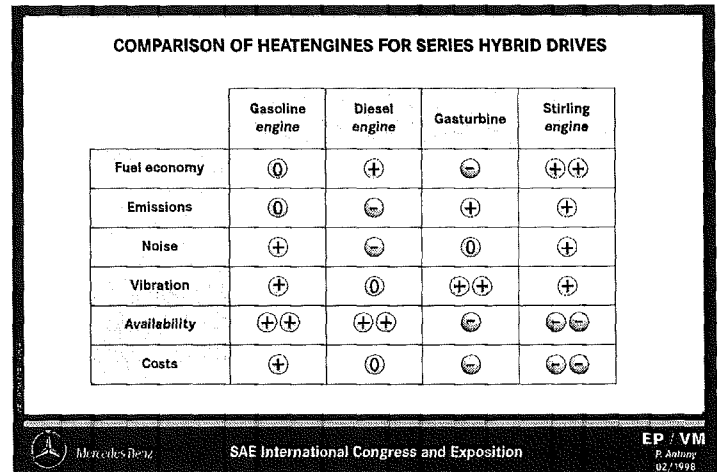Mercedes-Benz | SAE International Congress and Exposition | EP / VM | P. Antony 02/1998

Figure 6. Comparison of heat engines for series hybrids

The chart compares gasoline engines, diesel engines, gasturbines and stirling engines looking on consumption, emissions, noise, vibration, availability and costs.

For a short-term realization of our project, only the gasoline and diesel engine were acceptable. Finally the gasoline engine was chosen because of ist lower emissions.

The smallest available production engine at that time was the 4 cylinder 1.8 l gasoline engine. To reduce the raw emissions, especially hydrocarbons, the following measures have been carried out: use of ceramic valves, reduced top land height and Nikasil coating.

For the series hybrid an exhaust gas aftertreatment concept was developed which consists of active and passive components. The principle structure is a reproduction of the TLEV standard exhaust system, in order to minimize the vehicle modifications. The exhaust system comprises an air-gap insulated sheet-metal manifold, a header pipe which has an external insulation from the manifold flange to the entry into the underfloor catalytic converter, and a catalytic converter package.
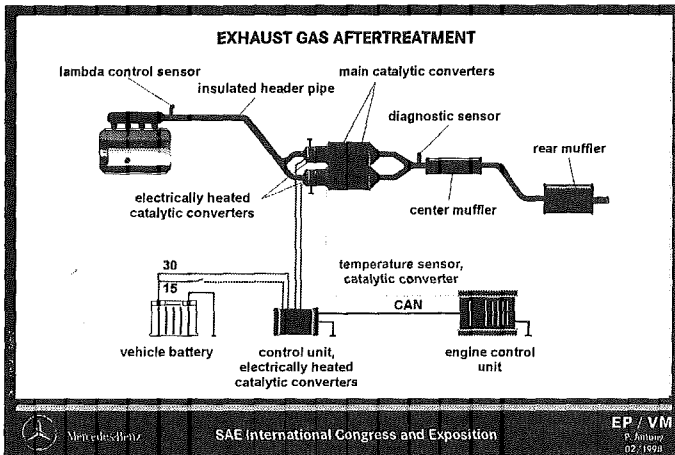
Figure 7. Exhaust gas aftertreatment system

As with the TLEV standard system the catalytic converter package has a twin-pipe design. The only difference is that there is one large-volume, electrically heated catalytic converter (EHC), upstream of each of the 2 conventional, insulated ceramic catalytic converters. The EHC's were designed for a heating power of 1.5 kW at 12V each.The command to start/stop heating the catalytic converter is given by the central control unit.

WARM-UP STRATEGY – For cold-starting the engine a warm-up strategy was developed which aims at achieving the lowest possible pollutant emission of the engine. Moreover, pre-conditioning of the exhaust gas aftertreatment system was intended to ensure that the pollutants are completely burnt by means of catalytic aftertreatment (primarily the hydrocarbons HC and CO). Figure 10 shows the correlations within the starting procedure.
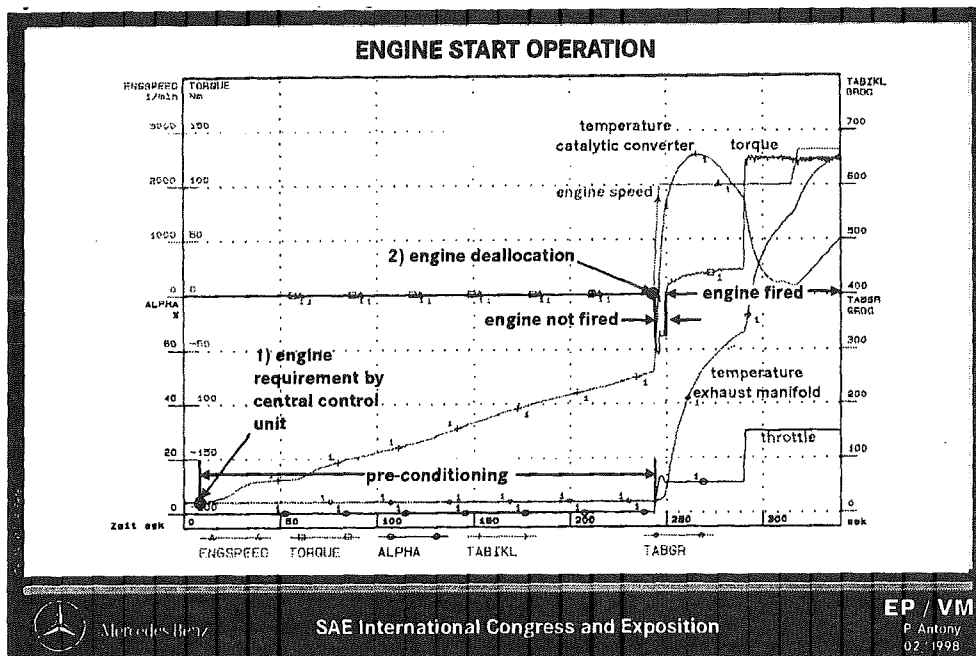

Figure 8. Starting procedure

At the timeline -1- the central control unit gives out the requirement of combustion engine operation.. This starts the pre-conditioning of the exhaust gas aftertreatment system, which means, the electrically heated catalytic converters are brought to a specified temperature . Once this value is reached, the central control unit gives the command -2- according to which the engine is motored to a specific engine speed by the generator. During this process the throttle valve is also brought into a defined position. After completion of these processes, the engine is fired.

Once the warm up is finished, the engine can now be started without any further peconditioning of the exhaust gas aftertreatment system, because the insulation measures that were taken make it possible to maintain a minimum temperature level of 400 °C in the catalytic converter package for a specific period of time.

For initial investigations a 4-cylinder spark-ignition engine was mounted on a dynamic test rig where in the FTP Cycle hydrocarbon emissions of on average 0.003 g/m could be reached.

ELECTRICAL MACHINES – In addition to the components for a conventional drive, an alternator and an electric motor must be installed on series hybrid drives, where the only key component not used any more is the transmission.

The following figure gives an overview of electric machines.

COMPARISON OF ELECTRIC DRIVES FOR HYBRID APPLICATION

	DC Motor	Asynchronous motor	Synchronous motor	Permanent magnet SM	Transversal flow motor	Switched reluctance motor
Power density	⊖⊖	⊙	⊙	⊕⊕	⊕⊕	⊙
Speed range	⊕	⊙	⊕⊕	⊕⊕	⊕⊕	⊙
Efficiency characteristic map	⊖	⊕	⊕⊕	⊕⊕	⊕⊕	⊕⊕
Development status	⊕⊕	⊕⊕	⊕	⊕	⊙	⊙

SAE International Congress and Exposition — EP / VM — P. Antony 02/1998

Figure 9. Comparison of electric machines

The call for the highest specific power inevitably follows from the performance requirements described earlier and the packaging situation in conversion cars. Permanently excited synchronous motors are clearly in the lead here. They achieve a maximum of about twice the specific power as asynchronous drives or magnetic reluctance drives.

Special permanently excited machines achieve these high specific continuous outputs (>=1kW/kg) at conceptional interesting speed levels. Additional transmission steps are thus dispensed with.

ELECTRIC MOTOR

Picture shows half a tandem motor

Technical data	Tandem electric motor
power	70 kW
peak power	75 kW
torque	1135 Nm
peak torque	1560 Nm
rated voltage	230 V
weight	68 kg
coolant	water

Rotor   Stator   Planetary gear   Housing

Source: Mannesmann Sachs

SAE International Congress and Exposition — EP VM — P. Antony 02/1998
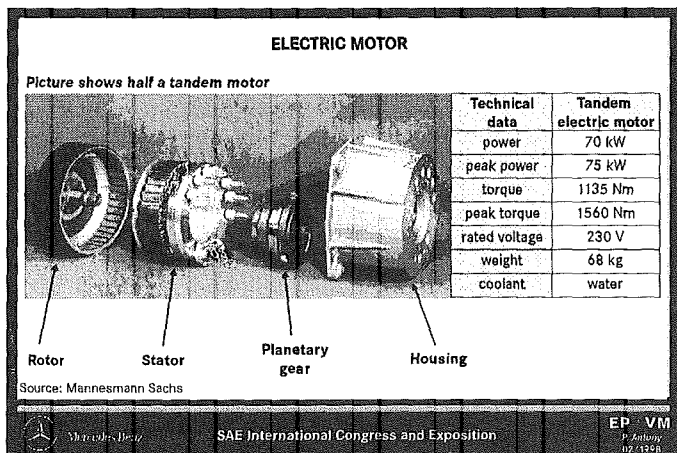
Figure 10. The F&S electric drive

A permanently excited synchronous machine by Fichtel & Sachs with high-pole external rotor was selected for our project.

The machines and associated electronics will be developed on an evolutionary basis also with regard to costs. Reduced use of materials and manufacturing costs and efforts due to optimized designs and progress in material technology (magnets) reduce the cost disadvantages of permanently excited machines compared with asynchronous machines. The power electronics for both systems can be considered as equal in price.

All in all, the further reduction in the costs of electric drives is of great importance for the marketability of hybrid drives and there is still some work to be done here.

Battery

ENERGY AND POWER DENSITY OF STORAGE SYSTEMS

Batteries — Target field for series hybrids — Flywheels — Supercapacitors

Energy [Wh/kg] vs Power [W/kg]

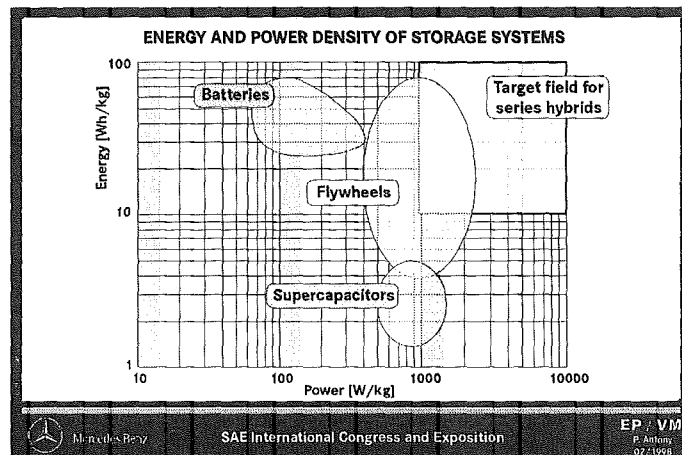SAE International Congress and Exposition — EP VM — P. Antony 07/1998

Figure 11. Energy and power of energy storage systems

The electrical storage requirements have already been mentioned: short-term power up to 55 kW with the lowest possible weight and volume. The energy content can be comparatively small.

This first suggests the idea of supercapacitors or flywheels. However, these technologies are still in an early development phase and the availability is problematic even for prototype test vehicles. In addition, the required energy content for these technologies, especially the supercapacitor is still very high.

The use of a battery as storage was therefore unavoidable.

The above requirements contrast with previous battery developments for electric drives. These were all directed towards the requirements of electric-driven vehicles only-thus towards range and energy content.

The battery produced the maximum power required due to its considerably larger overall size.

FMC 1016

Figure 12. Current battery systems

This figure gives an overview of the battery systems

The charging/discharging performance of available lead batteries is insufficient for this application and quickly drops off even more at low temperatures.

At >50 - 60% state of charge, the charge power must be drastically reduced, otherwise gassing voltage is exceeded. Even highly developed, more powerful lead batteries have this constraint.

The specific power is also too low in the case of the Na/NiCl (Sodium/Nickel Chloride) battery. For a hybrid vehicles, which from our piont of view should be independent from a charging infrastructure the necessity of keeping this battery system at its high operating temperature is unacceptable.

The Zebra battery is a typical electric vehicle battery or battery for a range extender - HEV.

Lithium batteries: in the meantime a first high-performance lithium/ion battery for HEVs has been announced. Whether it can also be charged with comparable power ranges is not yet clear.

This battery uses cobalt which is very expensive and rare. Work is continuing on alternatives materials (including manganese oxide).

Various safety aspects are still to be clarified for these batteries (in particular fire and explosion risk on overcharging and overheating).

The development of this system is being followed with interest.

The alkaline storages offer high performance even at relatively low charge states. This also applies to rapid charging at high states of charge (load leveling, recuperation).

These are the decisive parameters in this application.

For our series hybrid vehicle a NiMH battery (DAUG XX38) has been chosen.

A particular problem for a self-sufficient hybrid vehicle is the equalization of the state of charge between the cells, which is required regularly for all batteries. On an electric vehicle this can easily take place during each charging process, but during the operation of a hybrid vehicle a reset charge is not so easy to to be achieved.

The only known battery which has internal charge equalization and very rarely requires a "reset charge" is the DAUG "bipolar NiMH battery".
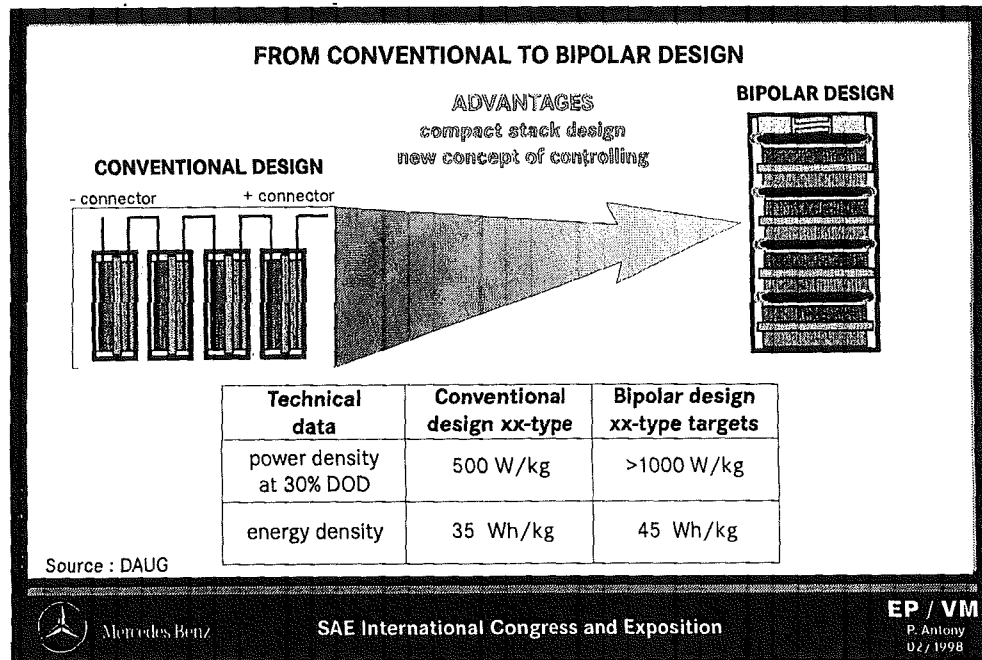
138

FROM CONVENTIONAL TO BIPOLAR DESIGN

ADVANTAGES
compact stack design
new concept of controlling

CONVENTIONAL DESIGN

BIPOLAR DESIGN

- connector   + connector

Technical data	Conventional design xx-type	Bipolar design xx-type targets
power density at 30% DOD	500 W/kg	>1000 W/kg
energy density	35 Wh/kg	45 Wh/kg

Source : DAUG

Mercedes-Benz   SAE International Congress and Exposition   EP / VM P. Antony 02/1998

Figure 13. Bipolar battery system by DAUG

The charge equalization between the cells of a cell bank (approx. 40 cells) takes place by means of hydrogen diffusion between the cells as the hydrogen pressure in the cell rises and falls with the state of charge.

Thanks to its low internal resistance, this concept has the potential for a high specific power above 1 kW/kg.

OPERATING STRATEGY

Owing to the complete separation of the auxiliary power unit from the drive system there is a high degree of freedom for the operating principle of the combustion engine. Both the operating point of the engine and the time at which the engine should run can be freely selected. This requires an intelligent engine operating strategy with the objective to optimize fuel efficiency, emissions and driveability.

To be able to investigate the effects of various operating strategies a simulation model was produced on the basis of MATLAB/SIMULINK.

STRATEGIES DEPENDING ON THE CHARGE LEVEL – In the literature we often find engine operating strategies with the charge level of the energy storage system as the basic control parameter.

FMC 1016

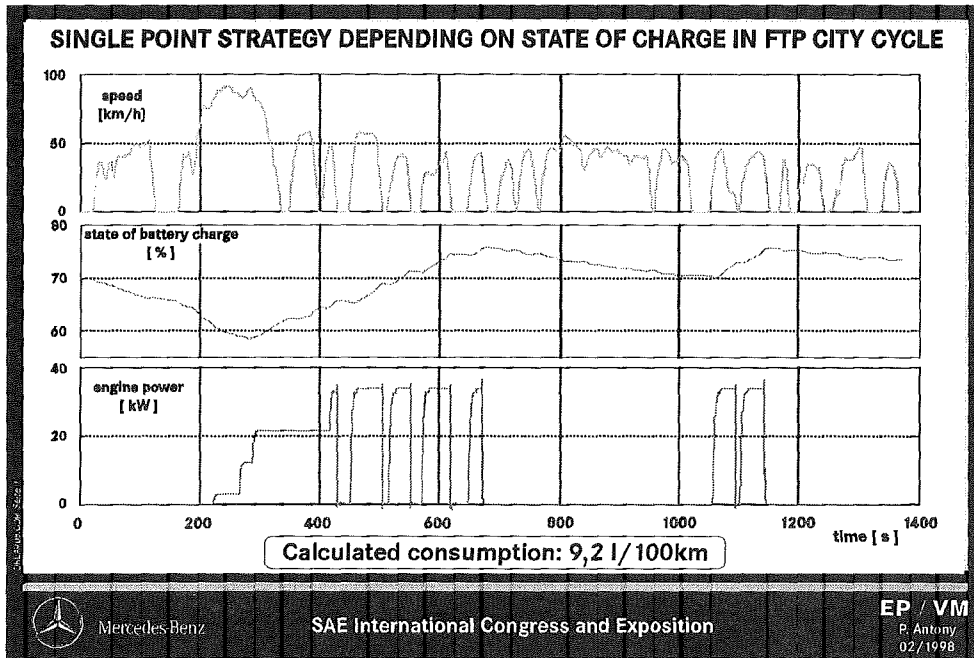**SINGLE POINT STRATEGY DEPENDING ON STATE OF CHARGE IN FTP CITY CYCLE**

Figure 14. Single-point strategy depending on state of charge in the FTP75 test

The engine is turned on and off to keep a defined range of state of charge.

Generally, these strategies are single-point strategies which means that the engine is running a constant operating point. The power delivered by the generator is produced in such a way that the combined efficiency of the auxiliary power unit has the optimum value.

An operating strategy tested on the series hybrid model regulates the charge level to between 70 and 75%. In addition to the charge level control, a speed-dependent control is superposed. If the vehicle speed falls below 5 km/h the engine switches from load to idle. As of a vehicle speed of 10 km/h the engine changes to load again.

This strategy leads to a calculated consumption of 9.2 l / 100km in FTP-City Cycle.

POWER-DEPENDENT OPERATING STRATEGY –

Another possible engine control parameter is the electrical power required by the electric motor, which needs to be provided by the auxiliary power unit and/or the battery.

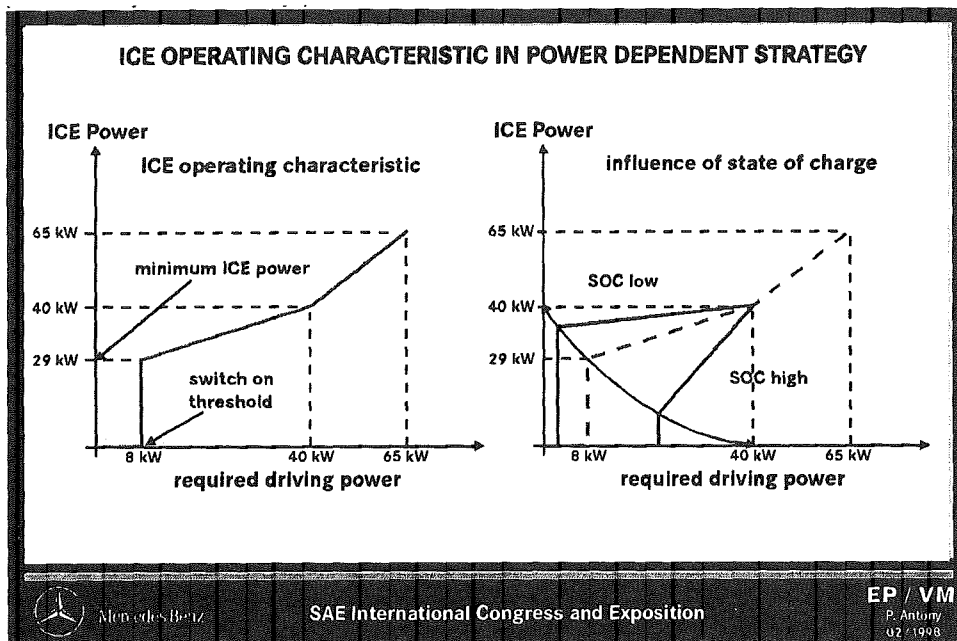**ICE OPERATING CHARACTERISTIC IN POWER DEPENDENT STRATEGY**

Figure 15. Engine operation characteristics

It is the objective to operate the engine in accordance with the power requirement in such a way that the overall efficiency of all systems is optimum at all times. This leads to an operating strategy as to bee seen in the picture.

140

As opposed to the strategies depending on the charge level it is not ensured with this strategy that the charge level of the battery remains within the desired limits.

For this reason the cut-in point needs to be lowered and the engine output increased when the charge level is too low and vice versa.
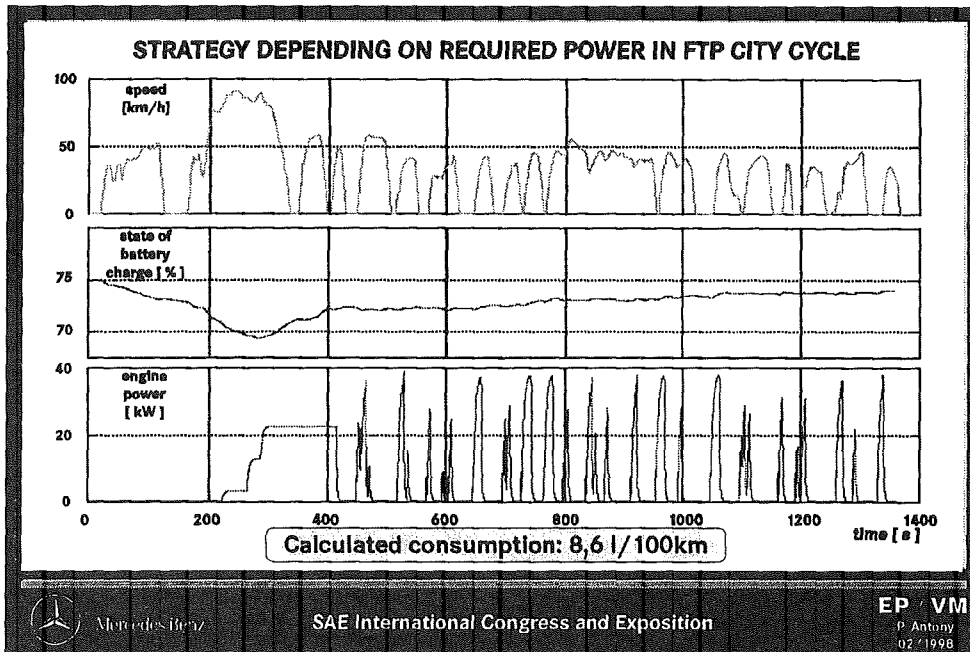

Figure 16.   Power-dependent strategy in the FTP75 test

The simulated fuel consumption of the power dependent strategy described was 8.6 l/100km.

The 7 % improvement in fuel economy compared to the state of charge dependant strategy was attained exclusively by an optimized engine operation. This comparison shows the relevance of a matured engine operation strategy.

TEST RESULTS

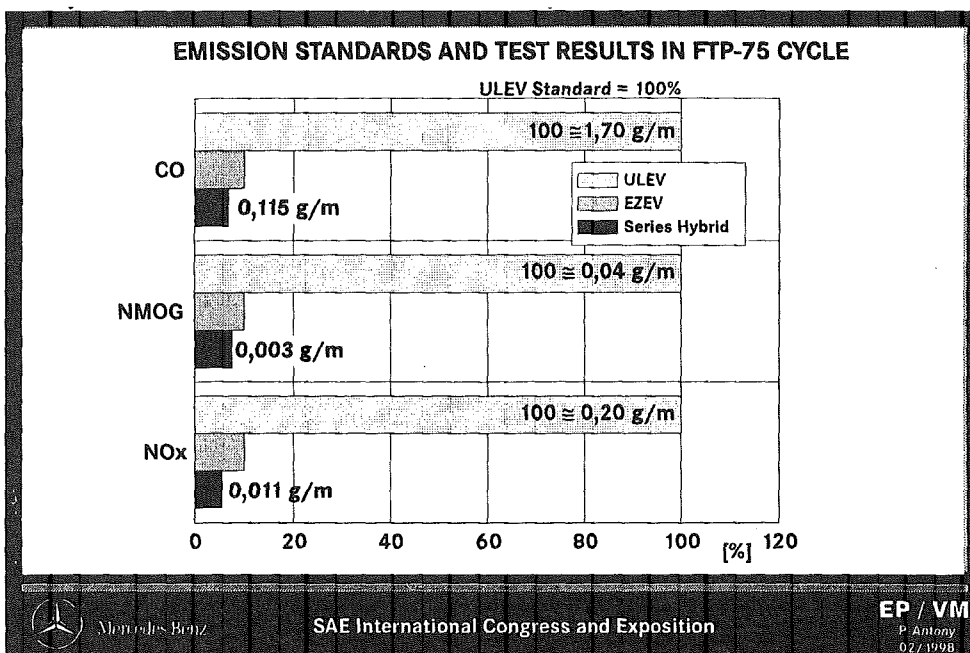Finally roller tests were carried out with both hybrid vehicles:

Figure 17.   Emission test results.

The tail pipe emissions of the series hybrid are within the EZEV level for all components hydrocarbons, carbon monoxide and nitrogen oxides. The tests showed very clearly the problem of measuring such low emissions especially concerning repeatability. Little differences in the initial and ambient conditions, the test sequence, con-trol processes and deposits in the exhaust system lead to large variance of the measured values.

The legal classification of such a "near zero emission vehicle" remains open particularly because of discussions about up-stream emissions and minimum pure electrical ranges.

VEHICLE COMPARISON

	1,8 l C-Class production car	Series Hybrid optimized for emissions	Series Hybrid optimized for fuel economy
Acceleration 0-100 km/h [sec]	12.0	14	14
Max. Speed [km/h]	193	>150	>150
Emission level FTP75 test	TLEV (with 2.3 l engine)	EZEV (Tailpipe emissions)	--
Fuel consumption [l/100km]	9.0	8.8	8.0
Vehicle weight [kg]	1350	1758	1758

Mercedes-Benz   SAE International Congress and Exposition   EP / VM
P. Antony
02/1998

Figure 18.   Consumption Test results

It was the objective of the development not to exceed the consumption of the 1.8l C-Class production car. In combination with EZEV emission level   this goal could be reached. When optimized on fuel consumption only, a significant advantage could be reached.

COSTS OF A HYBRID VEHICLE

Following our presentation of the technical possibilities of the series hybrid, we would like to analyze the costs.
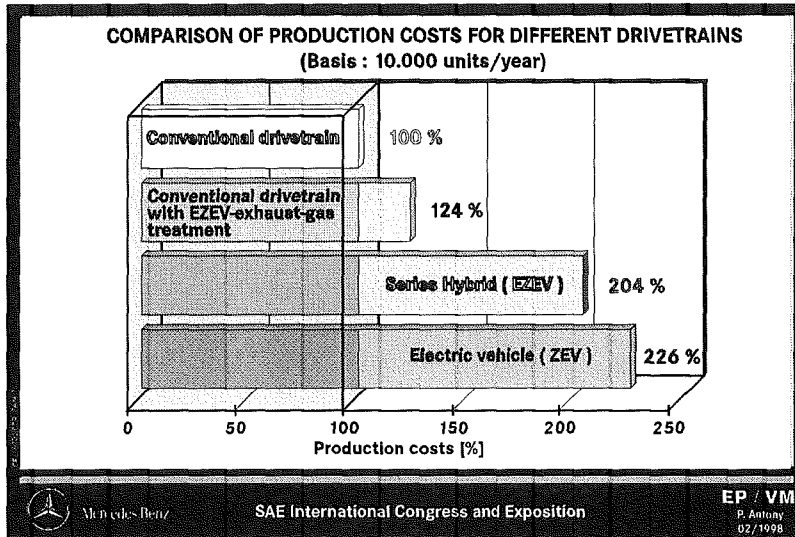
Figure 19. Comparison of costs

The illustration shows a comparison of the manufacturing costs of various technical concepts for meeting an EZEV/ZEV exhaust emission standard within a vehicle category.

The vehicle with conventional drive is the 100% base in our comparison. Note that the series hybrid car has even lower production costs than an electric vehicle with the same performance. The major impact of the battery costs is evident here.

Figure 20.

FINDINGS

It is possible to achieve extremely low pollutant emissions with a series hybrid drive. In the case of this main objective, there is little reduction in fuel consumption compared with a conventional drive.

With purely series hybrids, the component performance requirement is greatest compared with various concepts. This is because the electric wheel drive must be capable of delivering full acceleration power and the generator must deliver the power for a continuous maximum speed. The requirement for both reducing consumption and minimizing component sizes leads to mixed hybrid systems in which the combustion engine is involved in the wheel drive by means of a through-coupling or power split device.

THANKS

SAE The Engineering Society
For Advancing Mobility
Land Sea Air and Space ®

INTERNATIONAL

International Congress & Exposition
Detroit, Michigan
February 23-26, 1998

FMC 1016